Computer simulation and optimisation of solar heating systems for Cyprus

Ioannis M. Michaelides

School of Electronics and Manufacturing Systems Engineering,
Faculty of Engineering and Science

R. 'ELE: PHD

ENG

COMPUTER SIMULATION AND OPTIMISATION OF SOLAR HEATING SYSTEMS FOR CYPRUS

IOANNIS M. MICHAELIDES

A thesis submitted in partial fulfilment of the
requirements of the University of Westminster
for the degree of Doctor of Philosophy

School of Electronics and Manufacturing Systems Engineering,
Faculty of Engineering and Science,
University of Westminster, London

In collaboration with

Higher Technical Institute, Nicosia, Cyprus

April 1993

ABSTRACT

This thesis reports the results of research into the modelling and simulation of solar water and space heating for Cyprus, and the investigation of the factors concerning the optimisation of such systems. Further a number of design criteria, which can be used by consultants and designers of solar heating systems, have been established.

Five solar heating system configurations have been modelled using the component models of the TRNSYS programme. They concern thermosyphon solar water heating systems, active solar water heating systems, solar space heating systems, combined solar water and space heating systems and solar assisted heat pump systems for space and water heating. These models are used to simulate the thermal performance of the systems and investigate their cost effectiveness under the weather and socioeconomic conditions of Cyprus. The results of the simulations have been used to identify the optimum design criteria for such systems in the Cyprus environment.

The design criteria that have been established are concerned mainly with the solar collector and the storage tank and they are key design factors for a solar heating system. The design factors include the collector orientation and tilt angle, the collector to load factor which relates the collector surface area to the annual thermal load, the storage factor which relates the capacity of the storage tank to the collector size, the collector water flow flux, which relates the water flow rate through the collector with the collector area, and other criteria, which concern the auxiliary heat supply and the heat exchangers.

For space heating systems, in addition to the above factors, a new design criterion is introduced, the collector to floor area factor, which relates the collector area to the building floor area, while for domestic hot water systems, the collector to consumer factor is used to specify the collector surface area needed for each hot water consumer in the building.

This work has resulted in the publication of four papers in refereed International Journals and the presentation of three other papers at International Conferences. A list of publications is included in the Appendices.

LIST OF CONTENTS

LIST OF TABLES

LIST OF FIGURES

ACKNOWLEDGEMENTS

I would like to express my gratitude to my Director of studies, Dr W. C. Lee, for his constructive criticism and guidance. I am also indebted to Dr P. P. Votsis, who originally acted as Director of studies and then as local advisor, for his enthusiasm and encouragement. My appreciation is also due to Professor D. R. Wilson, for his stimulating interest and valuable advice throughout the work.

I am glad to place on record my gratitude to the Higher Technical Institute and its Director, Mr D. Lazarides, for the provision of research and other facilities. My thanks are also extended to all my colleagues who have assisted me and particularly Mr G. Iordanou, Head of the Mechanical Engineering Department, for his encouragement and support.

I am also indebted to the staff of the Applied Energy Centre of the Ministry of Commerce and Industry of the Republic of Cyprus for valuable discussions on energy matters.

My appreciation is also extended to the School of Electronics and Manufacturing Systems Engineering of the University of Westminster and particularly Mr K. E. Bird, Associate Head, for the facilities provided to me during my study visits to the University.

The financial assistance of the A. G. Leventis Foundation is also gratefully acknowledged.

Finally, I would like to dedicate this work to my wife Demetra and my two sons, Erineos and George, without whose love, understanding , patience and support, this work might never have been completed.

NOMENCLATURE

A, A_c	Collector area, m^2
A_f	Building floor area, m^2
b_o	Incidence angle modifier constant
C_A	Area dependent costs, US dollars
C_{AUX}	Auxiliary fuel cost, US dollars
C_c	Capacity rate of fluid on the cold side of a heat exchanger, $\dot{m}_c c_{pc}$
C_h	Capacity rate of fluid on the hot side of a heat exchanger, $\dot{m}_h c_{ph}$
C_E	Fixed costs, US dollars
C_{FA}	Auxiliary energy cost rate, US dollars/GJ
C_{FL}	Conventional fuel cost rate, US dollars/GJ
C_{LOAD}	Fuel cost of the conventional system, US dollars
C_{max}	Maximum capacitance rate in a heat exchanger, kJ h^{-1} K^{-1}
C_{min}	Minimum capacitance rate in a heat exchanger, kJ h^{-1} K^{-1}
COP	Coefficient of performance
c_p	Specific heat of working fluid, kJ kg^{-1} K^{-1}
c_{pc}	Specific heat of cold side fluid (heat exchanger), kJ kg^{-1} K^{-1}
c_{ph}	Specific heat of hot side fluid (heat exchanger), kJ kg^{-1} K^{-1}
d	Market discount rate, %
D	Down payment, % of original investment
DEG	Thermal performance degradation, %/yr
d_h	Diameter of collector headers, m
d_j, d_o	Diameter of collector inlet & outlet pipes, m
d_R	Diameter of collector risers, m
D_s	Diameter of storage tank, m
f	Solar fraction (fraction of the load that is met by solar)
F_{cc}	Collector to consumer factor, m^2 per consumer
F_{cf}	Collector to floor area factor, m^2 of collector per m^2 floor area
F_{cl}	Collector to load factor, m^2 per annual GJ
F_R	Collector heat removal factor
$F_R U_L$	Slope of the collector efficiency curve, kJ h^{-1} K^{-1} m^{-2}
$F_R(\tau\alpha)_n$	Intercept of the collector efficiency curve
F_s	Storage factor, l m^{-2}

G	Collector mass flux, kg h^{-1} m^{-2}
G_{test}	Collector mass flux at test conditions, kg h^{-1} m^{-2}
H_a	Height of auxiliary heating element above bottom of tank, m
H_c	Vertical distance between outlet and inlet of collectors, m
H_o	Vertical distance between outlet of tank and inlet to collector, m
H_r	Height of collector return above bottom of tank, m
H_t	Height of auxiliary thermostat above bottom of tank, m
HAUX	Auxiliary heat for space heating, GJ
HLOAD	Space heating load, GJ
HWAUX	Auxiliary heat for domestic hot water, GJ
HWLOAD	Domestic hot water heating load, GJ
i	Inflation rate, %
i_{FBUP}	Backup (auxiliary) fuel inflation rate, %
i_{FCF}	Conventional fuel inflation rate, %
I_h	Monthly average of the daily solar radiation incident on a horizontal surface, MJ m^{-2} day^{-1}
I_T	Total radiation incident on the (tilted) collector surface, MJ m^{-2}
L	Annual hot water load, GJ
LCC	Life cycle solar costs, US dollars
LCS	Life cycle solar savings, US dollars
L_h	Length of collector headers, m
L_i, L_o	Length of inlet and outlet piping, m
m	Mortgage, yrs
$\dot{m}_L$	Water flow rate to space heating load, kg h^{-1}
$\dot{m}_c$	Water flow rate on cold side of a heat exchanger, kg h^{-1}
$\dot{m}_h$	Water flow rate on hot side of a heat exchanger, kg h^{-1}
$\dot{m}_{sp}$	Water flow rate from main storage to hot water preheater, kg h^{-1}
M_S	Extra insurance, maintenance in year 1, % of initial investment
M_D	Total daily mass demand of hot water, l
N_D	Useful life for depreciation purposes, yrs
N_E	Period of economic analysis, yrs
N_L	Term of loan, yrs
N_R	Number of parallel collector risers
P_{aux}	Auxiliary energy input to tank, kW

PW	Present worth, US dollars
Q_{abs}	Energy absorbed from a cold source by a heat pump, kJ
Q_{air}	Energy absorbed from the ambient air by a heat pump, kJ
Q_{aux}	Auxiliary energy supplied to the system, kJ
Q_{dh}	Direct solar heat from storage to load, kJ
Q_{ei}	Electric energy required by the heat pump, kJ
Q_{env}	Heat loss from the storage tank, kJ
Q_{hp}	Heat output by the heat pump, kJ
Q_{ins}, QINS	Total radiation incident on the collector, kJ, GJ
QINPH	Heat supplied to water preheater, GJ
Q_{load}	Thermal load (hot water and/or space heating), kJ
QPLOAD	Heat from water preheater to load, GJ
Q_u, QU	Useful solar energy collection, kJ, GJ
R	Hot water preheat tank height to diameter ratio
S	Annual solar radiation on a horizontal surface per unit area, GJ m^{-2}
SAF	Solar–air fraction
t	Effective income tax rate (%), time
T_a	Ambient air temperature, °C
$T_{a,min}$	Minimum ambient temperature necessary for ambient air source heat pump operation, °C
TAUX	Total auxiliary heat, GJ
T_{ci}	Cold side inlet temperature, °C
T_{co}	Cold side outlet temperature, °C
T_{dh}	Minimum water temperature necessary for direct heating (collector–storage–load), °C
T_{evn}	Environmental temperature for losses from storage, °C
T_{hi}	Hot side inlet temperature, °C
T_{ho}	Hot side outlet temperature, °C
T_i	Temperature of the fluid at the collector inlet, °C
TLOAD	Total heating load (space and domestic hot water), GJ
T_{max}	Set temperature for cooling, °C
T_{min}	Set temperature for heating, °C
T_o	Temperature of the fluid at the collector outlet, °C
T_R	Room temperature, °C

T_{req}	Minimum required hot water delivery temperature, °C
T_s	Thermostat set temperature, °C
$T_{sh,min}$	Minimum water temperature necessary for heat pump operation using storage water source, °C
T_{so}	Temperature of water from storage tank, °C
U_L	Collector heat loss coefficient, kJ h^{-1} K^{-1} m^{-2}
UA	Constant characterising the building, kJ h^{-1} K^{-1}
$(UA)_{pi}$	Conductance for heat loss from collector inlet pipe, kJ h^{-1} K^{-1}
$(UA)_{po}$	Conductance for heat loss from collector outlet pipe, kJ h^{-1} K^{-1}
$(UA)_s$	Conductance for heat loss from storage tank, kJ h^{-1} K^{-1}
U_p	Heat loss coefficient of hot water preheat tank, kJ h^{-1} K^{-1} m^{-2}
U_s	Heat loss coefficient of storage tank, kJ h^{-1} K^{-1} m^{-2}
v	Wind velocity, m s^{-1}
V_p	Volume of hot water preheat tank, m^3
V_s	Storage tank volume, m^3

Greek symbols

α	Absorptance
β	Collector tilt angle, degrees from horizontal
γ_{htr}	Temperature control signal
ΔT	Temperature difference between the collector mean and the ambient air, °C
ΔU	Change in storage tank internal energy, kJ
ε	Heat exchanger effectiveness
ε_c	Effectiveness of the collector–storage tank heat exchanger
ε_L	Effectiveness of the space heating load heat exchanger
η	Efficiency
ρ_g	Ground reflectance
τ	Transmittance

ABBREVIATIONS

AUX	Auxiliary
ASHRAE	American Society of Heating Refrigeration and Air conditioning

	Engineers
Comm.	Commercial
COP	Coefficient of Performance
CY	Cyprus
CYS	Cyprus Organisation for Standards and Quality of Control
D	Diesel oil
DHW	Domestic Hot Water
Dom.	Domestic
E	Electricity
EC	European Community
El. Heating	Electric Heating
FH	From Horizontal
GDP	Gross Domestic Product
H	Hotel
HEX	Heat Exchanger
HFO	Heavy Fuel Oil
HTI	Higher Technical Institute
LCS	Life Cycle Savings
LFO	Light Fuel Oil
LPG	Liquified Petroleum Gas
MECU 85	Millions European Currency Units, at constant prices of 1985
MIT	Massachusetts Institute of Technology
P	Pump
R	Residential
SAHP	Solar Assisted Heat Pump
SDHW	Solar Domestic Hot Water
SHW	Service Hot Water
SOL	Solar
SWH	Solar Water Heater
SRCC	Solar Rating and Certification Corporation
TH	Thermostat
TSWH	Thermosyphon Solar Water Heater
toe	Ton oil equivalent
USD, US$	United States Dollar

CHAPTER 1

INTRODUCTION

1.1 Scope of work

In recent years, the public has become increasingly concerned about the rapid depletion and escalating costs of fuels. The increases in the oil prices and the rising demand for energy, have made people conscious of the wisdom of reducing the energy consumption through conservation of conventional sources of energy and exploitation of renewable energy sources. Solar energy is one such energy source that can probably make a vital contribution to our energy needs.

The present work is directed towards a very small subject area in the field of solar energy. It is an attempt to investigate the possibility of utilising solar energy for water and space heating for domestic and commercial purposes, and in particular to consider this in relation to the conditions of Cyprus.

There is a popular tendency to regard solar energy as "free". However, solar radiation must be intercepted and converted to useful thermal energy and this requires a capital investment and annual costs to operate and maintain the system. In practical terms, solar energy is definitely not "free". The cost is usually the most important single consideration in making a decision of whether or not to install a solar heating system.

The optimum economic choice for a heating system depends upon the projected costs of energy from various sources in the future. As indicated later in this thesis, given the current fuel costs and the capital costs of construction and installation, solar space heating in Cyprus is not the best economic choice at present; however, this might not be the case in the future. Undoubtedly, as more experience is gained with solar

heating systems, and as system components become more readily obtainable, manufacturing and installation costs will tend to decrease. Increasing costs for conventional sources of energy are inevitable and, ultimately, solar heating systems may well become an economic choice. Other factors such as personal choice or an interest in experimentation may also lead to the choice of a solar heating system.

The sizing of a solar heating system is a complex problem involving a number of interrelated factors which include collector area and performance, storage size, heating requirements, solar radiation, mechanical equipment sizing and system control, as well as an economic evaluation of the entire proposed system.

In Cyprus, the climatic weather conditions are such that Cyprus can be classified as one of the countries where the potential of solar energy utilisation is very high. During the past 30 years, the solar collector manufacturing industry has been very successful and it is estimated that about 33,000 m^2 of flat plate solar collectors are being produced each year. At present the use of solar energy is limited to domestic hot water applications and represent 9% of the total annual electricity consumption.

To enhance the utilisation of solar energy, a wider range of applications must be considered through careful design of cost effective solar–based energy systems which can be applied not only to domestic dwellings but also to large building complexes such as apartment blocks, hotels, sports centres etc. In order, therefore, to produce effective designs of such systems, it is necessary to optimise their performance in relation to various design parameters on the basis of Cyprus climatic and socio–economic conditions. This can be achieved through computer modelling and simulation of solar heating systems which will enable the synthesis of optimum design criteria for such systems. It is, therefore, very useful if a design tool is available which will take into consideration both the technical and economic aspects of the problem. This will help the designer to evaluate the cost effectiveness of a solar heating system and at the same time serve as a tool for sizing the system components.

The purpose of this research is two–fold. First, to develop suitable models for solar water and space heating systems for Cyprus. Second, to carry out computer

simulations of the performance of such systems over a wide range of operating conditions and for various design parameters in order to investigate some of the factors concerning the optimisation of the system. This will assist in the synthesis of design criteria which can be used by consulting engineers and designers of solar heating systems in Cyprus.

From the literature survey presented in Chapter 3 it is seen that the great majority of researchers followed the approach of modelling and simulation of solar systems to predict the performance of a system and investigate its optimum design parameters. Since the present work is essentially based on modelling and simulation of solar water and space heating systems, it would be appropriate to explain the value of modelling and simulation of solar systems and present some of the simulation models currently in use.

1.2 Modelling and simulation of solar heating systems

A solar energy system is an assembly of interacting components designed to collect solar radiation, convert it into heat or any other form of energy, store it and distribute it for use according to the needs. A solar space heating system, for example, is an assembly of various components, such as solar collector, storage tank, pumps etc, which collect solar radiation convert it into heat and store this heat in water to use it for space heating when needed.

The performance of solar hot water or space heating systems depends on the weather. Both, the building heating demand and the solar energy collected are time–dependent forcing functions, such as ambient air temperature, solar radiation and other meteorological variables acting on a solar heating system. As a result, solar heating systems always operate in transient modes, they are driven by weather which is variable and they are non–linear in their responses to solar radiation. Therefore, it is rather difficult to analyze solar energy systems based on their response to average weather conditions. On the other hand, the conduction of physical experiments is expensive, time consuming and non repeatable due to the variable weather conditions. It is however possible to "build" and "operate" them in computers by developing the

mathematical model of a system and simulating the performance of the system. The simulation is, in fact, a numerical experiment in which different designs and sizes of components can be tested to find the most suitable in terms of performance and cost. If the model has been validated against experimental data, reliable information can be obtained much more quickly and cheaply than by physical experiments. Modelling and simulation of solar systems can serve multiple purposes (Kreider and Kreith, 1981):

(a) They can organise complex systems into a more understandable format.

(b) Simulations can eliminate guesswork and reduce the expense of building prototypes. In cases where prototype solar energy systems should be built, a considerable cost savings can often be realised by substituting investigations using system models for some of the prototypes. In addition, a system model can predict the performance of a system for various sizes and types of components and for various operating and control modes.

(c) They can generate insight into system operation and component interactions. Some systems models may show only the final outcomes, such as the fraction of the heating load of a building met by solar on a monthly basis, but in many models the performance of subsystems and performance at shorter intervals is also investigated.

(d) Different system configurations can be tested and analyzed under identical conditions, for comparison purposes. When comparing the performance of prototype systems, it is difficult and rather impossible to establish repeatable conditions, while identical conditions can be specified when applying the same systems model to different systems or variations of the same system. The potential advantages in cost savings as compared to building prototype systems and in increased reliability and precision in such comparisons is obvious.

(e) System models can be used to identify the most important design considerations. The more complex a system is, the more difficult it is to intuitively identify what aspects of the system should be given most attention in research and development. A system model can be used to examine the quantitative consequences of a change in one or more design variables of a system. By comparing the effects of changing each design variable, a judgement can be made as to their relative importance. In a solar water heating system, for example, the collector area can be varied over a wide range without significantly affecting the solar fraction. At the same time, however, such a variation brings about a change in the system cost which means that the

system's performance is sensitive to collector area when its economics are included in the performance measure.

(f) Simulations facilitate the optimisation of solar systems. Optimisation of a system requires the implicit or explicit examinations of the performance of a system for a multiplicity of designs under identical external conditions and the identification of the design that is the best according to the measure of performance.

(g) They can be used to develop simplified design approaches. The results of many simulations can be used to develop generalised performance charts and synthesize design criteria for a solar system.

There are various approaches in solar systems modelling: mathematical models, simulations, empirical and physical models. Mathematical modelling is in fact the assembly of mathematical statements of well known physical laws. There are, however, systems which cannot be modelled mathematically, and other approaches, such as simulations, must be used. In contrast to mathematical models that are directly expressible in mathematical equations, simulation models are primarily procedural in nature, although they may use mathematical expressions. Simulation modelling is an important modelling approach for solar thermal systems, particularly for solar heating systems, since these systems do not lend themselves to mathematical modelling approaches.

There are various modelling approaches, which differ in purpose of use, complexity, accuracy and computational effort, like for example the TRNSYS simulation programme (Klein *et al.*, 1990), the f–chart (Klein *et al.*, 1976), STOLAR (Lameiro, 1977) and Bruno's method (Bruno and Kersten 1977). Of these models, TRNSYS and f–chart are the most popular in use. TRNSYS, which is a detailed simulation developed at the University of Wisconsin–Madison, will be presented in detail in a separate section in this chapter.

STOLAR is a STOchastic soLAR energy system model developed by Lameiro (1977). It consists of a statistical compression of hourly insolation and weather data and simplified system governing equations to form a mathematical systems model of residential solar water and space heating systems. The model focuses on transitions in storage tank temperature as the driving force for system behaviour. STOLAR

results matched TRNSYS (see below) fraction of solar predictions within 6% absolute difference for three test cities (Kreider and Kreith 1981). It has, however, a number of disadvantages; it requires large computer facilities, it does not provide monthly results, and is not applicable for commercial building systems.

Bruno's method is based on a sequential iterative solution scheme which requires only daily insolation and weather data. The daily behaviour of insolation and other external inputs to the system are modeled using equations whose form yields an exact solution to the systems governing equations. No major difficulties are perceived in the use of this systems model as long as the level of detail that the model provides is adequate. However, if more detail is required, or if an hourly reporting of system performance is needed, this model is not suitable.

F–chart is an example of a model that is based upon simulation results. The TRNSYS programme was used to model two specific configurations of space heating systems using both liquid and air heating collectors. The simulation studies were conducted using Madison climatological data. The f–chart model was then based upon correlations to results obtained from these simulation studies that were conducted by the use of the TRNSYS programme. The correlation was developed between the monthly fraction of load provided by the solar system and the dimensional parameters. These dimensional parameters were defined as the ratio between the collector gains and the monthly load and the ratio between the collector losses and the monthly load.

The f–chart model is a very valuable tool in the design of solar space and water heating systems since it provides a tool that may be used to very quickly estimate the monthly or yearly fraction of the load that would be supplied by a solar system, once the designer has specified the collector parameters and collector area. However, this model is accurate only for solar heating systems of a type comparable to that which was assumed in the development of the f–chart. In addition, this model does not provide the flexibility of detailed simulations and performance investigations as does TRNSYS.

1.2.1 The TRNSYS simulation programme

TRNSYS, an acronym for Transient Simulation programme, is a quasi-steady simulation model. This programme was developed by the members of the Solar Energy Laboratory at the University of Wisconsin-Madison. An early version of the programme was released in 1974. The programme consists of many subroutines which represent the various components commonly found in a solar system, such as the solar collectors, heat exchangers, stratified and fully mixed water storage tanks, space and domestic water heating loads, pumps, auxiliary heaters, thermostats, heat pumps, cooling devices, tees, valves, etc. There are also component routines to handle input of weather data or other time-dependent forcing functions and output of simulation results. Many components may operate in any of several modes, offering differing degrees of model complexity. Also, the capabilities of component routines may overlap. Building loads, for example, may be calculated using the simple "degree-hour" load model or with the more detailed transfer function zone component. Alternatively, TRNSYS can accept hourly loads generated by other load programs. A list of all component routines is included in the TRNSYS Manual (see Klein *et al.* 1990).

The mathematical models for the subsystem components are given in terms of either ordinary differential equations or algebraic equations. Heat exchangers, for example, are modelled using algebraic equations, while the storage subsystems are modelled by ordinary differential equations. Following is an example of a TRNSYS model for the counterflow heat exchanger illustrated in fig. 1.1a. The information flow diagram for the heat exchanger is shown in fig. 1.1b. The equations describing the operation of such a heat exchanger are:

$$\varepsilon = \frac{1 - \exp\left[-\frac{UA}{C_{min}}\left(1 - \frac{C_{min}}{C_{max}}\right)\right]}{1 - \left(\frac{C_{min}}{C_{max}}\right)\exp\left[-\frac{UA}{C_{min}}\left(1-\frac{C_{min}}{C_{max}}\right)\right]} \qquad (1.1)$$

$$T_{ho} = T_{hi} - \varepsilon \left(\frac{C_{\min}}{C_h} \right) \left(T_{hi} - T_{ci} \right) \tag{1.2}$$

$$T_{co} = T_{ci} + \varepsilon \left(\frac{C_{\min}}{C_c} \right) \left(T_{hi} - T_{ci} \right) \tag{1.3}$$

$$Q = \varepsilon \, C_{\min} \left(T_{hi} - T_{ci} \right) \tag{1.4}$$

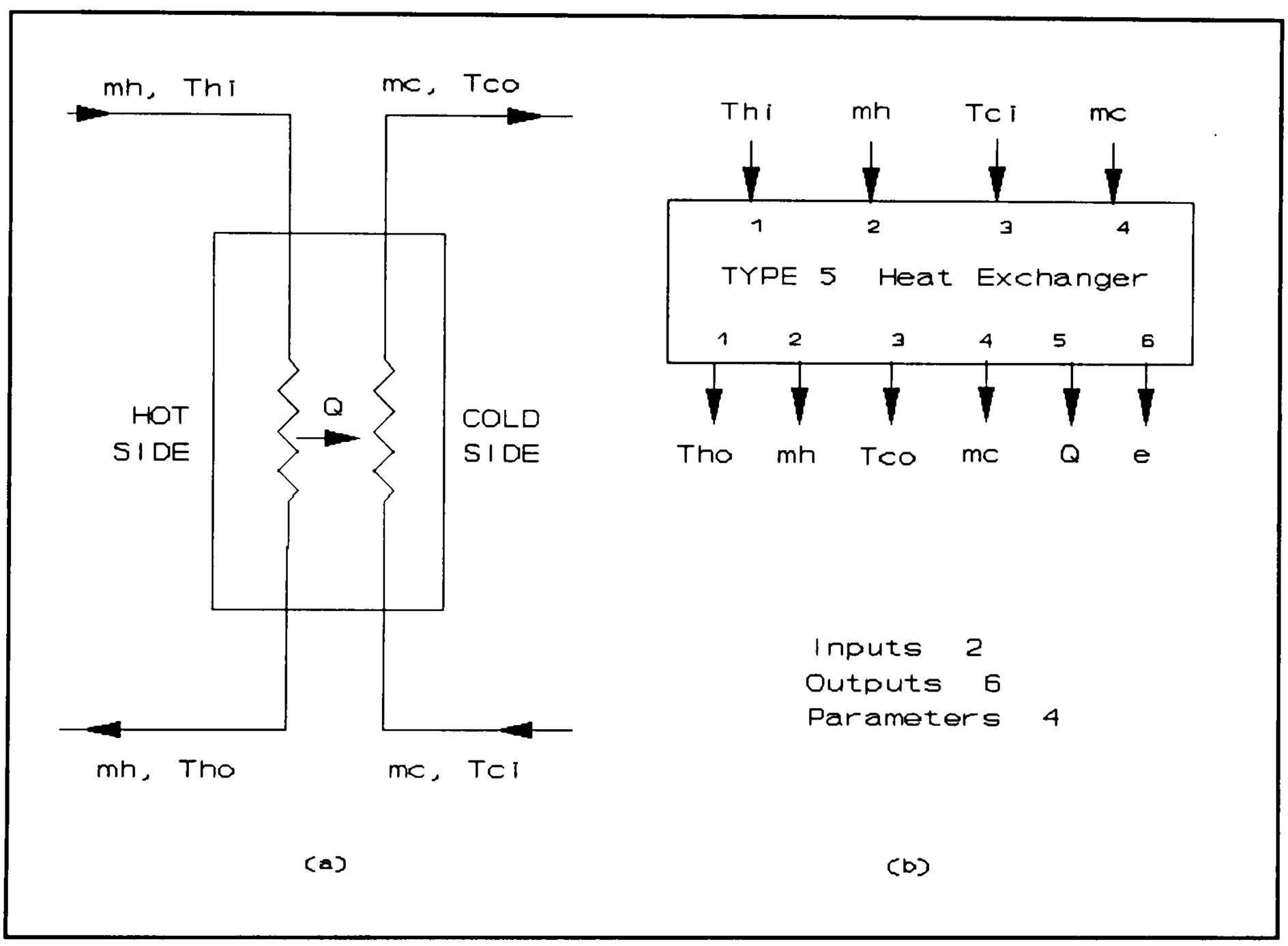

Fig. 1.1 Heat exchanger schematic (a) and information flow diagram (b)

The user must first identify the system components that comprise that particular system to be simulated and then must construct an information flow diagram to facilitate identification of the components and the flow of information between them. Connecting the system components in TRNSYS is analogous to connecting the real equipment with piping or wires. He then supplies values for all the parameters describing the system configuration selected for simulation. The organisation and processing of the required component subroutines, control strategies and data input

and output is carried out automatically through the TRNSYS simulation deck. The programme proceeds to the simultaneous solution of the algebraic and differential equations which represent the system components mathematical models. The numerical solution algorithm of the differential equations selected for TRNSYS is the Modified–Euler method. It is essentially a first order predictor–corrector algorithm using Euler's method for the predicting step and a trapezoid rule for the correcting step. The predicted values of the dependent variables are used to determine the corrected values. The two values are compared for convergence based on specified error tolerance. When the error tolerance is satisfied, the solution for that time step is complete and the whole process is repeated for the next time step. A more detailed account of the solution algorithm is given by Duffie and Beckman (1980).

The simulation of a system requires hourly weather data which must be representative of the location under investigation. The selection of typical weather conditions for a given location is very crucial in computer simulations for performance predictions and lead various investigators either to run long periods of observational data or to select a particular year, which appears to be typical from several years of data. Klein *et al.* (1976), have constructed the "average year" by selecting the monthly data from an 8–year period which corresponded most closely to the average monthly insolation and ambient temperature. In cases where hourly data are not available, the Weather Generator component, included in TRNSYS, generates a typical year of meteorological data given the monthly average values of radiation, temperature and humidity. A file of monthly average weather data for Nicosia has been created by the writer, in the format accepted by TRNSYS, as shown in Appendix A.

The economic evaluation of the systems under investigation is done using the TRNSYS subroutine of economic analysis, which performs a standard life cycle analysis based on the simulation of one year of solar system operation. It compares the capital and backup fuel costs of a solar system to the fuel costs of a conventional non–solar system. It is assumed that the solar backup system is identical to the conventional heating system, in that only the incremental costs of adding solar to the conventional system are considered. Payback time is defined as the time needed for cumulative fuel savings to equal the total initial investment, that is how long it takes to get an investment back by savings in fuel (see Duffie and Beckman 1980).

The detail of the economic output is dependent on the mode and parameters used. Mode 1 is the simplest method of calculating the life cycle costs and life cycle savings. It uses the P1 and P2 method as described by Brandemuehl and Beckman (1979) and Duffie and Beckman (1980). Mode 2, which is used in the simulations of this work, uses various economic parameters to calculate the yearly cash flows, life cycle costs, life cycle savings and payback periods. It also provides the user with options to calculate the rate of return on the solar investment, to consider income producing buildings , and to include tax credits. In both modes, the integrated cost of auxiliary energy use, i.e solar backup, at time t, is given by the formula

$$C_{AUX} = \int_0^t C_{FA}\, Q_{aux}\, dt \qquad (1.5)$$

where C_{FA} is the auxiliary energy cost rate and Q_{aux} the auxiliary energy supplied to the system. The integrated cost of the total load, i.e cost of conventional fuel without solar, at time t, is:

$$C_{LOAD} = \int_0^t C_{FL}\, Q_{load}\, dt \qquad (1.6)$$

where C_{FL} is the conventional energy cost rate and Q_{load} the system energy requirements.

In the present study, mode 2 is used. In this mode, the annual costs for both solar and non–solar systems to meet an energy demand can be expressed as:

$$Yearly\ cost = C_1 + C_2 + C_3 + C_4 + C_5 - C_6 \qquad (1.7)$$

where,

C_1 is the mortgage payment and includes interest and principal payment on funds borrowed to install the system;

C_2 is the fuel cost;

C_3 is the cost for maintenance and insurance;

C_4 represents the parasitic energy costs (running costs for pumps, fans, etc)

C_5 represents property taxes;

C_6 represents income tax savings, if applicable.

The difference between the cost of a conventional system and a solar system is the

solar savings, and they are expressed as:

$$Solar\ savings = S_1 + S_2 - S_3 - S_4 - S_5 - S_6 \qquad (1.8)$$

where,

S_1 represents fuel savings;

S_2 represents income tax savings, if applicable;

S_3 is the incremental mortgage payment, i.e the additional mortgage incurred by solar system;

S_4 is the incremental cost of maintenance and insurance;

S_5 is the incremental parasitic energy cost;

S_6 represents the incremental property tax, if applicable.

All of these costs and savings can be assumed to inflate at a fixed percentage each year. If a cost D is to be incurred at the end of the first year, at an inflation rate of i, the cost at the end of year N is:

$$D_N = D\ (\ 1\ +\ i\ )^N \qquad (1.9)$$

The discounted cost (present worth) at the end of year N, at a discount rate of d, is:

$$PW_N = \frac{D\ (1\ +\ i\ )^{N-1}}{(1\ +\ d\ )^N} \qquad (1.10)$$

These equations can be used to calculate the present worth of any cost in a series of inflating costs. A more detailed account of solar energy economics is given by Duffie and Beckman (1980).

Several studies (Anderson 1979, Freeman *et al.* 1979, Buckles and Klein 1980, Fanney and Klein 1983, 1987, Morrison and Braun 1985), have found that TRNSYS is capable of predicting the performance of solar heating systems within a good accuracy. Buckles and Klein (1980), compared the simulation results obtained from TRNSYS with experimental results , for several generic types of solar domestic water heating systems and they found an agreement which was within 5 per cent. According to Kreider and Kreith (1981), it has been shown, by analyzing the results of many validation studies, that the TRNSYS programme provides an accurate simulation program for the analysis of selected solar heating and cooling systems. The mean error between the simulation results and measured results on actual operating systems is under 10% for all state variables considered. These state variables include storage

temperature, collector inlet and outlet temperatures, collector mass flow rate, enclosure temperature, solar radiation on the tilted collector surface, and inlet and outlet temperatures of various types of heat exchangers.

Morrison *et al.* (1992) used TRNSYS to conduct a series of experiments at the European Community Joint Research Centre, Ispra, on a typical Greek solar water heater having a horizontal storage tank, and they reported a good agreement between the measured and the simulated results.

Thornton (1993) reports that the Solar Rating and Certification Corporation (SRCC) in the United States has created a new standard for rating and certification of solar domestic hot water (SDHW) systems and has chosen TRNSYS for the rating system. According to SRCC, the reasons for choosing TRNSYS for the rating system were seven–fold:

- models SDHW systems with first–principles approach;
- flexibility in modelling the existing variety of SDHW configurations;
- provides for simplified method of component substitution as opposed to expensive system test;
- enhances confidence in the validity of the results ;
- allows for literal input of component test results;
- provides a versatile framework for interfacing a model with system test data;
- provides ratings in a wide variety of climates and for locale–specific draw patterns.

1.3 Organisation of the thesis

The thesis is divided into eight chapters. Chapter one is an introduction to this work and has been written to present the problem and outline the objectives of the thesis. It also presents the concept of modelling and simulation of solar systems and highlights the benefits of employing this technique in solar heating systems. A part of this chapter is devoted to TRNSYS simulation programme which is the basic tool used in the simulations of the present work.

Since the study is confined to the climatic conditions of Cyprus, it was considered useful to devote chapter two to analyze the energy situation in the island and the exploitation of solar energy, with particular emphasis to water and space heating applications.

Chapter three is an overview of research and development in solar heating. It highlights the most important research activities in the field of solar water and space heating in the world.

Chapter four concerns the modelling and simulation of solar domestic hot water systems. It presents the models of thermosyphon and forced circulation solar water heating systems. The thermosyphon model is used to simulate the performance of a typical thermosyphon solar water heating (TSWH) system at different hot water consumption profiles. In the case of active solar domestic hot water (SDHW) systems performance simulations are run to investigate the optimum design criteria for that type of system for various applications and scenarios. An economic evaluation is included in both cases.

Chapter five is devoted to the development of a model for active solar space heating systems and the investigation of the optimum design criteria through computer simulation.

Chapter six deals with the formulation of a model for a combined solar hot water and space heating system and its performance simulation. The latter are carried out in order to investigate the optimum design criteria for the system.

Chapter seven concerns the modelling and simulation of solar assisted heat pump systems to provide service hot water and space heating. The performance of the system is compared to that of the conventional solar heating system.

Finally, in Chapter eight a summary of the work done is given along with the recommendations for future work.

CHAPTER 2

THE ENERGY PROFILE AND EXPLOITATION OF SOLAR ENERGY IN CYPRUS

2.1 Introduction

The purpose of this chapter is to present the energy profile of Cyprus with an overview of solar energy applications and their potential. Particular emphasis is given on water and space heating which is related to this work.

2.2 Geography and economy in brief

Cyprus is the third largest island in the Mediterranean and is situated at 33 degrees East of Greenwich and 35 degrees North of Equator. It has an area of 9,251 square kilometres and its population in 1990 was 706,900 inhabitants (Department of Statistics and Research, 1990). Its main sources of income are tourism, industry and agriculture.

The Cyprus economy is based on the free enterprise system. The private sector is the backbone of economic activity with the government's role being limited to safeguarding the system, indicative planning and the provision of public utilities.

In more recent years, the economy has been growing at an average rate of 6% (Planning Bureau, 1990). The Gross Domestic Product (GDP) approaches the two billion Cyprus pounds (approximately 4 billion US dollars) and the rate of inflation which reached a record of 13.5% in 1980 has declined steadily thereafter to a level below 5%. Near full-employment conditions prevail; the rate of unemployment in 1989 was 2.3% (Department of Statistics, 1989).

The *per capita* income in 1990 was US$ 9,600. In addition, during the period 1980–1989, the annual rate of growth of the Cyprus economy was constantly higher than the respective rates of growth of the EC member countries.

In the post–1974 period the economy has undergone major structural changes. The manufacturing and services sectors have become increasingly important as indicated by their contribution to GDP and their share in employment while the importance of agriculture is declining steadily.

International trade is of considerable importance to the economy of Cyprus. On the production side, the lack of raw materials, energy resources and heavy industry for the production of capital goods, necessitates the import of such inputs. On the demand side, because of the small size of the domestic market, exports are vital in supplementing aggregate demand for Cypriot agricultural, mineral and manufactured products. The main trading partners of Cyprus are the EC countries and the neighbouring Middle East countries.

The main characteristic of the balance of payments position is a wide deficit in the trade balance, which in the last few years, was more than offset by the increasing surplus on the invisible balance. Receipts from tourism, offshore business and other services have been the main factors for this development.

2.3 Climatic conditions

Cyprus has a Mediterranean climate characterised by hot dry summer and mild winter. Due to marine influences, the climate at the coastal areas is warmer in winter and cooler in summer. On elevated ground the temperatures are lowered by about 5 °C per 1000 m (Meteorological Service, 1975). The variation of air temperatures in Nicosia, representing the averages of the years 1941–1970, compiled from data taken from Meteorological Service (1985), is shown in fig. 2.1. The Cyprus climatic conditions are predominantly very sunny with an average daily solar radiation of about 5.4 kWh m^{-2} on a horizontal surface. According to the Meteorological Service (1985), this value is among the highest in the world and is mainly due to the long

daily sunshine duration, which is about 75% of the astronomical daylength, and consequently very favourable for solar energy applications.

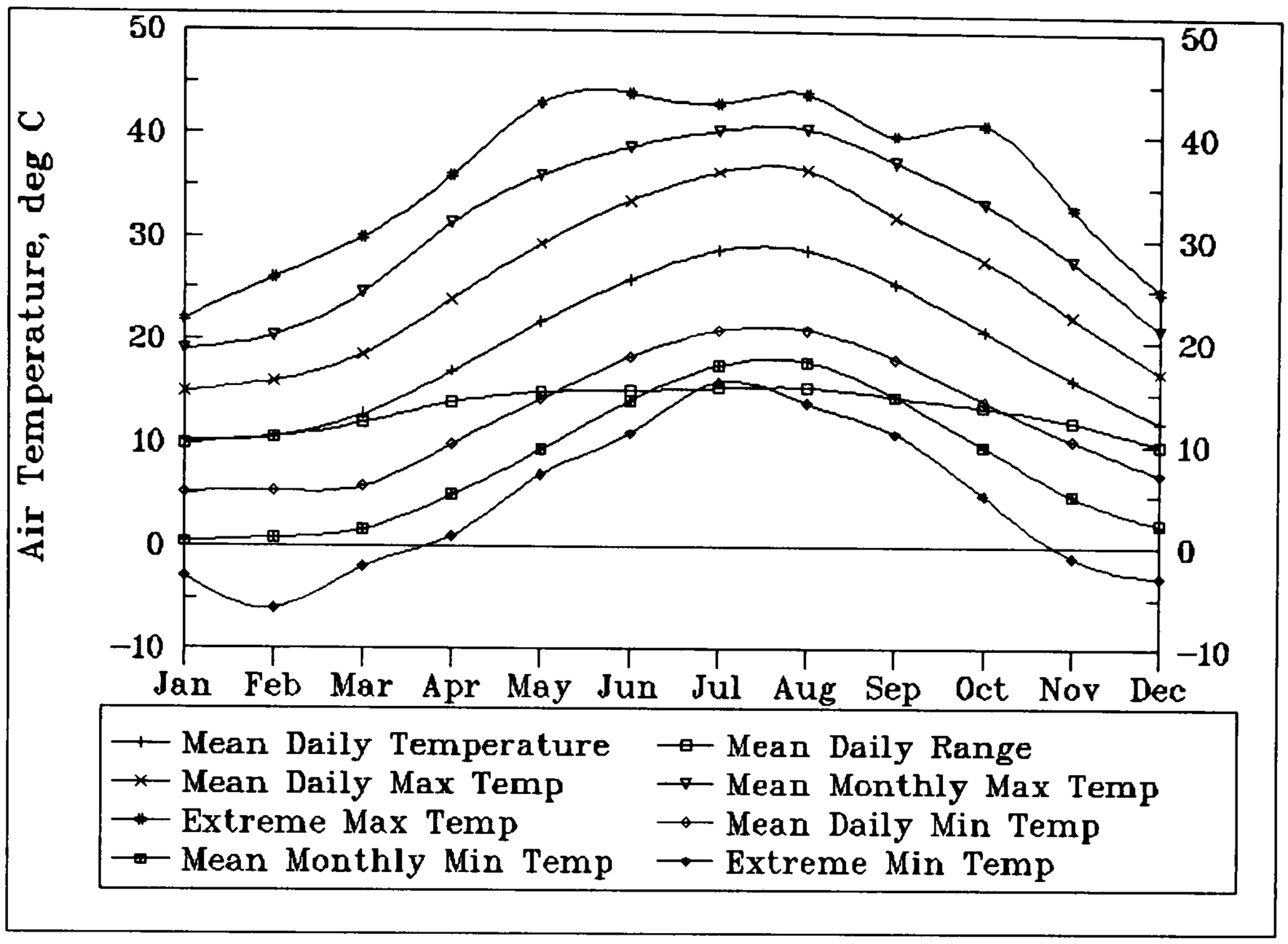

Fig. 2.1 Average air temperatures in Nicosia

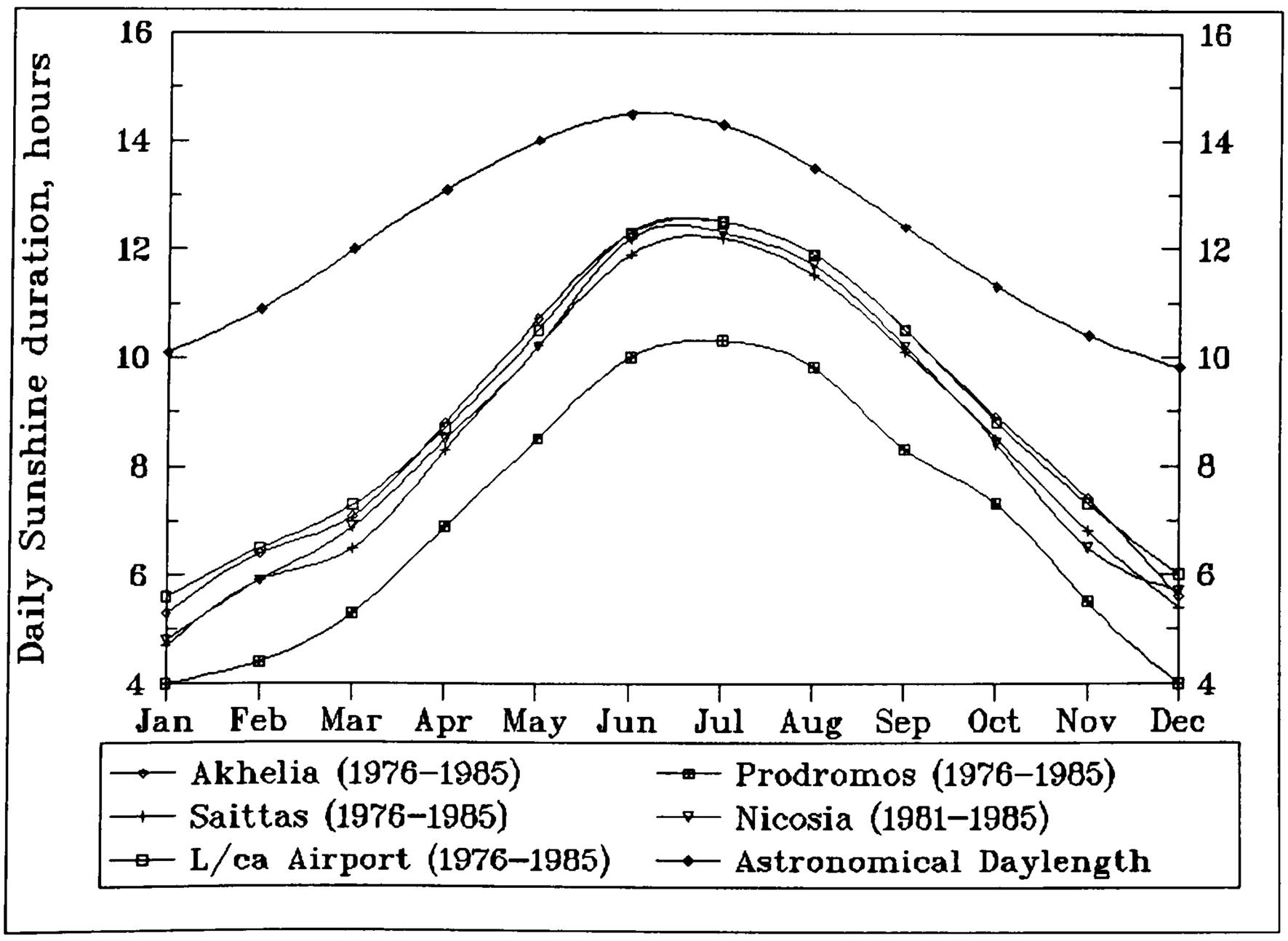

Fig. 2.2 Mean daily sunshine duration in Cyprus

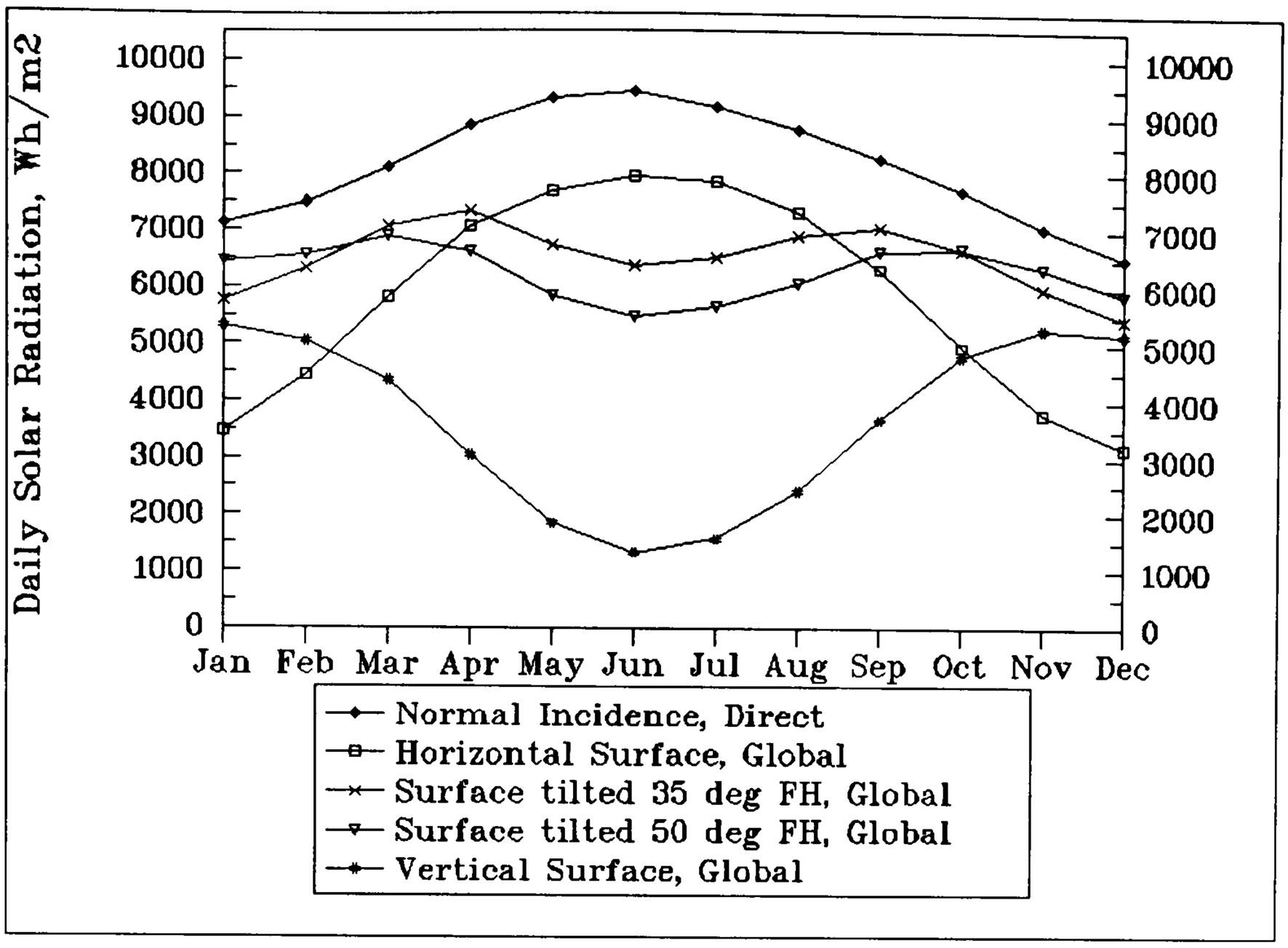

Fig. 2.3 Mean daily solar radiation in Cyprus

In the lowlands the daily sunshine duration varies from about 5.5 hours in winter to about 12 hours in summer. On the high mountains, the cloudiest winter months have an average of nearly 4 hours of bright sunshine per day and in July the figure reaches 12 hours. The mean daily sunshine duration for each month of the year, for various locations in Cyprus, is shown in fig. 2.2. Mean daily global solar radiation varies from about 2.3 kWh m^{-2} in December and January, the cloudiest months of the year, to about 7.2 kWh m^{-2} in July. The amount of global solar radiation received on a horizontal surface with average weather conditions is 1725 kWh m^{-2} per year (Hadjioannou, 1987). Of this amount, 69% reaches the surface as direct solar radiation (1188 kWh m^{-2}) and 31% as diffuse radiation (537 kWh m^{-2}). For the year as a whole, the amount of global solar radiation received by a surface inclined at 50° to the horizontal and facing south is 1817 kWh m^{-2} or 105% of that on a horizontal surface. However, the most important fact is that in the winter months, when the energy demand for heating is at its highest, this percentage is considerably higher. This is clearly shown in fig. 2.3, compiled from data taken from the Meteorological Service (1985) and Hadjioannou (1987).

2.4 The Energy scene

The annual energy consumption in Cyprus (government controlled area) for 1990 was about 1.62 million tons of oil equivalent (toe), including unbilled electricity in the area occupied by Turkish invasion forces. This corresponds to a per capita annual energy consumption of about 2.28 toe which is well above the world average of 1.59 toe/capita and below that of the European Community which according to Carvalho *et al.* (1991), is slightly more than double that for the world as a whole.

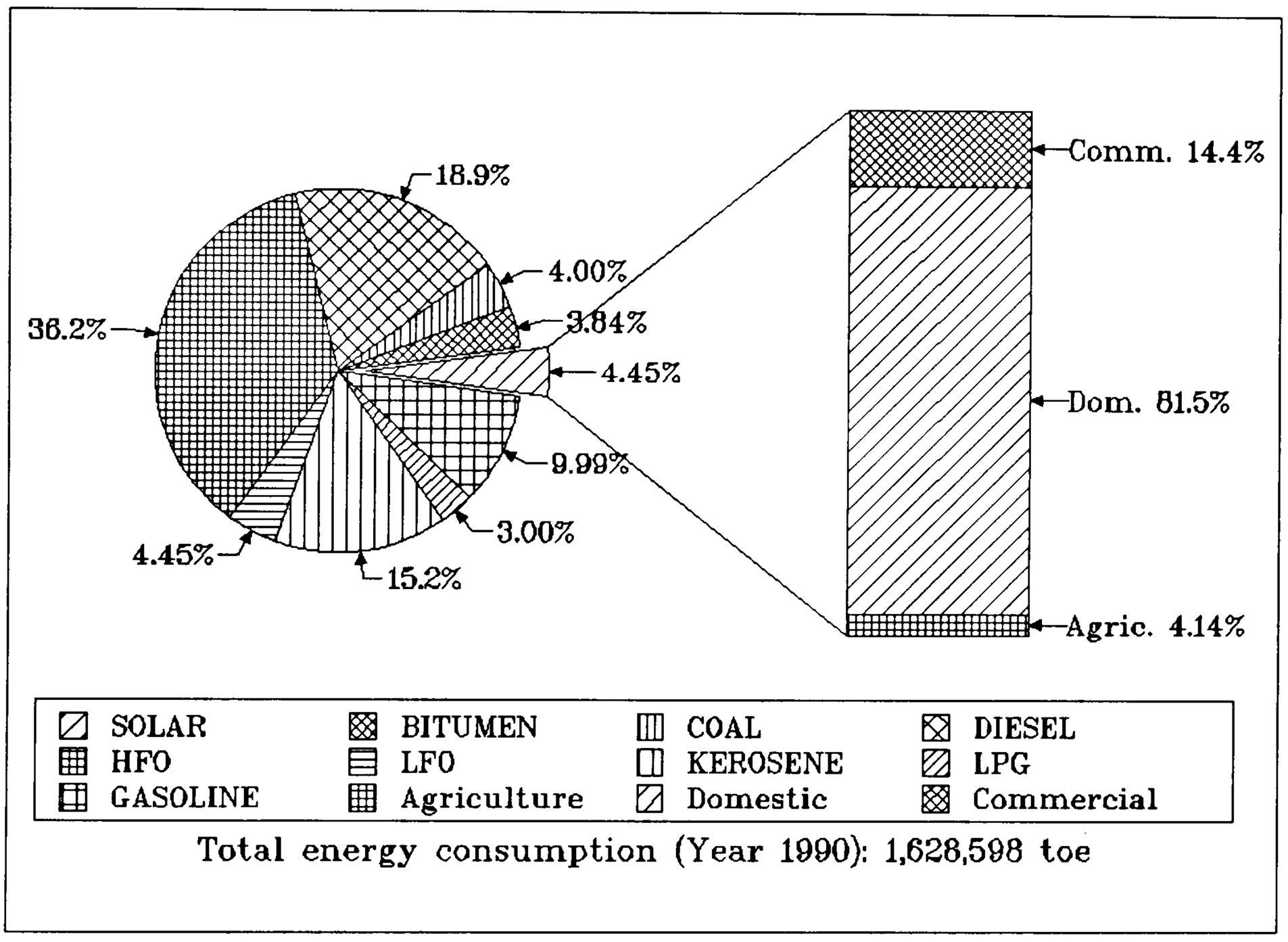

Fig. 2.4 Energy consumption in Cyprus

The forms of energy used in Cyprus and their percentage contribution to the final energy bill for 1990 are shown in fig. 2.4. A breakdown of the solar energy contribution is also shown in the same figure. The energy consumption by the various sectors of the Cyprus economy is illustrated in fig. 2.5, compiled from data taken from the Ministry of Commerce and Industry and the Department of Statistics and Research (1990). The commercial sector includes tourism (hotels and hotel apartments), public buildings, hospitals, offices, shops, supermarkets and restaurants.

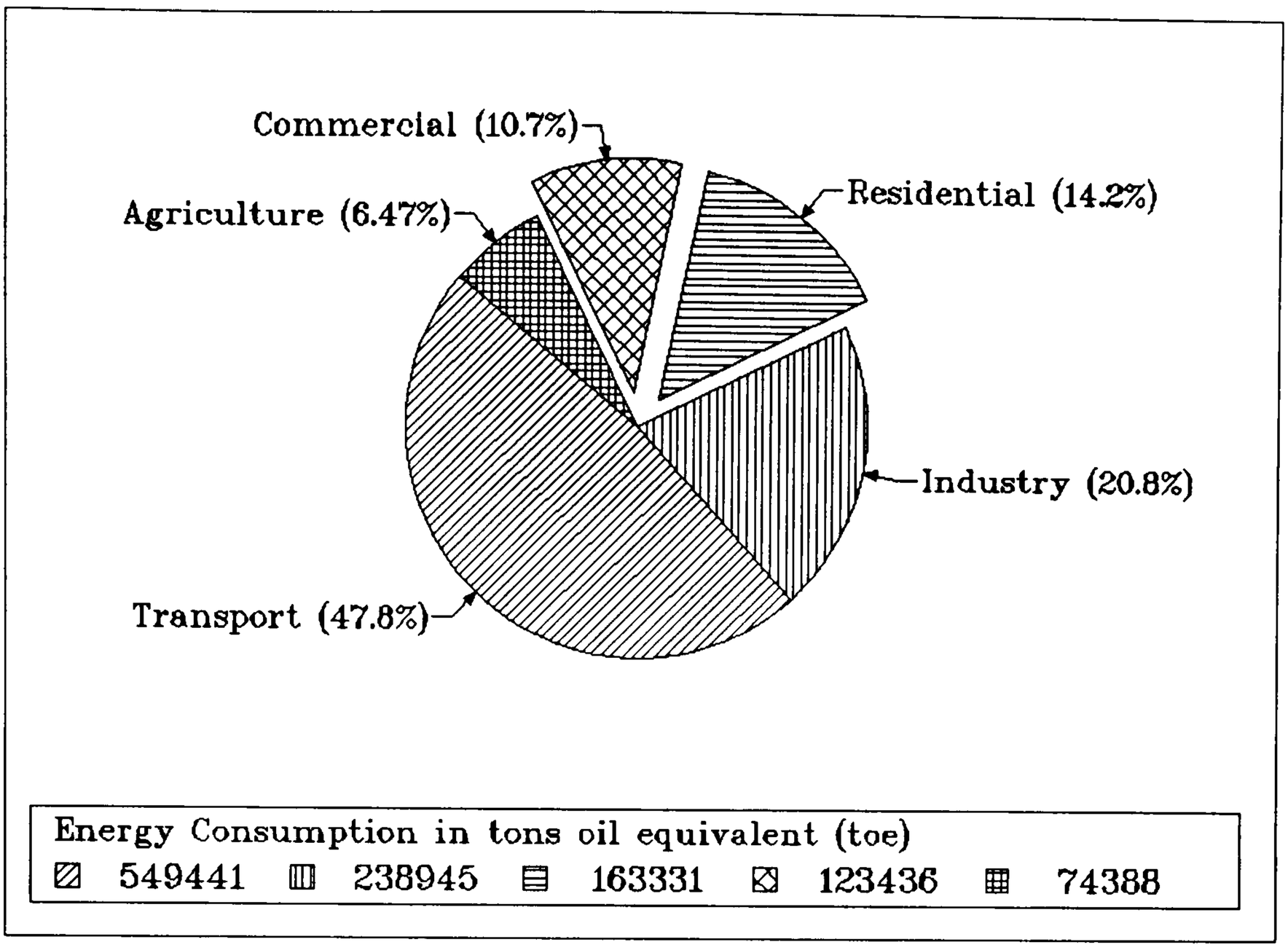

Fig. 2.5 Final energy consumption in Cyprus by sector

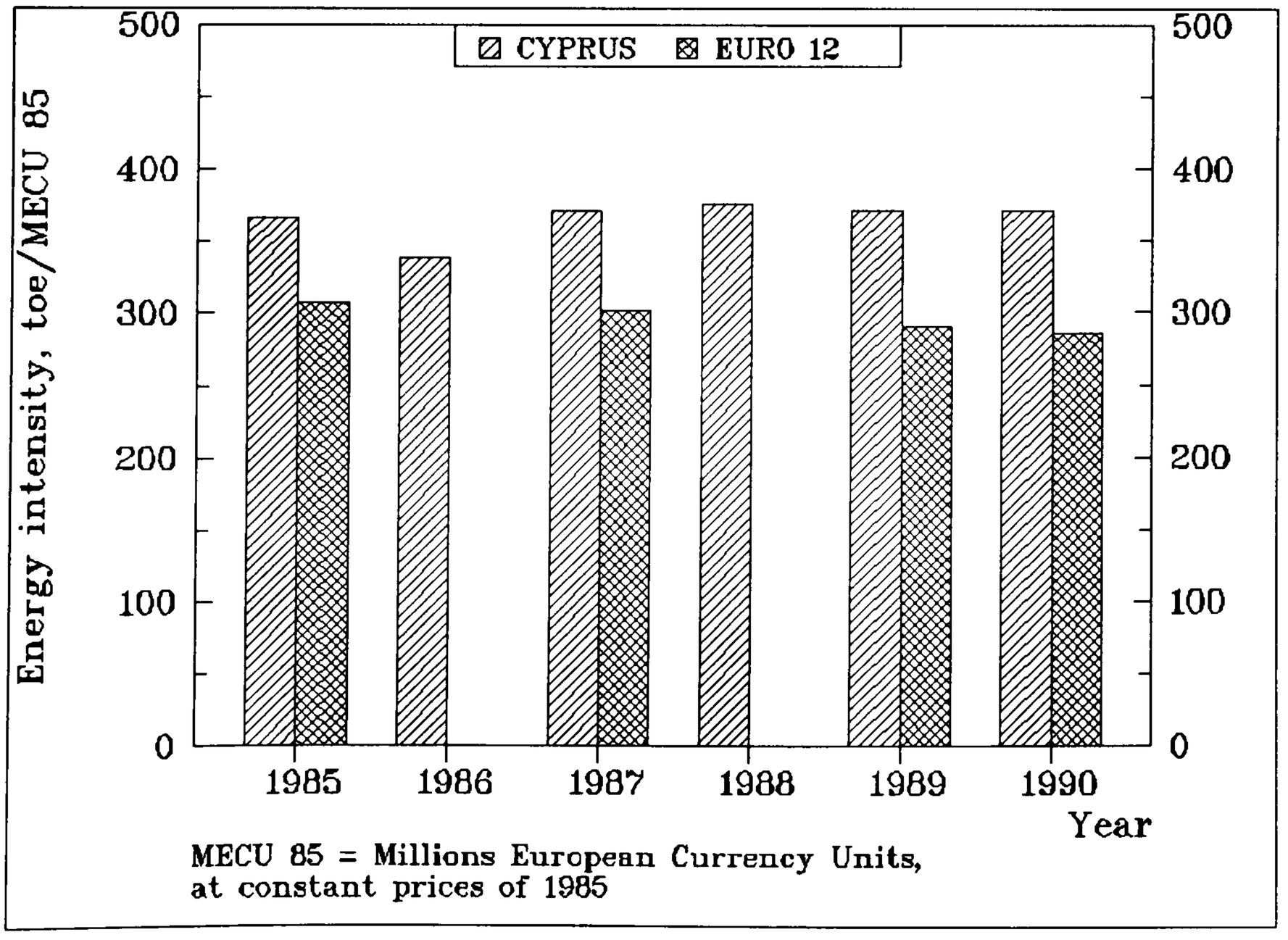

Fig. 2.6 Energy intensity in Cyprus

The amount of energy needed to produce a unit of Gross Domestic Product (GDP), i.e. the energy intensity, is shown in fig. 2.6. For comparison purposes, the energy intensity of the European Community is also superimposed. It can be seen from this figure that the energy intensity has remained at the same level during the period 1985–90 whereas in the case of the European Community a downward trend is shown of the order of 6.9% per year. According to Carvalho *et al.*, (1991), the world saw the fastest gains in energy intensity (1.3%), between 1980 and 1985. After 1985, intensity gains slowed down to 0.7% per year and this is mainly due to the combination of economic recovery and the oil price fall.

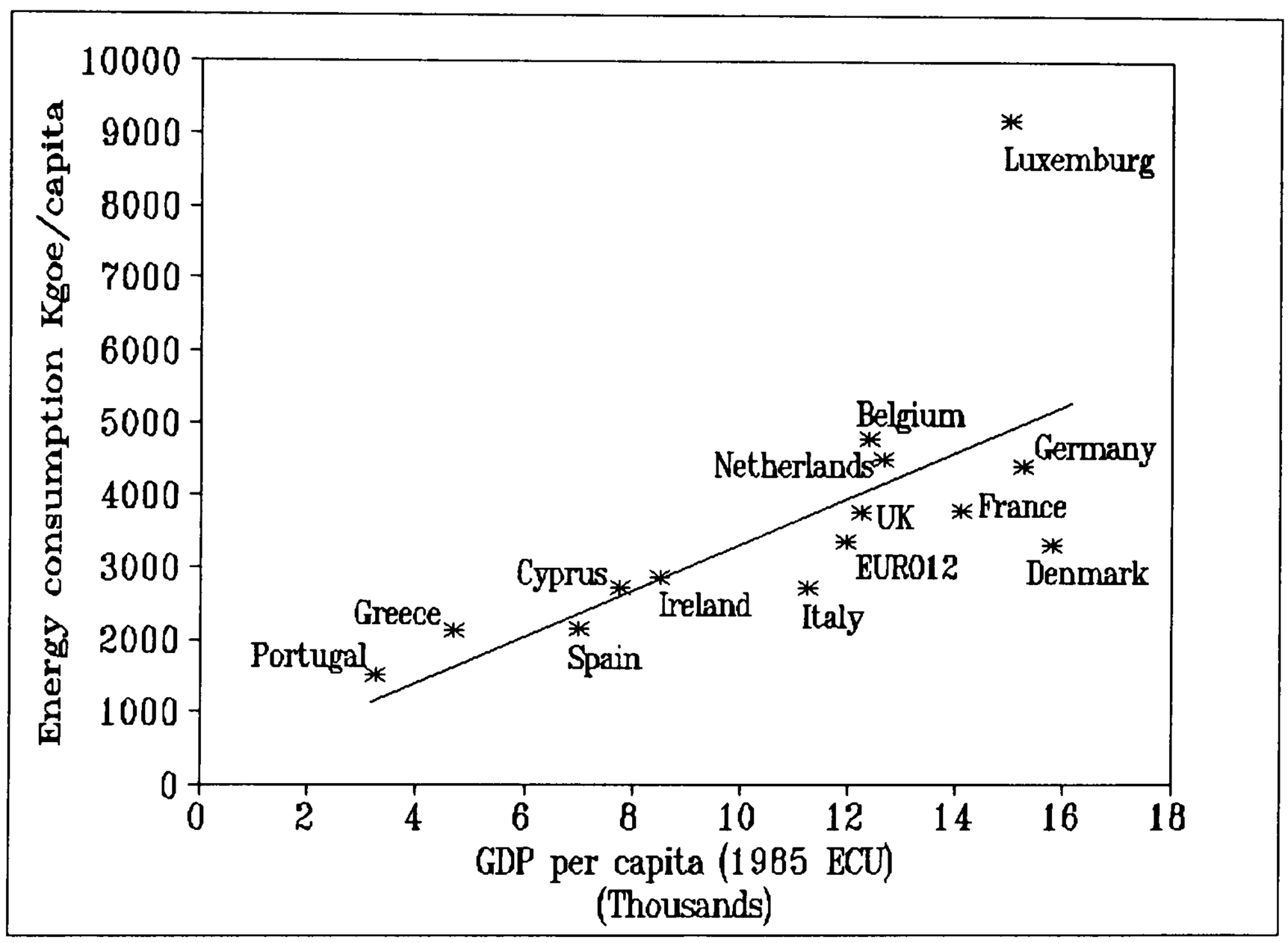

Fig. 2.7 Energy consumption per capita and GDP per capita in Cyprus and the European Community

Fig. 2.7, plotted from data obtained from Carvalho *et al.*, (1991), relates the energy consumption per capita with the GDP per capita, for Cyprus and the European Community. This is in fact a relationship between the economic activity and the energy consumption. Points above the straight line on the graph indicate a lower efficiency than the average whereas points below the line indicate a higher efficiency. Cyprus is nearly on the line, in about the same position with Ireland, Spain, Greece and Portugal. The above comparisons show that there is potential for energy

conservation and improvement of efficiency in Cyprus.

It appears from fig. 2.5 that the Residential and Commercial sectors together account for about 24.9% of Cyprus energy consumption. One common characteristic of these two sectors is the high consumption of heavy fuel oil (HFO), which is mainly used for the generation of electricity. In effect, this reflects the high consumption of electricity, mainly for air conditioning in hotels and hotel apartments. This is demonstrated by fig. 2.8, which shows the breakdown of energy consumption in a typical 4–star hotel, based on a survey conducted by Aristodemou *et al.* (1988).

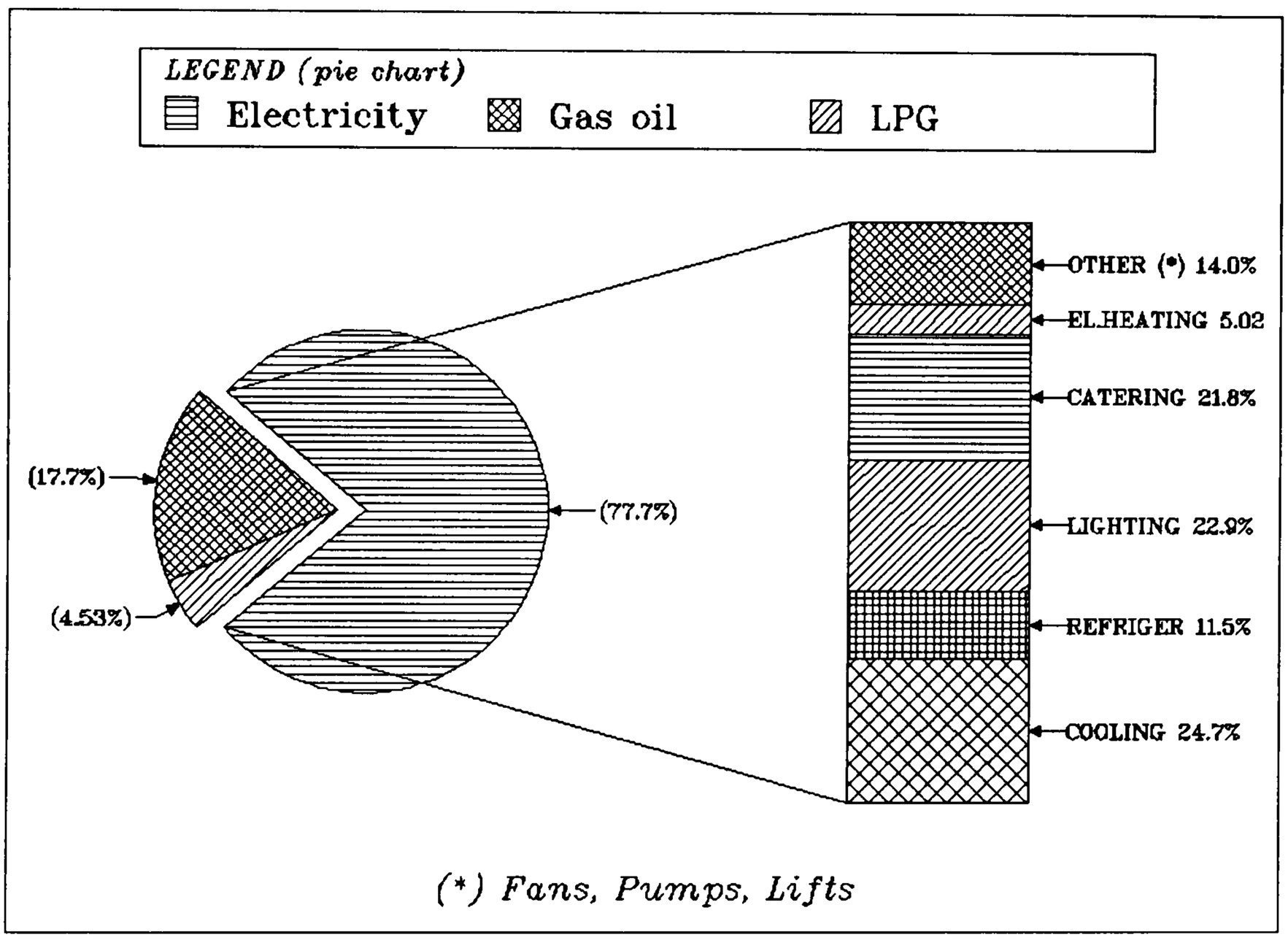

Fig. 2.8 Breakdown of energy consumption in a hotel

The contribution of domestic resources to meeting the energy needs of the country is estimated to about 5%, mainly from solar energy (water heating) and wood (cooking, heating). The rest, i.e. 95% of the total energy demand, is met by imported oil and coal. Cyprus imports more than half a million tons of crude oil, which is processed in the national refinery, and equal amounts of oil products. In addition, coal is imported and used exclusively for the needs of the two cement factories of the island. Fig. 2.9 shows the annual imports of crude petroleum and its cost for the years 1975 – 1990, based on information provided by the Department

of Statistics and Research (1990).

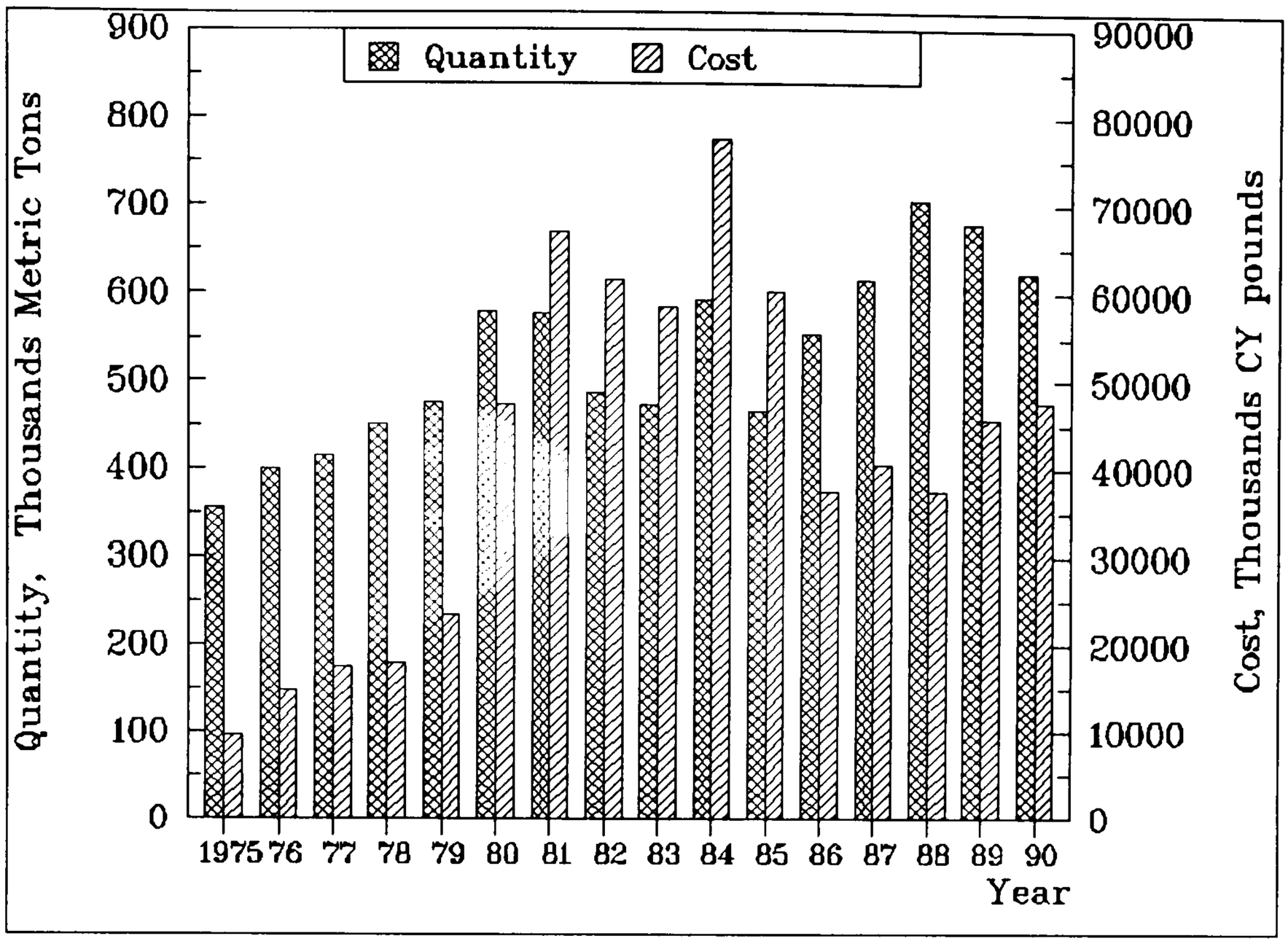

Fig. 2.9 Imports and cost of crude petroleum products in Cyprus

The almost full reliance of the island on imported oil in meeting its energy demand, together with the abundance of solar radiation and a good technological base, created favourable conditions for the exploitation and development of renewable energy sources.

The first application that has been historically developed in Cyprus, regarding renewable energies, is the use of windmills for irrigation purposes. In the early 1930's, hundreds of windmills were set up in the south–east coastal areas to irrigate small plots of vegetables (tomato, cucumber and potatoes). This application grew quickly but declined in the 1960's, when diesel pumps proliferated due to the very low oil prices. The 1973, oil crisis renewed interest in windmill technology, but the economic analysis, based on payback time, is still not in favour of windmills.

A second mass–extended utilisation of a renewable source of energy appeared in the early sixties; as solar water heaters were developed on a large scale in Israel, Cypriot manufacturers based their designs on Israeli products and quickly created a major

national industry, which is now one of the largest solar energy industries in the world, in terms of the number of annual square meters of solar collectors manufactured. Cyprus produces more than 33,000 m^2 of collectors per year and about 4% of the national energy demand is met by solar energy (Michaelides, 1992).

2.5 Solar water heating

The forms of energy used for domestic water heating are solar, electricity, gas, oil and wood. According to the 1982 Census of Housing, conducted by the Department of Statistics and Research (1982), 69.1% of households used solar energy for water heating, 19.9% electricity, 7.1% wood, 2.1% gas and 1.5% gas oil. In almost all cases where solar energy is used for water heating, electricity is used as an auxiliary source. There is, however, an increased interest in employing solar heating in new dwellings. According to Construction and Housing Statistics (1990), 93.3% of new dwellings built in 1990 have been equipped with solar water heating, as compared 87.3% 1987 and 84.4% in 1983. Fig. 2.10 indicates clearly the contribution of solar energy in water heating.

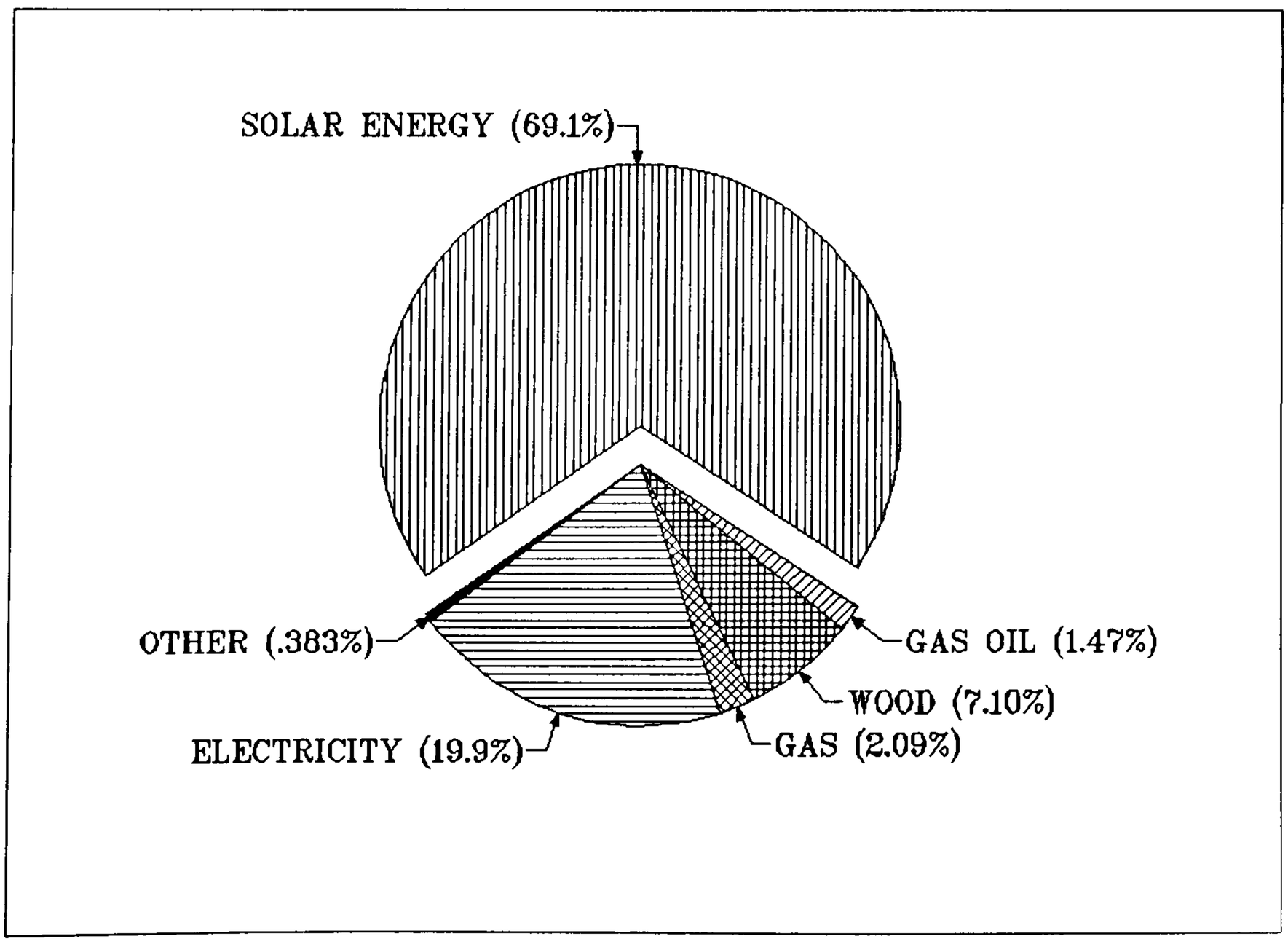

Fig. 2.10 Water heating in Cyprus

Cyprus began to manufacture Solar Water Heaters (SWH) in the early sixties. Cypriot industry of solar water heaters quickly expanded to reach 30,000 m^2 of collectors produced in 1983, by more than 20 manufacturers. Today, Cyprus produces more than 33,000 m^2 of flat-plate solar collectors per year. Figure 2.11, compiled from data taken from the Department of Statistics and Research (1990), shows the evolution of the production of solar water heaters in Cyprus for the years 1978-1989 as compared to electric water heaters.

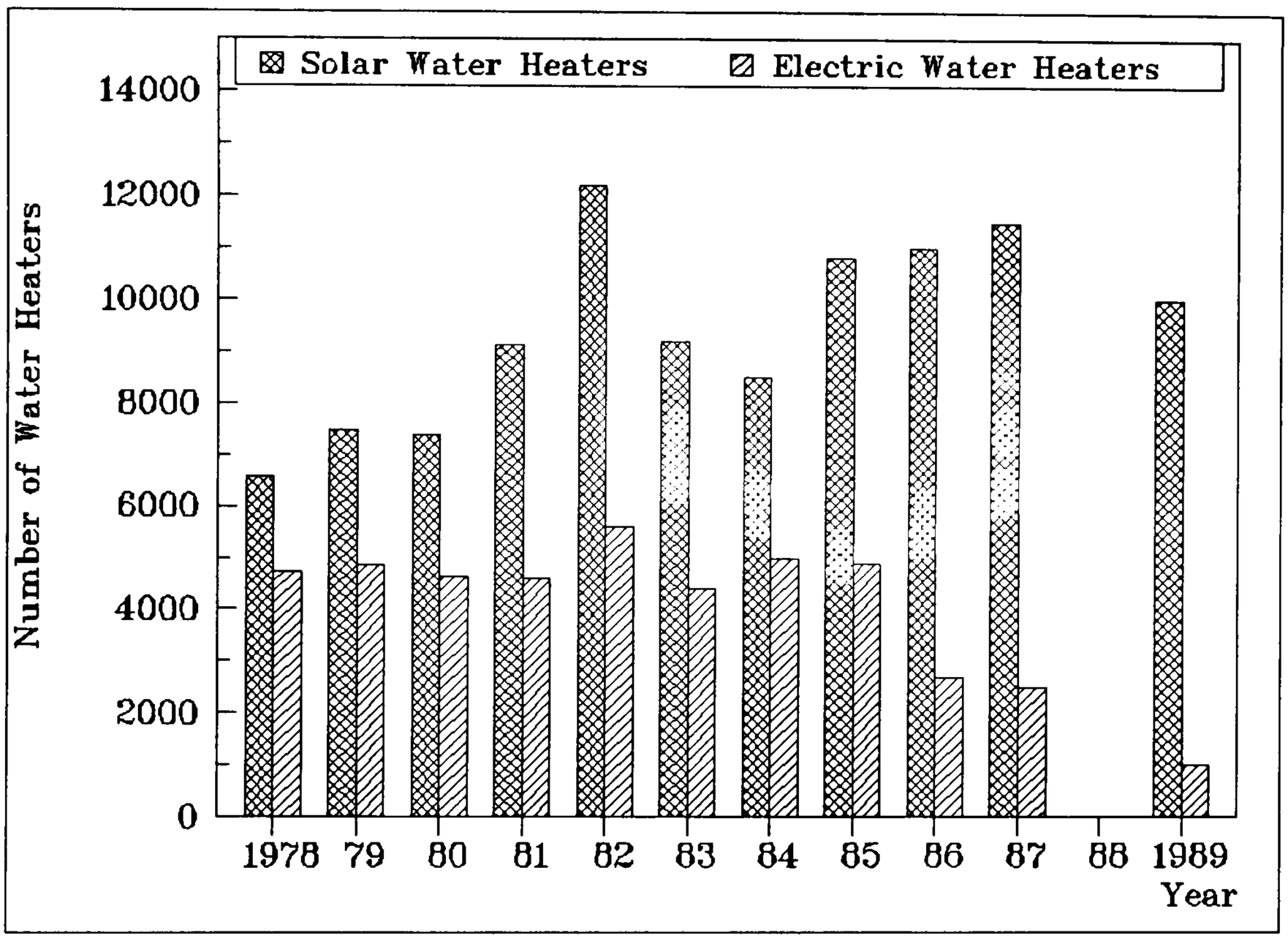

Fig. 2.11 Production of water heaters in Cyprus

A typical solar water heater in Cyprus consists of two flat-plate solar collectors having an absorber area of 3 m^2, a storage tank of 180 litres equipped with an auxiliary electric heater of 3 kW, and a cold water tank on top. The schematic of such a unit is illustrated in fig 2.12.

An important market potential exists for the development of solar water heaters in the residential and commercial sectors. There is much to be done in the tourism sector (hotels and hotel apartments and offices) and in collectively owned buildings (blocks of flats). It can be assumed that the number of collectively owned buildings using solar water heating, currently at around 15%, would gradually increase up to 40%

due to the development of new techniques for using solar energy in collective systems and to the application of computer based solutions that control the individual expenses of the tenants.

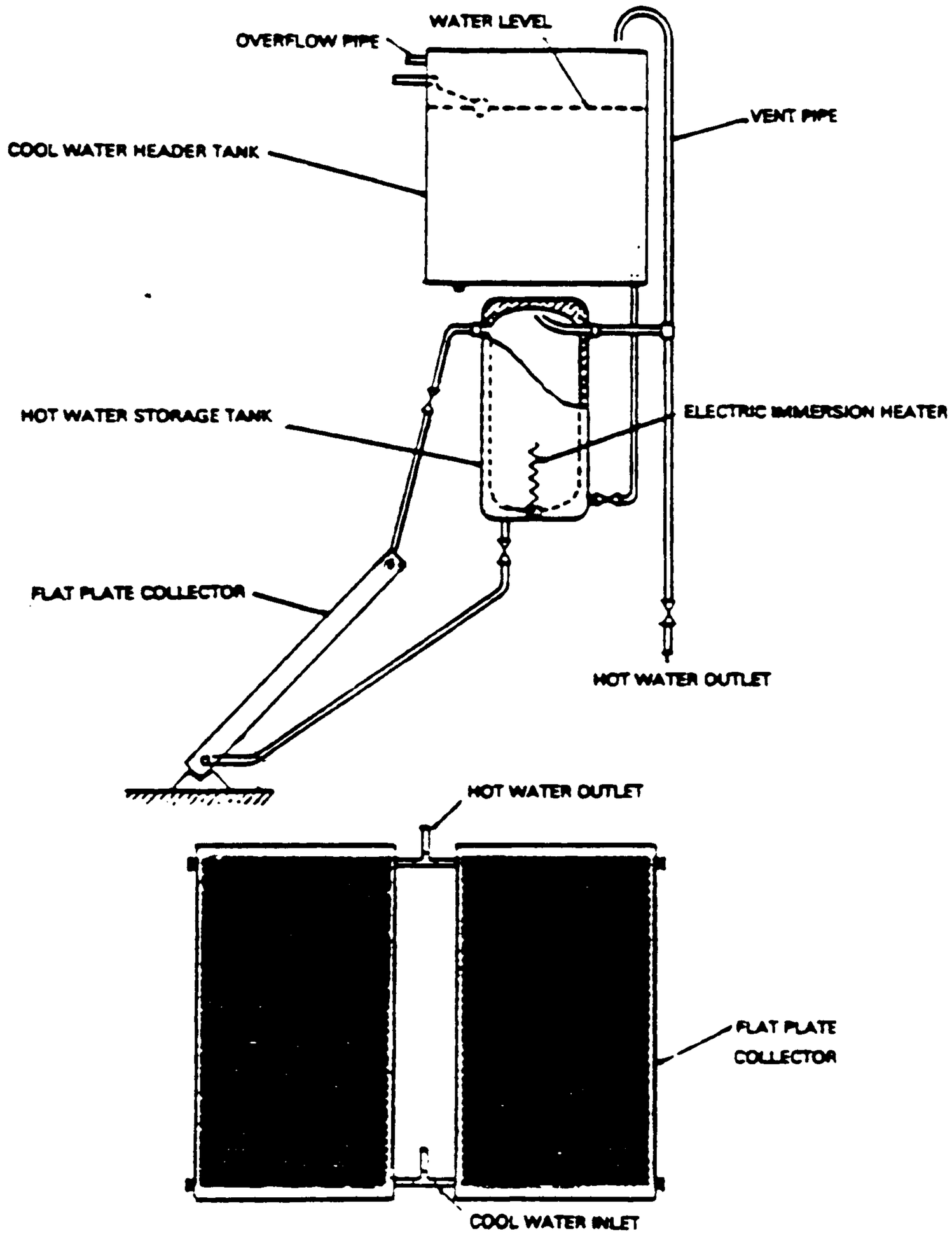

Fig. 2.12 Schematic diagram of a typical solar water heater in Cyprus. From CYS (1984)

2.5.1 Contribution of solar water heating to the national energy balance

It is estimated that the number of Solar Water Heaters (SWH) installed in Cyprus exceeded 130,000 units. This means one solar water heater per five people in the island. The estimated collector area installed in Cyprus, including central systems in hotels and hotel apartments, is about 400,000 m^2 out of which 360,000 m^2 are in

houses, 25,000 m^2 in flats and the rest in hotels and hospitals or clinics.

According to a study conducted by Michaelides *et al.* (1991), the estimated annual energy contribution of a typical SWH is about 1.05 MWh. It is also estimated that the savings in electricity as a result of using SWHs for water heating is of the order of 123 GWh of electricity, which represents about 9% of the national electricity consumption.

Different case studies have been carried out to investigate the cost effectiveness of solar water heating in the various sectors: individual houses, flats, hotels, hotel apartments and industry (Sema–Metra *et al.*, 1984; Michaelides *et al.*, 1992). The cost effectiveness of SWH's depends primarily on the "competing" source of energy. It has been concluded that:

(a) They are very competitive compared to the electric heating systems. Payback periods as low as 3 years have been observed for individual houses and 5 years for apartment buildings and hotel apartments.

(b) As long as the "competitor" is an oil–fired boiler system the payback period ranges from 7 to 15 years.

2.5.2 Standardization of solar water heaters

The Cyprus Organisation for Standards and Control of Quality (CYS) has formulated two standard specifications for solar water heating systems and flat plate solar collectors. These were adopted by nearly all major manufacturers to specify the required design characteristics and the manufacturing tolerances for their products. They were also used to provide the standard testing method for the evaluation of the thermal performance of flat plate solar collectors.

The first standard is the CYS 119:1980 Method of testing the performance of flat–plate solar collectors (CYS, 1980). For this purpose, a testing facility has been set up for the outdoor testing of flat–plate solar collectors, similar to that adopted by the Commonwealth Scientific and Industrial Research Organisation standard (Pott and Cooper, 1976). This facility is controlled by the Energy Service of the Ministry of

Commerce and Industry which issues test certificates and collector performance characteristics. These certificates are not quality marks but they serve the role of a document demonstrating that the collector's performance complies with the requirements of the standard.

The second standard is the CYS 100:1984 Standard Specification for Solar Water Heaters (CYS, 1984). It deals with solar water heaters intended for domestic use and specifies the requirements for the materials, construction, marking and performance of solar water heaters using water as the heat transfer medium.

Today, the standardisation work of the CYS continues at a more rapid pace aiming at harmonizing the initial standards with the European requirements and directives in the field of solar energy. For this purpose the Technical Committee of CYS for solar water heaters, whose chair is held by the author, is currently preparing the issue of a series of new standards to cover the durability tests and the short– and long–term test methods for solar water heating systems. The work of the European research programme on solar energy has allowed the development of a specialist group of European solar energy experts. The group's recommendations on collector perform–ance testing and test methods of solar domestic hot water systems are being used as basis to assist the preparation of the Cyprus standards. In order to provide the test facility which is required by the new standards, the CYS and the Ministry of Commerce and Industry have set up a modern and fully equipped testing centre. The experimental test ring employs an automatic data acquisition and control facility for outdoor testing, monitoring and analyzing the performance of both solar collectors and complete solar heating systems supplied by the manufacturers.

2.6 Solar space heating

The climatic conditions in winter are such that space heating is needed for a period of 4 to 5 months and the average number of degree–days (base 18 °C) for winter is estimated to be 950 degree–days.

For space heating, liquified petroleum gas (LPG) and kerosene are the most widely

used forms of energy, followed by oil and electricity. According to a Census of Housing conducted by the Department of Statistics and Research (1982), 70.7% of the households used LPG and kerosene stoves for heating, 3.3% oil–fired central heating systems, 3% electric stoves, 0.8% electric storage heaters and 22.2% either other methods of heating (fireplaces burning wood) or no heating at all. Fig. 1.13, compiled from data taken from the Department of Statistics and Research (1982), shows the various methods of space heating in Cyprus and their percentage contribution. It must be noted here that in the great majority of the dwellings using local heaters such as gas, kerosene and electric stoves, only one or a few rooms in a dwelling are heated. This is the reason why it is rather difficult to estimate accurately the share of heating in the country's energy consumption.

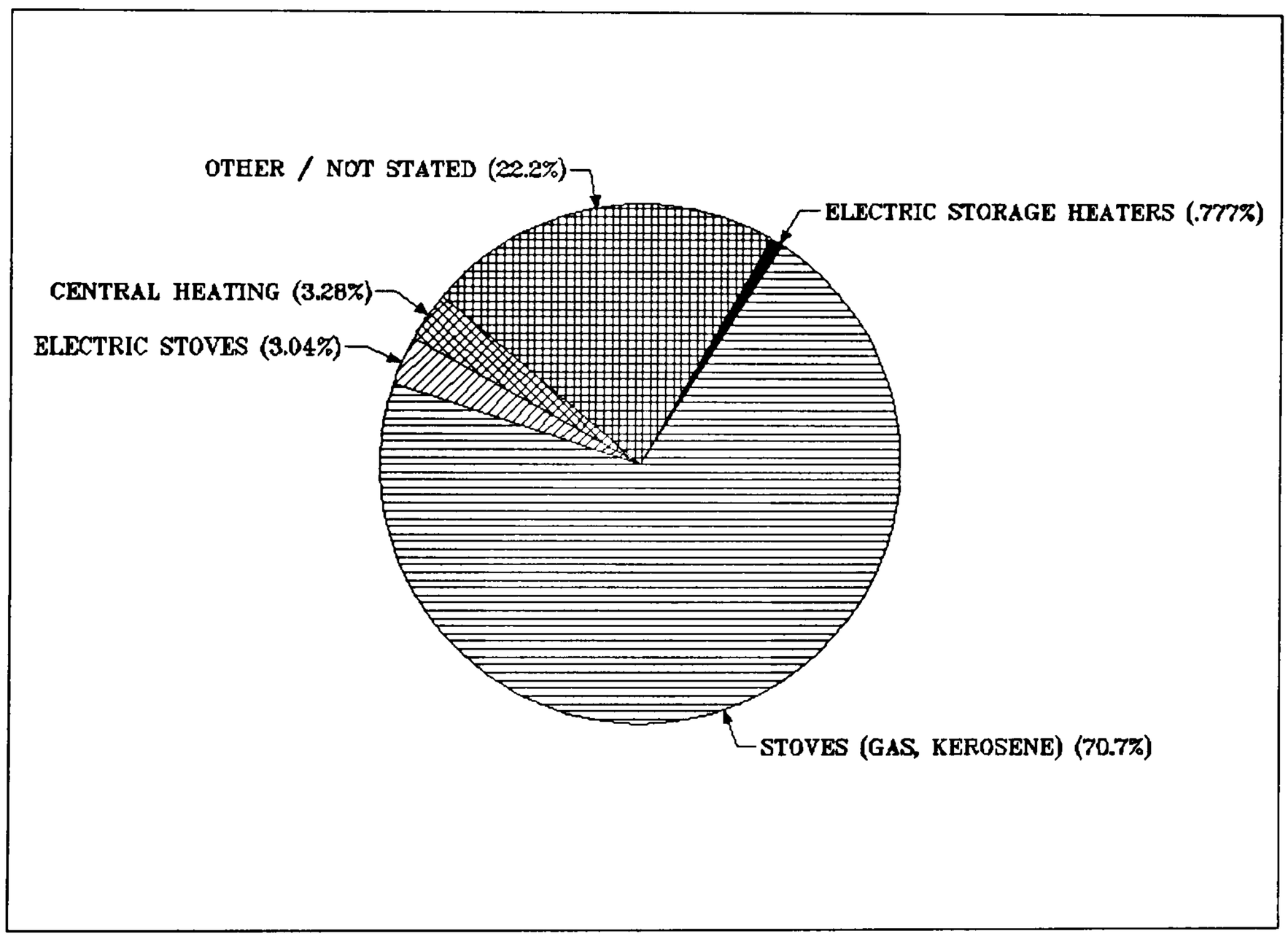

Fig. 2.13 Space heating in Cyprus

The current trend shows an increase in the application of central heating systems as a result of improved standards of comfort and living. According to the Department of Statistics and Research (1990), 40.4% of the new dwellings built in 1990 have been equipped with oil–fired central heating systems, as compared to 15.5% in 1987 and 9.5% in 1983.

For the commercial sector, there are no statistics. However, the majority of hotels employ oil–fired central heating systems with only a few users of electricity. The situation is the same for hospitals and clinics.

Solar energy has not been put into use for the heating of buildings except from very few cases where solar active systems have been combined with oil–fired central heating systems and floor heating in residential dwellings. However, performance data for these installations is not available and therefore no comprehensive conclusions as to their energy and economic performance can be drawn.

Based on the results obtained from an experimental installation which was monitored at the Higher Technical Institute (Michaelides, 1985), it can be concluded that the use of solar energy for space heating does not appear to be an attractive proposition under the conditions prevailing in Cyprus, due mainly to the following reasons:

(a) very high investment cost;
(b) high complexity of installation in existing buildings;
(c) short annual duration of optimal use leading to high depreciation costs and long payback periods;
(d) poor thermal insulation of buildings.

However, there is a need for research and development work in order to investigate the cost effectiveness of such systems. This can be achieved through modelling and simulation of solar systems. This will enable the thorough investigation of the capabilities and the performance characteristics of solar assisted heating systems at the design stage. Consequently, it will be possible to conduct parametric studies to determine the optimum system size for a particular application and to develop the necessary control strategies for optimum operation.

2.7 Other prospective solar energy applications

2.7.1 Solar heating of greenhouses

Greenhouses are mainly used for off–season production of vegetables and heating is

usually required in the night during the winter months. Investigations into the application of solar energy for greenhouse heating began in the late 70's and were expanded and intensified in 1981. Research work has been conducted by the Agricultural Research Institute (ARI) and included solar air and water collectors, water and rockbed storage systems, simple low grade heating systems for greenhouses, passive solar systems of water–filled plastic tubes and a pond collector. An effort was made to use only locally produced materials and make simple designs so that the farmers would be able to construct major parts or all the system themselves. The performance of the systems was monitored at the ARI by a micro–processor supported data–logger and was evaluated for at least one complete season. Some of the systems have been transferred to commercial farms in the major agricultural regions of the country and are tested under real operating conditions.

2.7.2 Solar cooling

The climatic conditions of Cyprus are such that summer air conditioning is necessary and a must in hot and humid areas and in some categories of buildings like hotels, hotel apartments, public spaces, luxury houses etc. At present, cooling is produced by electrically operated vapour compression refrigeration systems.

In the residential sector, only a very small number of houses are air conditioned. According to the Department of Statistics and research (1982), only 2.5% of the residential houses were air conditioned in 1982. 2.1% of the houses were equipped with individual room air conditioners and 0.4% had central systems.

In the commercial sector however, the situation is different. In the tourism industry, for instance, the great majority of hotels, mainly those classified as 3–, 4– and 5–stars, are equipped with central air conditioning systems. Of the other categories of hotels most of them use individual room air conditioners.

The trend is to install central air conditioning systems in almost all new large complexes of offices, hospitals and public buildings. It is estimated that in the commercial sector, cooling shares around 35% of the energy consumption and this

is in fact the main reason for the high electricity consumption which is observed.

Despite the fact that there are commercially available solar powered cooling systems, no application has so far been reported in the island. This is attributed to the high capital cost which yields very long payback periods and also to the lack of performance data of such systems operating under Cyprus climatic conditions.

There is therefore scope for research and development in this area in order to investigate the technical and economic feasibility of such applications as discussed earlier in the case of solar space heating.

2.7.3 Solar ponds

Solar ponds are natural or artificial lakes filled with brine, which are able to store heat in bottom layers , owing to the density gradient between bottom and surface. Stored heat can be consequently used for running a turbine and producing electricity.

Cyprus may have a good potential for the implementation of solar ponds, but the technical feasibility still has to be evaluated. There are two sites which might meet the technical requirements for a solar pond, the Salt lake of Limassol–Akrotiri (14 km^2) and the Salt lake of Larnaca (5 km^2). According to estimates made by Sema–Metra *et al.* (1985), the theoretical potential of these two lakes is 40–50 MW. Assuming that the system could work for 4000 to 5000 hours per year, the electricity production could be of the order of 200 GWh per year. However, a technical feasibility study should be made before any large scale application.

2.7.4 Photovoltaics

An alternative option of solar energy application would appear to be photovoltaic solar energy conversion. Only few applications exist in the island and these are of remote category. The drawback for this elegant source is the high capital cost but a breakthrough is possible which may result in drastic cost reductions.

CHAPTER 3

AN OVERVIEW OF SOLAR HEATING (LITERATURE SURVEY)

3.1 Introduction

The purpose of this chapter is to provide an overview of the developments in the field of solar water and space heating for buildings. This will include a brief description of the types of solar heating systems that are available and in current use, and their basic functions and key components will be presented. The above will be followed by a review of research work carried out in the field of solar water and space heating which seem to be relevant to the present work.

3.2 Historical perspective

It appears from the literature survey that the ancient Greeks were utilising solar energy for heating their houses. The classical Greek historian Xenophon, in his Memorabilia (see Kordatos and Varnalis, 1957), records some teachings of the Greek philosopher Socrates (470–399 B.C) regarding dwellings orientation:

> *"....Therefore, in houses facing south the sun's rays in winter penetrate into the porticoes, while in summer the sun path being right over our heads and above the roofs provides shade. Thus, this being correct, we should build the south side loftier in order to get the solar heat in winter, and the north side lower in order to keep out the cold winds in winter."*

The above teaching of Socrates constitutes today the basis of solar passive heating of buildings.

According to Hottel (1989), Godfrey L. Cabot marked the beginning of research in solar heating in 1938, by a donation to the Massachusetts Institute of Technology for

solar energy studies. As a result of this, the first solar heated house, a 16 x 31 foot one–storey combination office and solar laboratory, was built in 1939 in the United States and it is known as the MIT Solar House I. The solar system comprised 34 m^2 of triple–glazed collector located on the south–facing roof of the house which was built over an insulated storage tank having a capacity of 62 m^3 of water for interseasonal storage.

Experiments with Solar House I led to the conclusion that solar heating of houses was entirely feasible and the performance calculable, but such heating systems are too expensive. The MIT program resulted in development of methods of calculating collector performance which, according to Duffie and Beckman (1980), with some modification, are standard methods in use today. The MIT Solar House I was demolished in 1946 to make way for MIT Solar House II, which was built in 1947 in Massachusetts (see Szokolay, 1975). The house was a single storey laboratory, consisting of one room and eight cubicles of 1.2 m width each. The collection of solar energy was done by the south vertical wall which consisted of black–faced tanks, some containing water and some with eutectic salts for latent heat storage.

The above project was followed by Solar Houses III, IV and V with some improvements. According to Hottel (1989), the collector in Solar House IV was tilted to 60° southward to give optimum performance in winter, and water flowed through the collectors at a rate of approximately 40 kg/h per square metre of collector. The storage to collector ratio was around 95 l/m^2. The collector average efficiency was about 45% and the energy collected sufficed to supply 48% of the total house load for space heating and service hot water supply.

In Europe, according to Szokolay (1975), the first solar house appeared in France, in 1972, with the Chauvency–le–Chateau house and the Odeillo houses which employed rather passive solar heating. There is also the Milton Keynes house in Great Britain, constructed in 1974, which is basically an active solar heating system, employing flat plate solar collectors and water storage system, to satisfy partly the space heating and service hot water needs. In this project, the storage to collector ratio was 116 l/m^2 and the simulated performance of the system showed an average collector efficiency of 30% and an annual solar contribution of 59%.

A number of solar houses similar or slightly different from the above mentioned projects made their appearances in different locations in the world, mostly in the United States, Australia, Canada and France. Air is used as the collector fluid in some of them while the large majority have water systems and practically all the recent examples use water for collection and storage. Some form of auxiliary heat source is used in almost all cases, as it would be uneconomical to use a collector large enough to meet the heating and hot water load under severe weather conditions.

Having concluded to certain system configurations, researchers in solar heating concentrated their efforts on the development of design criteria for such systems, either through experimental investigations or through computer simulations. These criteria concerned mainly the collector area and the storage tank volume.

3.3 Solar space heating

3.3.1 Systems

The conversion of solar energy to thermal energy and the use of this energy to meet all or part of a building's heating load has been the primary application of solar energy to date. Two generic approaches exist: the passive approach and the active system. In the passive approach, the building itself is used to collect and store the solar heat. In active systems, special equipment is added to the building to collect, store and distribute the solar energy.

Active systems are composed of numerous components which can be assembled in a variety of configurations depending on the climatic and site conditions, architectural demands and economics. The basic element is the solar collector which is the device that collects solar radiation and converts it into heat.

Space heating can be done either with liquid solar collectors and water storage or with air collectors and rockbed storage. To control the flow of the heat transfer fluid, the system also includes components such as pumps, fans, valves, temperature sensors

and controllers. There is also the need for some other equipment, such as heat exchangers and auxiliary energy systems. The latter are necessary in order to boost the system in cases where the solar energy available is not enough to meet the heating load. However, the position of the auxiliary source of energy should be carefully examined in each case for effective utilisation.

According to Duffie and Beckman (1980), a solar active heating systems may have five basic modes of operation which are associated to same number of scenarios, depending on the conditions that exist in the system at a particular time. These are:

(a) Solar energy is available, but heat is not needed in the building, then the energy collected is added to the storage system.

(b) Solar energy is available and heat is needed in the building, then the energy collected is transferred directly to the load.

(c) Solar energy is not available, heat is needed in the building, there is thermal energy in the storage system; in such a case heat from the storage unit is used to meet the heating load requirements.

(d) Solar energy is not available, heat is needed in the building, the storage system has been depleted; in such a case auxiliary energy is used to meet the heating load requirements.

(e) Solar energy is available, heat is not needed in the building and the storage system is fully heated; under these circumstances, the energy collected is discarded.

Fig. 3.1 is a schematic of a basic air type solar heating system with a pebble bed storage system and auxiliary unit. In this system, the storage medium is held in the storage unit while air is the fluid used to transport energy from collector to storage and to the building. The five modes of operation are achieved by appropriate damper positioning. With this system it is not possible to combine modes by both adding energy to and removing energy from storage at the same time. The use of auxiliary heater can be combined with energy supply to the building from collector or storage if the supply of heat from the latter is inadequate to meet the loads. A by–pass is provided to by–pass the collector and storage unit when auxiliary alone is being used to provide heat.

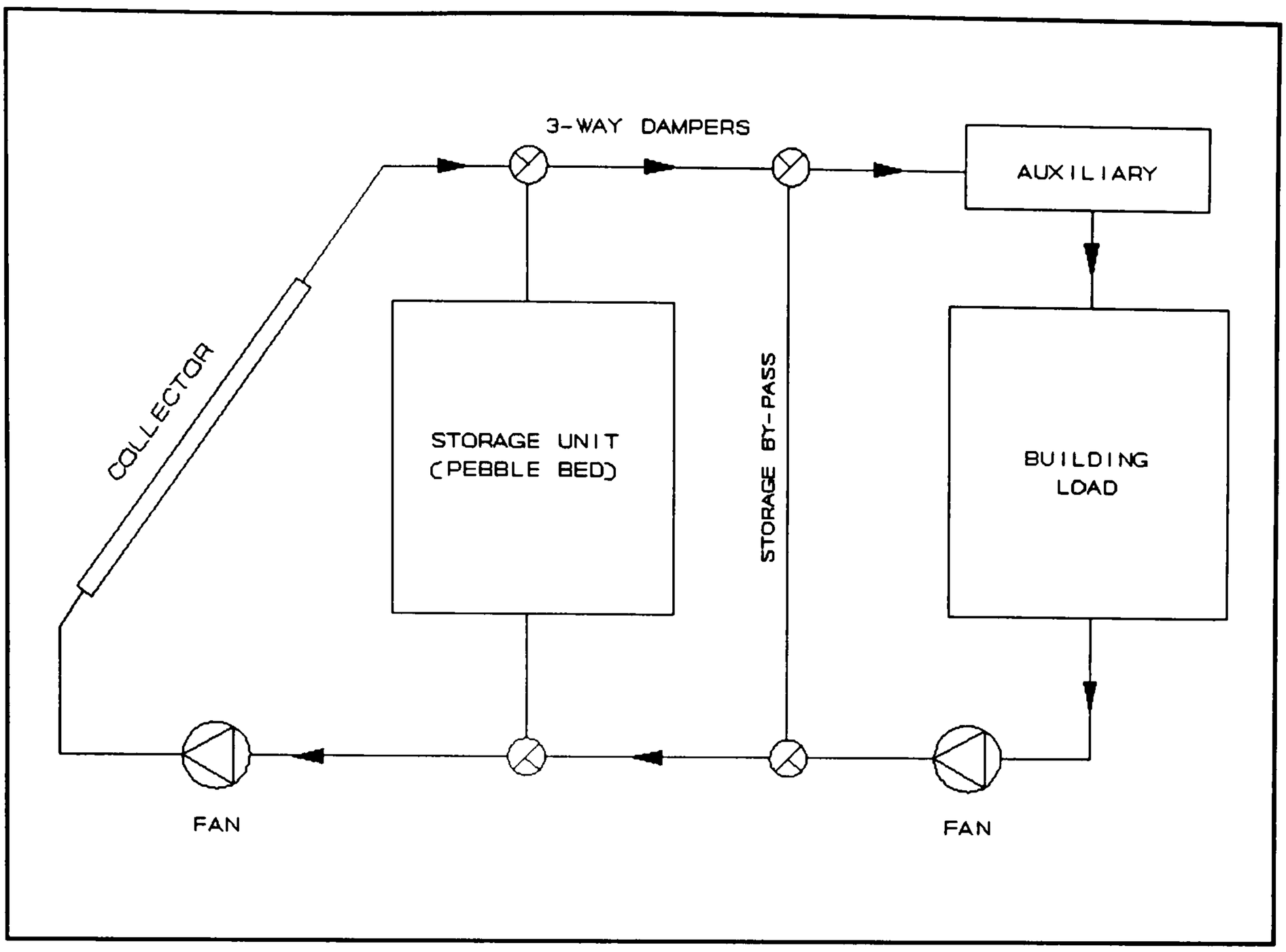

Fig. 3.1 Schematic of basic air-type solar heating system

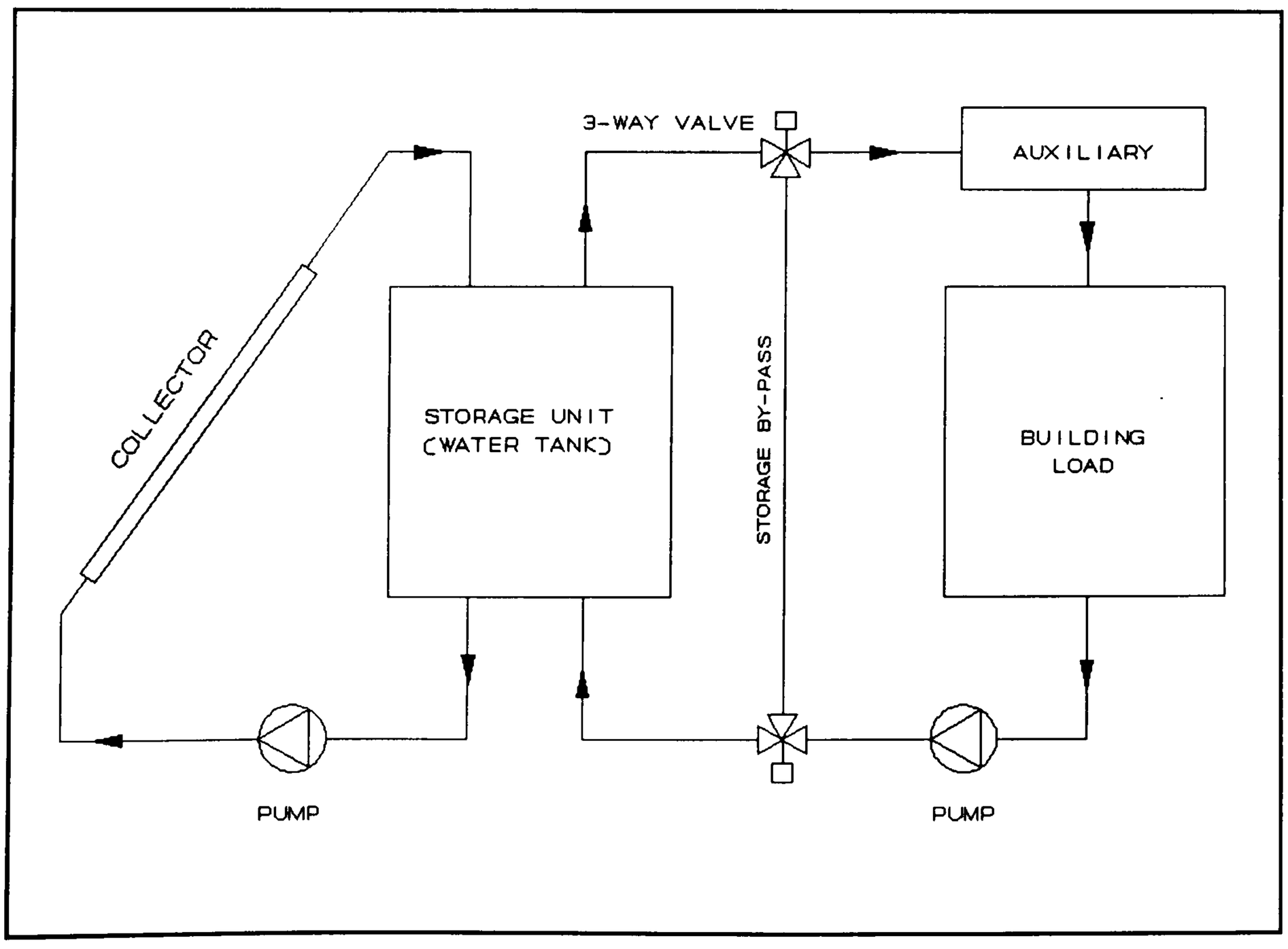

Fig. 3.2 Schematic of basic liquid solar heating system

Systems using air as the heat collection medium have the advantage of no problem with freezing and overheating in the collectors as might happen in water operating systems. Corrosion problems are also minimized as the working fluid is air. Conventional control devices are readily available that can be applied to these systems. Disadvantages include relatively high fluid pumping costs, relatively large volumes of storage, noise from the fans, and the difficulty of adding conventional absorption air conditioners to the systems.

Fig. 3.2 is a schematic of a basic water heating system, with water tank storage and auxiliary energy source. This system allows independent control on the solar collector–storage subsystem on the one hand, and storage–auxiliary–load subsystem on the other, as solar heated water can be added to storage at the same time that energy is removed from storage to meet the building heating load. Solar radiation is absorbed in the collector, the temperature of water being pumped through the collector increases, and the heated water is transferred to the storage tank or in some cases directly to the heat distribution system. The thermal storage unit is usually essential because heat is ordinarily required at night and during cloudy periods. The solar collector and thermal storage unit can operate independently of heating demands, so solar energy can be collected and stored whenever there is sufficient incident solar radiation.

Advantages of water heating include use of a common heat transfer and storage medium, smaller storage, relatively easy adaptation to supply energy to absorption air conditioners, and relatively low energy requirements for pumping of the heat transfer fluid. In climates where freezing is a problem, the following solutions may be introduced:

(a) The collectors may be designed to be drained during times when they are not operating or when freezing is a possibility.

(b) Antifreeze solutions can be used in the collector, but this would require a heat exchanger to transfer the energy to the water.

Liquid solar heating systems will probably operate at lower water temperatures than conventional water heating systems and thus require additional heat transfer area to transfer the required heat into the building. Care should be taken for cases of

excessively high temperatures so as to avoid boiling and pressure build–up.

An auxiliary source of energy is required as a backup to the solar system for use when the solar collector–storage subsystem is unable to meet heating demands. Although the collector and storage could be sized large enough to meet the full heating requirements throughout the year, the cost would be prohibitive in most climates. An economical design involves a smaller solar system and an auxiliary furnace or boiler capable of meeting the full heating demand when solar collection is not possible and when stored heat is inadequate. This combination results in more effective use of the solar equipment throughout the heating season and a lower annual total cost. There are several methods of supplying auxiliary heat in a liquid solar system for space heating. In virtually all practical solar heating designs, auxiliary heat is supplied to the fluid stream in which heat is distributed to the various zones in the building. In most of the systems the auxiliary source of heat is best used in parallel with the solar supply from storage rather than in series with it, so that only one source is used at a time. The series design is seldom used because some of the heat supplied to the water passing through a thermostatically–controlled auxiliary boiler would flow on through the load exchangers and be accumulated in the solar heat storage tank. The resulting temperature rise in solar storage would reduce collector efficiency and capacity for solar heat storage.

A more detailed schematic diagram of a liquid based solar heating system is illustrated in fig. 3.3. A collector heat exchanger is shown between the collector and storage tank allowing the use of antifreeze solution in the collector. In fact, the use of such a heat exchanger increases the system cost and it also reduces the system efficiency. Its effect on the system performance will be investigated in the present study. Relief valves are also included for dumping excess energy in cases where the collector operates at excessive temperatures. A load heat exchanger is also employed to transfer energy from the storage tank to the heated rooms. An auxiliary source of energy is employed, in this case in parallel to the solar system, in order to assist the system in case of non adequate energy supply from the collector–storage subsystem. In some cases, the auxiliary is placed in series with the solar system. The effects of this arrangement will be investigated in this work.

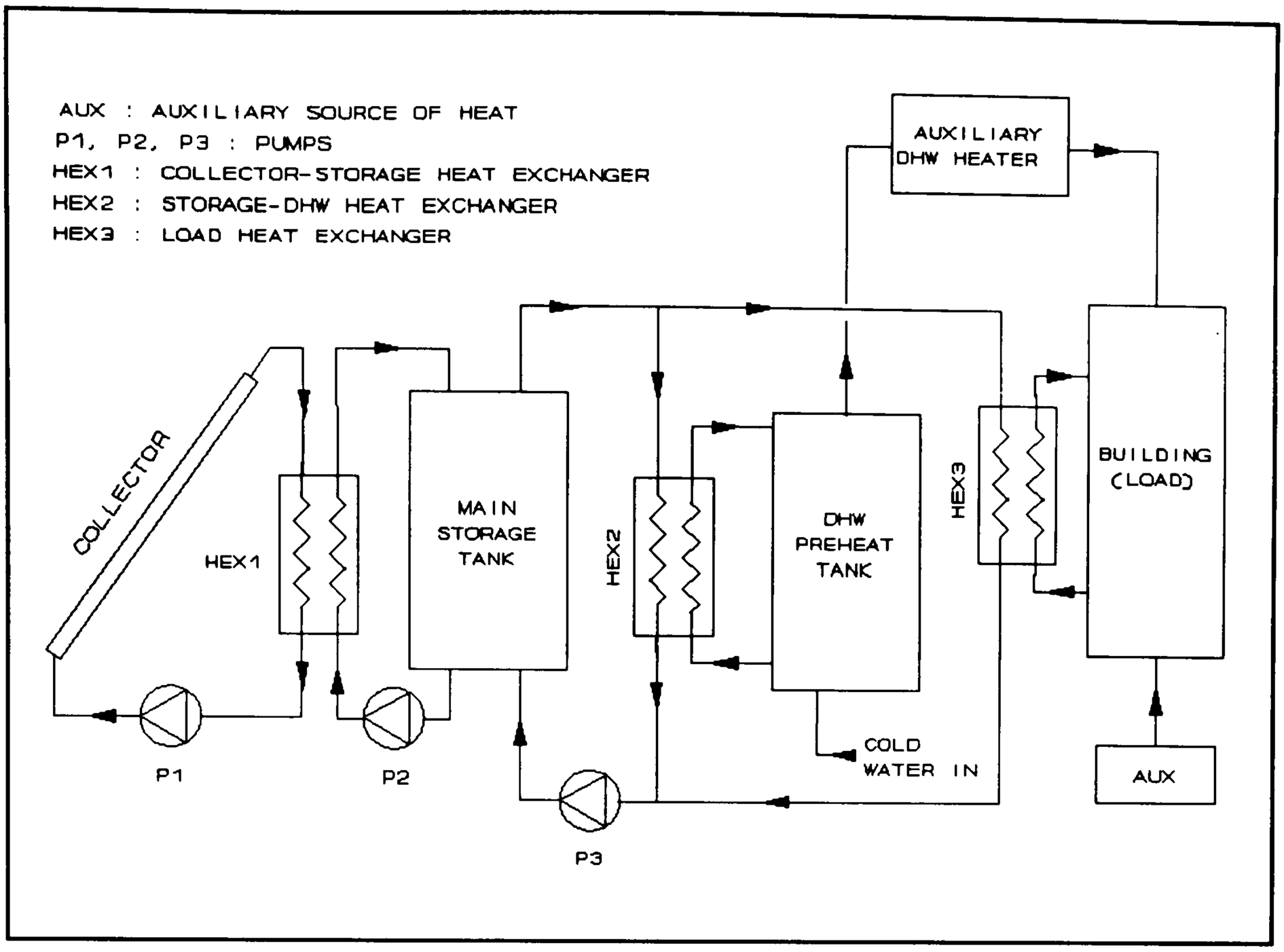

Fig. 3.3 Detailed schematic of a liquid based solar heating system

The load heat exchanger, i.e the heat exchanger which transfers the heat from the solar system to the building, must be adequately designed to avoid excessive temperature drop and corresponding increase of temperature in the storage tank and the collector. According to Duffie and Beckman (1980), the parameter describing this heat exchanger is $\varepsilon_L C_{min}/UA$, where ε_L is the effectiveness of the heat exchanger, C_{min} is the lower of the two fluid capacitance rates (mass flow rate times specific heat capacity of the fluid) in the heat exchanger, usually that of air, and UA is the building overall heat loss coefficient–area product. Klein *et al.* (1976), studied the effect of load heat exchanger size on the performance of a solar space hating system for residential applications. They found that the dimensionless parameter $\varepsilon_L C_{min}/UA$ provides a measure of the size of the heat exchanger needed to supply solar heat to a specified building. In conclusion, they suggest that reasonable values of $\varepsilon_L C_{min}/UA$ for solar space heating systems, when costs are considered, are between 1 and 3.

The temperature difference between the collector and the storage tank must be adjusted so that there will be no heat loss from the storage tank, via the collector,

under any conditions. To maintain this condition, the temperature at the top of the collector must be 8–12 °C higher than that of the storage tank, when the pump is switched on (Rusch, 1978). This temperature difference must be chosen for the following reasons:

(a) The heat loss from the pipes connecting the collector to the storage tank accounts for 1–3 °C, depending on the length.

(b) The tolerances of the detector and the controller account for 1–2 °C.

(c) For effective heat transfer, the minimum temperature difference at the heat exchanger should be at least 3–5 °C.

(d) The system must only be put into operation when more useful energy is produced than the energy required by the pump, the minimum temperature difference being 3 °C.

One of the basic problems in conventional liquid solar heating systems is that the system often cannot collect heat when insufficient solar energy is available, consequently an auxiliary energy supply is required to meet the heating load. On the other hand, heat pumps, use mechanical energy to transfer thermal energy from a source at a lower temperature to a sink at higher temperature. Heat pumps may use air or water as their energy source, and dual source machines are under development that can use either, but the most important application of air– or water–source heat pumps occurs when they collect heat under conditions of low insolation. One of the systems which could overcome these problems is the combined solar and heat pump system widely known as solar assisted heat pump system (SAHP).

There are three possible configurations of solar heat pump systems, namely the series, the parallel and the dual system. The schematic diagrams of these systems, taken from Freeman *et al.* (1979), are illustrated in figs. 3.4 to 3.6. In the series system (see fig. 3.4) the evaporator of the heat pump is supplied with heat energy from the solar system. The system is arranged and controlled so that solar heat can be added to the building directly from the storage tank when the storage temperature is high enough.

The parallel system shown in fig. 3.5, employs an air–to–air heat pump and a water–to–air load heat exchanger. The operation of this system is the same as a conventional solar system, but with the heat pump supplying the auxiliary energy.

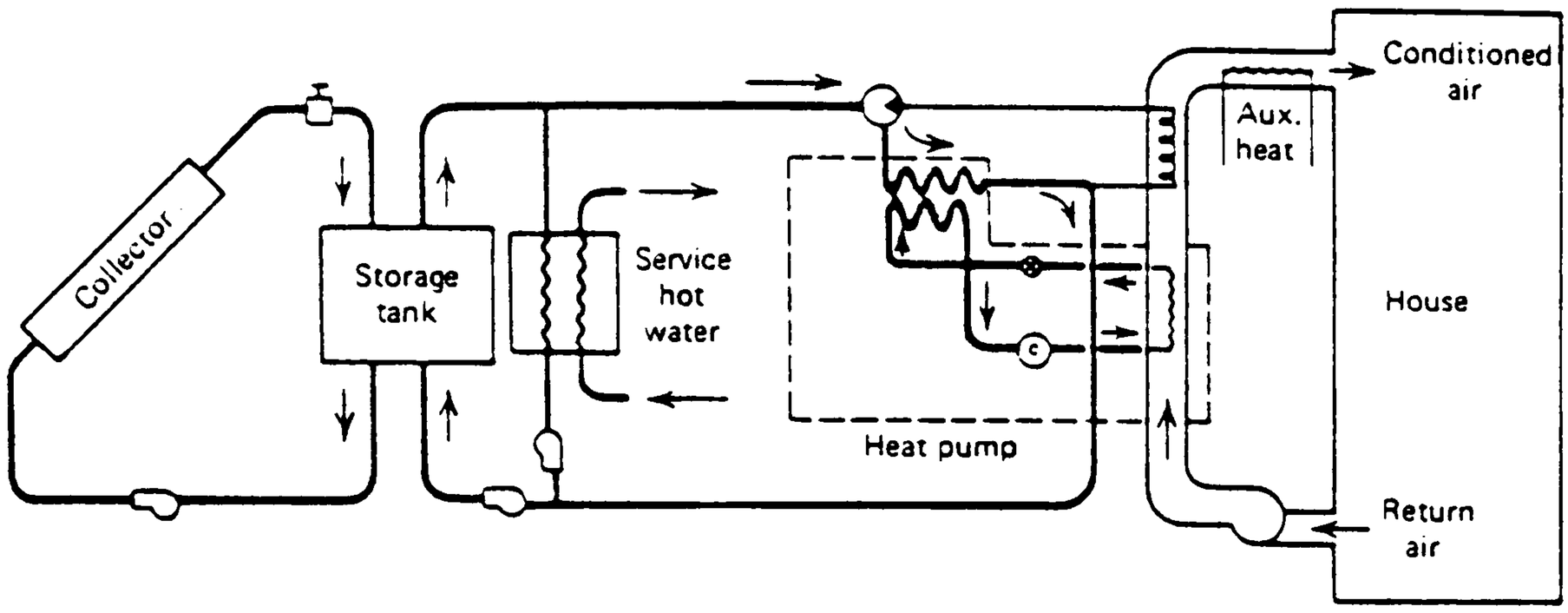

Fig. 3.4 Schematic of a series solar heat pump system. From Freeman *et al.* (1979)

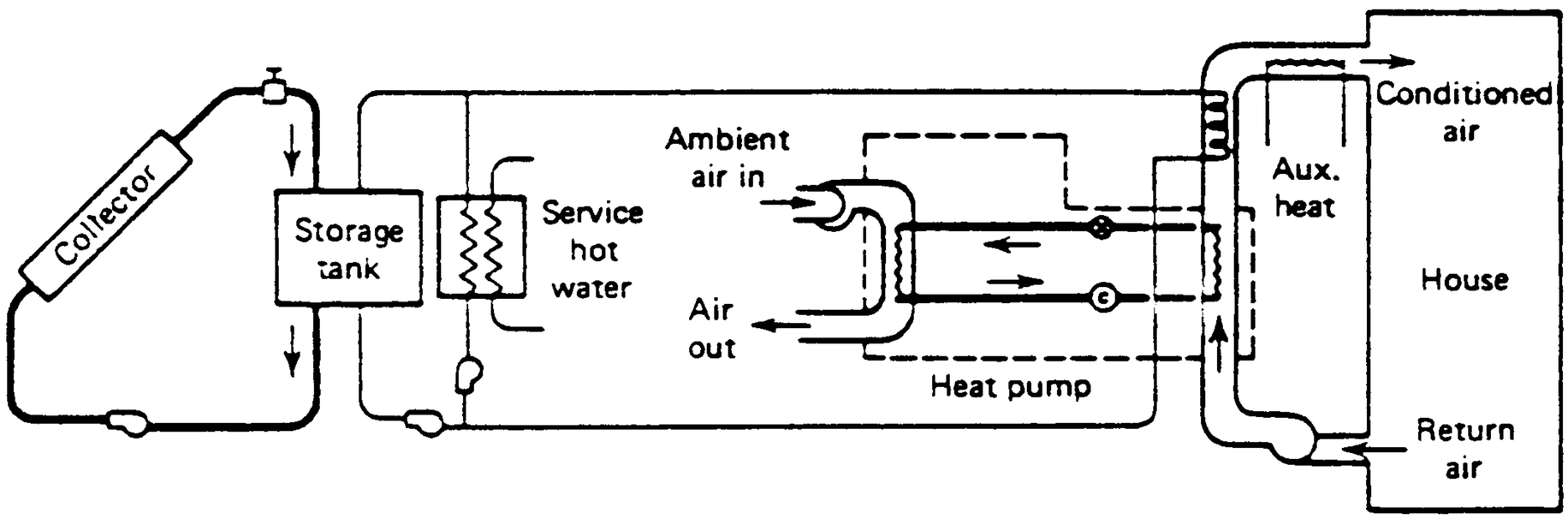

Fig. 3.5 Schematic of a parallel solar heat pump system. From Freeman *et al.* (1979)

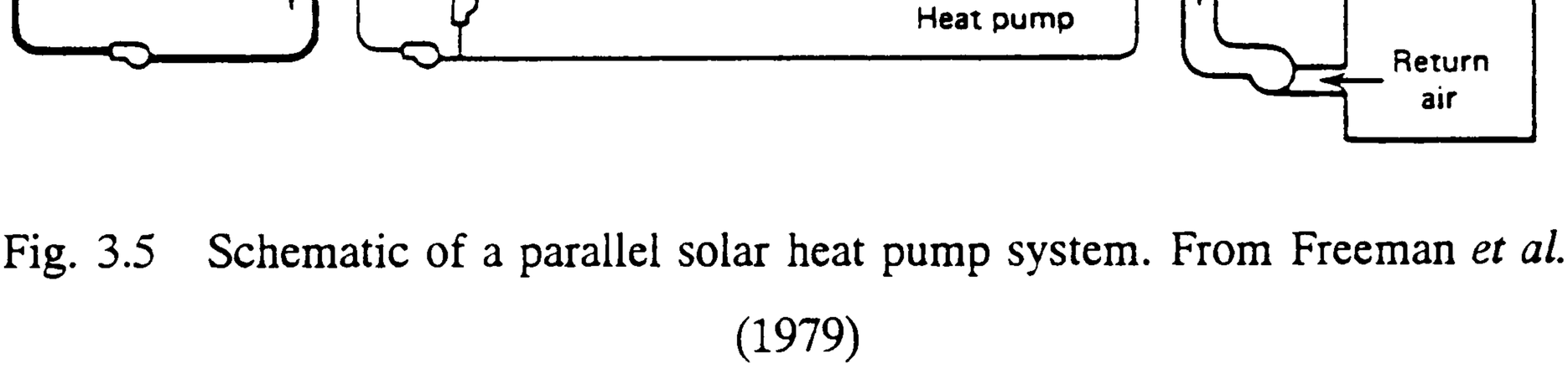

Fig. 3.6 Schematic of a dual source solar heat pump system. From Freeman *et al.* (1979)

In the dual source system shown in fig. 3.6, the heat pump evaporator is supplied with energy from either the water in the storage system or from ambient air. Solar energy can be supplied directly to the building. This system however needs careful design of the control mechanism to select the source which gives the higher coefficient of performance, that is the higher of the two source temperatures.

3.3.2 Research and Development

A method for optimising the design and predicting the annual costs of solar heating of buildings was presented by Lof and Tybout (1973). This model was applicable only to regions of relatively mild climate and where sunshine was plentiful. Lof and Tybout correlated the size of storage tank to the collector area and suggested that the range for the storage capacity per unit collector area should be from 200 to 300 kJ $m^{-2} K^{-1}$ which corresponds to 50–75 kg of stored water per square meter of collector area. In addition, they indicated that the performance of solar heating systems is rather insensitive to the amount of storage capacity within this general range.

Phillips (1981) suggested that the ratio of storage capacity to the collector area does not account for the fact that all collectors do not have exactly the same performance. He introduced a dimensionless storage factor expressed in terms of the ratio of storage capacity to collector area and the collector characteristics. This factor, however, implies that each collector in the system should be treated separately, which is neither practical nor convenient for design purposes.

Hunn *et al*. (1977) developed a computer model which simulates the effects of hourly weather conditions on the performance and cost of a combined solar/conventional heating system for buildings in cloudy, northern climates. This model, which in fact was evolved from that of Lof and Tybout, exhibits the effects of several system and cost parameters on system cost so that optimal designs can be determined. They found that the collection of solar energy from diffuse sky radiation is significant and amounts to about 25% of the total on an annual basis. They also studied the effect of the number of glazing in the collector and concluded that two sheets of glasses are optimal for cold, cloudy climates. They found that the optimal storage capacity ranges

from 204 to 408 kJ m^{-2} K^{-1} , being 204 for low collector–fuel cost combinations and 408 for high collector–fuel cost combinations. They also found that combined solar/conventional costs are only moderately sensitive to interest rate and amortisation period. This information is useful to a design engineer but the range of recommended values is large and therefore difficult to make a choice. To narrow this range, it is necessary to optimise a system after taking into consideration the economic and other parameters related to the location where the system is to be installed. This will be investigated in the present study.

Kovarik and Lesse (1976) studied the problem of optimal control of flow through the collector. They showed that the efficiency of the collector increases with the flow through the collector and that if the amount of energy collected is the only criterion of performance, maximum flow rate is to be applied whenever there is a positive gain from the collector, except in systems with stratified storage.

Kern and Harris (1975) and Felske (1978) considered the optimum tilt angle of south facing collectors and studied the effect of off–south orientation of collectors in solar heating systems. Felske concluded that the optimum collector tilt is quite insensitive to azimuthal angle but is a function of the mean fluid temperature and that for a given azimuthal angle an optimum collector tilt exists which is between 3° and 10° less than the latitude. He also found that within ±10° of the optimum, the collector performance is about the same.

Brandemuehl and Beckman (1979) developed a procedure for assessing the economic viability of a solar heating system in terms of the life cycle savings of the system over a conventional heating system. The life cycle savings is expressed in a generalised form by introducing two economic parameters which relate all life cycle cost considerations to the first year fuel cost or the initial solar investment cost. Using the generalised life cycle savings equations, they developed a method for calculating the solar heating system design which maximizes the life cycle savings.

Barley (1979) derived an algorithm for choosing insulation levels, as well as solar collection area, so as to minimise the overall cost of constructing and heating a building. The general algorithm is applicable with any solar performance prediction

method and with economic criteria where the cost is a linear function of collection area and of auxiliary energy consumption. It has been shown that the ratio of solar collector area to the annual space heating load has an economically optimal value, corresponding to an optimal solar heating fraction, which is independent of the magnitude of the load.

Lunde (1979) presented a new method for the prediction of the performance of solar heating systems using well mixed storage. This method predicts monthly and annual system performance over a wide range of system variables including minimum storage temperature, storage capacity and geographic location. In the same study, Lunde correlated the performance of solar heating systems with the ratio of the collector area to the heating load (m^2/GJ). He simulated the performance of a solar heating system under the weather conditions of six different locations in the United States, at collector to load ratios ranging from 0 to 1.32 m^2/GJ. He demonstrated that this ratio is a good design parameter for predicting the performance of a solar heating system but he did not investigate the optimum design values for such applications.

Gandhidasam (1987) studied the effect of incorporating heat exchangers in solar water heating systems. For a two–loop solar heating system and using a heat exchanger in the storage tank, increases in the capacity–rate ratio cause the overall effectiveness to decrease. For any heat exchanger effectiveness, as the collector effectiveness increases the capacity–rate ratio varies linearly and becomes smaller.

Elsayed (1989) developed an analytical model based on longterm averaging of solar data for the determination of the optimum tilt angle of the collector at any orientation for a given period of time that varies from one month to few months or a year, and examined the effect of the various parameters, such as ground reflectivity and number of glass covers, on the value of the optimum tilt angle. He concluded that the radiation absorbed by a collector is reduced by less than 3% when the tilt angle is changed by ±10°, and by less than 4% when the tilt angle is changed by ±15°.

Ammar *et al.* (1989) used TRNSYS to determine the performance of the standard space and domestic water heating systems in Alexandria, Egypt. They investigated the optimum parameters for water–based systems for the weather and socioeconomic

conditions of Alexandria. They suggested that for optimum operation the collector orientation should be equal to the latitude, the storage to collector area should be of the order of 300 kg m^{-2} and the water mass flow rate through the collector should be 50 kg h^{-1} m^{-2}.

Freeman *et al.* (1979) used TRNSYS to study the performance of combined solar heat pump systems for residential space and domestic hot water heating. They simulated the thermal performance of different system configurations and found that the combination of a heat pump and a solar energy system alleviate the disadvantages that each has when operating separately: (a) the energy collected by a solar system in winter is too low in temperature to be useful for direct solar heating; (b) the coefficient of performance of a heat pump is low at low ambient air temperatures in winter.

A solar assisted heat pump system with a conventional backup unit was simulated by McArthur *et al.* (1978). The performance of the system as a function of collector area and thermal storage volume was evaluated to determine the fraction of the space heating and domestic hot water load that was supplied by the solar–assisted system. This information was used to compute the payback period based on cumulative costs, for each variation of the system's parameters when compared to a conventional system. They found that the optimum combination of collector and storage for the building they investigated was 30 m^2 and 3.5 m^3 of collector and storage respectively, which correspond to a storage ratio of 117 l/m^2. The above combination resulted to 37% fuel savings. However, the economics of the system were marginal and the payback period was slightly less than the life of the mortgage.

Anderson *et al.* (1980) developed a method for predicting the performance of parallel solar–heat pump systems. This method requires as inputs the fraction of the space and water heating load met by solar energy and the fraction of the load that would have been met by the same heat pump operating without a solar system. The procedure then combines these results in a way which accounts for the interaction of the solar system and the heat pump and yields the performance of the combined system. The standard deviations of the errors associated with the equations and assumptions used in predicting performance through simulations are within 1.3 per

cent of the total load, which according to Anderson *et al.* (1980), is well within the uncertainties introduced by solar system parameters and heat pump performance data.

A study of the economic performance of a solar system and several solar–assisted heat pump systems (SAHP) for residential heating has been conducted by Hatheway and Converse (1981). The study was based on a computer simulation which is supported by monitoring data from an existing installation. Three different SAHP configurations as well as conventional solar and air–to–air heat pump systems were evaluated:

(a) the series system in which the solar storage serves as the energy source for the heat pump;

(b) the series off–peak system in which the heat pump in the series system operates only during certain periods of the day under a special electric rate structure;

(c) a parallel system in which oil was operated during the period of peak electricity price;

(d) a peak/off–peak parallel system in which oil was operated during the period of peak electricity price. Hybrid air–to–air heat pump/oil systems were also evaluated.

The results indicated that the air–to–air heat pump/on–peak oil system was the most economic when there was a peak/off–peak electricity price differential. Without price differential, the air–to–air heat pump/oil system was still superior. The solar/oil system was the most economic only when the electricity price was doubled. In this study, however, the solar collector area has not been optimised but it was chosen to fit the available roof area.

3.4. Solar water heating

3.4.1. Systems

The production of service hot water for domestic use by means of solar energy constitutes one of the most popular and economically feasible applications of solar

energy. Solar water heating systems can be classified according to how the water is heated (directly by the sun or by means of a heat exchanger), and according to how the water is circulated through the system. Systems where the circulation of water is done by natural convection as a result of temperature differences, are known as thermosyphon systems, while systems employing a pump are known as forced-circulation systems.

The most common configurations of solar water heating systems are illustrated in fig. 3.7, taken from Duffie and Beckman (1980). Thermosyphon solar water heating systems usually consist of a flat plate solar collector connected to an insulated storage tank, with the tank positioned at a higher level than the collector as shown in fig. 3.7a. Hot water from storage flows directly into the building for domestic use. No pumps are required and very few valves are used.

Water flow in a thermosyphon system is by natural convection, driven by the density difference between hot and cold water. The water in the collector expands as it is heated by the sun, becoming less dense, and rises through the collector into the top of the storage tank. It is replaced by the cooler water that has sunk to the bottom of the tank, from which it flows down into the collector. There the water is reheated, and circulation continues as long as the sun is shining. Since the driving force is only a small density difference (and not a pump), larger than normal pipe sizes must be used to minimize pipe friction. Connecting lines must be well insulated to retain heat and sloped to prevent formation of air pockets which would stop the circulation.

At night, or whenever the collector is cooler than the water in the tank the direction of the thermosyphon flow will reverse, cooling the stored water. One way to prevent this is to place the top of the collector well below the bottom of the storage tank. Kreider and Kreith (1977) suggested that the top header of the collector should be at least 30 cm below the cold leg fitting on the storage tank. To provide heat during an extended cloudy period, an electrical immersion heater can be used in the storage tank; or the solar unit can be connected to a conventional water heater that turns on when the stored water reaches some preset minimum temperature.

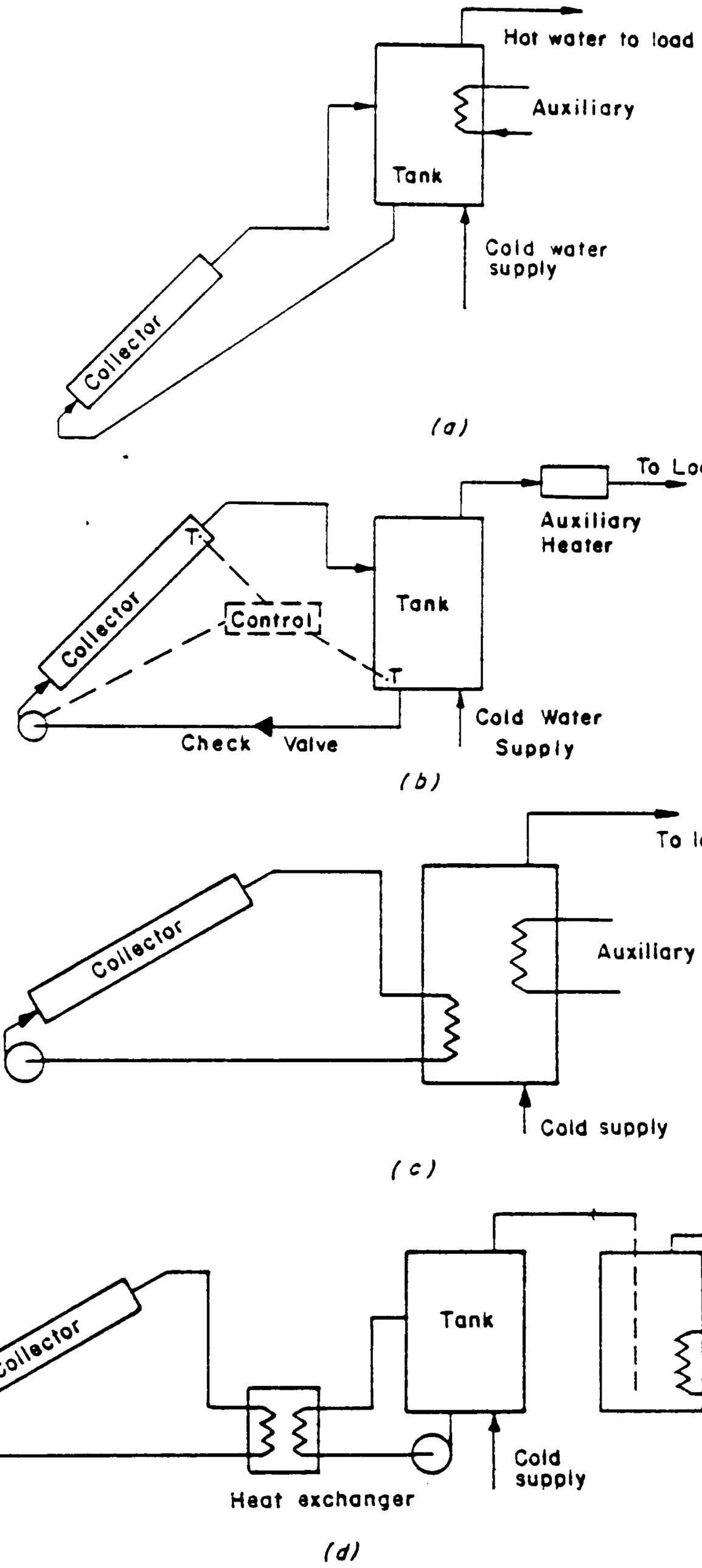

Fig. 3.7 Schematics of common configurations of solar water heating systems. *(a)* A natural circulation (thermosyphon) system. *(b)* One tank forced circulation system. *(c)* System with antifreeze loop and internal heat exchanger. *(d)* System with antifreeze loop and external heat exchanger. Auxiliary is shown added in the tank, in a line heater, or in a second tank; any of these auxiliary methods can be used with any of the collector–tank arrangements. From Duffie and Beckman (1980).

Fig. 3.7b shows an example of a forced circulation system where a pump is required. This is usually controlled by a differential thermostat which is turning on the pump when the temperature at the top header of the collector is higher than the temperature of water in the bottom of the storage tank by a sufficient margin to assure control stability.

In climates where freezing temperatures occur, systems are equipped with a heat exchanger between the collector and the storage tank, as shown in figs. 3.7c and 3.7d. The collector heat exchangers can be either internal or external to the tank.

When solar energy cannot maintain the desired water temperature, backup energy can be supplied most cheaply by an auxiliary source, which is usually placed in the line leaving the storage tank to the load. In some cases, an electric heating coil is often used inside the storage tank to provide extra heat for the domestic hot water. This electrical element should be installed near the top of the tank to take advantage of the stratification within the tank (hot water at the top, cold near the bottom); this reduces the on–time of the heating element.

3.4.2. Research and Development

Extensive investigations have been made for studying the various aspects of solar heating systems for the production of service hot water. Ong (1976) investigated the effect of the height between the collector and the storage tank of a thermosyphon solar water heater, both analytically and experimentally. The analytical results showed that the mean system efficiency and the mean storage tank temperature increased with increased tank height and also with increased solar radiation. The experimental results indicated that by increasing the height of the tank, the water mass flow rate was increased and resulted to lower collector temperatures and hence higher collector efficiencies. He did not, however, recommend an optimum height.

Beckman *et al.* (1976) used the results of many simulations with TRNSYS programme to develop the f–chart method which was in the form of generalized performance charts which correlated the performance of a particular type of system

with its design parameters and the weather. However, this method was applicable only for systems with separate preheat and auxiliary tanks, and systems having a preheat tank loss coefficient of 0.42 W/m^2 °C. Overall, the f–chart method is an accurate tool for sizing domestic water heating systems with well insulated storage tanks, but it is not valid for comparing the performance of systems with differing amounts of storage tank insulation. The method is also not applicable to many process water heating systems where cold water enters the system above 20°C and/or the desired set temperature is greater than 70°C.

Baughn and Crowther (1978) studied the effect of varying the vertical height of the hot water storage tank above the solar collector of solar water heaters. This investigation was carried out experimentally for three different conditions: clear sky, high levels of insolation and under conditions of no consumption of water. The experimental system consisted of 2 m^2 of collector and a storage tank of 120 l connected together by pipes of 25 mm diameter. The tests were conducted at three different elevations of the lower outlet of the storage tank relative to the upper outlet of the collector, namely 67 mm above and 30 mm and 83 mm below. It was found that the system efficiency was relatively insensitive to the elevation difference between the storage tank and the collector. The study did not consider the effect of nocturnal reverse circulation of water from the storage tank to the collector.

A detailed information on thermosyphon system behaviour was provided by Shitzer *et al.* (1979). They studied the water temperature distribution along the collector tubes, measured the water flow rates in the system which was found to generally follow the pattern of variation of the solar insolation, and tested the validity of an analytical model developed for the estimation of the water flow rate. Results showed relatively linear temperature distribution along the collectors and in the storage tank when no water consumption was allowed. Water flow rate was found to follow the pattern of variation of the solar radiation and reached a maximum of 950 cm^3/min.

Fanney and Liu (1980), measured the performance of one thermosyphon solar water heater and five forced circulation systems over a year and compared the predictions of several simulations. They found that the thermosyphon system gave slightly better performance than the closest equivalent pumped system.

Parker (1981) studied the performance characteristics of a thermosyphon solar water heating system, installed in a house, under dynamic conditions of normal operation. This investigation showed that there was a substantial heat loss from the long runs of pipe connecting the storage tank to the collectors and there was also evidence of a small amount of back circulation at night despite the 2 metres difference in height between the tank and the panels.

Braun *et al.* (1983) used the results of hundreds of TRNSYS simulations of a solar hot water system to develop a design method for solar water heating systems, which was in fact an improvement of the f–chart method. They assumed a fully mixed storage tank and a daily hot water consumption pattern similar to that developed by Rand Corporation Survey (Mutch 1974). The resulting procedures overcome the main limitations of the f–chart method concerning the water set temperature, water mains temperature and the preheat tank loss coefficient. The results obtained with the improved method agree with detailed TRNSYS simulation results within 2 per cent on an annual basis and 3 per cent for monthly comparisons.

Morrison and Braun (1985) developed a simulation model for thermosyphon solar water heaters, which has been adopted by TRNSYS, to study the relative merits of pumped and thermosyphon solar hot water systems. Thermosyphon and active solar water heating systems were found to have very similar performance if both were operated with a daily collector to load volume ratio of 1. However, thermosyphon systems performed better than high collector flow rate pumped systems due to the advantage of stratification in the thermosyphon storage tank. They have also found that thermosyphon solar water heaters with horizontal storage tank do not perform as well as vertical tank systems, since the short conduction path in horizontal tanks results in significant heating of the preheat zone, i.e it results to fully mixed conditions. They also reported a good agreement between the simulation results and experimental data for two test locations.

Extensive investigations into the performance of thermosyphon solar water heaters were also reported by Morrison and Tran (1984). They developed a finite element simulation model for predicting the longterm performance of thermosyphon solar water heaters and compared the simulation results with the measured performance of

six systems supplying typical domestic hot water loads. The performance of single tank thermosyphon systems was found to improve as the flow through the collector was reduced to approximately 1 tank volume per day and thermosyphon systems were found to be slightly more efficient than equivalent pumped circulation systems.

Carrington *et al.* (1985) studied the hot water consumption profiles for seven New Zealand households. They found that there is a high proportion of low volume draws, 50% yielding less than 2–3 litres, depending on the household, and the draws tend to be separated by relatively short intervals, 50% following the previous draw by not more than 10–20 minutes. Most users exhibited a double peaked draw–off structure, the major demands occurring in the morning and evening. This was in agreement with the electric power supply authority records confirming that the electric power demand for hot water heating also has this structure.

The effect of thermal stratification in the storage tank of a solar water heating system has been studied experimentally by Tiwari *et al.* (1985). Experiments have been conducted at Delhi and concerned two large scale thermosyphon solar water heating systems, each one comprising an insulated storage tank 1000 l capacity, connected to 12 solar collectors having a total surface area of 18 m^2. It was found that stratification was significant during the first day of the experiment and became less significant during the night and subsequent days of the experiment, as a result of mixing of storage tank water. The effect of stratification on the annual solar fraction of the system has not been investigated.

A technoeconomic model for a hybrid solar forced circulation water heating system was developed by Goyal *et al.* (1987). Two options of auxiliary energy use, electric and diesel, were considered. They have taken into account the life, capital cost and the maintenance cost of the system to calculate the cost of useful energy for different values of collector area and storage tank capacity. Two different profiles for hot water consumption have been used, showing a variation with hour in the day. The simulations showed that the annually averaged solar fraction, which represents the total useful energy provided by the solar collectors as a fraction of the total energy required for meeting a certain hot water demand at a specified temperature, keeps on increasing with an increase in collector area and storage tank capacity. However, the

percentage increase in the solar fraction diminishes non–linearly with increasing collector area and/or storage capacity and the cost of the solar system increases linearly with the collector area and storage tank capacity. In view of the above, Goyal *et al.* concluded that the cost of useful energy can easily be chosen as a key parameter for the optimisation of collector area and storage tank capacity for a specific hot water consumption profile. They also studied the effect of government subsidy on the optimum collector area, tank capacity and the minimum cost of the useful energy. As expected, the government subsidy makes the system more economical.

Gandhidasam (1987) studied the effect of incorporating heat exchangers in solar water heating systems. He found that for a two–loop solar heating system, using a heat exchanger in the storage tank, when the capacity–rate ratio increases, the overall effectiveness decreases. For any heat exchanger effectiveness, as the collector effectiveness increases the capacity–rate ratio varies linearly and becomes smaller.

The effects of heat exchanger length in forced circulation solar water heating systems have been studied by Fahmy and Sadek (1990). They concluded that the system efficiency, with heat exchanger, rises asymptotically towards its maximum (when withdrawal is direct from the storage tank) when the heat exchanger length is increased infinitely. This means that, to get the maximum possible performance of the system, one should either use a very long heat exchanger tube or dispense with it altogether. However, the use of a heat exchanger becomes indispensable when antifreeze and corrosion inhibitors are to be added in the collector.

Morrison *et al.* (1992) used TRNSYS programme to investigate the effect of the load pattern on the performance of a typical Greek solar water heater at the Joint Research Centre, Ispra. The results indicated only a minor variation of delivered energy with load pattern. The delivered energy was highest for an evening draw off due to a reduction of tank heat loss at night. The delivery for a distributed load was similar to the morning peak load for volume deliveries less than one tank volume. For load volumes greater than one tank volume the morning and evening loads reached maximum delivery, whereas the distributed load output continued to increase as a result of larger draw off during the middle of the day.

CHAPTER 4

MODELLING AND SIMULATION OF SOLAR WATER HEATING SYSTEMS

4.1 Introduction

This chapter concerns the modelling and simulation of solar water heating systems for residential and commercial applications. The following two systems, described in chapter 3, will be investigated:

(a) Thermosyphon solar water heating systems, which are mostly applicable to residential houses and flats, and

(b) Active or forced circulation solar hot water systems, which are applicable to rather larger–scale applications, such as blocks of flats, hotels, hospitals, etc.

For each of the above cases, the system model is formulated using the component routines of TRNSYS and an executable file is generated for the system simulation. In the case of Thermosyphon Solar Water Heater (TSWH), since this is a rather standardised, and in fact a well established, system in Cyprus, we considered that there is no need to develop any design criteria. However, a number of simulations should be run in order to investigate the performance characteristics of a typical Cypriot TSWH under different hot water consumption profiles, and the payback period of the system for different economic and technical parameters. Such an investigation will provide a detailed understanding of the phenomena involved in the system operation which will help in further improvements in the system performance.

The case of active systems will be treated in a different and rather more detailed way in order to investigate the optimum design criteria for the system. The investigation will cover small scale applications such as residential for example, and larger scale applications such as blocks of flats and hotels.

4.2 Structure of domestic hot water (DHW) consumption

Hot water demand varies widely from person to person, from day to day and from location to location. It has to do with the users habits, the weather and socio–economic conditions of a place. This is very clearly shown by a study conducted by Carrington (1985) where seven New Zealand households were found to have seven different consumption profiles. Four of them showed a high consumption in the morning hours and low in the evening, one showed a high consumption in the evening hours and two showed high consumption in both morning and evening. According to Gillet *et al* (1981), variations may be in the range of 25–160 litres per person per day although an average figure would appear to be nearer the lower limit. British Standard BS 5918:1981 (1981) assumes a daily hot water consumption of 175 litres at 60°C for a household and gives the hour–by–hour demand of hot water for the British Standard reference solar hot water system.

In the absence of monitored data for Cyprus, a number of consumption profiles have been constructed, based on surveys conducted by the author. Seven different consumption profiles have been used in the simulations of this work, representing equal number of scenarios for houses, flats and hotels, as shown in Table 4.1. Profile DOM1 represents a low consumption pattern of 30 litres per person daily at 45°C while profile DOM2 represents a consumption of 40 litres per person at 50°C. Profile DOM3 is based on a typical domestic hot water load pattern known as RAND distribution (Mutch, 1974). The water consumption patterns for each of the above scenarios are illustrated in figs. 4.1 to 4.7. which show the distribution of hot water consumption per person throughout the day.

It must be noted, however, that hot water demand may be subject to wide variation in both magnitude and time distribution. Even in households in which a regular schedule of hot water usage is maintained, it is unlikely that the daily hot water demand will be the same from one day to the next.

Profile code	Application	Daily HW consumption (l/person)	Temperature (°C)	Consumption pattern
DOM1	Houses, Flats	30	45	Michaelides
DOM2	Houses, Flats	40	50	Michaelides
DOM3	Houses, Flats	40	50	RAND
DOM4	Houses, Flats	40	50	Michaelides
HOT1	Hotels	40	50	Michaelides
HOT2	Hotels	50	50	Michaelides
HOT3	Hotels	60	60	Michaelides

Table 4.1 Domestic hot water consumption profiles

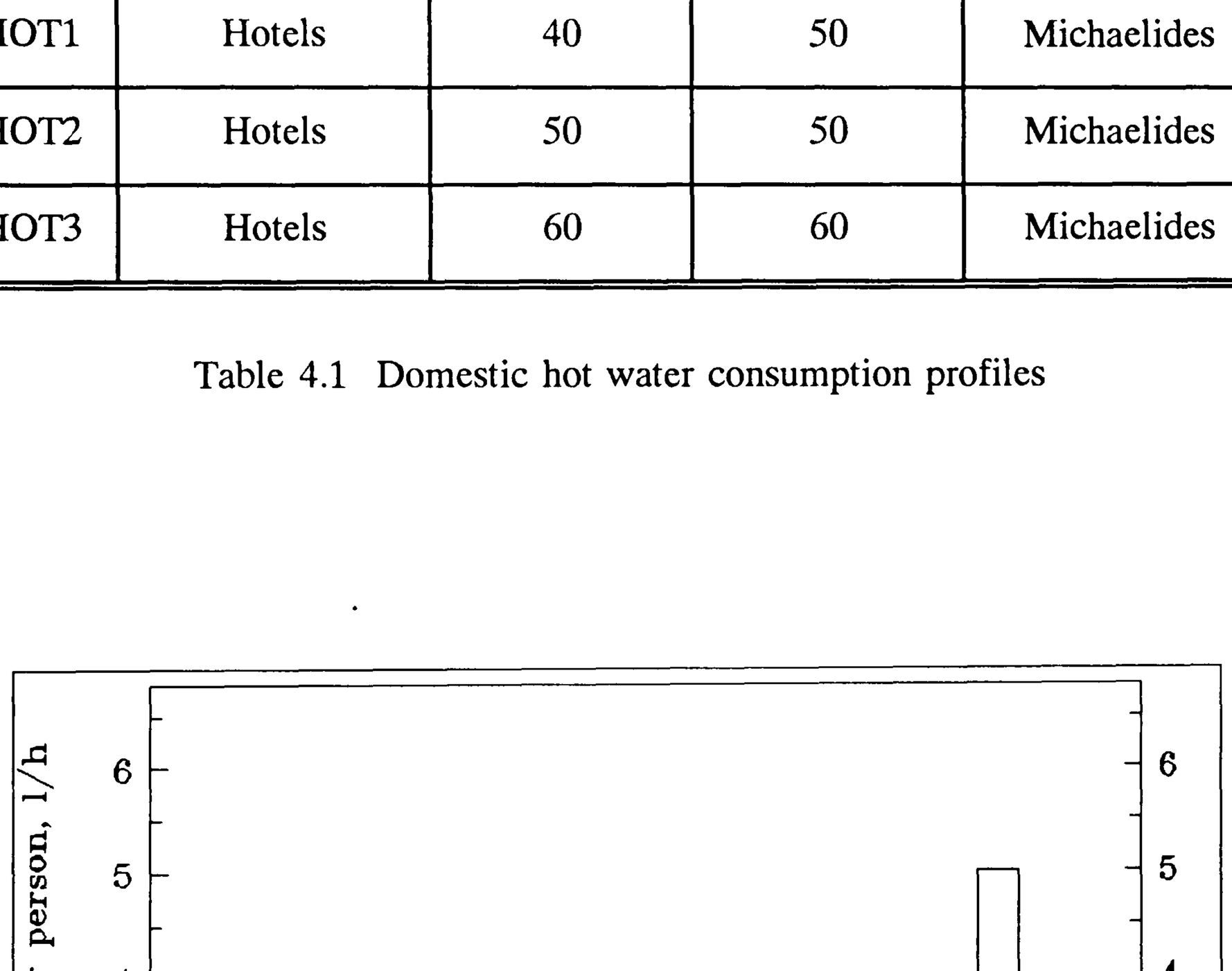

Fig. 4.1 Hot water consumption profile DOM1

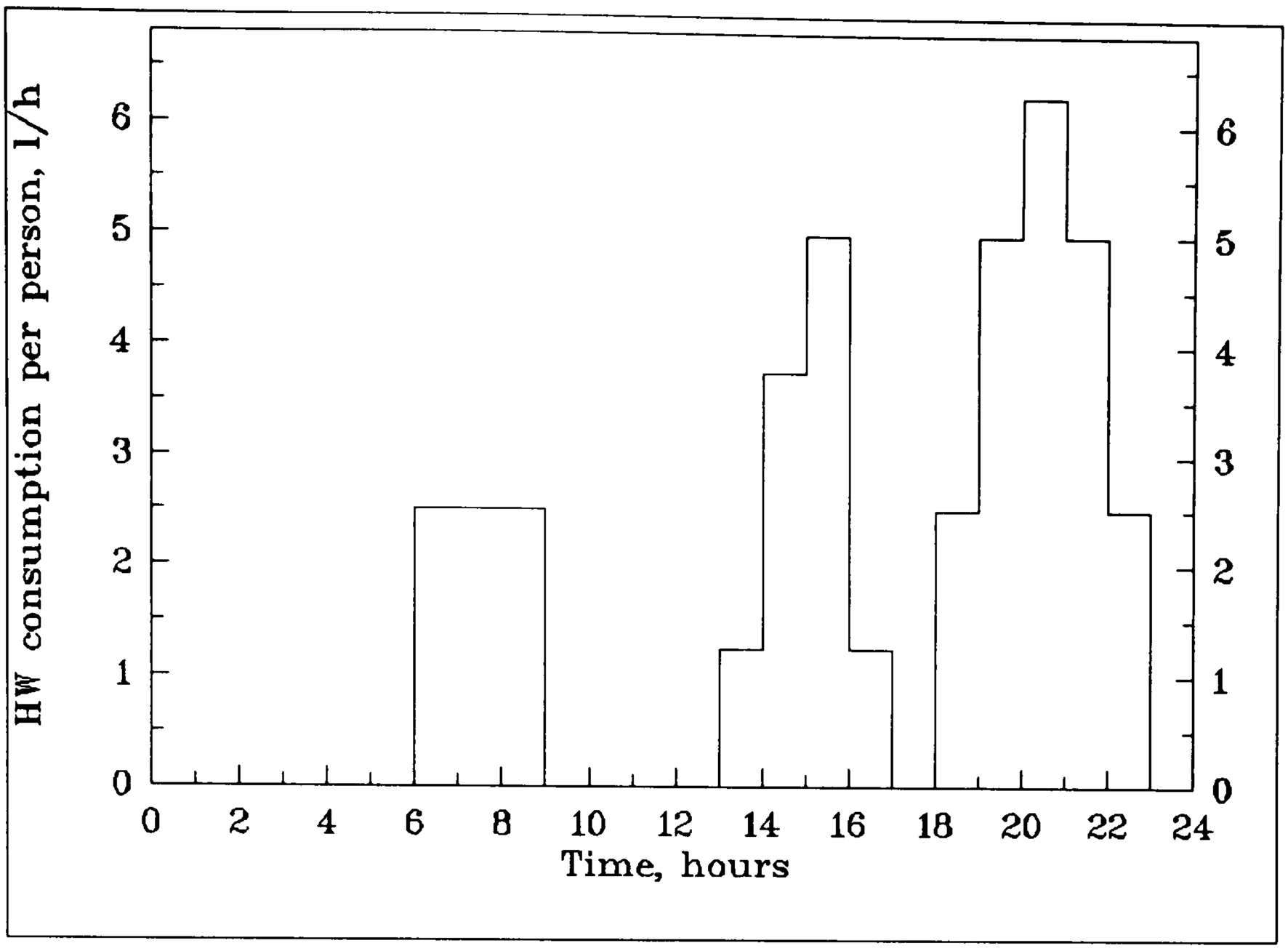

Fig. 4.2 Hot water consumption profile DOM2

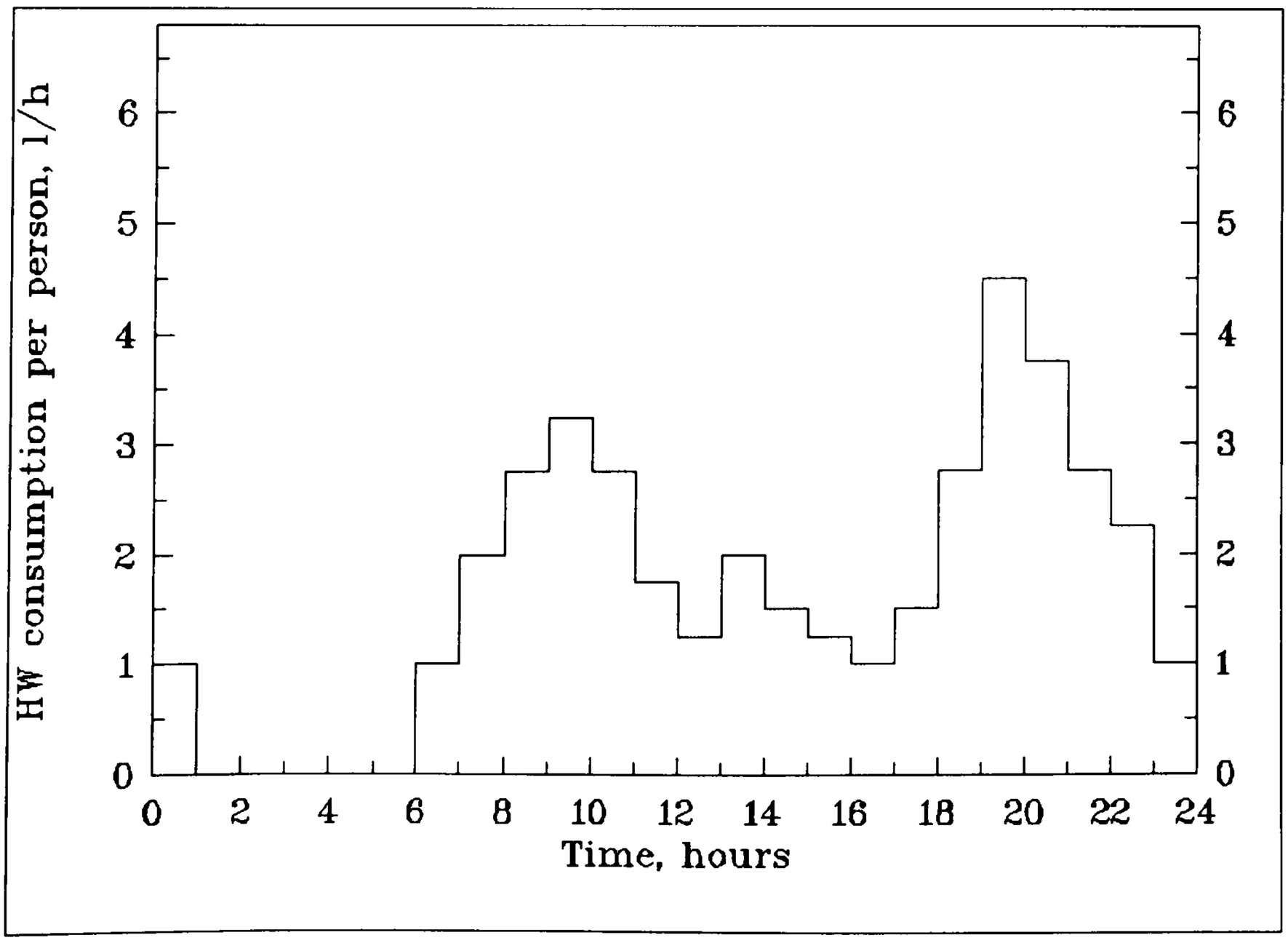

Fig. 4.3 Hot water consumption profile DOM3

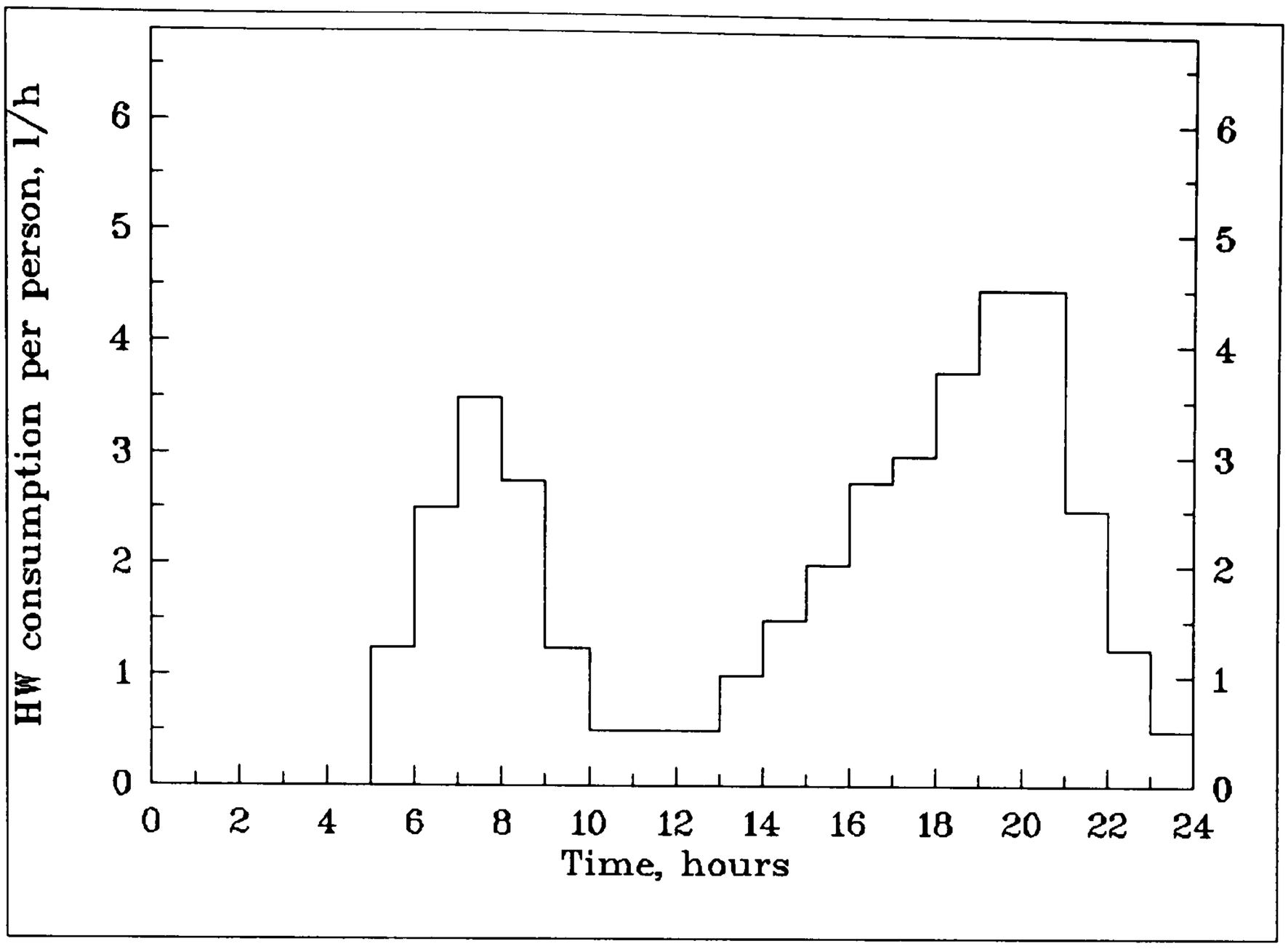

Fig. 4.4 Hot water consumption profile DOM4

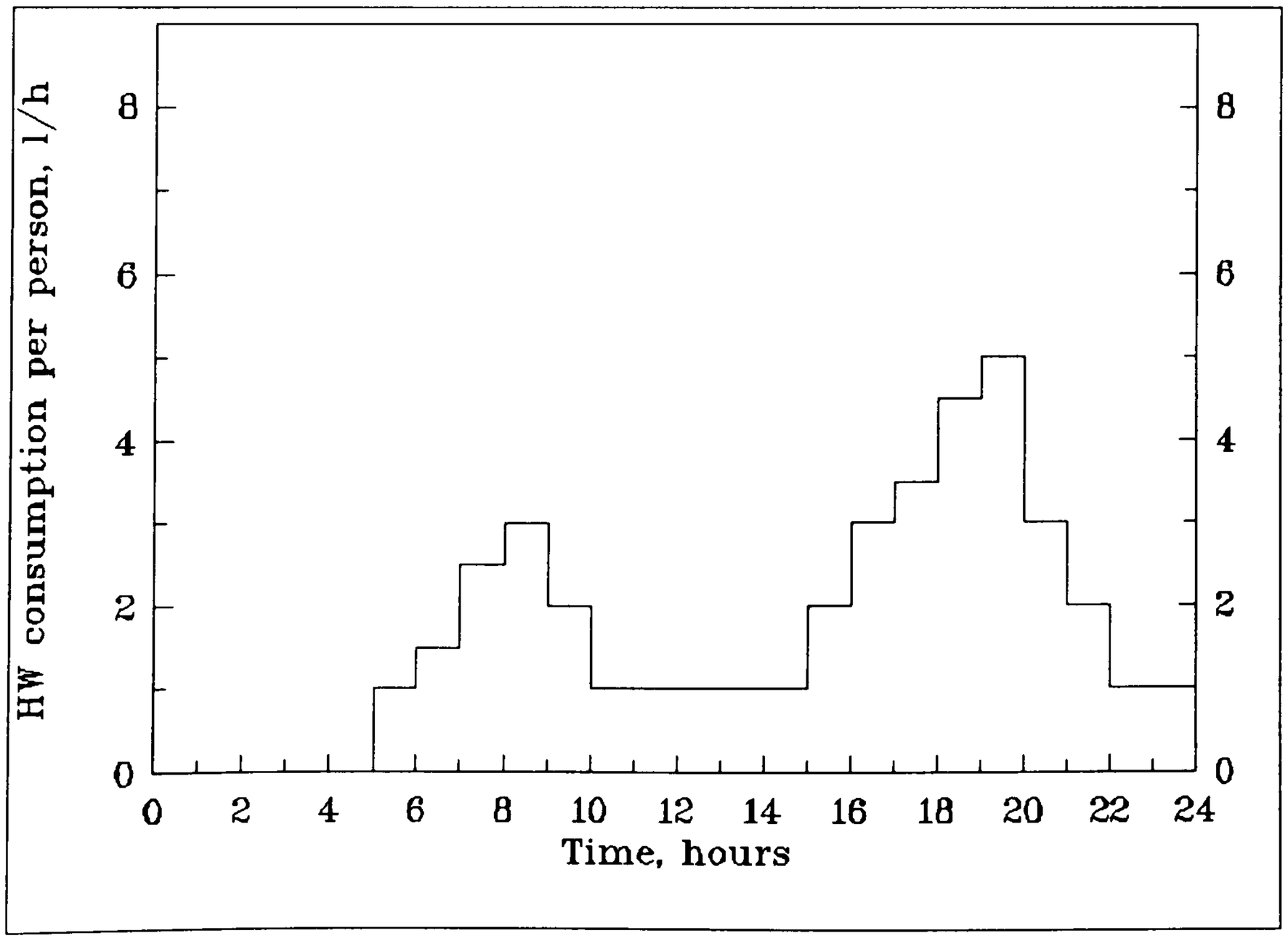

Fig. 4.5 Hot water consumption profile HOT1

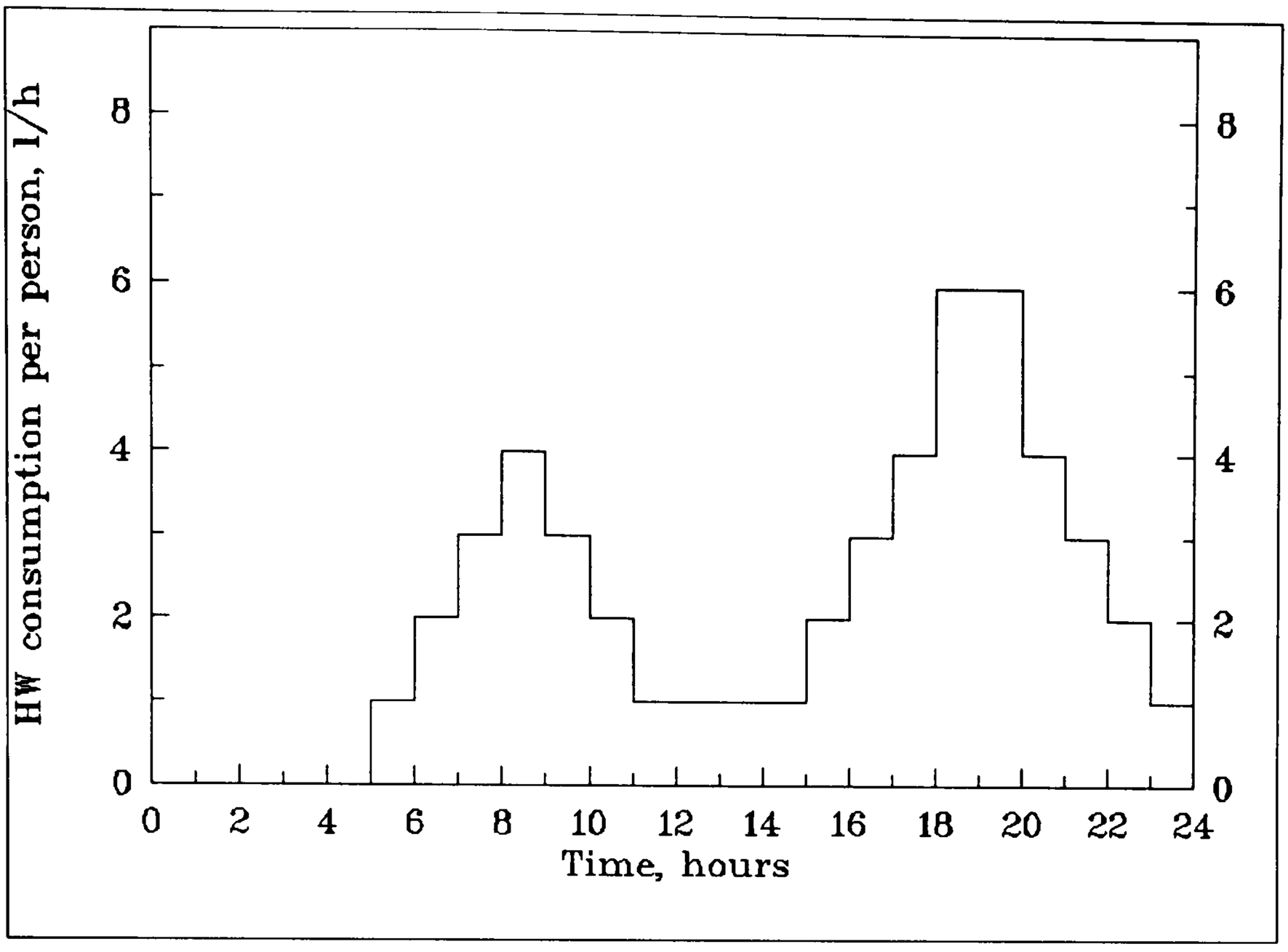

Fig. 4.6 Hot water consumption profile HOT2

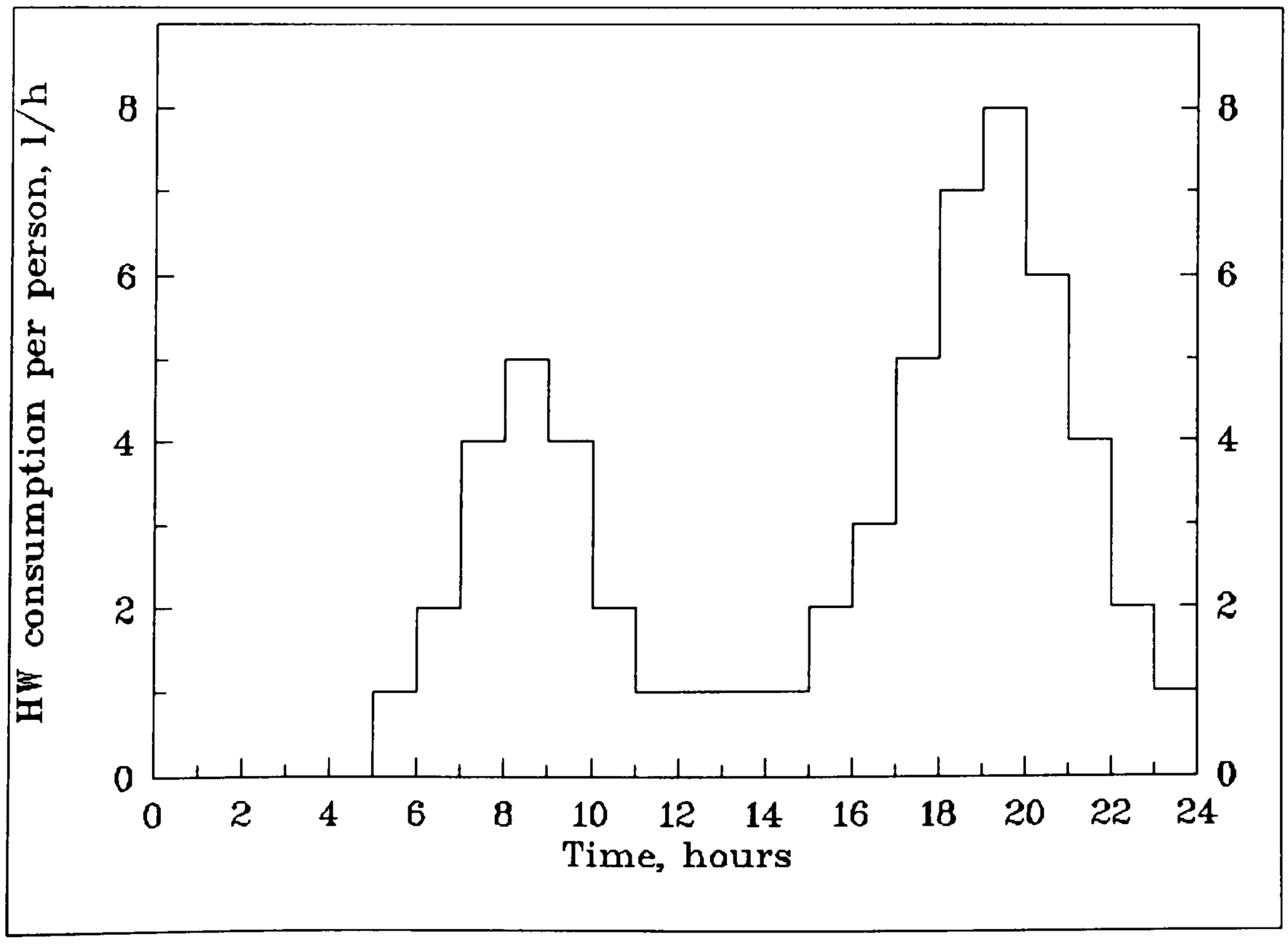

Fig. 4.7 Hot water consumption profile HOT3

4.3 Weather data for simulations

The simulation of a system requires hourly weather data which must be representative of the location under investigation. The selection of typical weather conditions for a given location is very crucial in computer simulations for performance predictions and lead various investigators either to run long periods of observational data or to select a particular year, which appears to be typical from several years of data. For example, Klein *et al* (1976) have constructed the "average year" by selecting the monthly data from an 8–year period which corresponded most closely to the average monthly insolation and ambient temperature. In the absence of such an "average year" for Cyprus, monthly average values for the years 1984 – 1987 of the daily solar radiation and air temperatures, taken from the Cyprus Meteorological Service (see Hadjioannou, 1987 and Meteorological Service, 1975), have been used in the simulation. These are shown in Table 4.2.

Month	T_a (°C)	I_h (kJ/m^2 day)	v (m/s)
January	10.3	8,568	3.09
February	10.9	11,948	4.12
March	13.2	15,836	3.61
April	17.1	20,624	4.12
May	21.9	23,267	4.64
June	26.3	25,304	5.15
July	29.0	25,758	5.15
August	28.8	22,835	4.64
September	25.8	18,846	4.12
October	21.5	13,892	3.61
November	16.4	9,896	3.09
December	12.0	8,269	3.09

Table 4.2 Monthly average values of weather data for Nicosia.

The above monthly average values are used by the Weather Generator subroutine of the TRNSYS programme to generate hourly data as required for the simulation. A file of monthly average weather data for Nicosia, based on Table 4.2 has been created by the author, in the format acceptable by TRNSYS and is used in the simulations which follow with the name CYDATA.DAT (see Appendix A).

4.4 Thermosyphon solar water heating systems

4.4.1 System description

The schematic diagram of the system under investigation is shown in fig. 4.8. It consists of two flat plate solar collectors having a total surface area of 3 m^2, tilted at 42 degrees from horizontal, an insulated horizontal storage tank of capacity 180 litres equipped with a 3 kW electric heater and interconnecting piping. The collectors are connected in parallel through the supply headers, each employing ten evenly spaced parallel copper pipes embossed by semi–circular grooves formed in the flat plate absorber. This system is rated to meet the hot water requirements of a family of four. The parameters and other pertinent technical details of the system are given in Table 4.3.

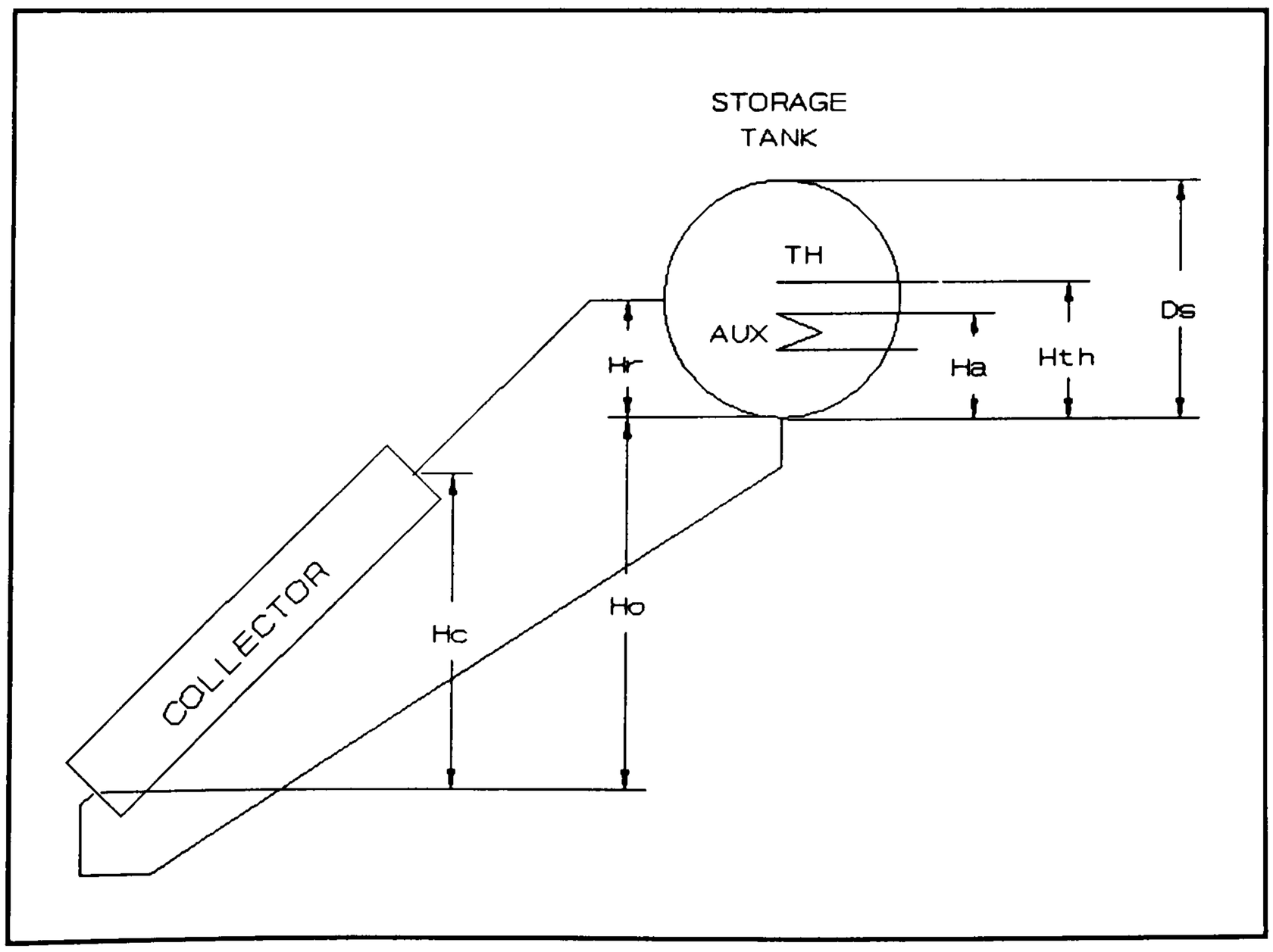

Fig. 4.8 Schematic diagram of the thermosyphon system under investigation

A_c	3 m^2
$F_R(\tau\alpha)_n$	0.77
$F_R U_L$	24.4 kJ h^{-1} m^{-2} K^{-1}
G_{test}	54 kg h^{-1} m^{-2}
β	42 degrees from horizontal
N_R	20
d_R	12 mm
d_h	26 mm
L_h	1900 mm
d_j, d_o	20 mm, 20 mm
H_c	1000 mm
H_o	1150 mm
H_r	250 mm
H_a	300 mm
H_{th}	370 mm
L_j, L_o	2000 mm, 520 mm
$(UA)_{pi}$, $(UA)_{po}$	1.6 kJ h^{-1} K^{-1}, 0.5 kJ h^{-1} K^{-1}
V_s	180 litres
D_s	500 mm
$(UA)_s$	4.65 kJ h^{-1} K^{-1}
P_{aux}	3 kW

Table 4.3 Design parameters for the thermosyphon solar water heater

4.4.2 System modelling

The simulation of a thermosyphon solar water heating system can provide a mean of analyzing the dynamic performance of the system in response to selected meteorological data and load profiles. Like most solar energy systems, the thermosyphon solar water heater is modular and the simulation model for the system can be formulated by connecting models of each of the system components.

For the simulation of this system the TRNSYS model for thermosyphon system (TYPE 45) is used, as described in the TRNSYS Manual. In addition to the above component model, there are certain other subroutines which have to be included in the model to facilitate the system simulation. Thus, a solar radiation processor, TYPE 16, should be included in order to convert the solar data into a form usable by the collector model. In order to calculate the monthly and yearly efficiency of the solar collector, the integrated quantities of solar radiation at the collector tilt angle, and the useful energy gain of the collector are needed. Therefore, a quantity integrator TYPE 24 must be included. The integrator must have a printer TYPE 25 attached to it to output the monthly integrated values.

With the choice of component modules completed, it is necessary to determine the TRNSYS information flow. Due to its modular approach, TRNSYS connects components together via an input/output scheme. This scheme is analogous to connecting pipes and wires in a real system. For example, the collector receives as input the flow rate, which is an output of the pump (in forced circulation systems), the solar radiation and ambient temperature (from the weather generator), and outputs the collector temperature. The user must identify where each input of every component in the system is coming from. In this manner, the user creates a coupled set of equations that TRNSYS must solve. This process is referred to as creating the TRNSYS input file.

Each component in the simulation also requires the specification of time independent variables (parameters) in order to solve the component model. For example, the TYPE 45 thermosyphon subsystem requires as parameters the collector area, fluid specific heat, and the number of collectors in series (among others). It is these

parameters that the user will wish to change periodically in order to perform parametric analyses. With the choice of the timestep, beginning and ending times for the simulation, and the selection of the control statements, the user is ready to run the simulation. Finally, in order to evaluate the economics of the system, an economic analysis (TYPE 29) is needed. The simulation input file JM1.DAT for the thermosyphon solar water heating system described is shown in Appendix B1.

4.4.3 Analysis of simulation results

Many simulations were run to investigate the performance of the system under different scenarios of daily hot water consumption profiles on a daily and a yearly basis. In this study, the performance of the solar heating system will be expressed in terms of its solar fraction, f, which is defined as the fraction of the hot water load provided by solar and can be calculated from the following relationship:

$$f = \frac{Q_{load} - Q_{aux}}{Q_{load}} \tag{4.1}$$

where Q_{load} = hot water energy requirement

Q_{aux} = auxiliary energy supplied to the system

Simulation results including the useful solar energy collected by the system, auxiliary energy needed to meet the load, heat losses from the storage tank and other useful information were also obtained. These results were used to determine the monthly and annual solar fraction of the system and to plot a number of graphs to correlate the various parameters of the system, e.g the flow rate, the efficiency, the tempera–tures and the solar fraction with time, and the efficiency with the thermosyphonic flow rate of water. It must be noted here that these results assume the same daily load profile throughout the year. This is not quite true during the summer period, where the consumption pattern is somewhat higher. However, during this period, the required hot water temperature is not as high as in winter. Consequently, the total thermal energy requirements are reasonably constant throughout the year. The system was also simulated to investigate its behaviour without any imposed load. A detailed economic analysis was also performed.

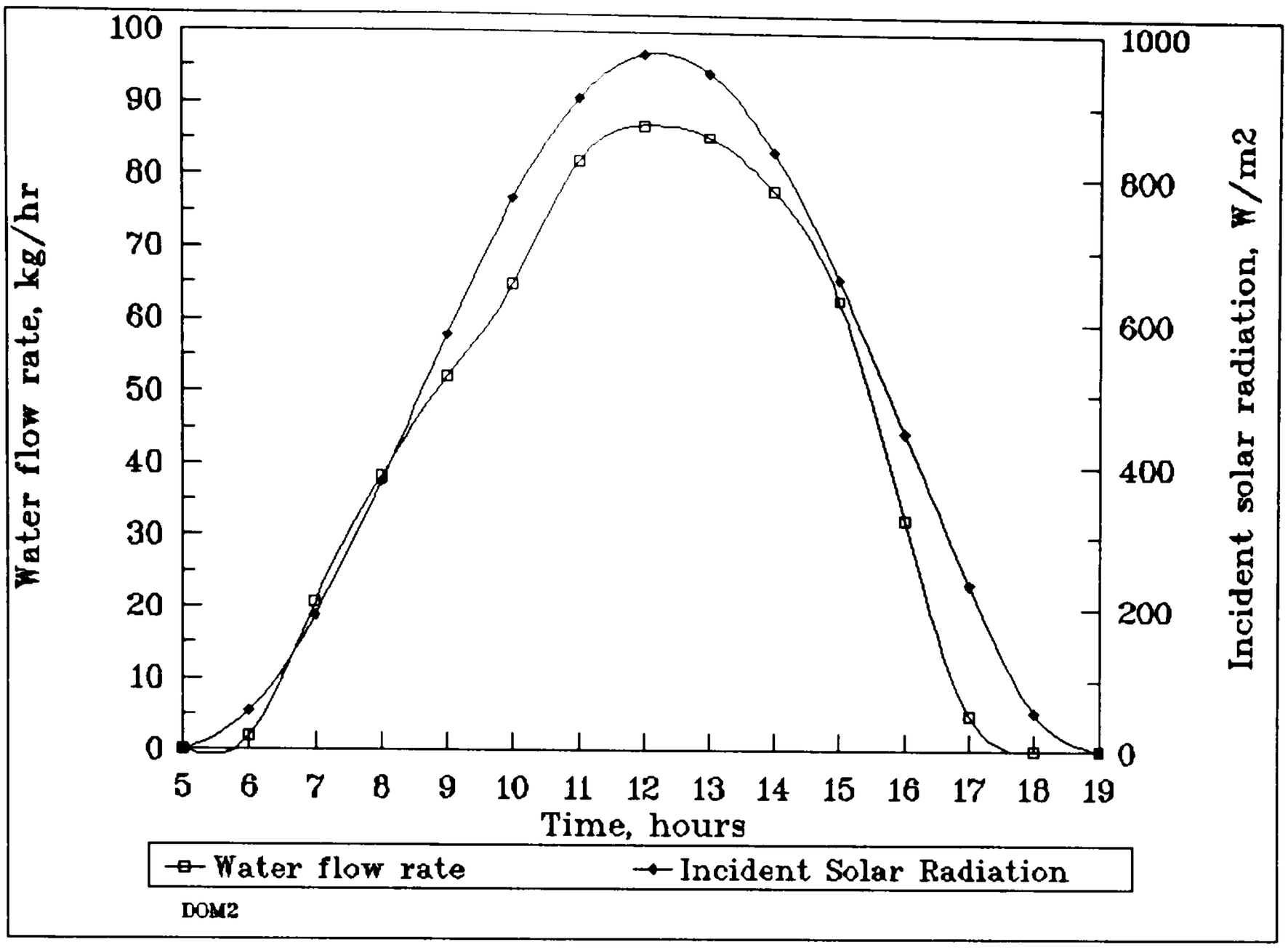

Fig. 4.9 Variation of the incident solar radiation and water flow with time, for consumption profile DOM2

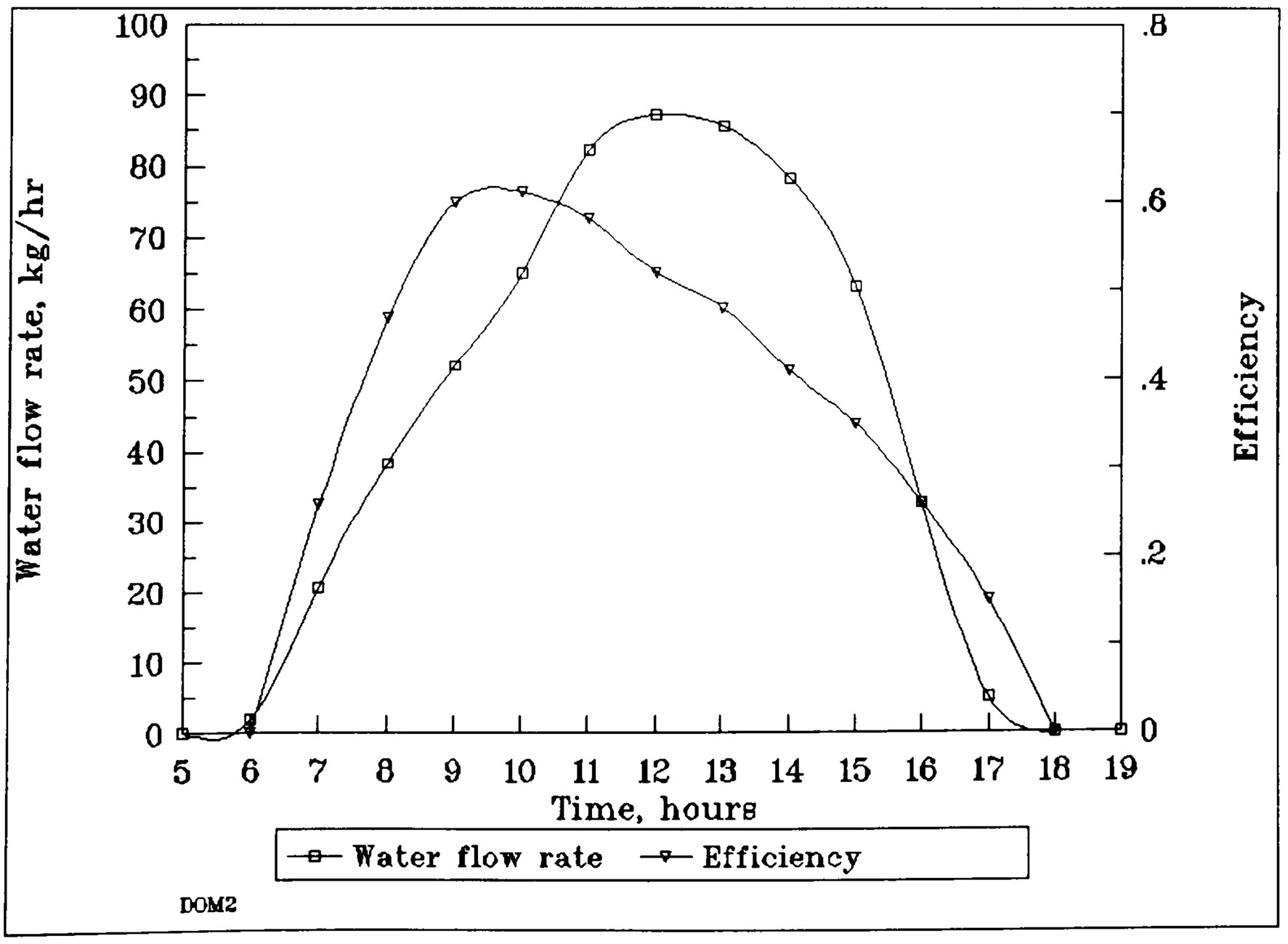

Fig. 4.10 Variation of thermosyphon water flow and efficiency with time, for consumption profile DOM2

Figure 4.9 shows the variations of thermosyphonic flow and incident solar radiation with time for the consumption profile DOM2. As expected, water flow rate in the system was found to follow the pattern of variation of the solar insolation. The flow rate increases during the morning hours to reach a maximum of about 86 kg/h at solar noon, corresponding to approximately 28.7 kg/h per m^2 of collector, and then starts to decline in the afternoon hours as the solar radiation decreases. The same pattern of variation was also observed for the other cases studied including the one without imposed load. The above values are slightly higher than those reported by Shitzer *et al*. (1979) for a similar system tested in Israel and Pafelias *et al.* (1990) for a similar system tested in Greece.

Figs. 4.10 – 4.13 illustrate the variation of the system efficiency with time for four different scenarios. Also shown in these figures is the variation of water flow rate. The system efficiency follows a pattern which is slightly different from that of flow rate. It increases rapidly during the morning hours to reach a maximum of about 60% at around 9.00 a.m. solar time in all four scenarios. There is however a remarkable difference in the afternoon hours where the best efficiency pattern is obtained in the case of high consumption. Thus, at 4.00 p.m. the efficiency of the system without load becomes zero (see fig. 4.11) while in the case of load profile DOM2 the system collects energy at an efficiency of about 25% (see fig. 4.10). This can be attributed to the fact that the temperature of water entering the collector in the system without load is higher than that with load and therefore the collector is operating at high temperature difference, $T_i - T_a$, corresponding to low efficiency. It is interesting to note that the peak of efficiency does not coincide with that for thermosyphonic flow because maximum flow occurs at maximum temperature difference across the collector and therefore lower efficiencies.

In correlating the efficiency with the thermosyphonic flow, it should be noted that the pattern of variation is more or less the same in all three cases, with slight differences in the case without imposed load. It is seen from figs. 4.14 and 4.15 that, in the morning hours, the efficiency rises slowly as the water flow rate increases, and it reaches a maximum of 60% when the flow is 55 kg/h, that is 18.3 kg/h per m^2 of collector. As the flow rate increases further, the efficiency declines very slowly to drop down to 52% at 83 kg/h with consumption profile DOM2 and down to

approximately 50% at the same flow rate without imposed load.

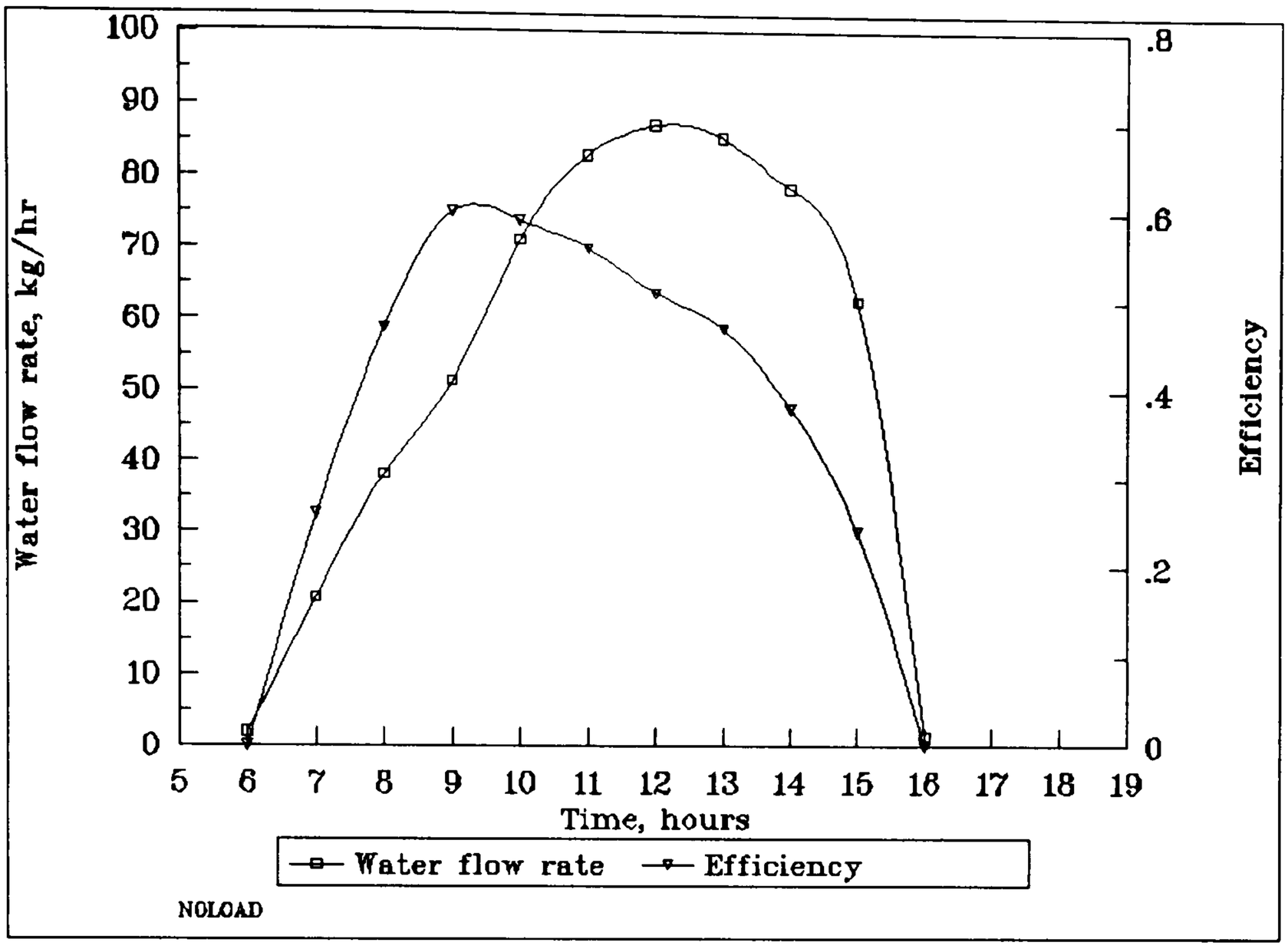

Fig. 4.11 Variation of thermosyphon water flow and system efficiency with time, without imposed load

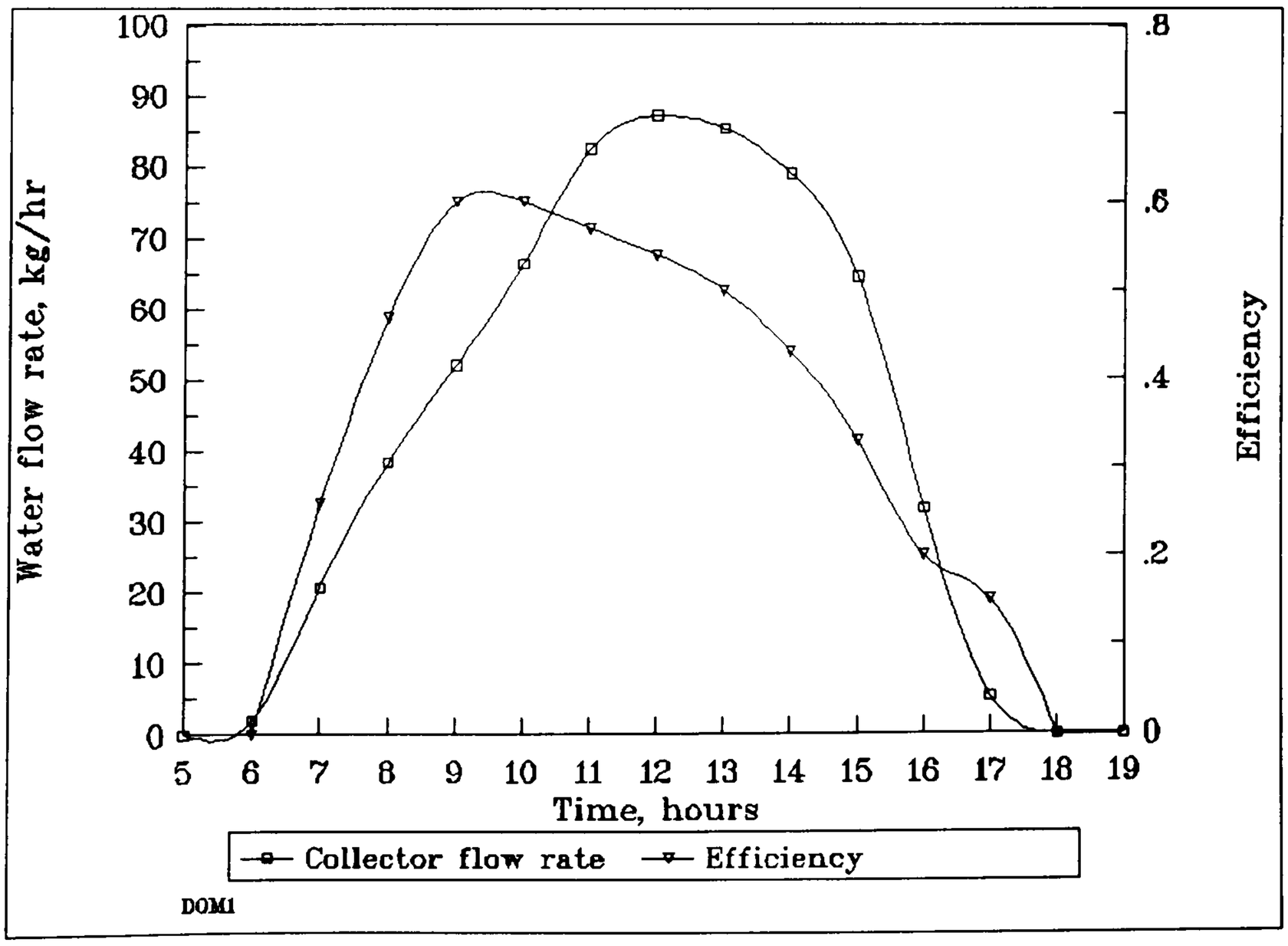

Fig. 4.12 Variation of thermosyphon water flow and efficiency with time, for consumption profile DOM1

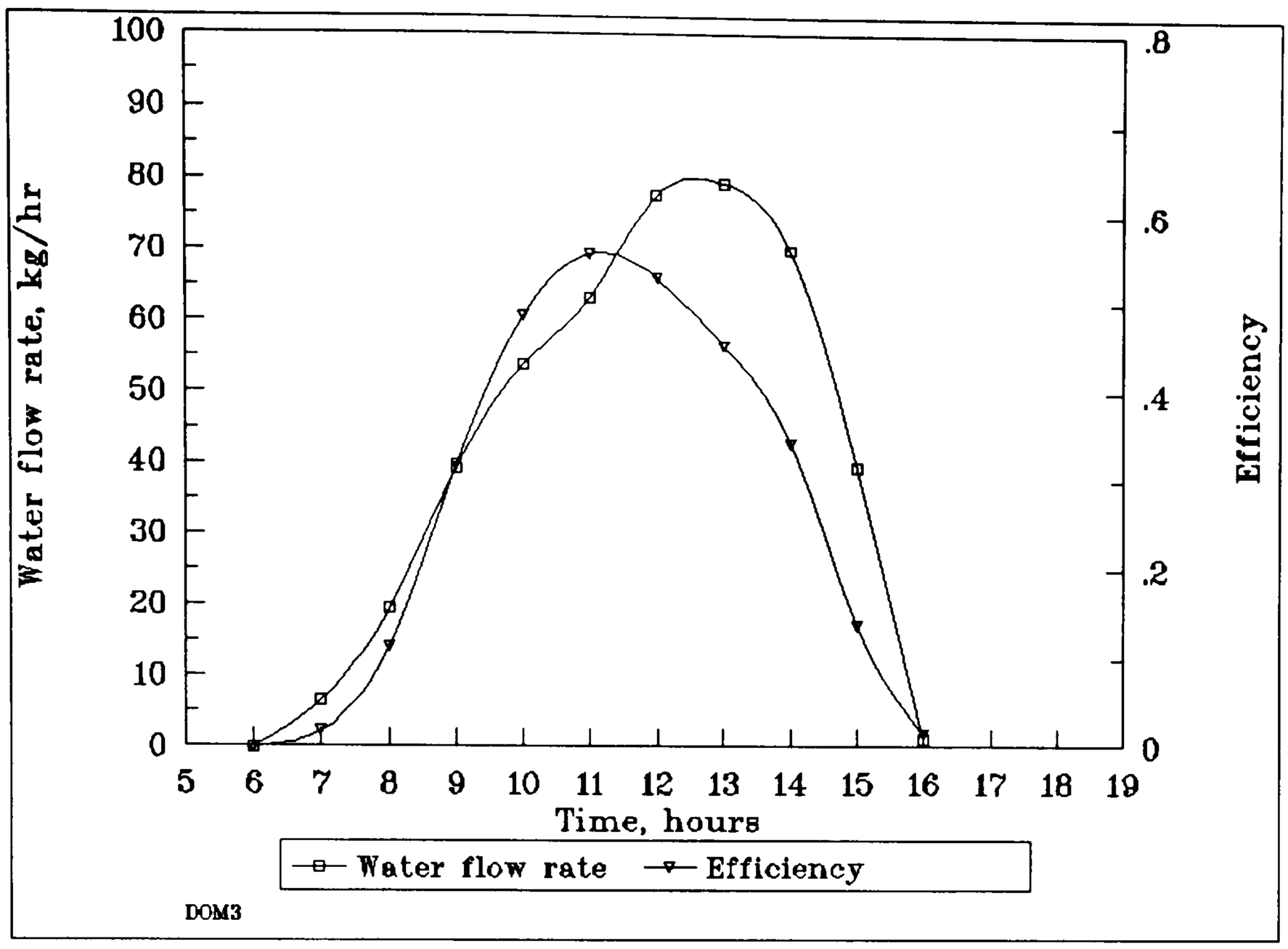

Fig. 4.13 Variation of thermosyphon water flow and efficiency with time, for consumption profile DOM3

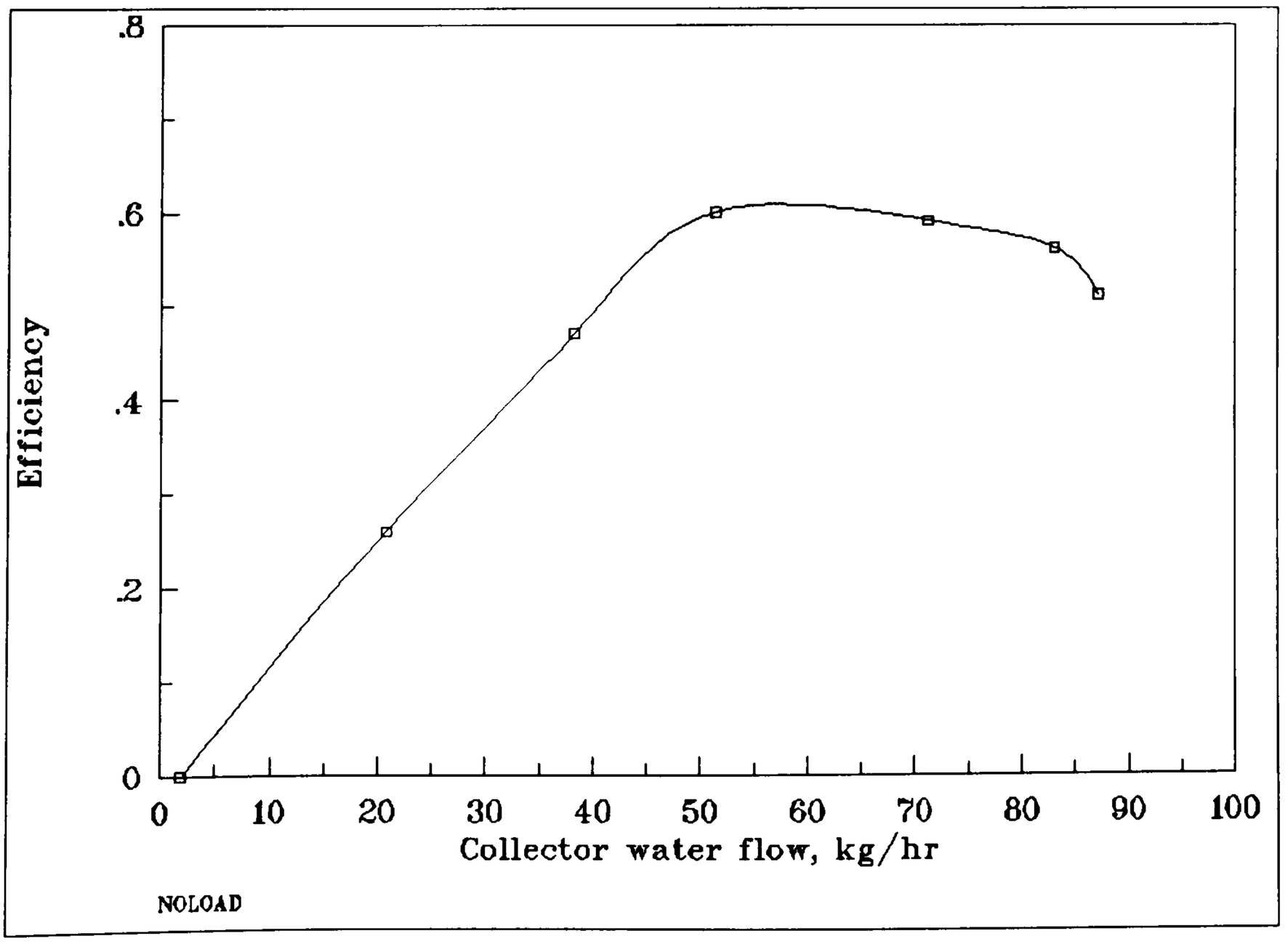

Fig. 4.14 Variation of efficiency with flow, without imposed load

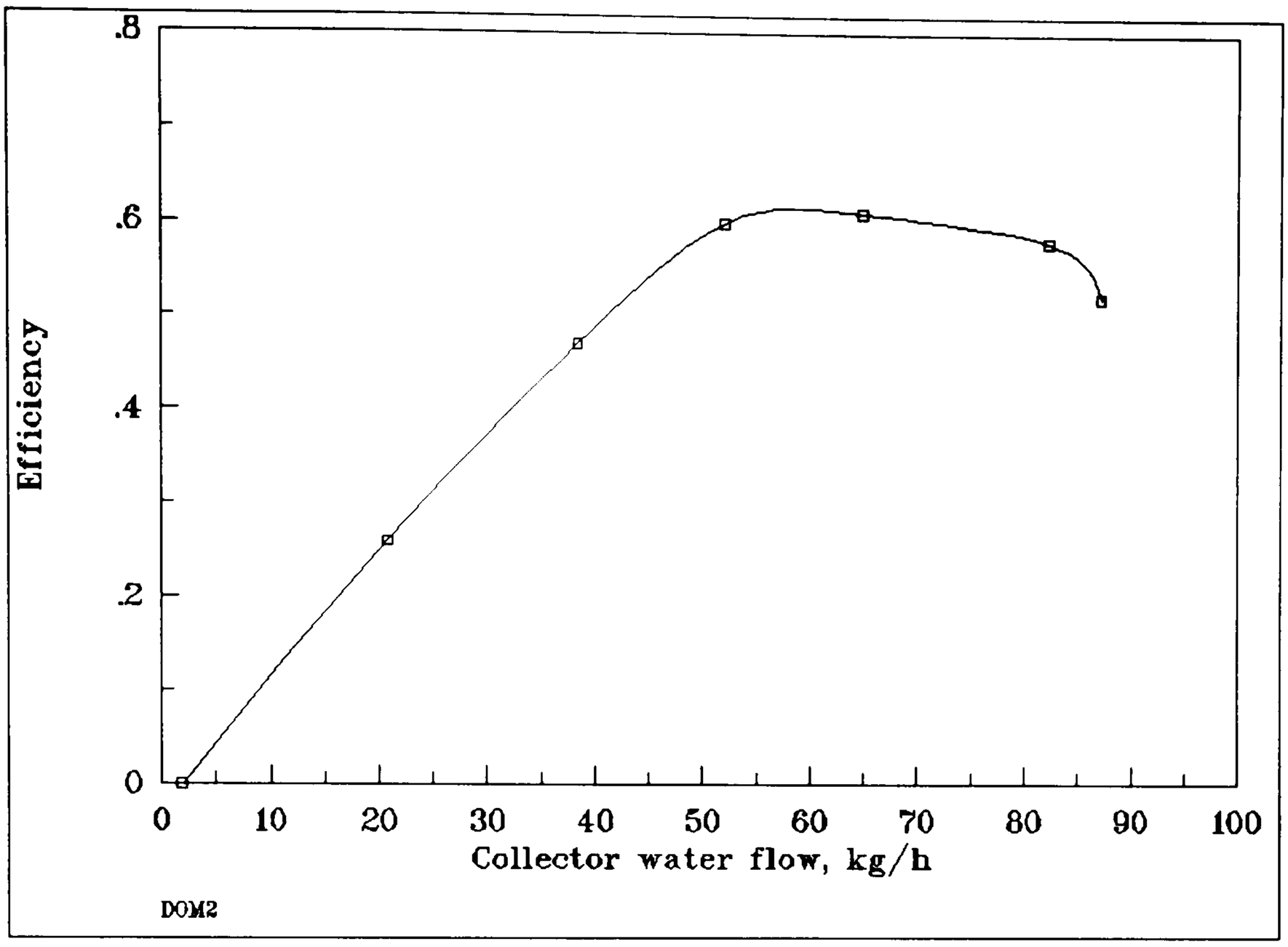

Fig. 4.15 Variation of efficiency with flow, for consumption profile DOM2

The variation of collector inlet and outlet temperatures and their difference, with time is shown in figs. 4.16 and 4.17 for the systems with and without water consumption respectively. It is clear from the figures that the collector temperatures start rising in the morning hours following the variation pattern of the solar radiation, but they reach their peak values at around 2.00 p.m. in the case with water consumption profile DOM2 (see fig. 4.16), and at 4.00 p.m. without imposed load (see fig. 4.17). The highest temperature was obtained for the system without load and reached 72 °C at the collector outlet, at 4.00 p.m. In the case of consumption profile DOM2 the maximum temperature attained at the collector outlet was 69 °C at 2.00 p.m. It is interesting to note that the temperature difference between the collector inlet and outlet starts rising in the morning to reach a maximum of about 18 K, in all cases, at 9 a.m and drops down in a slow rate afterwards until the next hot water draw off. The variation of the temperature difference follows the pattern of the variation of efficiency.

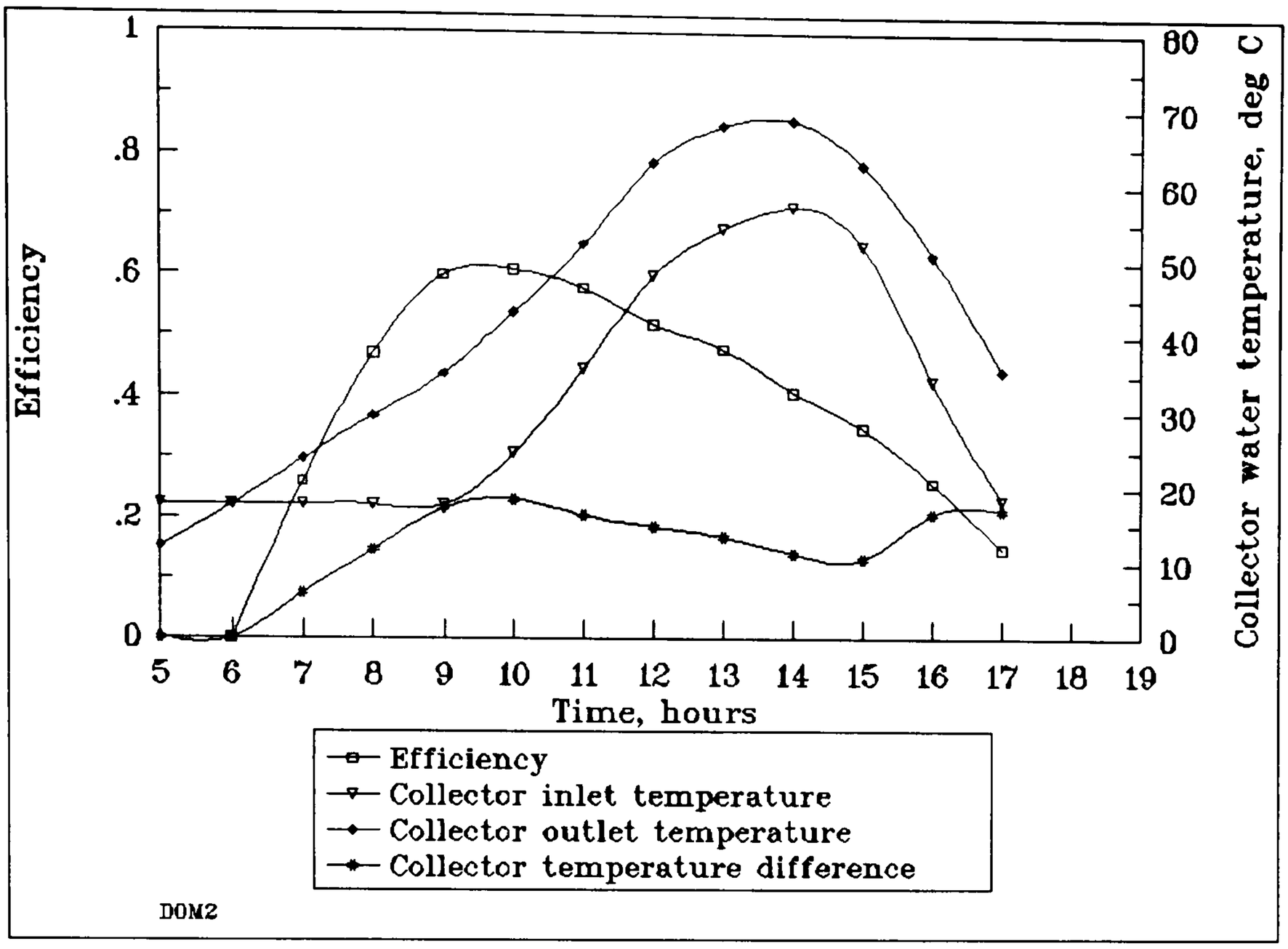

Fig. 4.16 Variation of collector water temperatures and efficiency with time, for consumption profile DOM2

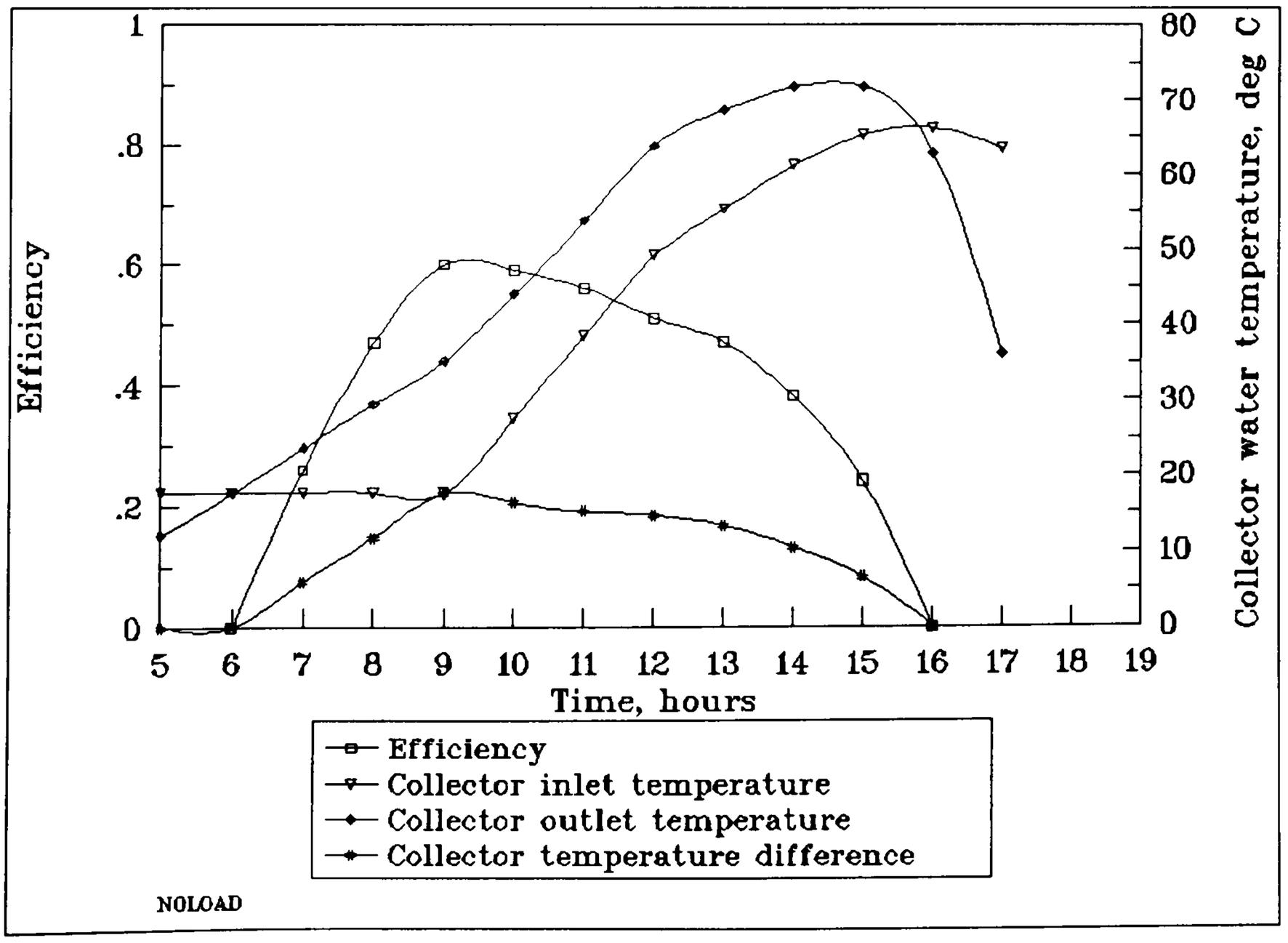

Fig. 4.17 Variation of collector water temperatures and efficiency with time, without imposed load

The variation of the annual solar contribution for the consumption profiles investigated are shown in fig. 4.18. In this figure, f, the solar fraction, is defined as the ratio of the useful solar energy supplied to the system and the energy needed to heat the water if no solar is used. In other words, f is a measure of the fractional energy saving relative to a conventional system. It must be noted here that these results assume the same daily load profile throughout the year. This is not quite true during the summer period, where the consumption pattern is somewhat higher. However, during this period, the hot water temperature requirements are not as high as those in winter. Consequently, the total thermal energy requirements is reasonably constant throughout the year. For the high profile consumption case (DOM4), the yearly solar fraction is approximately 63% as compared with 89% for the low profile consumption case (DOM1).

With reference to fig. 4.18, it must be noted that the useful energy collected during seven months of the year, namely April to October inclusive, is greater than the load in the case of the low consumption profile DOM1; in this case the solar fraction is taken as 1.

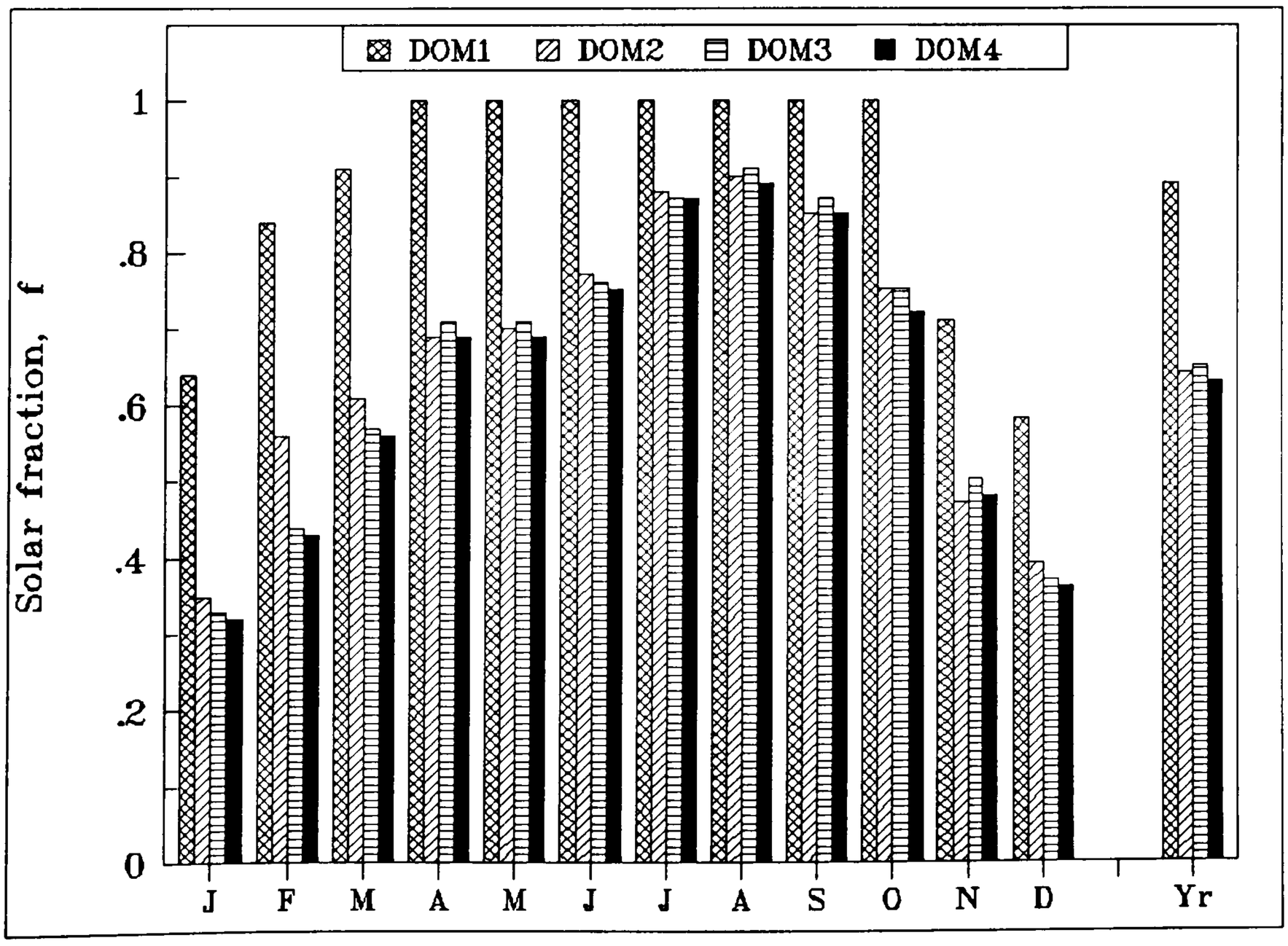

Fig. 4.18 Predicted solar fraction of a thermosyphon solar water heater at various hot water consumption profiles

With a high hot water consumption profile, the solar system never meets fully the hot water demand and the useful solar energy collected is fully utilised. This is not the case with the low consumption profile, where the solar fraction is greater than unity for a substantial period of the year. This means that the energy collected is greater than that required to meet the load and in fact, an amount of energy remains unused. In these cases the solar fraction is taken as unity.

The effect of the hourly distribution of hot water usage was investigated by simulating the annual performance of the system subject to four alternative hot water consumption patterns. The simulation results for these consumption profiles are shown in Table 4.4. and they indicate that TSWH systems are relatively insensitive to the hourly distribution of hot water usage. There is however a large difference in the case of profile DOM1 but this is due to the fact that the design hot water temperature is lower than that of the other cases.

Profile	Solar fraction	Payback period	
		Electricity	Diesel oil
DOM1	0.89	3	9
DOM2	0.63	2	7
DOM3	0.65	2	8
DOM4	0.64	2	8

Table 4.4 Predicted solar fraction and payback period for various consumption profiles

With regard to the economics of the system it is necessary to state the conditions under which the present simulation results were obtained. A thermosyphon solar water heater of the type described in this study costs about US$ 1000, and it also includes the cost for the supply and installation of a cold water tank and a supporting structure. However, when the cost of cold water tank and supporting structure as

well as the cost of additional storage capacity required by solar are subtracted, the incremental cost incurred by the solar system is about US$ 500. The cost of electricity is taken as 36 US$/GJ while that of diesel oil is taken as 7.4 US$/GJ. The economic parameters used in the simulation are shown in Table 4.5.

Parameter	Value	Parameter	Value
C_{FA}	36 US$/GJ	d	8%
C_{FL}	7.4 US$/GJ	M_S	1%
N_E	20 years	i	5%
D	30%	t	9%
m	9%	N_D	20 years
N_L	3 years	i_{FCF}	5%/yr
i_{FBUP}	5%/yr		

Table 4.5 Economic parameters used for the economic analysis

The simulation results concerning the economics of the system, with a low consumption profile and using electricity as the backup source of energy, are shown in Appendix B2. In this case, the annual energy requirements are 7.56 GJ. Under these conditions, the payback period, i.e the time needed for the cumulative fuel savings to equal the total initial investment, is 3 years. This means that it takes 3 years to get the investment back by savings in electricity. The rate of return on the solar investment is 81.7% and the annualized total cost with solar is 17 US$/GJ as compared to 53 US$/GJ without solar. With a high consumption profile like that of DOM2, the annual energy requirements are about 11.48 GJ and the payback period is reduced to 2 years. In this case, the rate of return is greater than 100%. It is therefore evident that the use of a thermosyphon solar water heater is a cost effective option as an alternative to electric water heaters.

The situation is somehow different when the comparison is with diesel oil. With a

low consumption profile, the payback period is 9 years and the rate of return on the solar investment is 10.4%. The annualized total cost with solar is 9 US$/GJ and the annualized energy cost without solar is 11 US$/GJ. With a high consumption profile, however, the payback period is reduced to 7 years and the rate of return on the solar investment increases to 16%. This implies that the thermosyphon solar water heater cannot compete with diesel–oil fired water heating systems. The predicted annual solar fractions for the consumption profiles studied and their corresponding payback periods are shown in Table 4.4.

4.5 Forced circulation systems

4.5.1 System description

The schematic diagram of the system to be employed is shown in fig. 4.19. It consists of a number of flat plate solar collectors, an insulated storage tank, a pump to circulate water from the collector to the storage tank, an auxiliary heating system in line with the taps and a number of controls to provide an efficient operation of the system. With regard to the auxiliary source of energy, it must be noted that two alternative solutions are investigated: diesel–oil fired boiler and electric immersion heater. The first alternative is associated with a high initial cost as compared to the second one which is cheaper to buy and install but more expensive to run. The system is designed to meet the hot water requirements of houses, blocks of flats, hotels, hotel apartments and hospitals.

4.5.2 System modelling

The performance of a SDHW system is dependent upon the prevailing weather conditions and the hot water consumption patterns. Both the energy collected and the load are functions of solar radiation, ambient air temperature, wind velocity and other meteorological variables which may be viewed as a set of time dependent forcing functions acting on the system. The system model should be formulated in such a way that all these factors will be taken into consideration when its performance is

investigated through computer simulations.

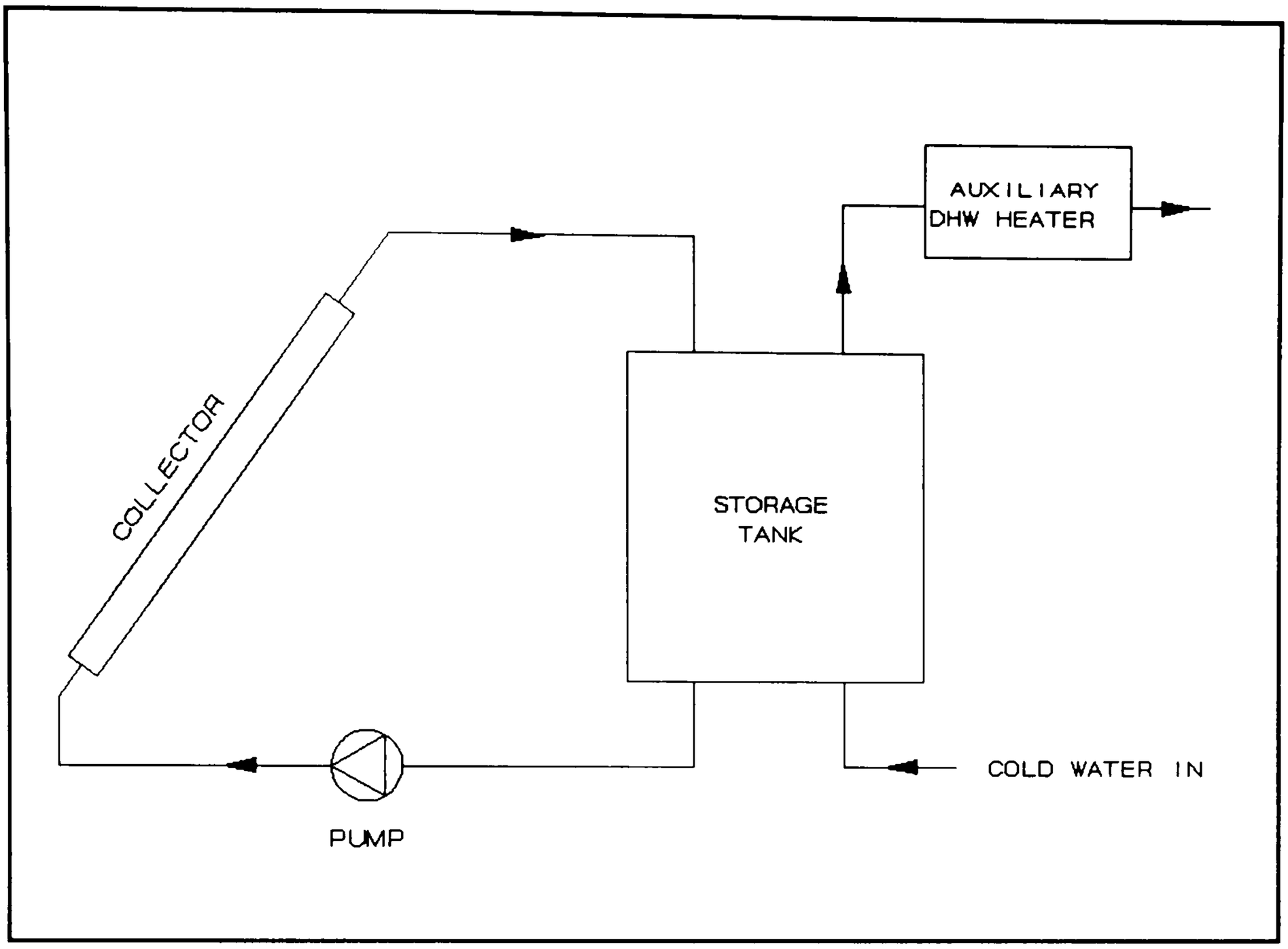

Fig. 4.19 Schematic diagram of the basic forced circulation solar hot water system

After referring to the TRNSYS manual, it was determined that the following component routines with the appropriate choice of inputs and parameters should be used to model the system:

(a) a TYPE 1 flat–plate solar collector;

(b) a TYPE 2 controller;

(c) a TYPE 3 pump;

(d) a TYPE 4 stratified storage tank;

(e) a TYPE 6 auxiliary heater ;

(f) a TYPE 14 load.

In addition to the above component models, there are certain other subroutines which have to be included in the model to facilitate the system simulation. Thus, a solar radiation processor, TYPE 16, should be included in order to convert the solar data into a form usable by the collector model. In order to calculate the monthly and yearly efficiency of the solar collector, the integrated quantities of solar radiation at

the collector tilt angle, and the useful energy gain of the collector are needed. Therefore, a quantity integrator TYPE 24 must also be included. The integrator must have a printer TYPE 25 attached to it to output the monthly integrated values. Finally, in order to evaluate the economics of the system, an economic analysis (TYPE 29) is needed.

The simulation input file JM2.DAT for the forced circulation solar water heating system under investigation is shown in Appendix C.

4.5.3 System design parameters

A large number of parameters are required as inputs to the system model. These include physical parameters, such as collector and storage tank size, as well as thermal parameters such as heat exchanger efficiencies and heat loss coefficients. A number of assumptions have been made for the system simulation, concerning the storage tank, solar collector configuration, pipe losses and controllers. The system is defined as having one, fully mixed storage tank at uniform temperature at any instant in time. The solar collector is defined as consisting of a single panel, regardless of the total area, and the working fluid in the collector loop is water. The collector loop circulating pump is activated whenever the collector outlet temperature is higher than the inlet temperature by a differential of 8–10 K. When modelling the pump controller in TRNSYS, a one degree dead band temperature difference is employed to prevent numerical instability (see Minnerly *et al.* 1991).

For the optimisation of the design parameters it is necessary to assume that the system will have to meet a certain load. Since forced circulation systems are mostly intended for large scale applications rather than residential, the system under investigation will concern a block of flats. Each flat is supposed to accommodate 4 persons, each consuming 40 litres of hot water at 50 °C daily as per consumption profile DOM4 (see Table 4.1 and fig. 4.4).

Whenever it is necessary to define the values of some parameters in the model in order to investigate the effect of varying another parameter, approximate values are

used. For example, for the investigation of the optimum tilt angle of the collector, it is necessary to specify the collector and storage tank sizes. Based on the thermosyphon system we may start the simulation with the assumption that 3 m^2 of collector will be adequate for each flat, for the purpose of the simulation. Thus the size of the collector will be taken as 30 m^2. Then, assuming a storage ratio of 50 litres per m^2 of collector, the storage tank should have a volume of 1500 litres of water. In a similar way all other parameters are defined and yearly simulations are run.

It is also important to note that the collector parameters concerning the performance characteristics of the flat–plate collector, i.e $F_R(\tau\alpha)_n$, F_RU_L and G_{test}, were investigated experimentally at the Collector Testing Centre of the Ministry of Commerce and Industry, according to CYS:119:1980 (CYS, 1980). Some of the parameters used in the simulation are shown in Table 4.6. The economic parameters used in the simulations are the same as those used for thermosyphon solar systems and are shown in Table 4.4.

$F_R(\tau\alpha)_n$	0.78
F_RU_L	24.4 kJ h^{-1} K^{-1} m^{-2}
G	50 kg h^{-1} m^{-2}
G_{test}	54 kg h^{-1} m^{-2}
b_o	0.1
β	To be optimised
ρ_g	0.2
U_s	1.2 kJ h^{-1} K^{-1} m^{-2}

Table 4.6 Simulation parameters for the forced circulation system

4.5.4 Optimisation of collector tilt angle

According to Duffie and Beckman (1980), the best surface azimuth angles for maximizing incident solar radiation are 0° in the northern hemisphere or 180° in the southern hemisphere and deviations of 20 or 30° have a small effect on total annual energy collection. The results obtained in the present study are based on the assumption that the collector is oriented due south.

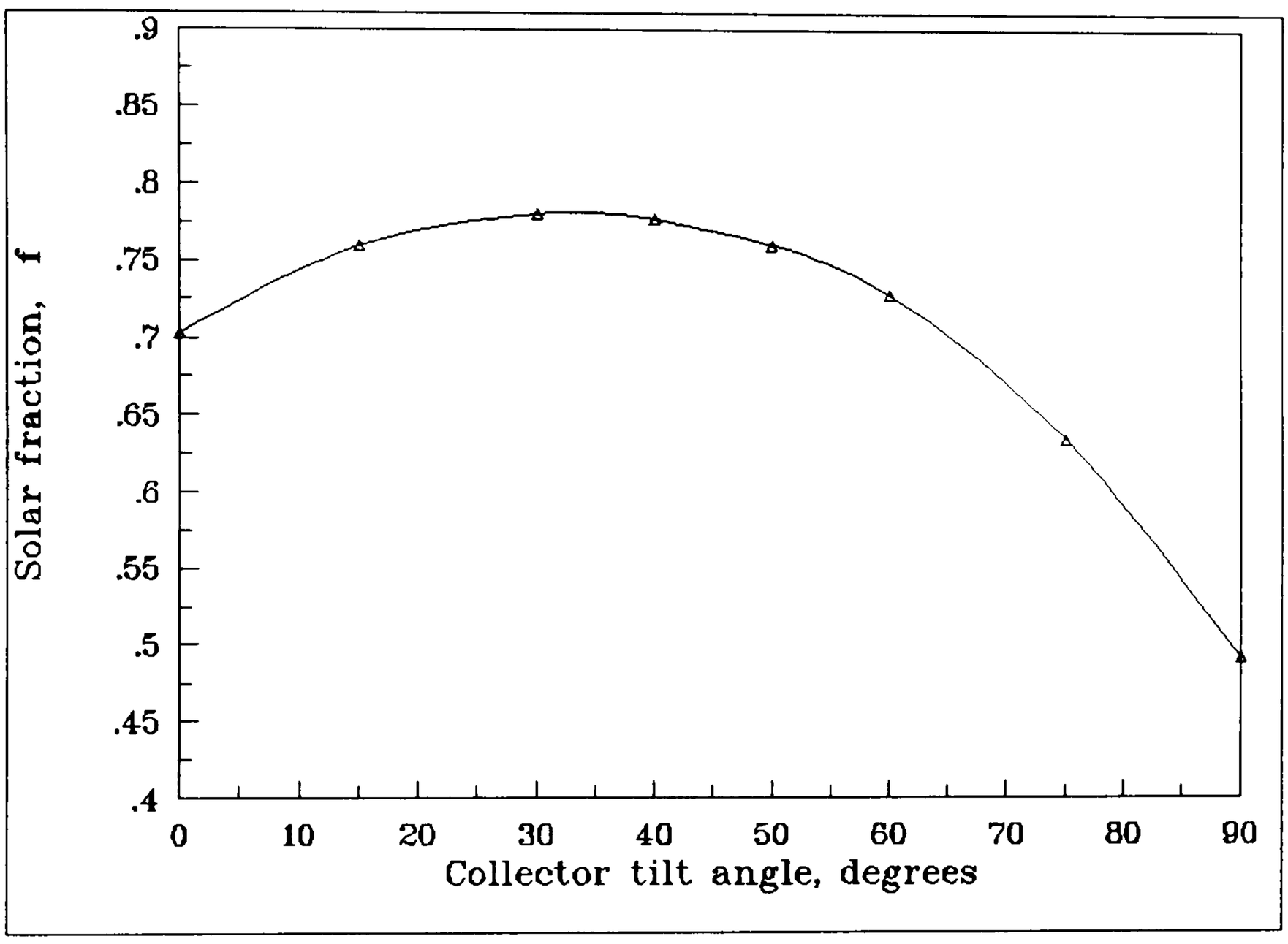

Fig. 4.20 Variation of yearly solar fraction with collector tilt angle

A number of simulations over a period of one year were run to obtain results for various collector tilt angles, ranging from 0° (horizontal) to 90° (vertical). These results were used to calculate the yearly solar fraction of the system. Fig. 4.20 shows the variation of the solar fraction with the collector tilt angle. It is evident from this figure that the system performance becomes maximum when the collector tilt angle is around 35° from the horizontal. Therefore, the optimum tilt angle is 35° and is equal to the latitude angle. It is also indicated that there is a range of values from 25° to 45° for which the system solar fraction is nearly as high as with 35°. This is in agreement with Felske (1978) who found that within ±10° of the optimum tilt angle, the collector performance is about the same. This is because at tilt angles between

25° to 45° the incident solar radiation falls on the collector almost perpendicularly, therefore minimising the reflected and maximising the transmitted and absorbed solar radiation components. For collector tilt angles beyond 50° from horizontal, the system solar fraction decreases dramatically with an increase in the tilt angle. This is attributed to the fact that the angle of incidence deviates from the normal direction of the collector surface resulting in higher reflection of solar radiation.

For subsequent simulations, the collector tilt angle is fixed at 35° from horizontal. This value is selected to represent good design practice.

4.5.5 Optimisation of collector size

With the collector tilt angle fixed to 35° from horizontal, a number of simulations were run to investigate the optimum size of the collector, i.e the surface area of the collector which will bring about maximum savings throughout the lifetime of the system. The annual solar fraction of the system and the collector average efficiency are also related to the collector area. The system was simulated at one hour time–steps.

The simulation results were used to plot the graphs of fig. 4.21 which show the variation of the system annual solar fraction, the system yearly average efficiency of solar energy collection and the system life cycle savings with the collector area.

It is interesting to observe the variation of the collector average efficiency with the collector area. A small collector area is associated with a high efficiency while a large collector area is associated with a low efficiency. This can be explained by the fact that in the case of small collector area the relatively high demand for hot water keeps the water temperature in the storage tank and thus in the collector inlet at low levels. As a result of this, the temperature difference between the collector and its environment is small, thus reducing the collector heat losses to low levels. On the other hand, if the collector area is large, the water in the storage tank will have a relatively higher temperature and consequently the collector heat losses will increase.

With regard to the system solar fraction, the situation is completely different. Solar fraction is low at small collector areas and it increases as the collector area increases. The rate of change is high at low collector areas and slows down at larger collector areas. However, larger sizes of collectors are associated with higher capital cost and the question which arises in such cases is what is the optimum economic size of the collector. This is investigated by the economic analysis which takes into consideration a number of economic parameters related to the system, similar with those used in the case of thermosyphon solar systems, including the costs of conventional and backup energy. The results of the simulations showed that the life cycle savings increase as the collector area increases to reach a maximum corresponding to a collector area of approximately 40 m^2 and then decreases as the collector area increases. Thus, the optimum collector size is approximately 40 m^2 which corresponds to 4 m^2 per flat or 1 m^2 per consumer (see also fig. 4.22). This is slightly greater than the case of a thermosyphon solar water heater where 3 m^2 of collector are used for a family of four, i.e. 0.75 m^2 per person.

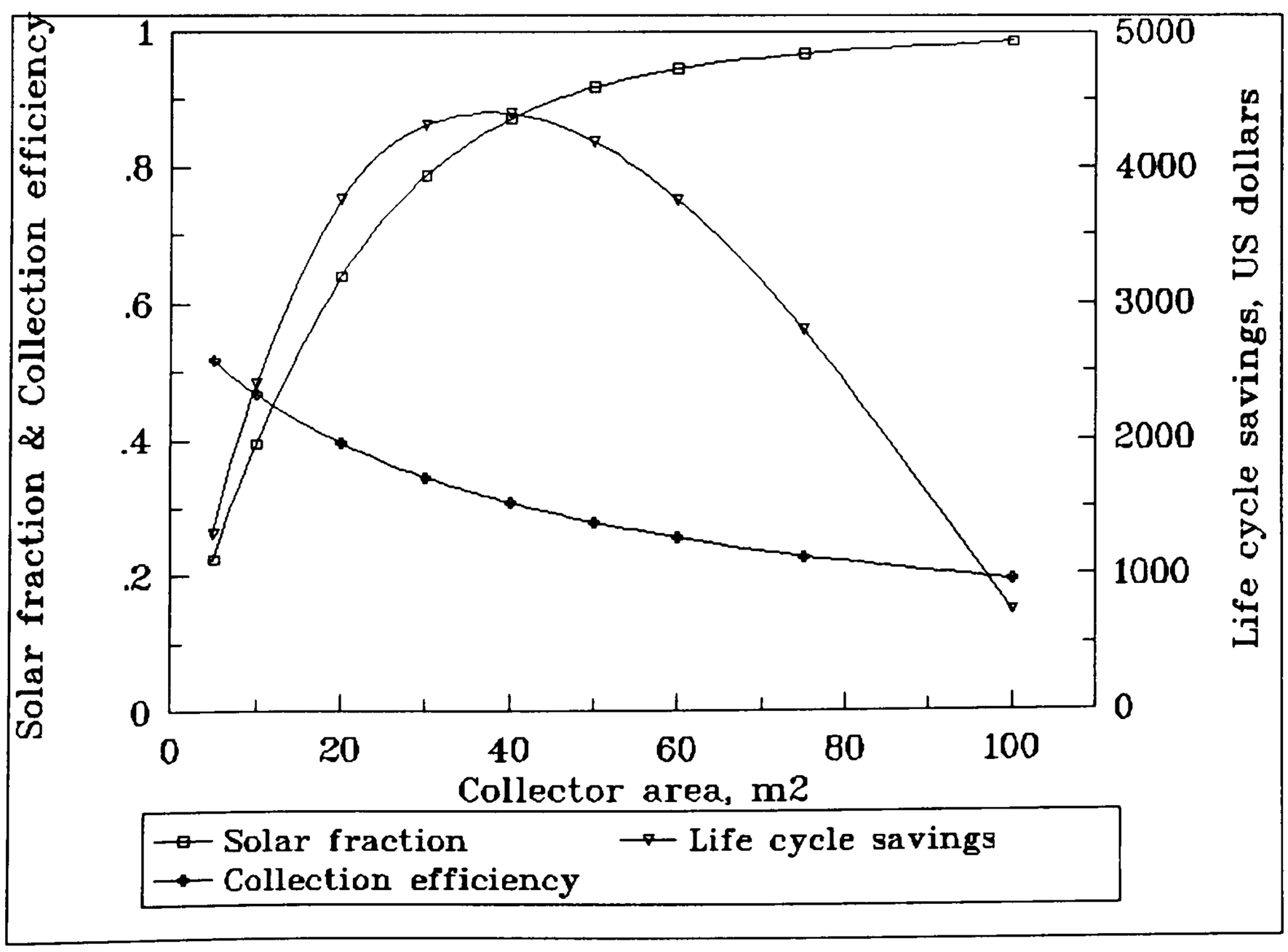

Fig. 4.21 Variation of annual solar fraction, average efficiency of collector and life cycle savings with the collector area

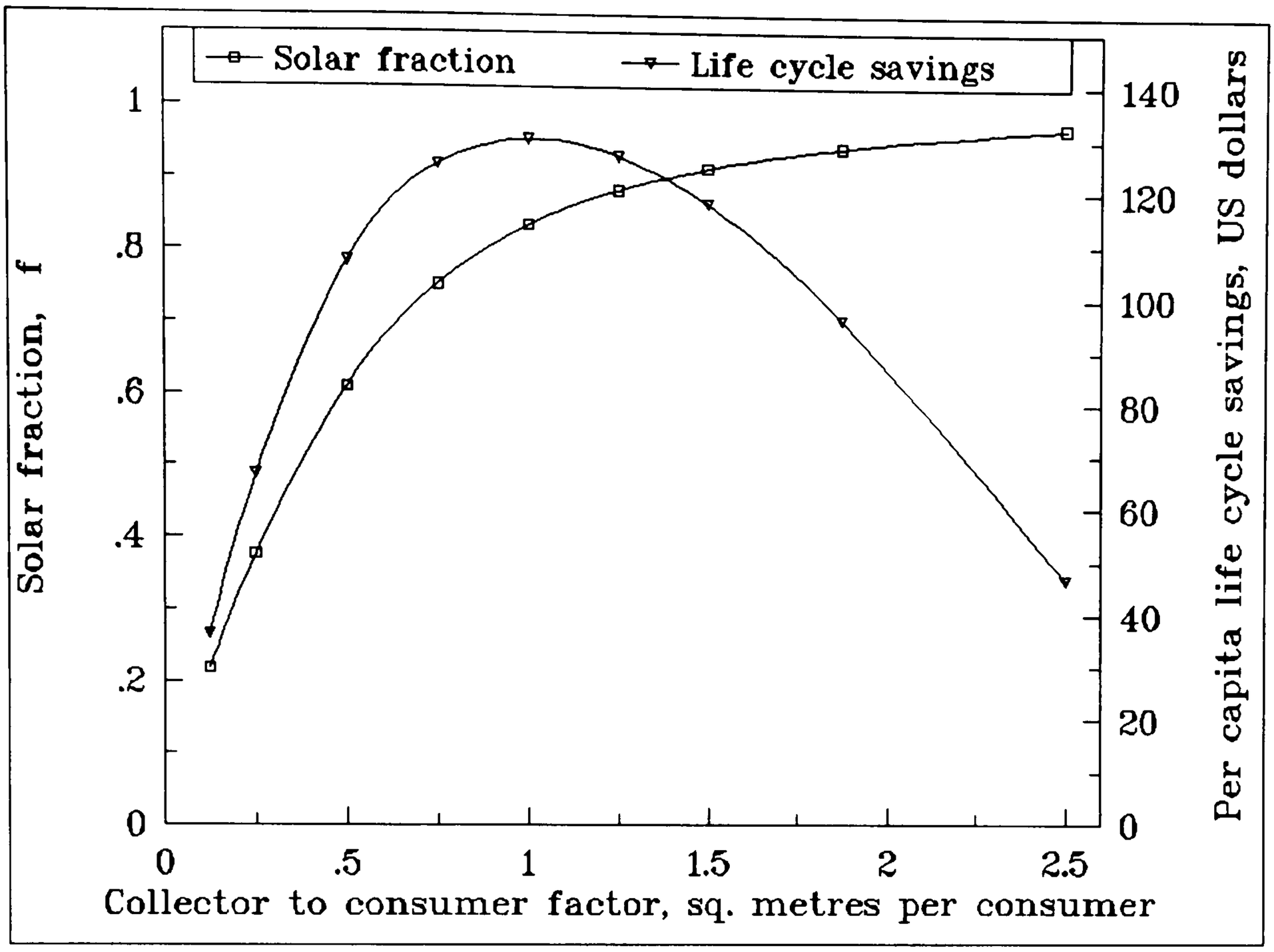

Fig. 4.22 Effect of collector to consumer factor F_{cc} on solar fraction and life cycle savings

The graph of fig. 4.22 can be used to estimate the collector area required to meet a pre-selected solar fraction, on the basis of number of consumers in the building. However, this approach assumes a certain hot water load imposed by each consumer, similar to that considered in the simulations, i.e DOM4. For this reason, and in order to relate the collector area directly to the load, the results of the simulations were used to correlate the solar fraction and the life cycle savings with the collector to load factor, F_{cl}, which is a dimensional factor relating the collector surface area to the annual hot water load. It is defined as the ratio of collector area over the hot water annual load and is expressed in m^2 per annual GJ.

This correlation is illustrated in fig. 4.23 which shows the variation of the system solar fraction and life cycle savings with F_{cl}. It is seen from this graph that the optimum collector to load factor is approximately 0.5 m^2 per annual GJ. This means that the optimum collector area required for each GJ of annual thermal load is 0.5 m^2.

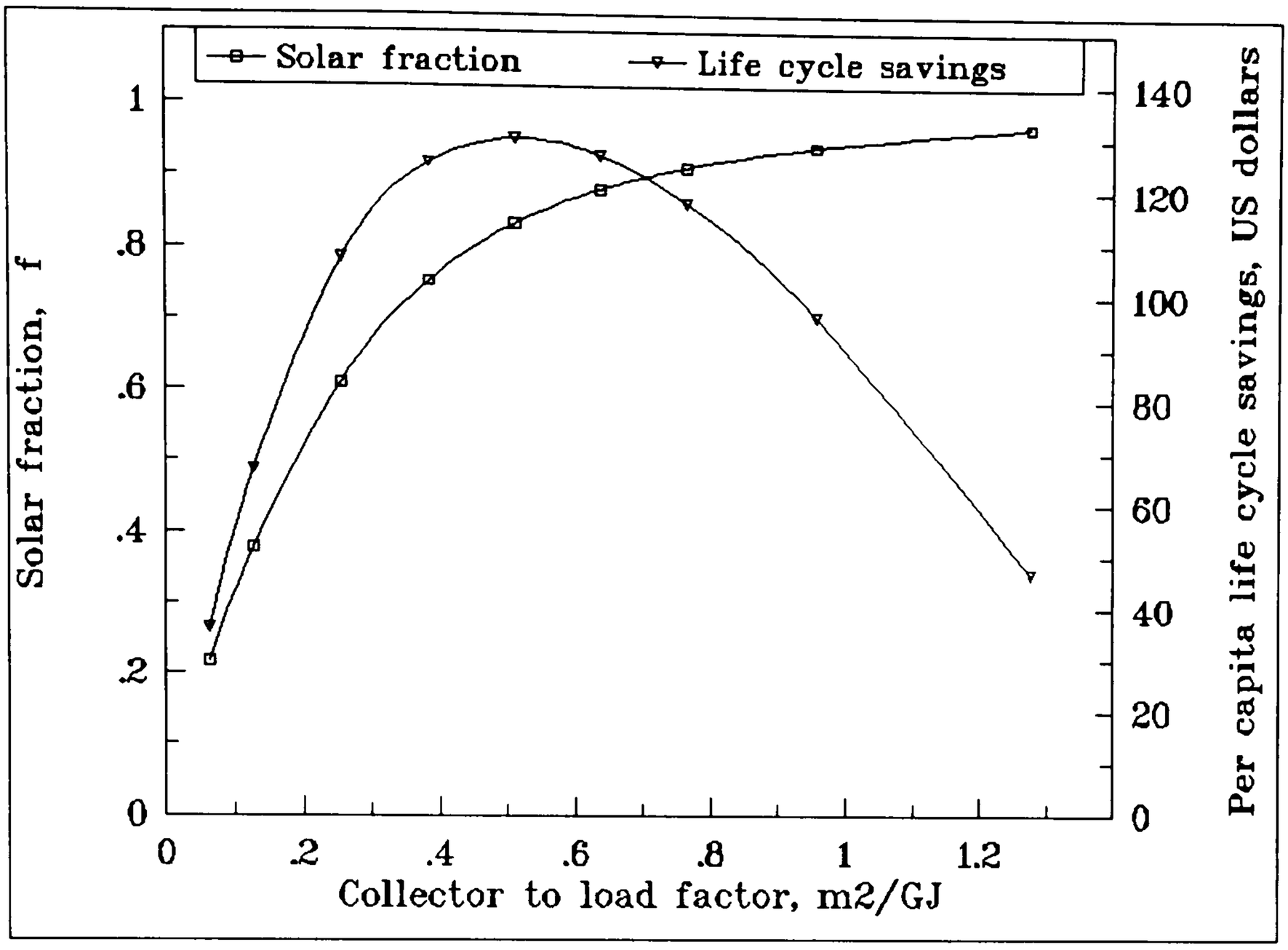

Fig. 4.23 Effect of collector to load factor, F_{cl}, on annual solar fraction and life cycle savings, for residential applications

Under the above optimum condition, i.e. 40 m^2 of collector coupled to a 2000 l storage tank, the collector average efficiency is about 31% and the system solar fraction is approximately 85%. The monthly average efficiency of collection of solar energy and the solar fraction of the system are shown in fig. 4.24. Under these conditions, where the backup fuel is diesel oil, the payback period is 8 years. This means that it takes 8 years to get the investment back by savings in fuel. The rate of return on the solar investment is 14.9% and the annualized total cost with solar is 13 US$/GJ as compared to 19 US$/GJ without solar. The situation is, however, different and in favour of solar when the comparison is done with electricity as backup energy, assuming the same collector area. The payback period in such a case is 4 years and the rate of return on the solar investment is greater than 100%. The annualized total cost with solar is 13 US$/GJ as compared to 40 US$/GJ without solar. The payback period is slightly greater than that reported by Michaelides *et al.* (1992) for thermosyphon solar water heating systems using electricity as backup energy. It is therefore evident that solar water heating is a cost effective option as an alternative to electric water heating but it is no competitive to a diesel–oil fired water heating system.

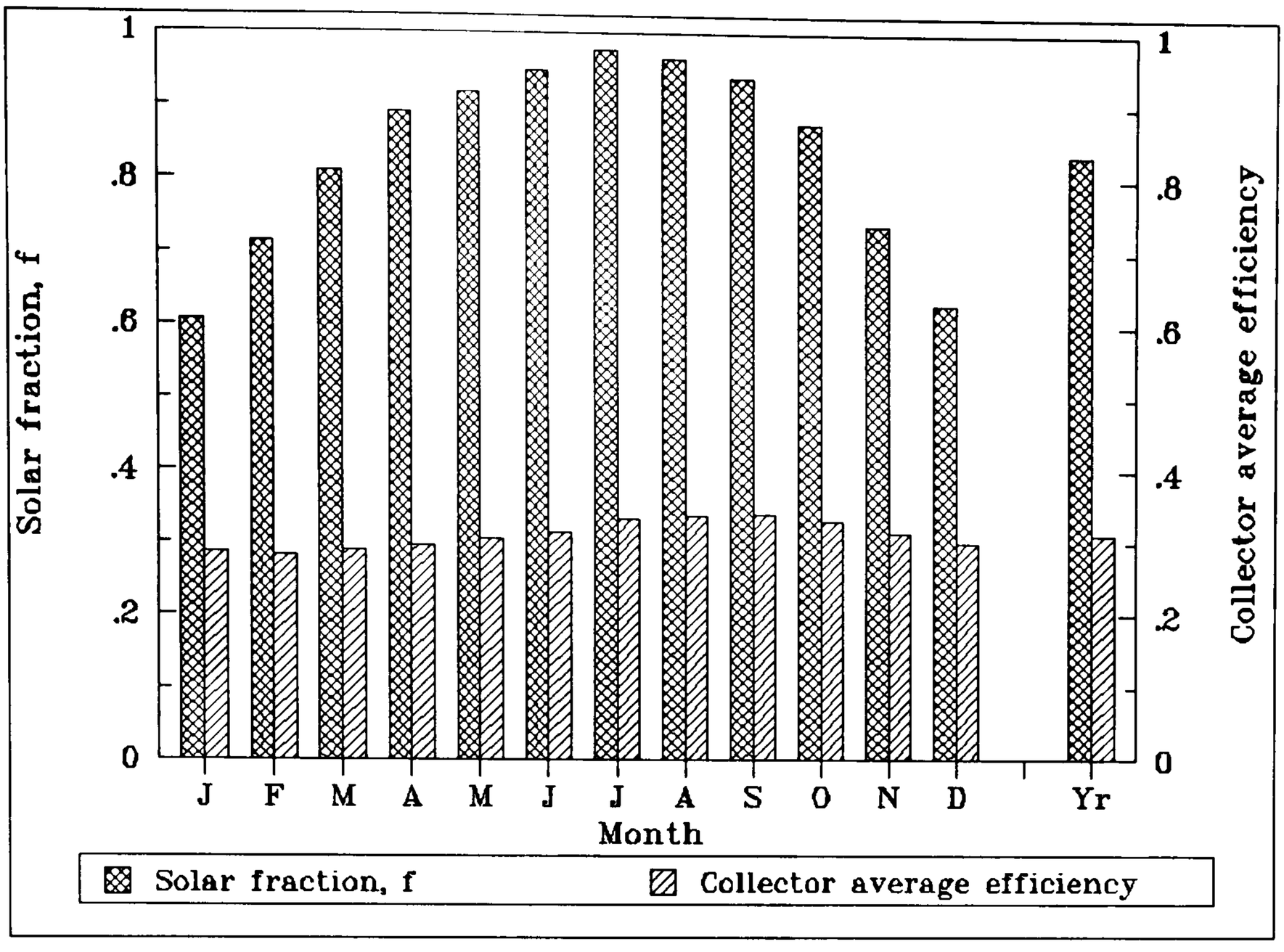

Fig. 4.24 Predicted monthly solar fraction and collector average efficiency at optimum collector area

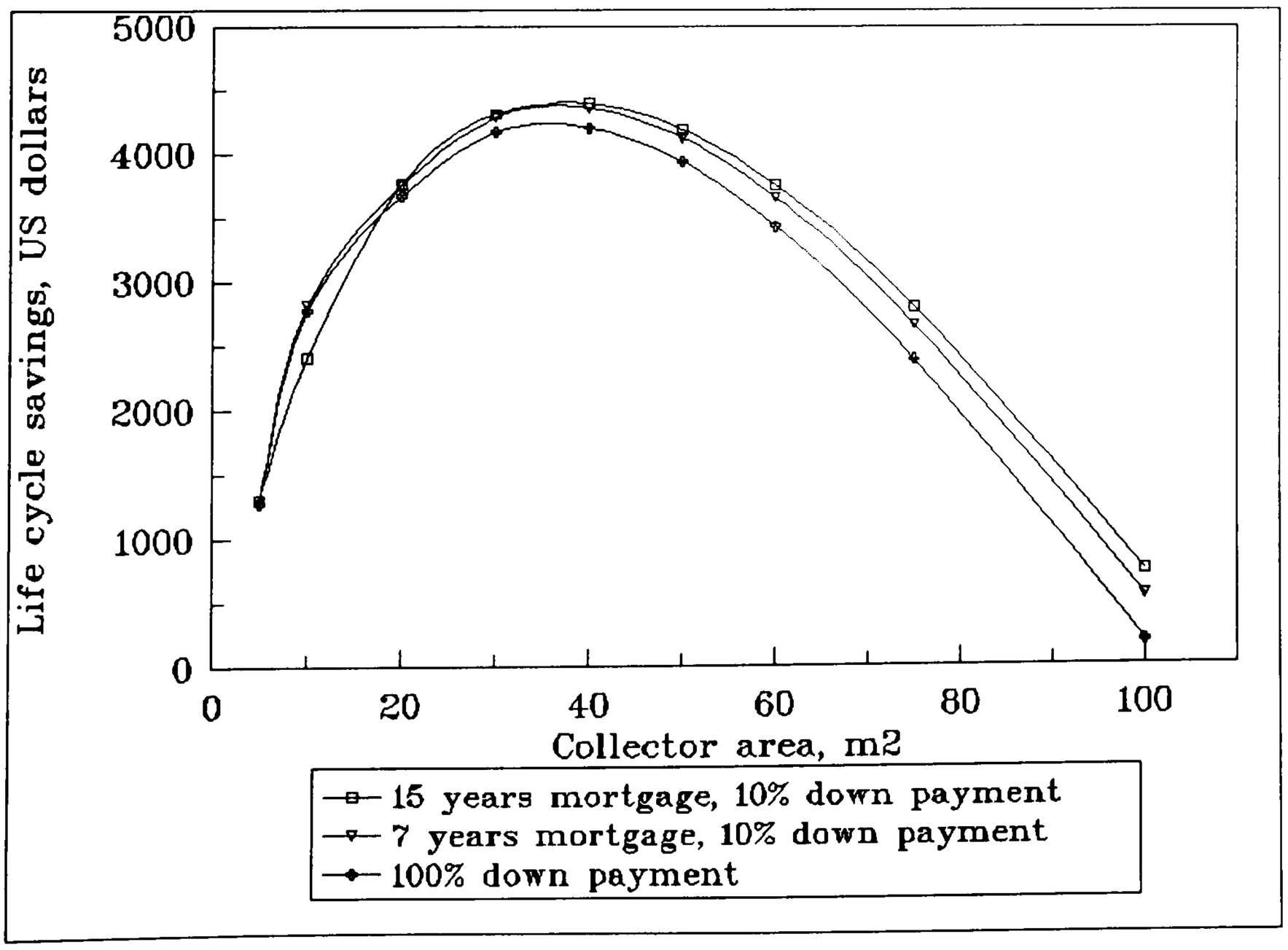

Fig. 4.25 Effect of mortgage period and down payment on life cycle savings

Another interesting piece of information is that the mortgage period does not bring significant changes in the optimisation of the system. This is illustrated in fig. 4.25 where life cycle savings are plotted against collector area for various terms of mortgage and payment, i.e. 15 years mortgage with 10% down payment, 7 years mortgage with 10% down payment and 100% down payment. There is a slight reduction in the life cycle savings in the case of 100% down payment but the optimum collector size is about the same in all three cases.

4.5.6 Optimisation of storage tank size

The sizing of the storage tank is equally important as the sizing of the collector. A small storage capacity, for example, will cause the collector to operate at reduced efficiency while a larger storage tank, which is associated to higher costs, will indirectly contribute to a higher collector efficiency. This is why the storage tank capacity is usually related to the collector aperture area by the parameter F_s which will be called the system heat storage factor and will represent the ratio of the storage tank capacity to the collector aperture area in litres per square metre. An economic study by Lof and Tybout (1973) suggests a storage capacity of 200 to 300 kJ m^{-2} K^{-1}. However, this is a wide range to be used for design purposes.

A number of simulations were run, using the optimum collector area tilted at 35°, to investigate the optimum storage factor for the system. The simulation results were used to plot the graphs of fig. 4.26 which relate the system solar fraction and its life cycle savings to the storage factor F_s.

It can be seen from fig. 4.26 that the solar fraction increases with the storage factor. However, the rate of increase is higher for storage factors in the range of zero to 40 l/m^2 and slows down for values greater than 50 l/m^2. This shows that storage factors higher than 50 l/m^2 are associated with high system performance. Considering the economics of the system, it can be easily seen that the system life cycle savings become maximum when the storage factor is approximately 50 l/m^2 which is the optimum storage factor. It is interesting to note that the life cycle savings decrease dramatically when the storage factor is reduced below 40 l/m^2 which is in agreement

with the solar fraction curve. This is explained by the fact that high storage capacities result in higher capital costs which outweigh the benefits from increased energy savings.

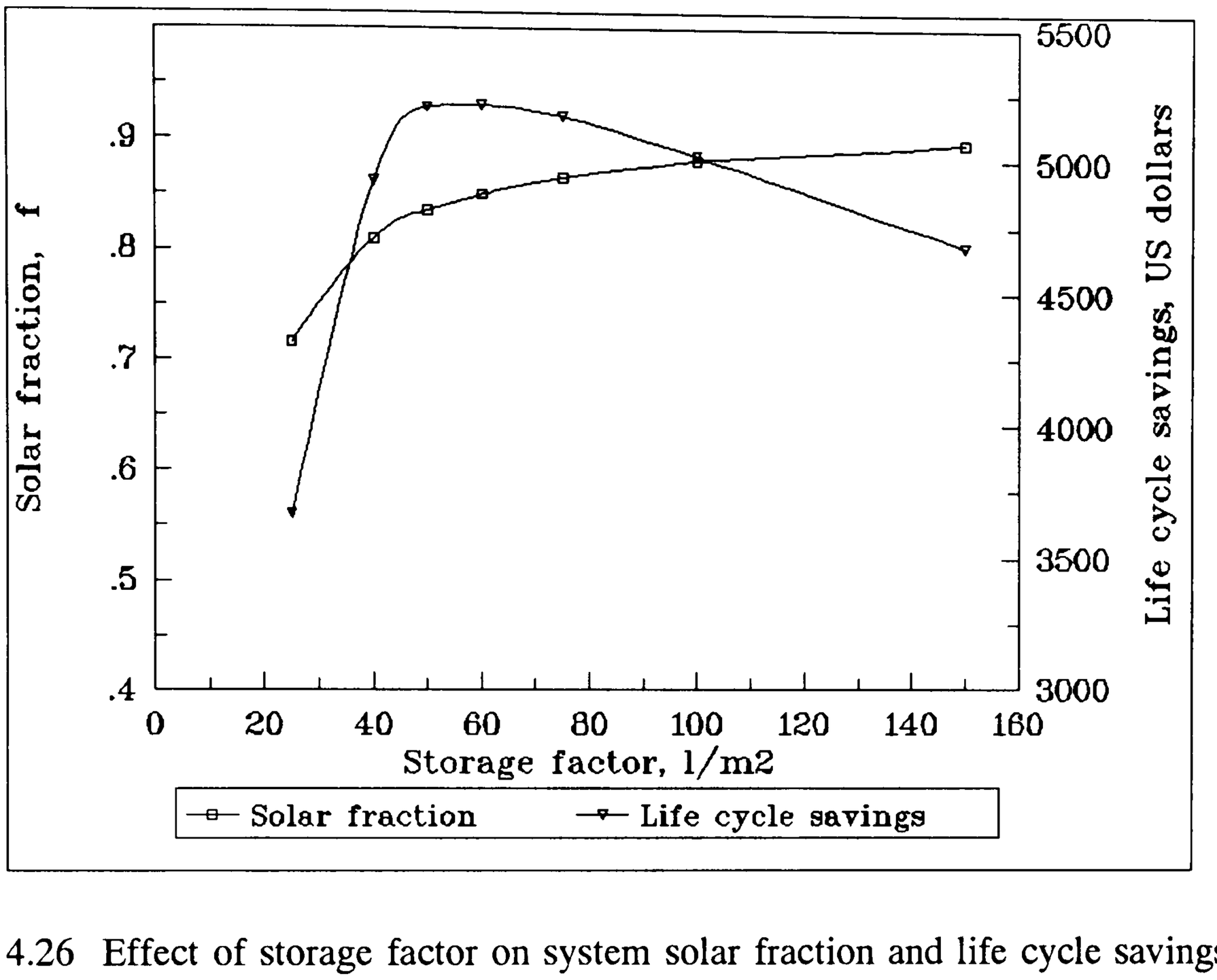

Fig. 4.26 Effect of storage factor on system solar fraction and life cycle savings

4.5.7 Effect of stratification in the storage tank

The previous simulations were run with the assumption that the storage tank is fully mixed. To investigate the effect of stratification, the storage tank is assumed to be divided into three separate, thoroughly mixed, isothermal layers of equal height. A number of simulations were run, keeping all the other parameters the same as with fully mixed simulation. The results of the simulations were used to plot the graphs of fig. 4.27 which demonstrates the differences in the results for stratified and fully mixed storage tanks.

It is interesting to note the difference between the average efficiency of collector in the two cases, where the case of stratified storage tank shows a superiority. This increase in the case of stratified storage tank is due to the reduced collector inlet

temperatures. The above results from the fact that in a three section tank the temperature of water at the lower level of the tank, which is the supply to the collector, is lower than that of the top. The reduced inlet temperature to collector causes a reduction in collector heat loss, and therefore a rise in collection efficiency.

An increased collector efficiency would have an effect on the system solar fraction which in fact shows a slight increase as compared to the case of fully mixed storage tank. This is clearly demonstrated in the same figure; however, the increase in the solar fraction is not as high as in the case of the collector efficiency. This is due to the increased heat losses from the top of the storage tank which is at a higher average temperature than the fully mixed case.

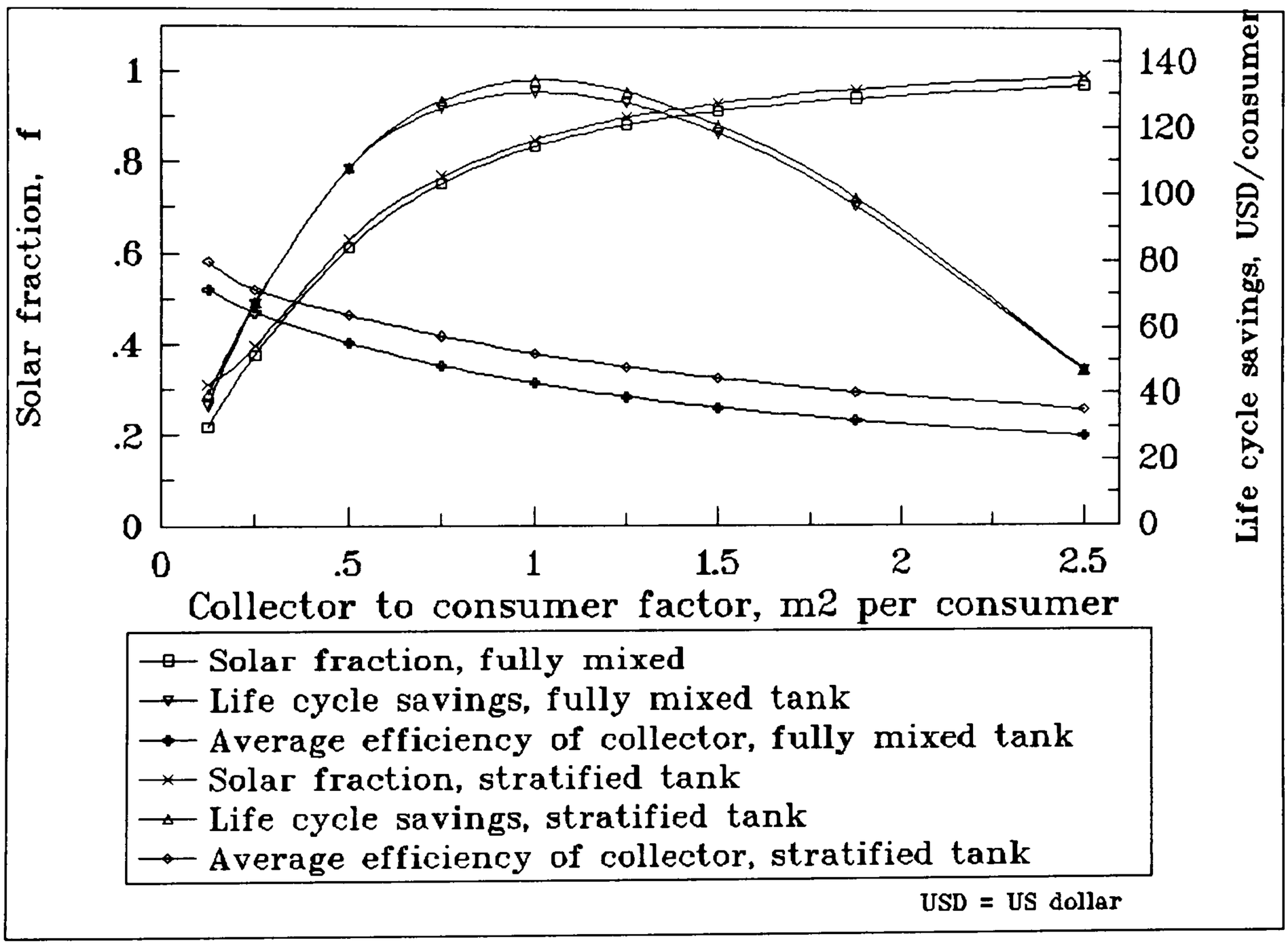

Fig. 4.27 Effect of stratification on solar fraction and life cycle savings

With regard to life cycle savings, the difference is slightly in favour of stratified storage tank. However, this slight increase does not bring a distinct change in the optimum collector area which is approximately the same as in the fully mixed case, i.e one square metre per consumer.

4.5.8 Optimisation of collector mass flux

In forced circulation systems like the one under investigation, there is always the question of water mass flow rate through the collector. It is evident that a very low flow rate will result to the development and maintenance of very high temperatures in the collector which will bring about a reduction in the collector efficiency and thus the cost effectiveness of the system. In the present study, the effect of flow rate on the system performance will be investigated in terms of the collector mass flux, G, which will be the ratio of flow rate through the collector to the collector aperture area and will be expressed in kg h^{-1} m^{-2}.

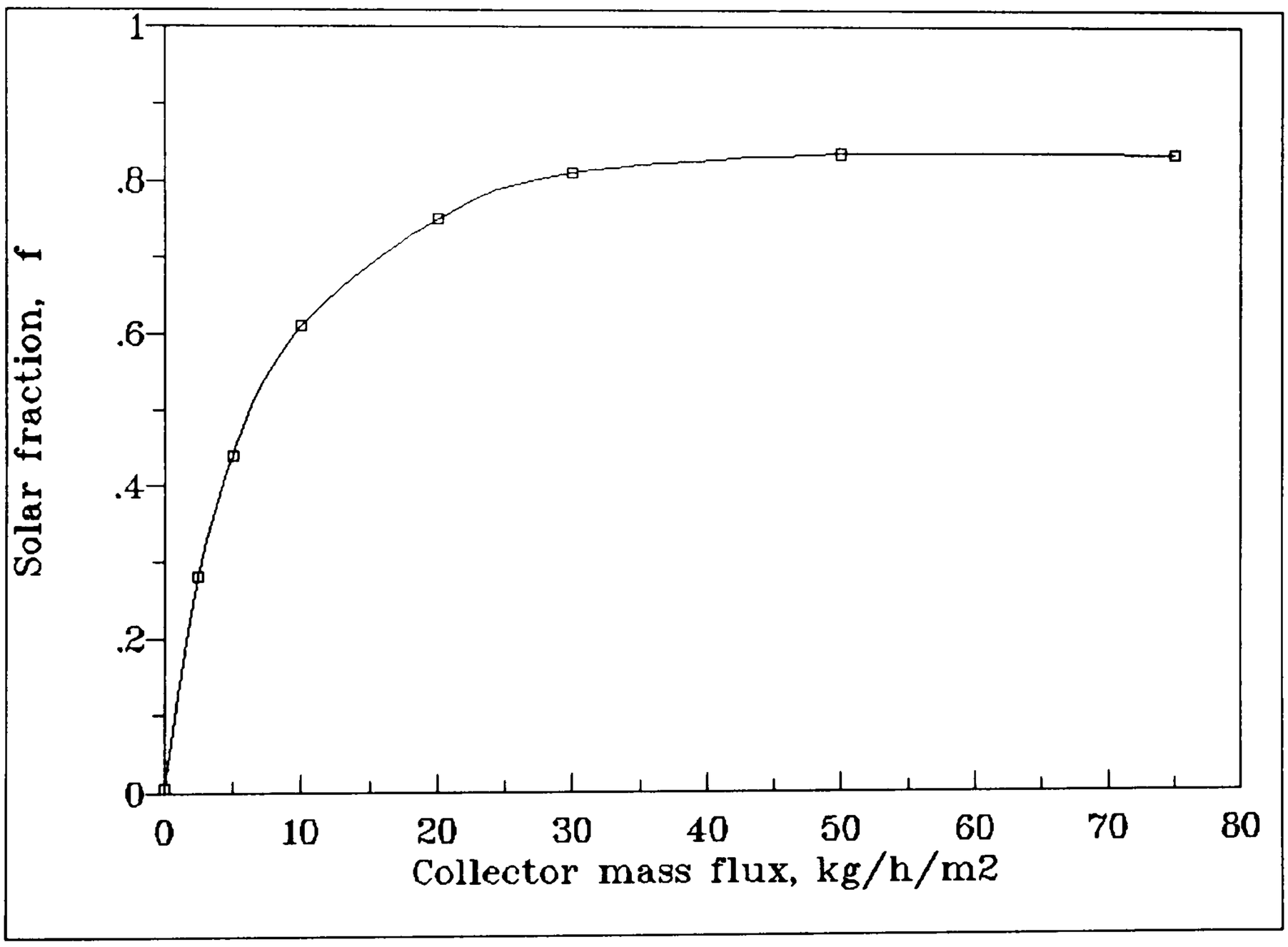

Fig. 4.28 Effect of the collector mass flux, G, on the system solar fraction

The system was simulated for different mass flow rates and the results were used to plot the graph of fig. 4.28 which shows the effect of varying the collector mass flux on the system solar fraction. It is clearly demonstrated that the solar fraction is very low when the collector mass flux is kept at low levels but it increases rapidly as G increases from 0 to 10 kg h^{-1} m^{-2} when it reaches a value of approximately 0.6. The solar fraction reaches a maximum of about 0.8 at 50 kg h^{-1} m^{-2} and then levels off as the collector mass flux increases.

4.5.9 Auxiliary heater

The degree of reliability of a solar water heating system to meet a certain load can be provided by a combination of properly sized collector and storage tank and an auxiliary energy source to back up the system in case of insufficient solar energy. The question which usually arises in dealing with this part of the system is what size of auxiliary heater and where to install it. The size is easily determined once the collector and storage tank sizes are decided. With regard to the positioning of the auxiliary energy unit, there are two possible arrangements:

(a) Built–in the storage tank, where the auxiliary energy source is integrated in the storage tank, and

(b) External, in line to the load, which requires a heater separate from the storage tank.

A set of simulations was done in order to examine the merits of each configuration. The results of these simulations were used to plot the graphs of fig. 4.29 and fig. 4.30 which compare the monthly average efficiency of collector and the system solar fraction respectively for the two arrangements. It is clearly shown that the arrangement with external auxiliary unit has a higher collector efficiency and is definitely superior to the built–in configuration. This is explained by the fact that the system uses the maximum possible solar energy from the storage tank without driving up the collector temperature. The storage tank is maintained at lower temperatures as compared to the built–in configuration where it is continuously kept at the design set temperature, thus resulting to higher heat losses. This is more distinct in the case of winter months where the difference in heat losses is much greater than the yearly average. This is because in winter the temperature difference between the storage tank and its surrounding is higher than that occurring in summer.

Another interesting piece of information is that with external auxiliary the fluctuation of the collector average efficiency throughout the year is smaller than that for the case with the built–in auxiliary heater. It fluctuates between 28% and 33% as compared to 18% and 32% in the built–in auxiliary configuration.

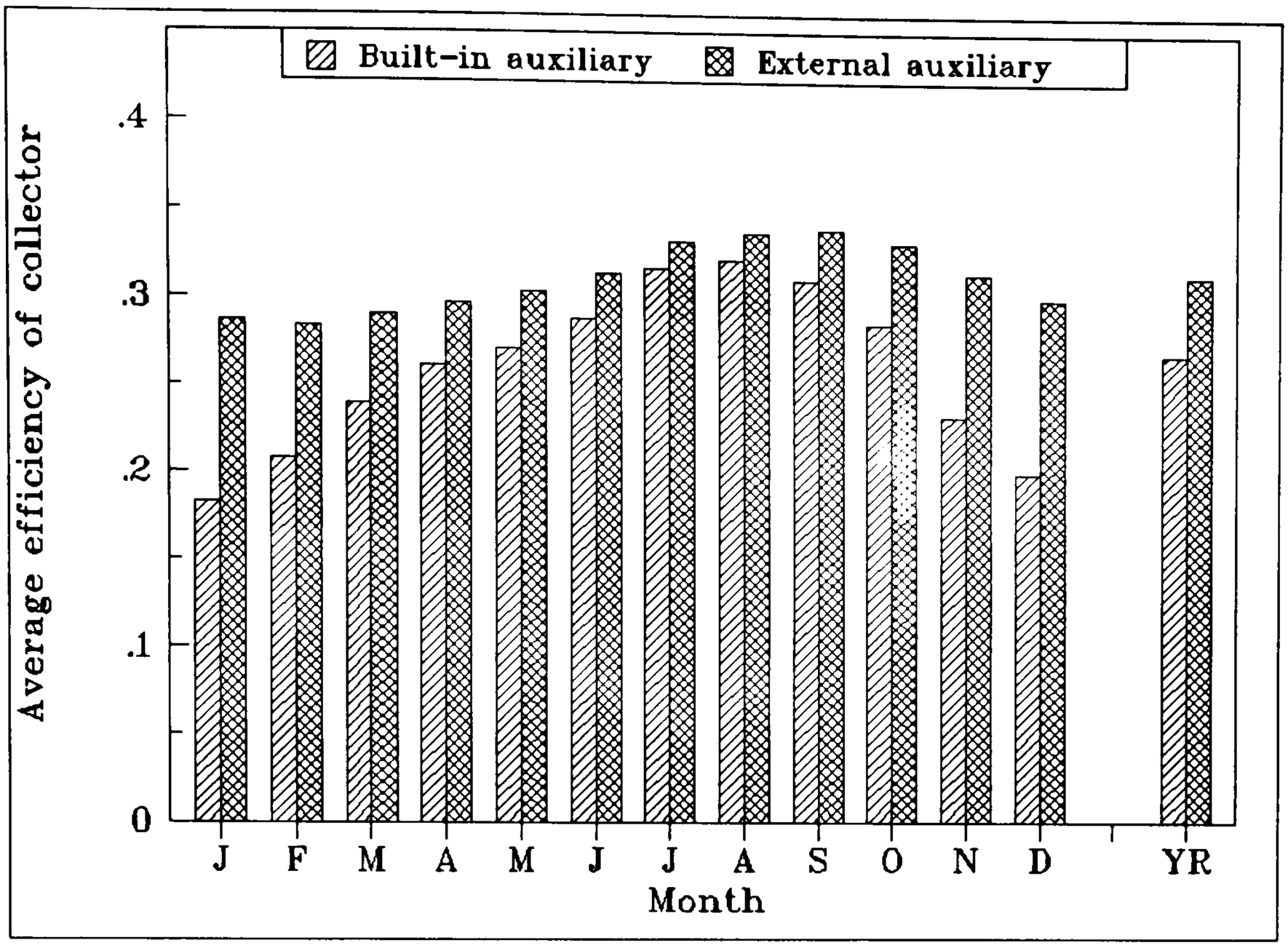

Fig. 4.29 Variation of collector average efficiency in built-in and external auxiliary configuration

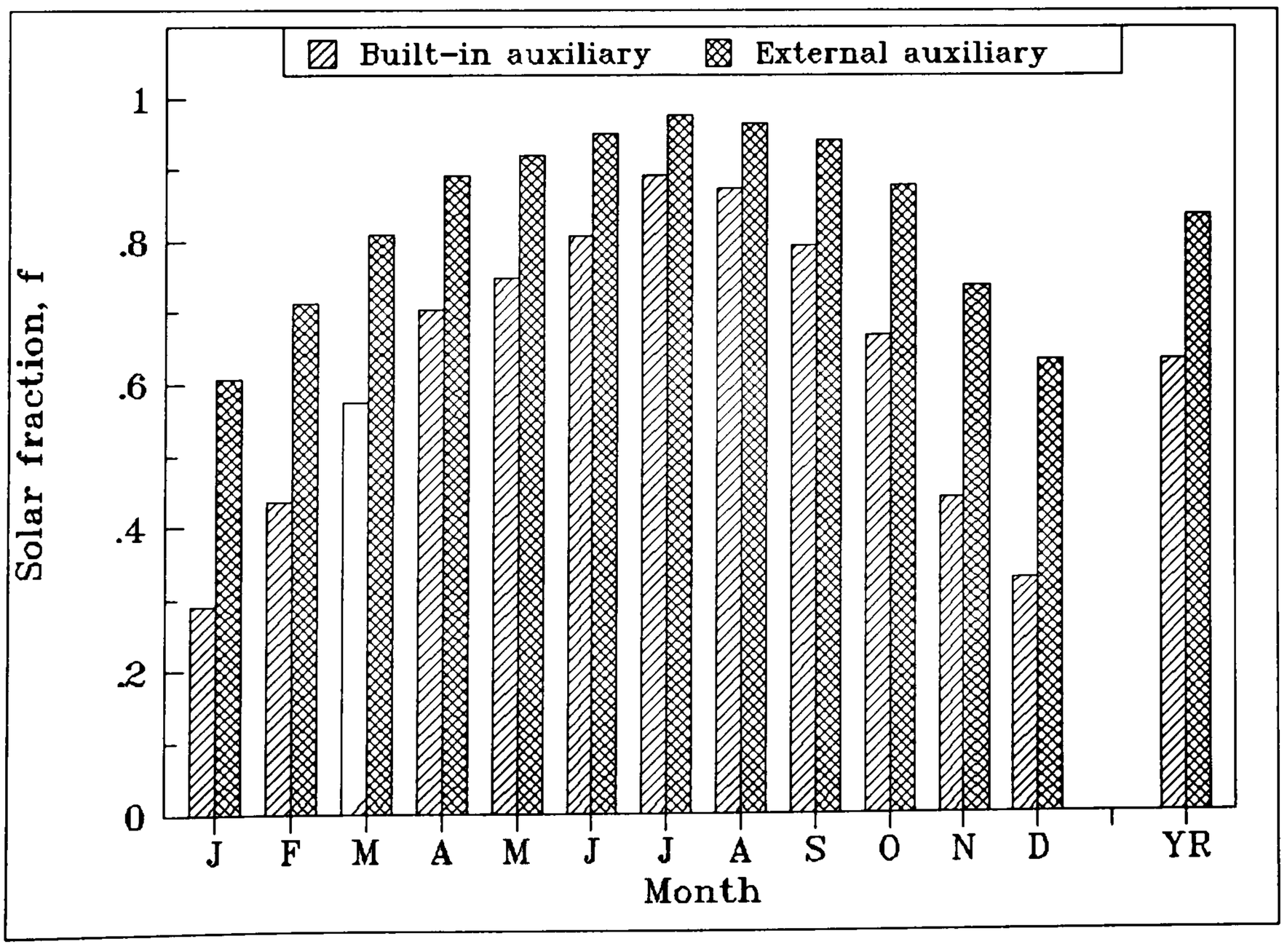

Fig. 4.30 Variation of system solar fraction in built-in and external auxiliary configurations

The effect on the solar fraction is demonstrated in fig. 4.30 where the superiority of external auxiliary is very distinct and is in agreement with that of the collector efficiency. It is interesting, however, to note the great difference in favour of external auxiliary, during winter months where the solar fraction in January for example is two times greater than the solar fraction of the system employing a built–in auxiliary unit.

4.5.10 Optimisation of collector size for hotel applications

The forced circulation solar water heating system used for the simulation of residential applications could also be employed for the production of service hot water in hotels. The question which usually arises in this category of applications is whether solar is a cost effective alternative as compared to conventional methods of water heating which employ oil–fired boilers and hot water calorifiers. A set of simulations was done to investigate the optimum collector area factor for such an application and predict the performance of such systems at different hot water consumption scenarios.

The parameters used in these simulations are those used in the simulations of residential applications, the only difference being in the hot water consumption patterns. Three sets of simulations were run, one for each hot water load profile applicable to hotels, i.e. HOT1, HOT2 and HOT3 described at the beginning of this chapter (see Table 4.1 and figs. 4.5 – 4.7). The parameters used for the economic analysis were identical for all scenarios for the purpose of comparison. The simulation results were used to plot the graphs of fig. 4.31 which shows the variation of annual solar fraction and per capita life cycle savings with the collector to consumer factor F_{cc} for the three scenarios.

It is interesting to note that the solar fraction increases with collector area . The situation, however, is not the same with the life cycle savings which reach a maximum corresponding to about 0.8 m^2 per consumer for the low load profile HOT1, 1 m^2 per consumer for the medium load profile HOT2 and 1.2 m^2 per consumer for the high load profile HOT3. This means that the optimum collector to

consumer factors are 0.8, 1 and 1.2 m^2 per consumer respectively for the low, the medium and the high hotel load profiles, as compared to 1 m^2 per consumer in residential applications.

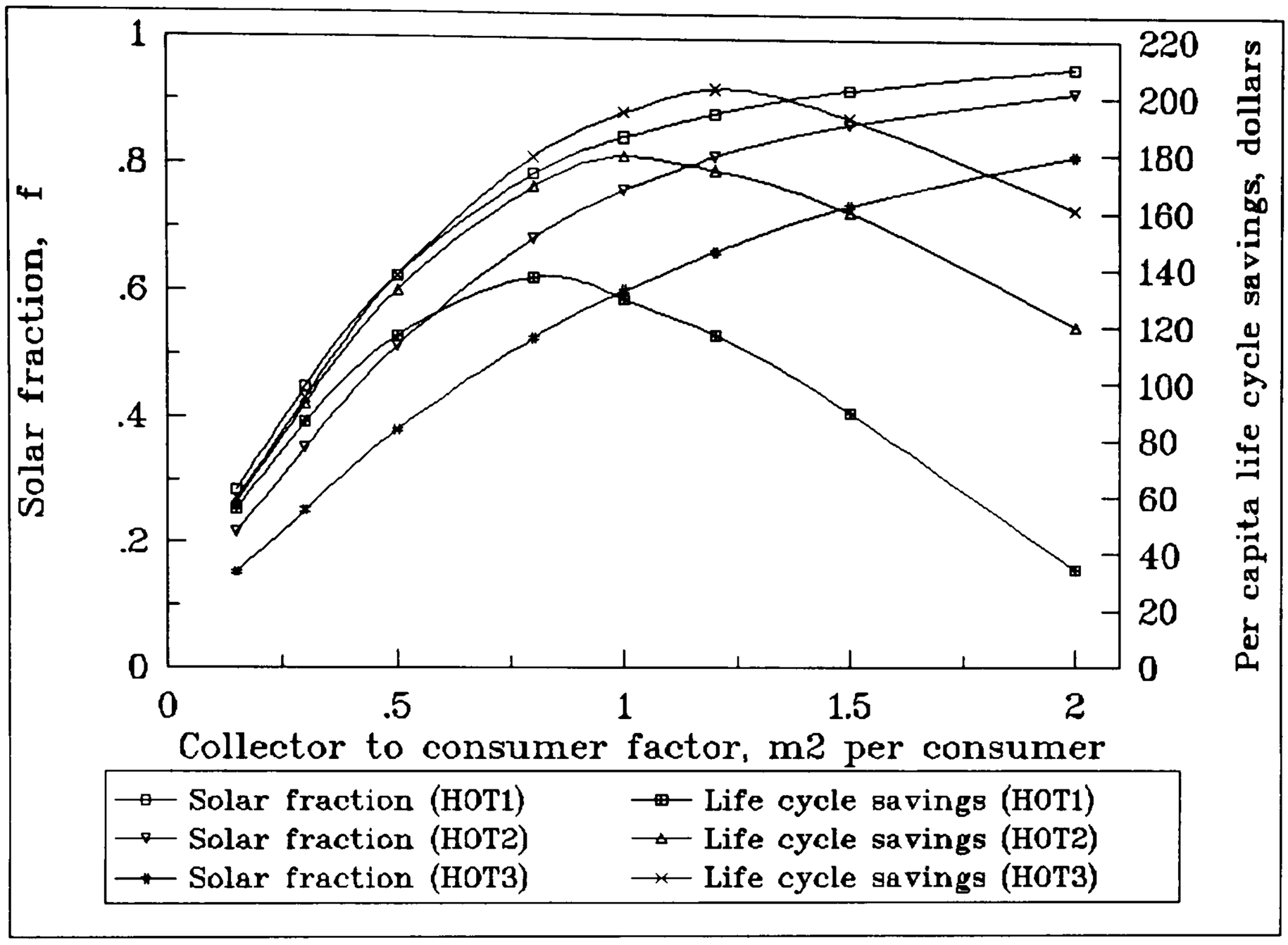

Fig. 4.31 Optimisation of collector to consumer factor, F_{cc}, for hotel applications

As in the case of residential solar water heating, the above graphs can be used to determine the collector size for a pre–selected annual solar fraction, provided that the consumption pattern is one of those used in the simulations or similar to them. However, for the reasons explained in the case of residential applications, it is also useful to relate the solar fraction and life cycle savings to the dimensional factor F_{cl} which involves the collector size and the annual hot water load. For this purpose, the results of simulations were used to plot three additional graphs, namely figs. 4.32, 4.33 and 4.34, which show the variation of the annual solar fraction and life cycle savings with the collector to load factor F_{cl}, for low, medium and high load profiles respectively. From the above figures it can be seen that the value of F_{cl} for the low load profile HOT1 is about 0.4 m^2 per annual GJ (see fig. 4.32), F_{cl} for load profile HOT2 is approximately 0.35 m^2 per annual GJ (see fig. 4.33), and that of the high load profile HOT3 is approximately 0.3 m^2 per annual GJ (see fig. 4.34) which show that the optimum collector sizes are different and are dependent on the load profile.

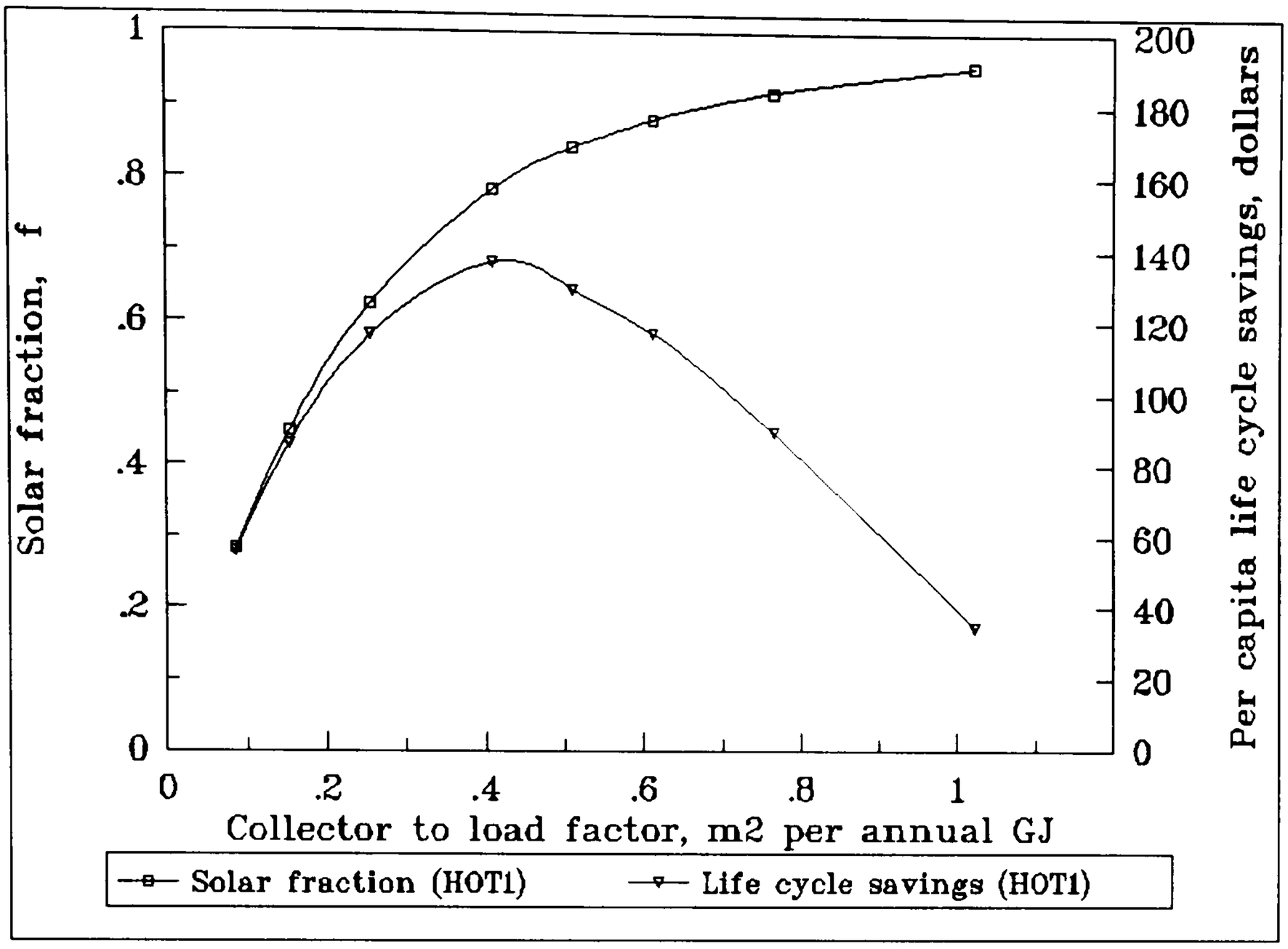

Fig. 4.32 Optimisation of collector to load factor, F_{cl}, for hotel applications of low load profile HOT1

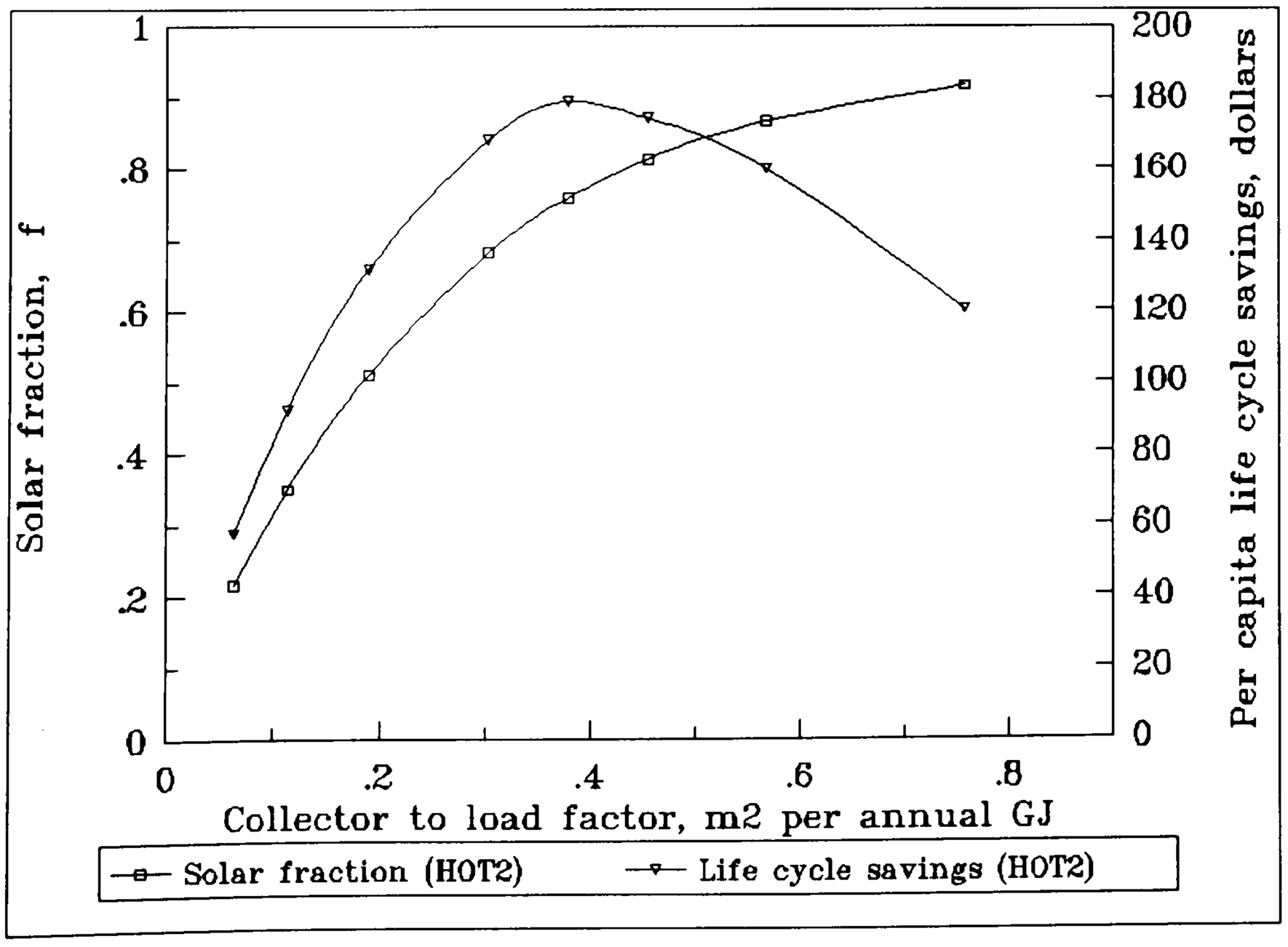

Fig. 4.33 Optimisation of collector to load factor, F_{cl}, for hotel applications of low load profile HOT2

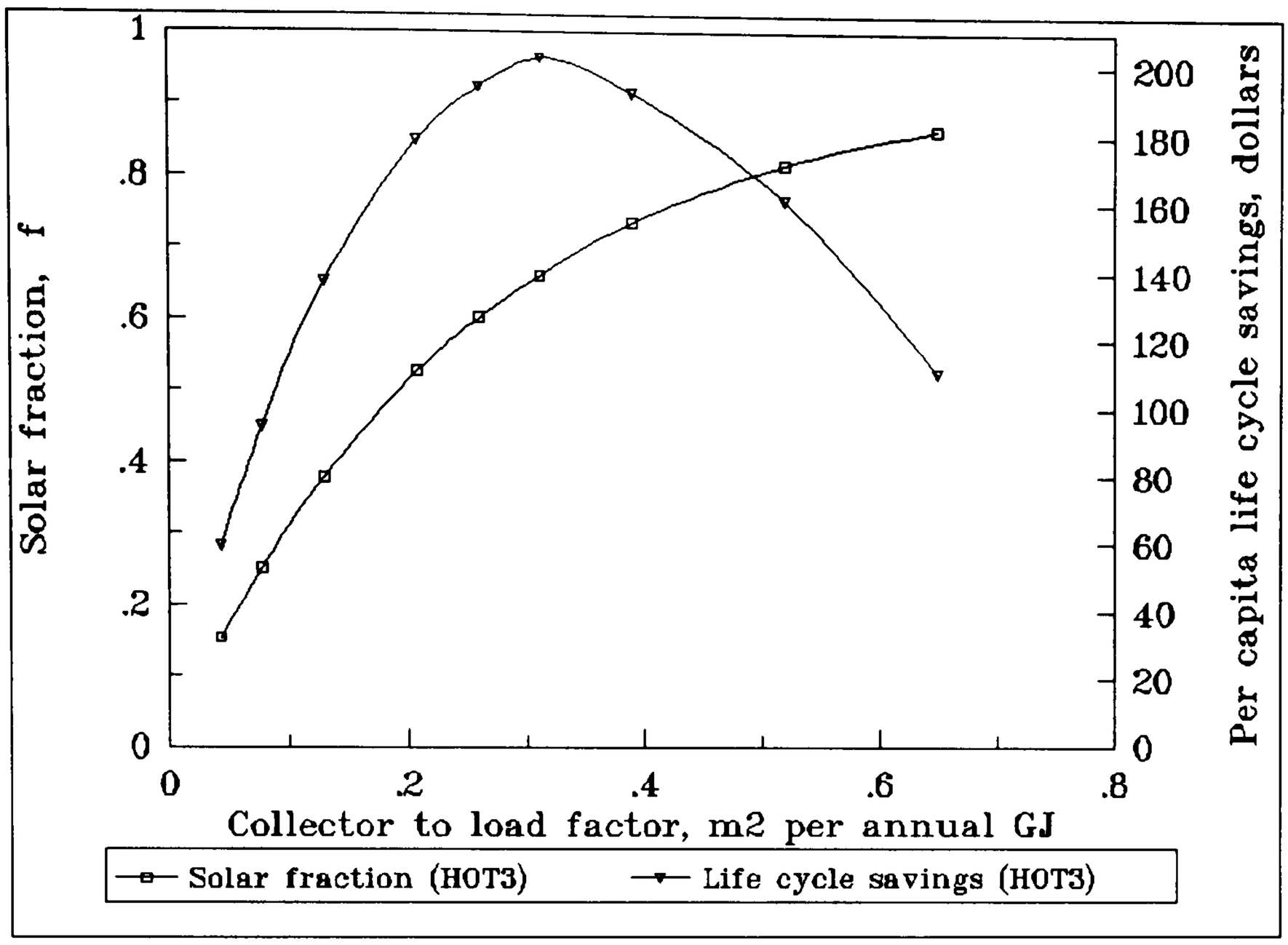

Fig. 4.34 Optimisation of collector to load factor, F_{cl}, for hotel applications of high load profile HOT3

A summary of the results concerning optimum collector sizes and payback periods for hotel applications is shown in Table 4.7. The optimum collector to consumer size varies from 0.8 to 1.2 m^2 per consumer for low and high load profile respectively which indicates that a larger collector is economically justified as the consumption of water increases (load profile HOT1 assumes 40 l per person while profile HOT2 assumes 50 l per person). The optimum collector to load factor decreases as the annual thermal load increases and varies from approximately 0.4 to 0.3 m^2 per annual GJ respectively.

The payback periods corresponding to the optimum design criteria, for the low load profile HOT1 is 8 years while for high load profile HOT3 this figure reduces to 7 years. The difference is attributed to the fact that consumption profile HOT3 assumes a higher load (60 l of water at 60 °C as compared to 40 l at 50°C for HOT1) which results to an increased utilisation of the collectors and generally the solar system.

In the preceding simulations the conventional fuel and the back up energy were assumed to be diesel oil which is the traditional energy source used for service water heating in the hotel industry in Cyprus due to its low cost (7.4 dollars per GJ as compared to 36 dollars per GJ for electricity). For this reason, any comparison with electricity is out of scope. It must be noted, however, that a set of simulations have been run for an economic scenario which assumes electricity as conventional and back up energy. The simulation results demonstrated that the solar system would be a cost effective and attractive alternative with a payback period of about 4 years and an annual solar fraction of nearly 0.9.

Load profile	Annual load GJ	OPTIMUM			Solar fraction	Payback period years
		A_c m^2	F_{cc} m^2/consumer	F_{cl} m^2/GJ		
HOT1	587	235	0.8	0.4	0.80	8
HOT2	893	300	1.0	0.35	0.75	7
HOT3	1156	345	1.2	0.3	0.65	7

Table 4.7 Optimum design criteria for hotel applications

An additional set of simulations was run with all three scenarios, assuming an optimum collector area factor of 0.8 m^2 per person for all cases, to investigate the performance of the system for each scenario. The results of the simulations were used to plot the graph of fig. 4.35 which shows the variation of monthly solar fraction for each load profile. The solar fraction in all three cases is lower in the winter months and gets higher in summer. This is in agreement with the variation of solar radiation throughout the year. The summer high values are also attributed to the higher solar radiation and the reduced heat losses from the storage tank due to low temperature differences between the storage unit and its surroundings. A comparison of the solar fraction of each scenario shows a higher contribution to the hot water energy demand in the case of low load profile, as expected.

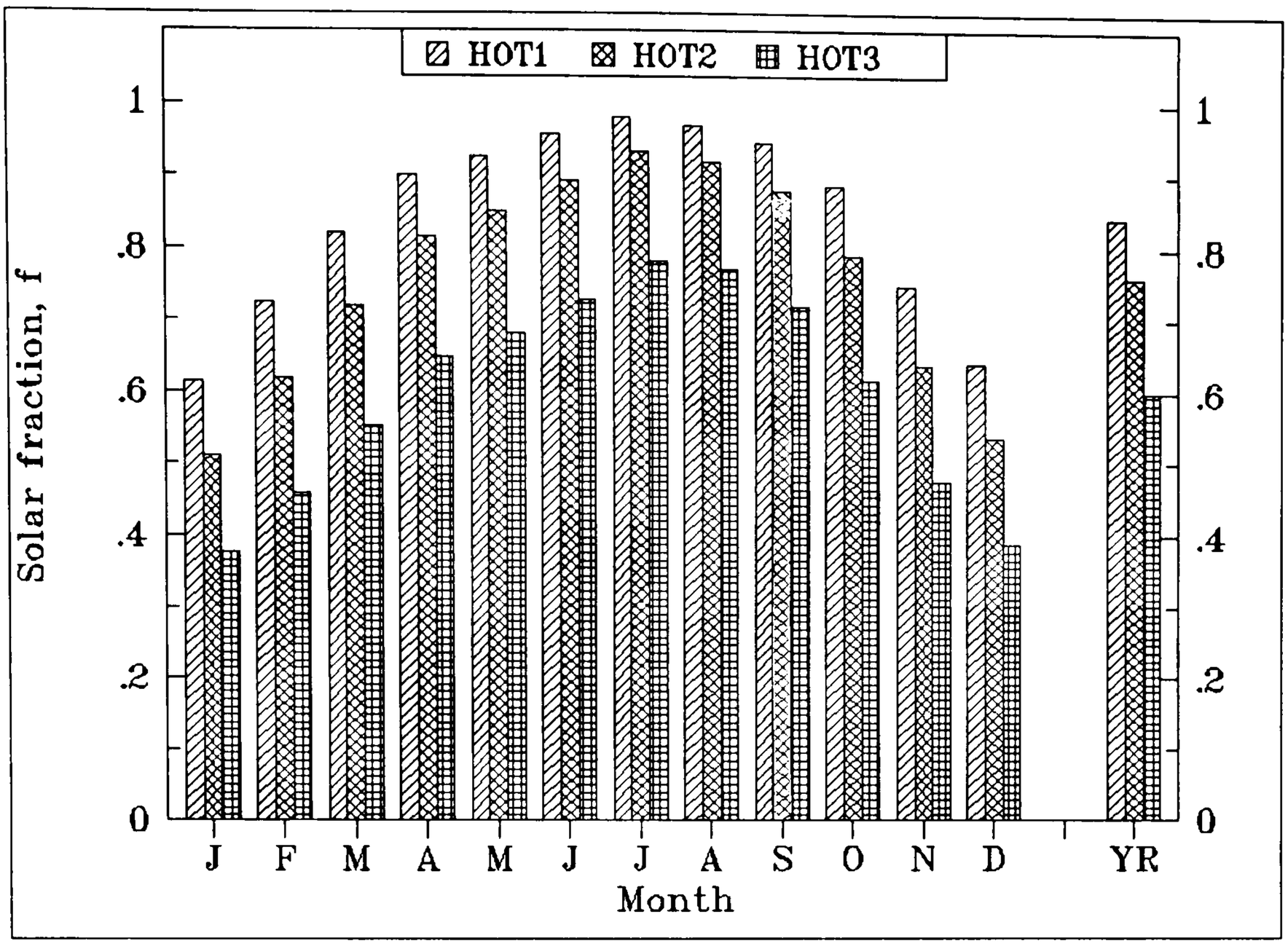

Fig. 4.35 Monthly solar fraction for three different hotel load profiles

CHAPTER 5

MODELLING AND SIMULATION OF SOLAR SPACE HEATING SYSTEMS

5.1 Introduction

The components of a solar space heating system must be well selected, properly sized, and carefully assembled in order to ensure that the system will function properly. Collectors, heat storage units, pumps, controls, heat exchangers and auxiliary heaters must be combined into an efficient and cost effective system. In a liquid–based heating system, heat from the collector is usually delivered directly, or by a heat–exchanger, to water storage, and the heating demand is met by supplying heat from storage. An auxiliary fuel or electric heater is needed to provide heat when stored solar energy is insufficient to meet the demand. Such occasions can occur on excessively cold weather or after successive cloudy days. A practical solar system must function automatically, provide the desired comfort level in the building at all times, require little maintenance, and operate reliably over a long period of time.

Following the selection of the system to be employed, the collector area and storage volume are determined, the liquid flow rate through the collector is established and pumps are selected. The heat exchanger size is based on the desired heat delivery rate. The auxiliary unit is sized to meet that part of the building heating load that can not be met by the solar system. If adequate attention is not given to details of sizing, layout and assembly, the system may not perform as expected, even if the best available components are selected.

Proper sizing of space heating equipment requires knowledge of the heating load in a building. This applies to solar systems as well as to conventional equipment. Oversizing of conventional space heating equipment leads to inefficient operation.

On the other hand, undersizing is not acceptable from a standpoint of comfort. Oversizing of solar systems is not advisable because of high initial cost, while undersizing may not provide significant savings of conventional fuels. It is therefore important to make accurate calculations of heating loads for proper sizing of solar as well as conventional equipment.

The performance of solar systems is governed by a number of parameters. These include the collector efficiency, collector tilt angle, storage tank size relative to collector area, rate of water flow through the collector, use of heat exchanger in the collector–storage subsystem, the heat exchanger effectiveness, the building characteristics, the method of transferring the collected energy to the building, etc. For a solar system to be efficient and effective the above factors have to be optimised; this can be achieved either through experimental investigations which, however, are time consuming, expensive and not repeatable, or through modelling and simulations which can provide much of the same thermal performance information as physical experiments with less time, effort and expense.

The objective of this chapter is to investigate the effect that these parameters have on the performance of a solar space heating system and investigate the optimum design criteria for a cost–effective and efficient system. The above will be achieved through modelling and simulations for the reasons explained in Chapter 1.

5.2 System configuration

A schematic layout of the solar heating system under investigation is shown in fig. 5.1. It is a water–based active solar heating system and comprises a number of flat–plate solar collectors coupled to a water storage tank. In addition, there is a load heat exchanger and two circulating pumps which are used to maintain the required water flow rate through the collector–storage and the storage–load heat exchanger sub–circuits. Auxiliary heating is provided by using conventional heaters to supply any shortfall in the heat energy that is supplied by the storage.

The system is arranged to collect solar heat in a liquid, deliver the heat to a liquid

storage subsystem either directly or indirectly through an optional liquid–to–liquid heat exchanger, and supply heat from the storage tank to the space heating equipment. When solar heat cannot meet the demand of space heating, auxiliary heat is supplied from the conventional auxiliary heating unit shown.

The most commonly used liquid in the collector loop is a mixture of water and ethylene glycol (ordinary automobile radiator antifreeze), although propylene glycol or alcohol and water mixtures may also be used. A centrifugal pump, usually at the lowest position in the loop, circulates the liquid mixture through the collectors, at a flow rate to be optimised. An expansion tank with open vent or pressure relief valve is installed preferably at the highest point in the loop.

A heat exchanger and water heat storage are used in systems with non–freezing liquids because of the excessive cost of filling a thermal storage tank with such expensive liquids. Such an arrangement will separate the collector liquid from the storage tank liquid and provide the possibility of using antifreeze additives in the collection circuit if needed. However, this arrangement will require a second pump. The other alternative is to avoid the use of collector heat exchanger so that the collected solar heat is delivered directly to the storage tank. In such a case, there is saving of capital equipment and maintenance costs for the collector heat exchanger and the storage pump. Furthermore, the temperature drop across the collector heat exchanger (ranging from 0 to 6 °C) is eliminated with a net result of an improvement in system efficiency.

Heat from a solar hot water storage tank may be distributed to living spaces either as hot water or as warm air. For water distribution, methods and equipment commonly used in conventional hydronic heating systems are employed. When activated by a room thermostat, a pump draws solar–heated water from the top of the storage tank, through one of several types of heating coils in each heated space in the building and returns the water to the lower part of the tank.

Solar–heated water can be distributed in conventional hydronic systems involving multiple fan–coil exchangers, pipe coils embedded in floors and ceilings, and cast iron hot water radiators.

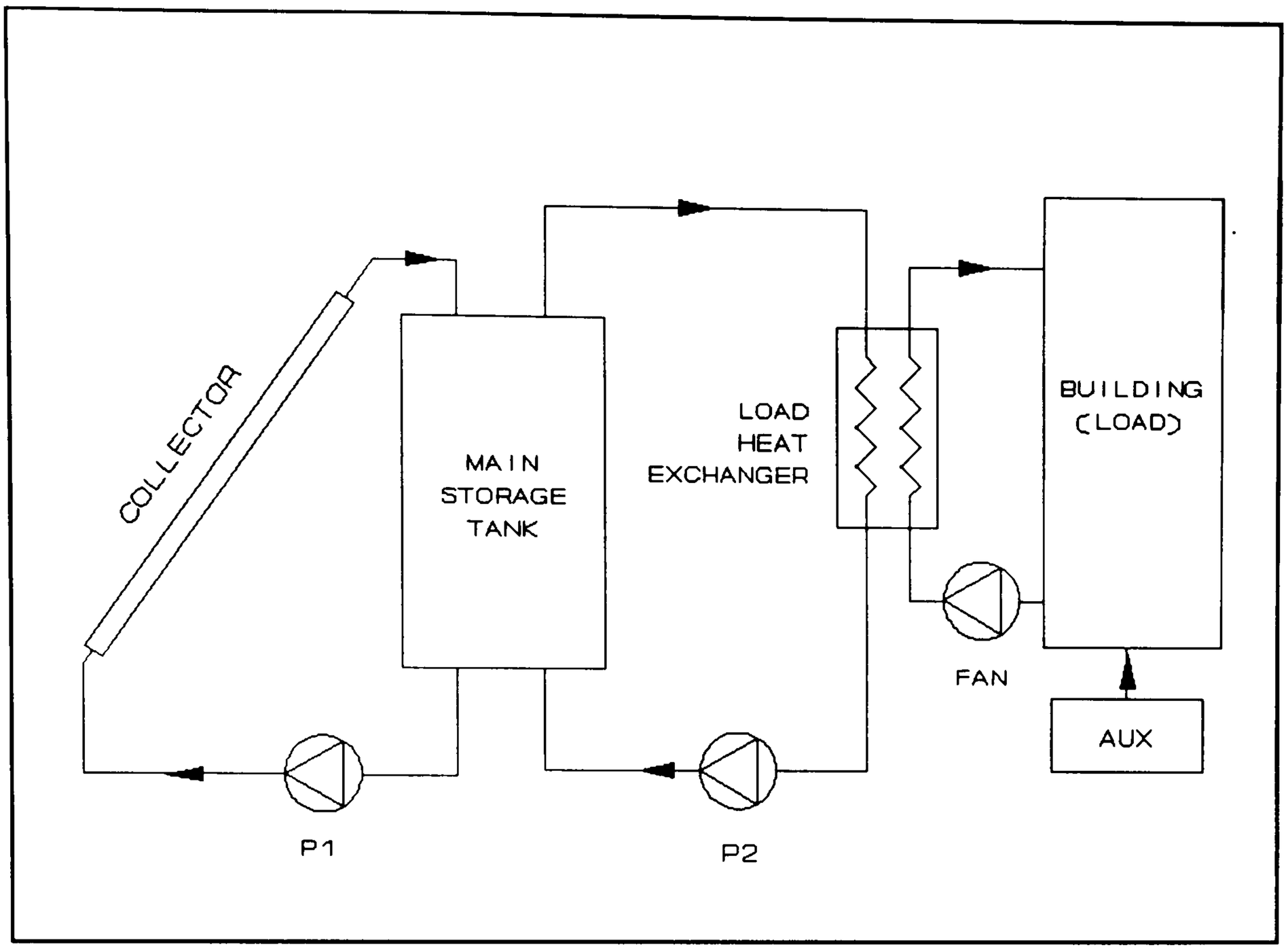

Fig. 5.1 Solar space heating system schematic diagram

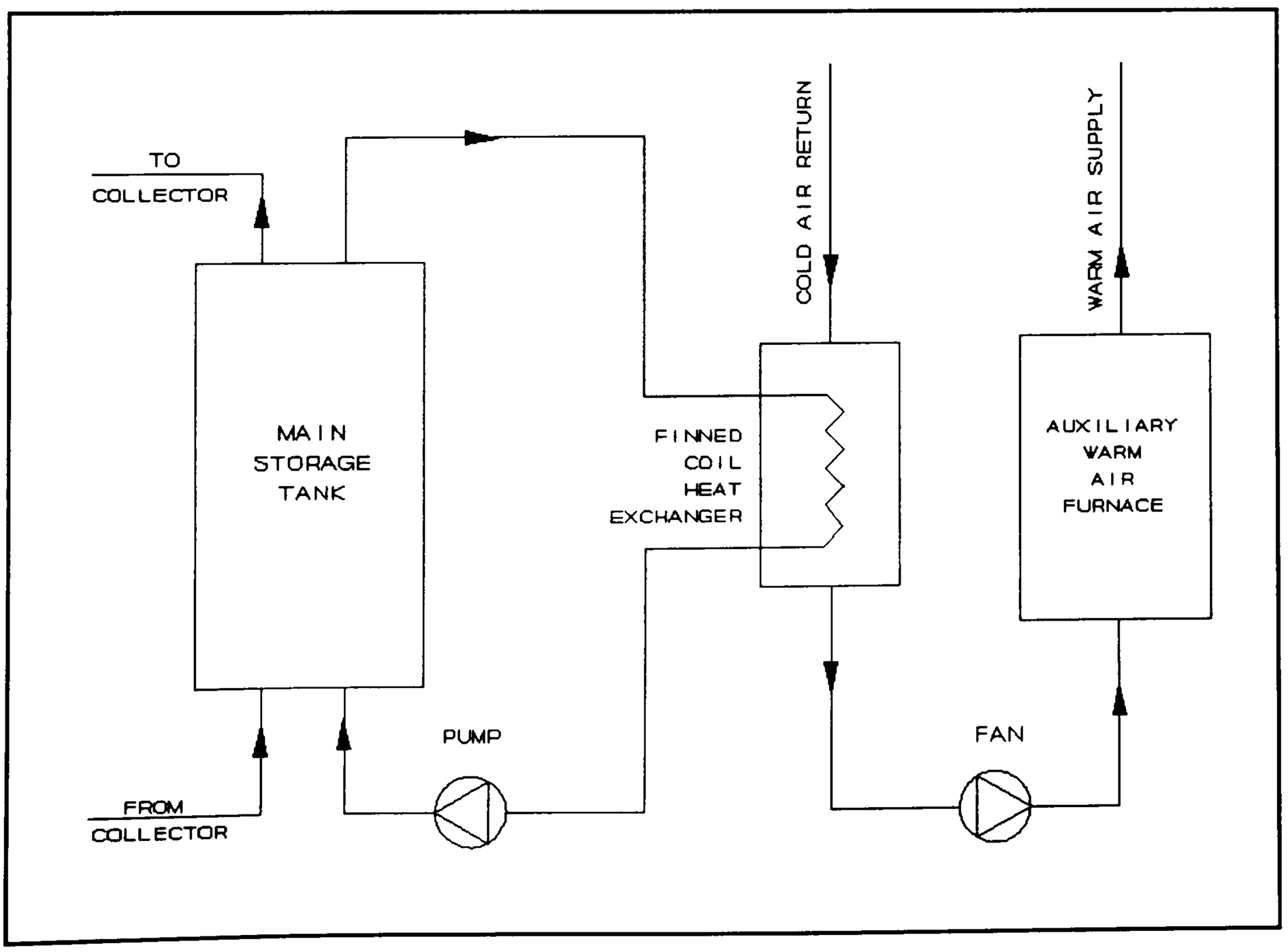

Fig. 5.2 Solar space heating with auxiliary furnace

In ducted warm air heating systems, hot water is supplied from solar storage to a finned coil heat exchanger in the main air duct and returned by a centrifugal pump to the storage tank (fig. 5.2). Air is circulated through the heat exchanger by a fan, and is usually heated from about 20 °C, which is the room temperature, to a temperature ranging from 26 to 30 °C, depending on the temperature of the hot water supplied from the storage tank. A conventional warm air furnace is usually employed in this system so that the temperature of air supplied from the solar coil can be boosted by the auxiliary heater.

5.3 The simulation model

There are three possibilities for modelling the building energy loads with TRNSYS. However, for relatively quick estimates of heating requirements, the space heating load model of TRNSYS known as Energy/(Degree–Day) TYPE 12 model, may be used. In this case, the building is modelled through the use of a single conductance (UA) for heat loss. A single energy balance on the structure is performed each simulation timestep.

The energy/(degree–day) concept has been shown by ASHRAE (1981) to be useful in estimating the monthly heating load of a structure. In this space heating load model, the energy/(degree–day), or more appropriately the energy/(degree–hour), concept is extended to estimate the hour by hour heating load of a structure. According to Klein *et al* (1990), the hour by hour space heating load estimated in this manner may be significantly in error, but over a period of time, the model may provide reasonable estimates of overall energy quantities. Furthermore, the model does provide an estimation of the space heating load with minimal computational effort.

There are four modes of operation in TYPE 12 which give flexibility in control and auxiliary strategy. Modes 1, 2 and 3 are compatible with energy rate control. Modes 1 and 2 model a zero capacitance structure maintained at a constant set temperature for heating. Mode 3 allows the room temperature to float between set points for heating and cooling (if required), T_{min} and T_{max}. A singled lumped capacitance is

used in this analysis. If the room temperature would fall below T_{min} or rise above T_{max}, then the energy required to maintain either limit is output as the heating or cooling requirement. Mode 4 models a single lumped capacitance house compatible with temperature level control.

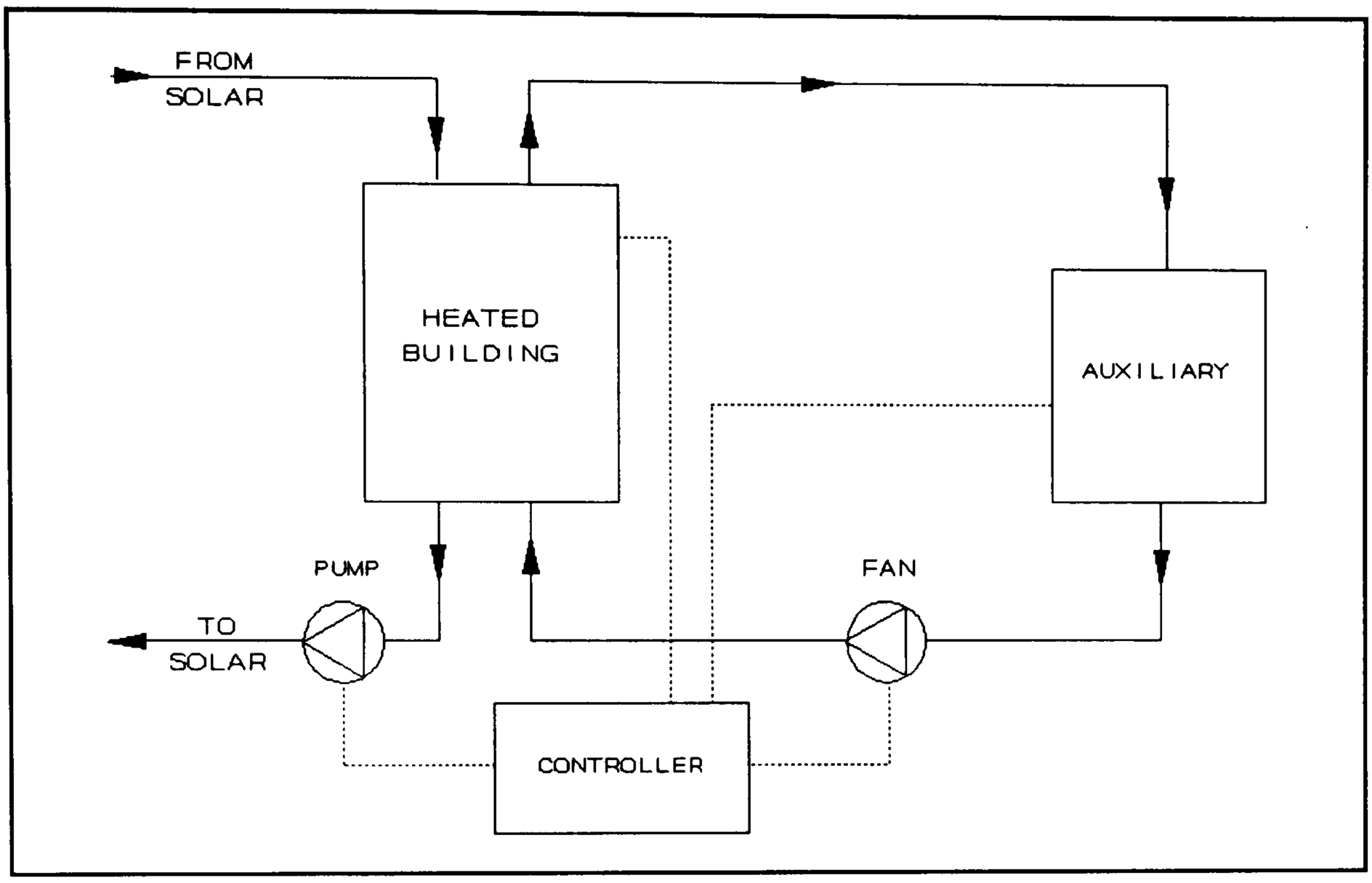

Fig. 5.3 Mode 1, parallel auxiliary

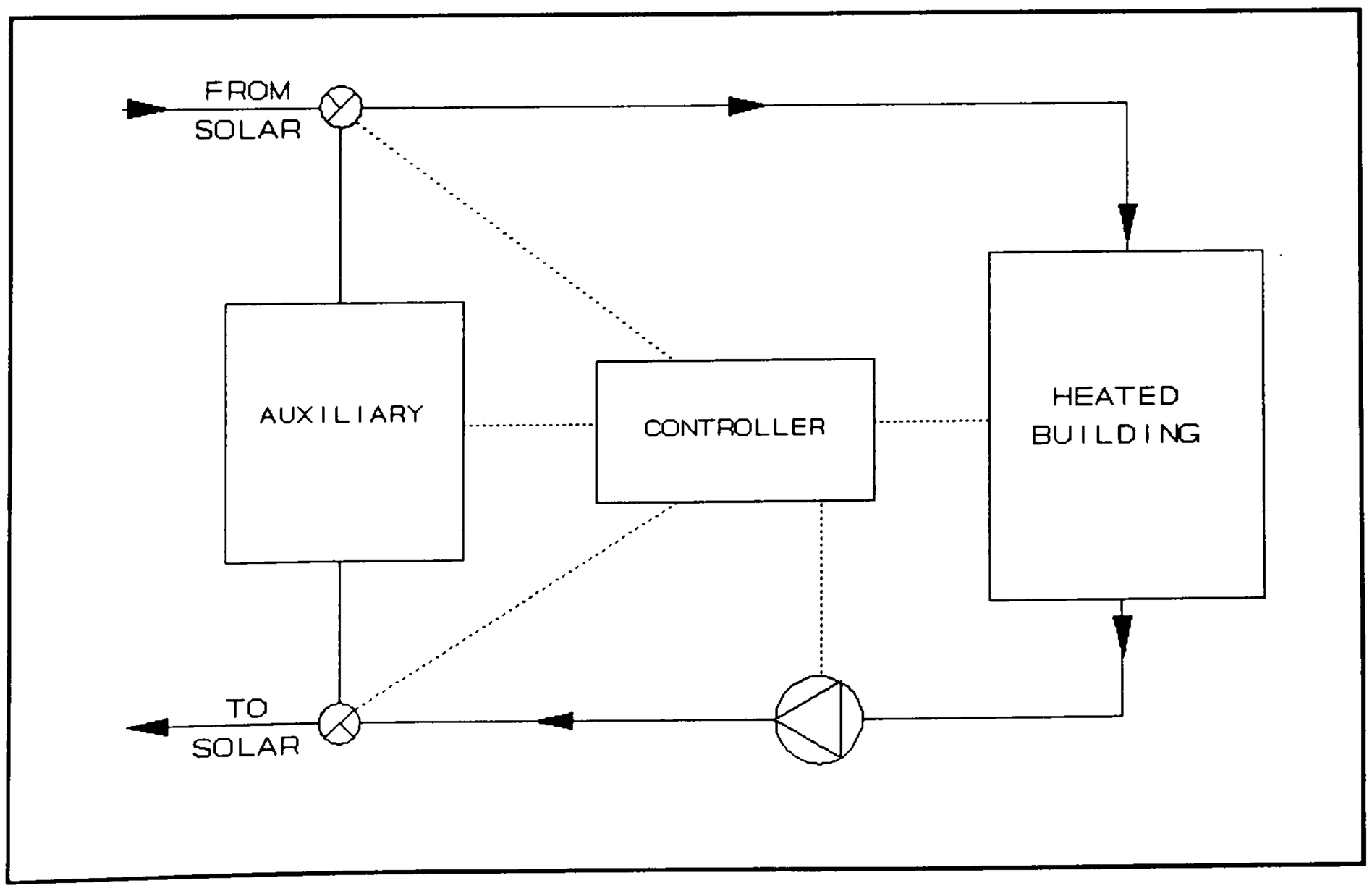

Fig. 5.4 Mode 2, series auxiliary

This component provides the user with two methods of supplying auxiliary energy to the load. Mode 1 is the parallel auxiliary mode and Mode 2 is the series, or "bypass" auxiliary mode. In mode 1, auxiliary energy makes up only that part of the load which cannot be extracted from the flow stream coming from the solar collector and storage subsystem (see fig. 5.3). In mode 2, auxiliary supplies the entire load via the by–pass circuit when the flow stream cannot meet the load (see fig. 5.4). A detailed description of the mathematical model is given by Klein *et al.* (1990).

The following TRNSYS component routines with the appropriate choice of inputs and parameters should be used to model the system:

(a) a TYPE 1, Flat–plate solar collector

(b) a TYPE 3, Pump

(c) a TYPE 2, Pump controller

(d) a TYPE 4, Stratified storage tank

(e) a TYPE 12, Energy/(degree–day) space heating load

(f) a TYPE 54, Weather generator

(g) a TYPE 16, Solar radiation processor

(h) a TYPE 24, Quantity integrator

(i) a TYPE 25, Printer

(j) A TYPE 29, Economic analysis.

A brief description of each of the above models is presented in Appendix D. The simulation input file JM3.DAT for the solar space heating system under investigation is also shown in Appendix D.

A large number of parameters and inputs (about 85 parameters and 40 inputs) are required as inputs to the system model as in the case of solar water heating system. These include physical parameters, such as collector and storage tank size, as well as thermal parameters, such as heat exchanger efficiencies and heat loss coefficients. A number of assumptions have been made for the system simulation, concerning the storage tank, solar collector configuration and controllers. Whenever it is necessary to define the values of some parameters in the model in order to investigate the effect of varying another parameter, approximate values are used as done with solar water heating.

1. Solar Collector	
A_c	5 – 200 m^2
G_{test}	54 kg h^{-1} m^{-2}
G	50 kg h^{-1} m^{-2}
$F_R(\tau\alpha)_n$	0.78
F_RU_L	24.4 kJ h^{-1} K^{-1} m^{-2}
ε_c	0.1 – 1.0
b_o	0.1
β	0 – 90° from horizontal
ρ_g	0.2
2. Storage system	
V_s	1.5 – 14.0 m^3
U_s	1.2 kJ h^{-1} K^{-1} m^{-2}
$\dot{m}_L$	1800 kg h^{-1}
3. Load	
UA	4000 kJ h^{-1} K^{-1}
T_R	20 °C
$\varepsilon_L C_{min}$	400 – 40000 kJ h^{-1} K^{-1}

Table 5.1 System simulation parameters

Some of the most important simulation parameters of the system are shown in Table 5.1. In this table the collector parameters concerning the performance characteristics of the flat–plate collector, i.e. $F_R(\tau\alpha)_n$, F_RU_L and G_{test}, were investigated experimentally at the collector Testing Centre of the Ministry of Commerce and Industry, according to CYS:119:1980 (CYS 1980). It must also be noted that the ground reflectance was taken as 0.2, following the recommendation of Liu and Jordan

(1963) who suggest that this parameter should be 0.2 where there is no snow and 0.7 when there is snow cover.

For the optimisation of the design parameters it is necessary to assume that the system will have to meet a certain load. In the present study the system is designed to meet the space heating load of a house having a floor area of 200 m^2, characterised by a heat loss coefficient, UA, of 4000 kJ h^{-1} K^{-1}. The weather data are the same as those used for the solar water heating systems and are shown in Table 4.2.

The performance of the system will be expressed in terms of its solar fraction, f, which is defined as the fraction of the space heating load provided by solar energy and can be calculated from the following relationship:

$$f = \frac{Q_{load} - Q_{aux}}{Q_{load}} \qquad (5.1)$$

where Q_{load} is the space heating load and Q_{aux} is the auxiliary energy supplied to the system.

5.4 Optimisation of design criteria

Several system design criteria are investigated, in order to establish the range of optimum values. These include collector slope, collector size, heat storage capacity per unit collector area, water flow rate through the collector, load heat exchanger characteristics and auxiliary energy. To this effect the economics of the system are very essential and need to be treated in conjunction with the thermal performance of the system. For this purpose, the Economic Analysis subroutine of TRNSYS has been included in the system model. The economic analysis presented in Chapter 1 is also applicable to solar space heating.

The costs of solar heating equipment include purchase and installation of all collectors, storage tank, pumps, controls, ductwork, piping, heat exchangers, etc., and are considered as the incremental costs, that is, the difference in cost between the solar heating system and a conventional heating system. Operating costs include

costs of auxiliary energy, parasitic (ancillary) power, maintenance, etc. It is assumed that the costs of components which are common to both, conventional and solar heating systems, e.g the furnace, load heat exchanger, ductwork, fans, controls, and the maintenance costs of this equipment are identical. As a result of the above, all references to solar heating system costs, or conventional system costs, refer to the cost increment above the common costs.

Parameter	**Value**	**Parameter**	**Value**
C_{FA}	36 US$/GJ	d	9%
C_{FL}	7.4 US$/GJ	M_S	1%
N_E	20 years	i	5%
D	50%	t	9%
m	9%	N_D	20 years
N_L	15 years	i_{FCF}	5%/yr
DEG	1%/yr	i_{FBUP}	5%/yr

Table 5.2 Economic parameters used for the economic analysis

Several economic criteria have been proposed and used for evaluating and optimising solar heating systems and these are described in detail by Duffie and Beckman (1980). In the discussion which follows, two of these criteria are used; these are the life cycle savings and the payback period. Life cycle savings (LCS) or net present worth (PW) is defined as the difference between the life cycle cost of a conventional fuel–only system and the life cycle cost of the solar plus auxiliary energy system. Payback period is defined in many ways (see Duffie and Beckman). For the present study, however, payback period will be defined as the time needed for the cumulative fuel savings to equal the total initial investment, that is, how long it takes to get an investment back by savings in fuel.

Some of the economic parameters used in the simulations which follow are shown in Table 5.2.

5.4.1 Optimisation of collector tilt angle

The orientation and tilt angle of the solar collector should be dealt with carefully when designing a solar heating system. A collector should be mounted to face due south (northern hemisphere) for maximum solar gain, although any orientation within 20° off–south is acceptable (see Felske, 1978). With regards to the collector tilt angle, the collector should be kept as close to normal to the incoming solar radiation for maximum heat gain. The optimum tilt angle depends on site latitude and solar application. Detailed studies by Lof and Tybout (1974) have shown that the optimum collector tilt for solar space heating is approximately the location latitude plus 15°, i.e ϕ+15°. Carg (1982), also recommends the value of ϕ+15° as the optimum tilt angle. However, Kern and Harris (1982), optimised the tilt angle based on beam radiation and concluded that the optimum tilt angle in the heating season is about ϕ+(10 to 30°). This shows that when it comes to a real design it is better if one takes into consideration the conditions prevailing to the particular location. In the present study, a number of yearly simulations were run to get results for various collector tilt angles. These results were used to calculate the annual solar fraction of the system, and the graph of fig. 5.5 was plotted to show the variation of the solar fraction with the collector tilt angle.

It is evident from this graph that the system performance becomes maximum when the collector slope is around 50 degrees from the horizontal, which is in excellent agreement with the results of Lof and Tybout (1974). However, there is a range of values from 40° to 55° which brings about maximum performance. This is because at tilt angles between 40° to 55° the incident solar radiation falls on the collector almost perpendicularly, therefore minimising the reflected and maximising the transmitted solar radiation components. At collector tilt angles outside the range of 40° to 55° from horizontal, the solar fraction falls off drastically. This is mainly due to the displacement of the collector plane away from the normal conditions of the incident solar beam.

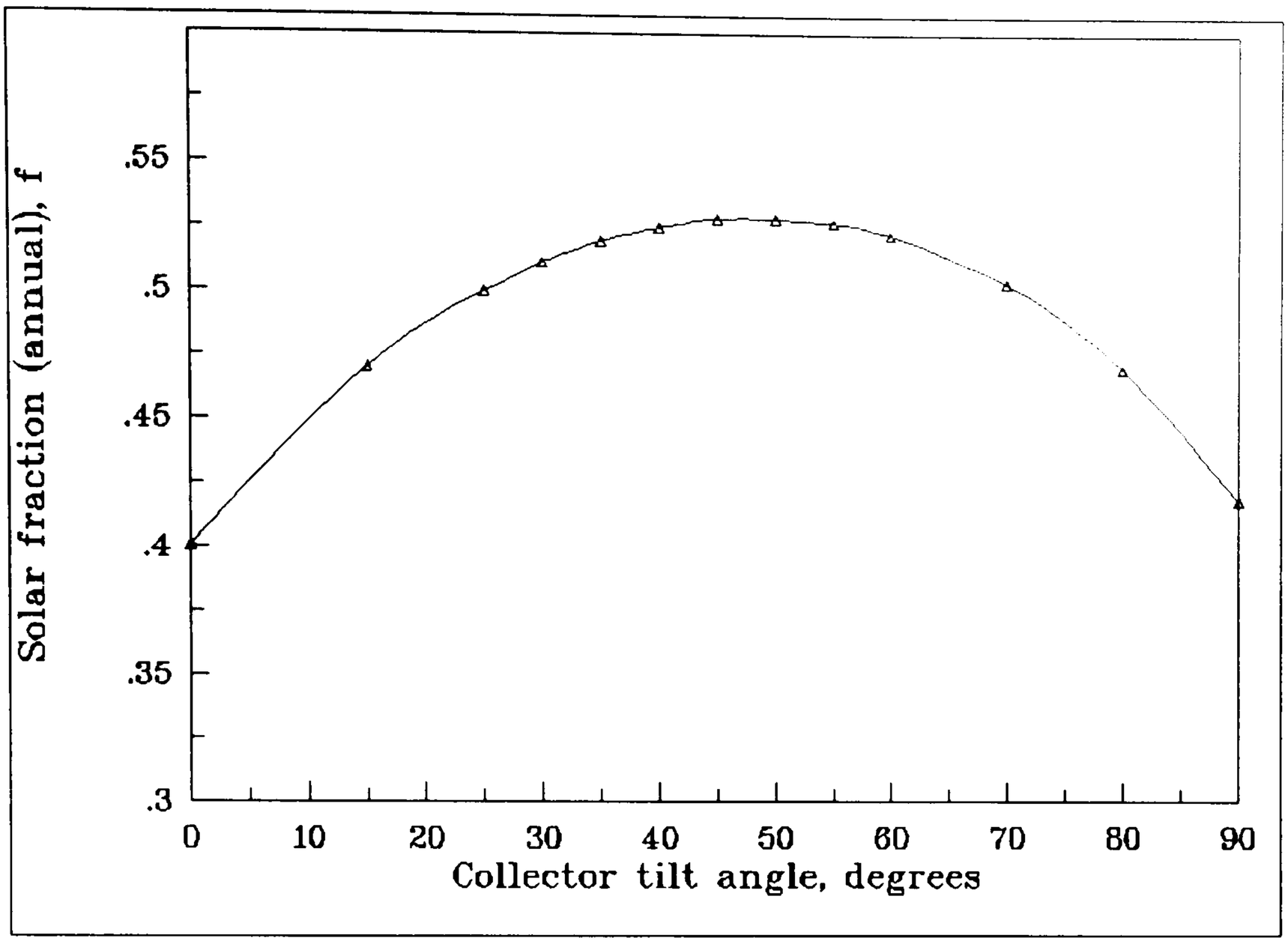

Fig. 5.5 Optimisation of collector tilt angle

The curve of fig. 5.5 is useful in cases where the collector tilt angle is dictated by architectural considerations. In such instances, this curve can be used to demonstrate the effect that the imposed collector slope has on the annual solar fraction and consequently on the thermal performance of the system. For subsequent simulations, the collector tilt angle is fixed to 50 degrees from horizontal. This value is selected to represent good design practice.

5.4.2 Optimisation of collector size

Given a certain load that is some function of time through a year, a type of collector and a system configuration, the primary design variable is the collector size. System performance is much more sensitive to collector area than to any other variable (Duffie and Beckman, 1980).

A set of simulations was run for different collector areas, assuming a collector slope

of 50° from horizontal, a storage factor of 50 l/m^2 and a water flow rate through the collector equal to 50 kg/h per m^2 of collector. The results of the simulations were used to plot graphs relating the annual solar fraction and life cycle savings of the system to the collector area A_c, the collector to floor area factor F_{cf} which is defined as the ratio of collector area A_c to the building floor area A_f, and the collector to load factor F_{cl} which is defined as the ratio of collector surface area to the annual space heating load. These are shown in figs. 5.6 to 5.8. This approach is considered useful because it offers the flexibility to the designer to base his design on either of the parameters and do some kind of cross-checking in determining the optimum collector area of a solar space heating system.

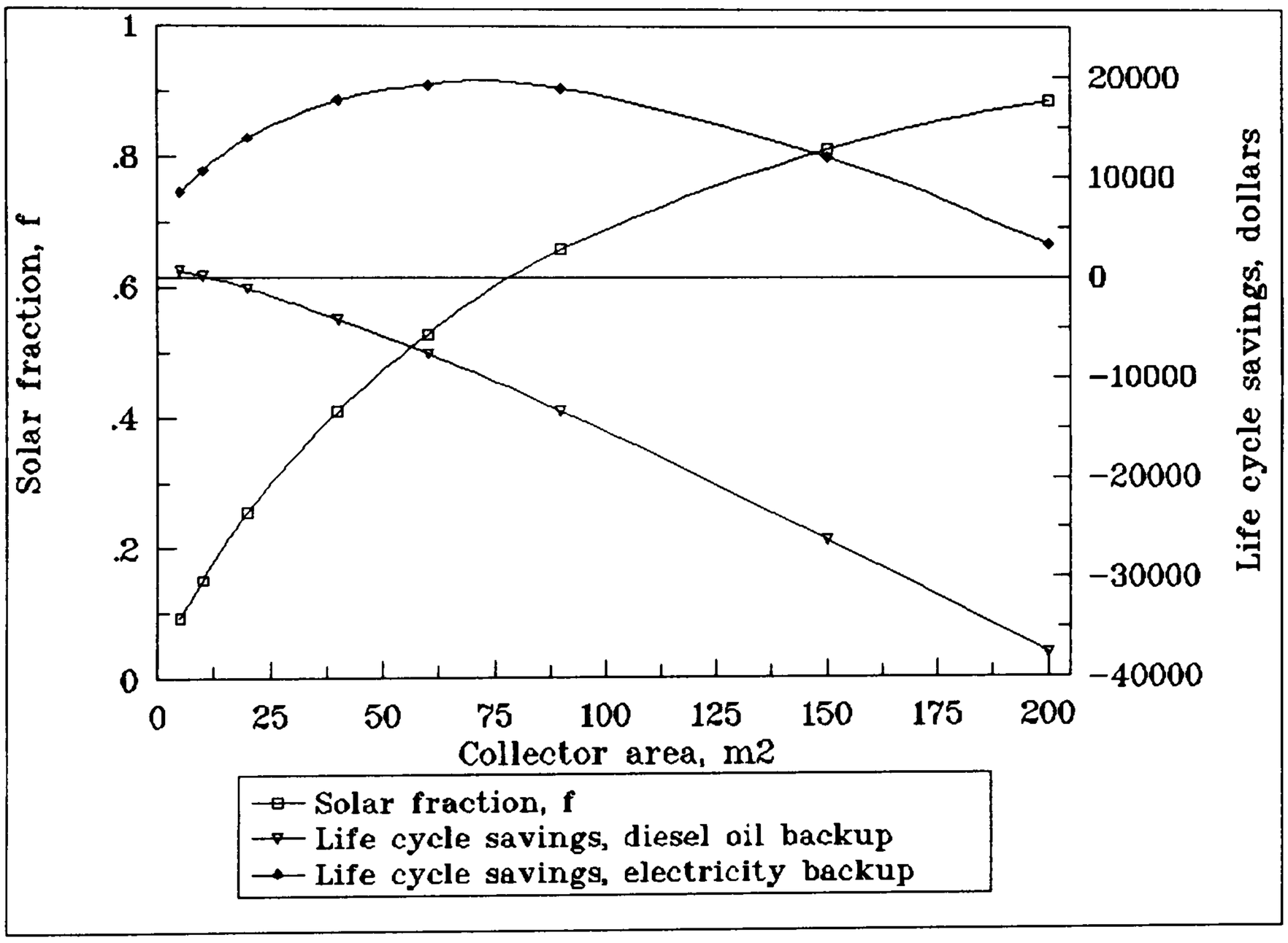

Fig. 5.6 Annual solar fraction and life cycle savings as a function of collector area, for diesel oil and electricity backup energy

It is interesting to note, in all graphs, the distinct difference in the results between diesel-backed-up and electricity backed-up systems. When using an oil-fired boiler as auxiliary, the life cycle savings are negative at large collector areas and increase as the collector area decreases. The curve of life cycle savings tends to reach a maximum as the collector area approaches zero. At the same time, it is seen from the results that the payback period varies from 9 years to values which exceed the

expected lifetime of the system, i.e higher than 20 years (see Table 5.3). It is, therefore, evident that solar space heating is not cost effective and in fact cannot compete with conventional heating systems which use diesel oil fired boilers.

A_c (m^2)	**Diesel oil backup**			**Electricity backup**		
	f	LCS (US$)	Payback (years)	f	LCS (US$)	Payback (years)
5	0.093	627	9	0.093	8517	3
10	0.151	98	11	0.151	10574	4
20	0.255	−1119	13	0.255	13882	4
40	0.410	−4152	15	0.410	17643	5
60	0.528	−7629	17	0.528	19224	5
90	0.658	−13415	20	0.658	18837	6
150	0.812	−26237	> 20	0.812	12020	8
200	0.888	−37558	> 20	0.888	3262	10

Table 5.3 Summary of simulation results, diesel oil and electricity backup

The results are more in favour of solar when the system is compared to conventional heating systems using electricity as energy source. It appears from the graphs that the life cycle savings curves corresponding to electricity backed−up systems have maxima. These maximum points represent the optimum size of collector for a given set of collector and electricity costs. Thus, fig. 5.6 shows that the optimum collector area for the system under investigation is about 70 m^2. Fig. 5.7 indicates that the optimum collector to floor area factor, F_{cf}, is 0.35 m^2 per m^2 of building floor area. From fig. 5.8 the optimum collector to load factor, F_{cl}, is approximately 0.55 m^2 per GJ of annual heating load.

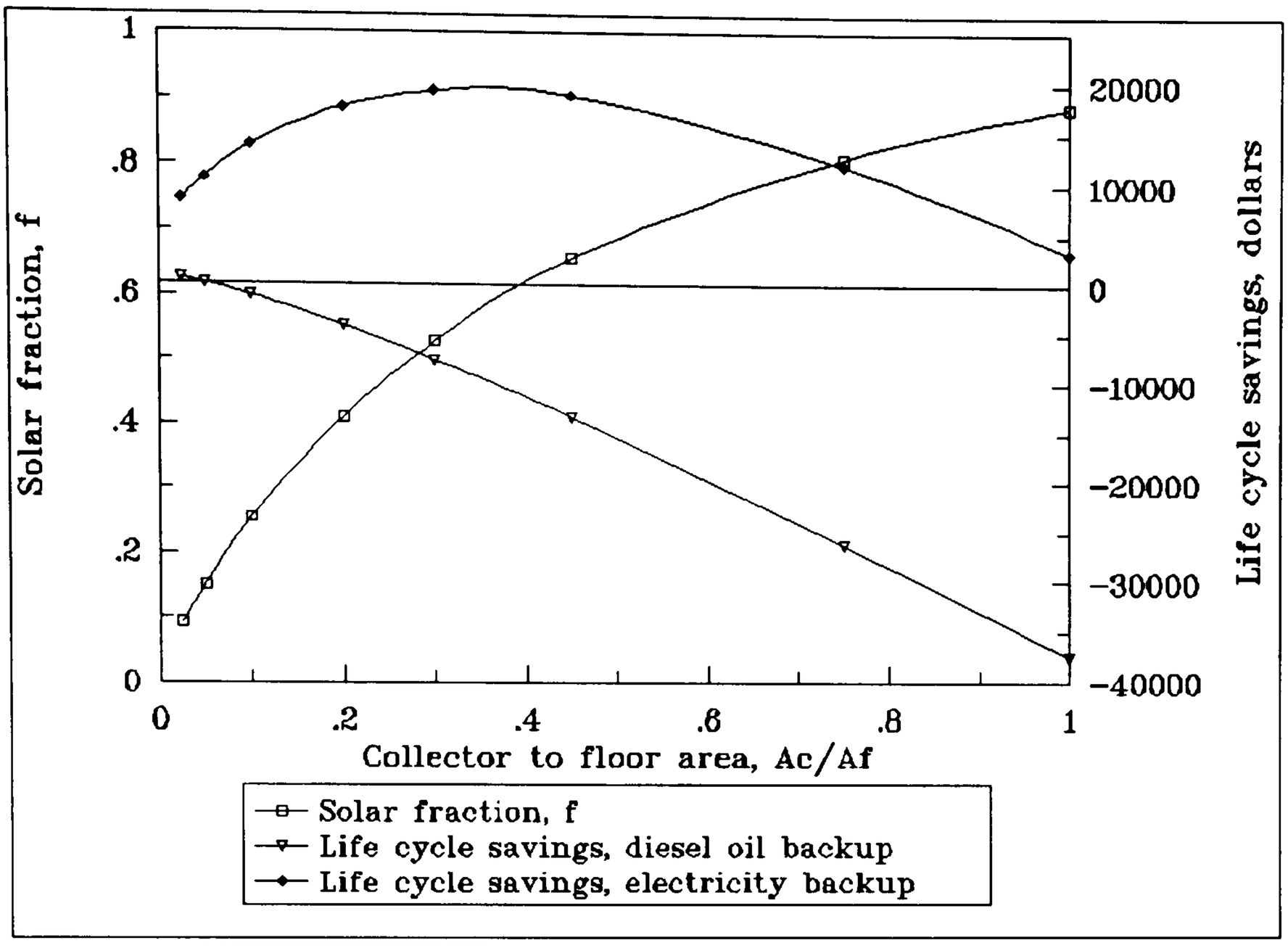

Fig. 5.7 Annual solar fraction and life cycle savings as a function of collector to floor area factor, F_{cf}, for diesel oil and electricity backup energy

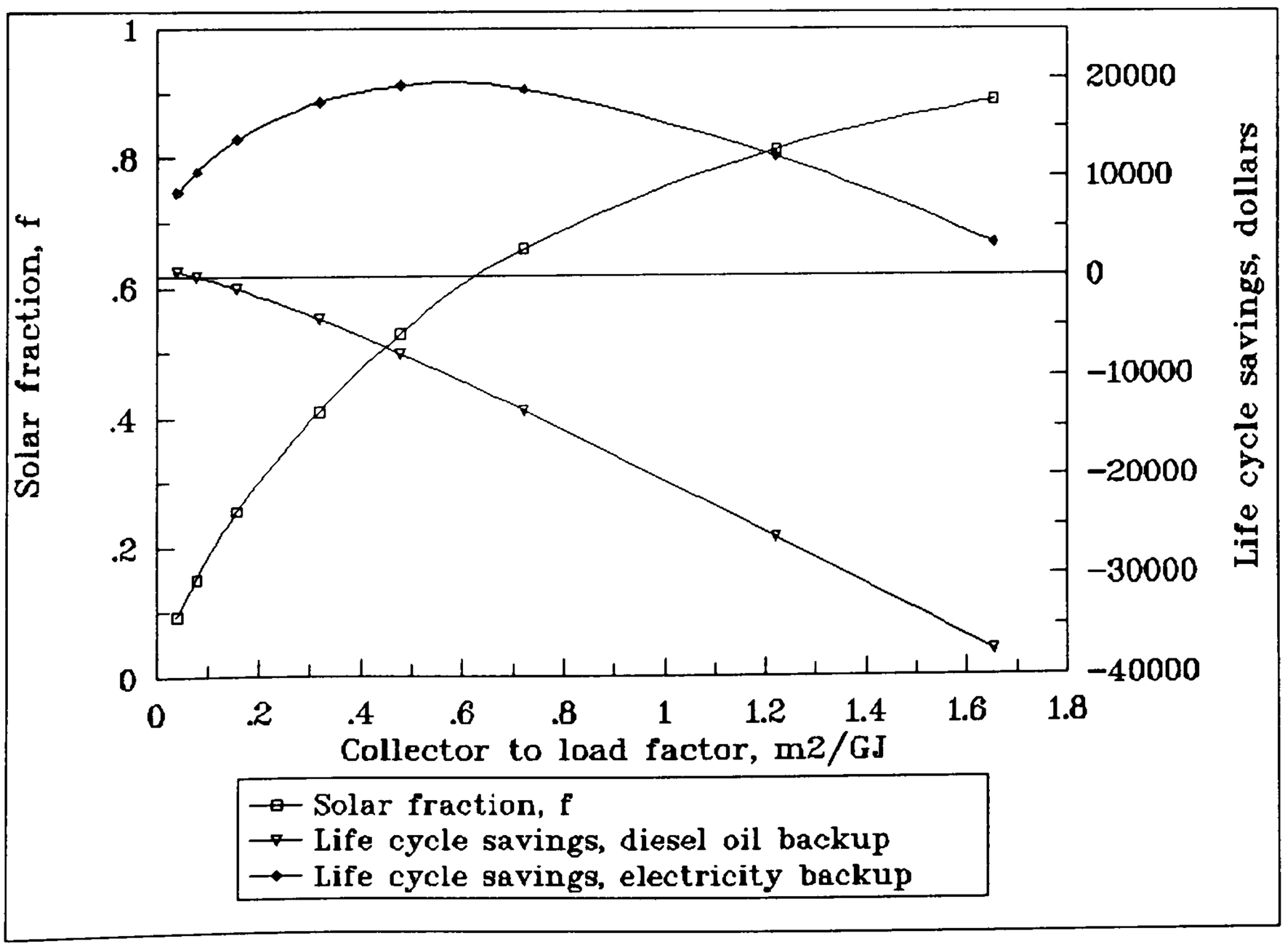

Fig. 5.8 Annual solar fraction and life cycle savings as a function of collector to load factor, F_{cl}, for diesel oil and electricity backup energy

The annual solar fraction, f, is dependent on the size of solar collector and increases at a decreasing rate as the collector area increases. At optimum collector area, the solar fraction is approximately 0.6, which means that 60% of the space heating load of the building is met by solar while the rest is supplied by the auxiliary unit. The curves of figs. 5.6 – 5.8 could be used to predict the annual solar fraction of a solar space heating system at any imposed collector size.

It has been found that solar space heating is not a cost effective application when compared to conventional oil–fired heating systems. For this reason, subsequent simulations will assume that electricity is used as backup energy and the optimisation will concern only solar heating systems backed–up with electricity.

5.4.3 Optimisation of storage capacity

Storage of solar thermal energy is required in solar heating systems so that solar heat can be delivered to the building during non–sunny periods. The volume of storage needed is principally dependent on collector area. In liquid–based systems where solar heat is first collected in storage before delivery to the load, the storage unit should be large enough for all–day solar heat collection without penalising collector efficiency, and small enough to raise the temperature in storage to meet the load.

A number of annual simulations were run by keeping the collector area constant at the optimum value of 70 m^2 and varying the storage capacity from as low as 0.5 m^3 to as high as 14 m^3 of water , in order to investigate the effect that the storage capacity has on the system performance. The storage capacity is related to the collector area by the storage factor F_s, defined as the ratio of storage tank volume V_s to the collector area A_c and is expressed in litres per m^2 of collector (l/m^2). The results of these simulations were used to plot the graph of fig. 5.9, which shows the effect of storage factor on the system life cycle savings and the annual solar fraction.

Fig. 5.9 indicates that with little storage the amount of solar heat provided is limited because solar heat could be delivered and used only during the day when the thermostat calls for heat. The contribution of solar energy to the building heating

load increases rapidly with storage size and the life cycle savings reach a maximum corresponding to an optimum storage capacity which is within the range of 45 to 50 l/m^2. As the storage volume continues to increase, the solar fraction also increases. The optimum range of storage factor is associated with an annual solar fraction ranging from 0.56 to 0.58 which leads us to the conclusion that it is more beneficial to use a storage factor of 50 l/m^2. This means that storage capacities greater than the above value do not make the system cost effective in spite of the fact that they cause an increase in the annual solar fraction and the annual savings in energy.

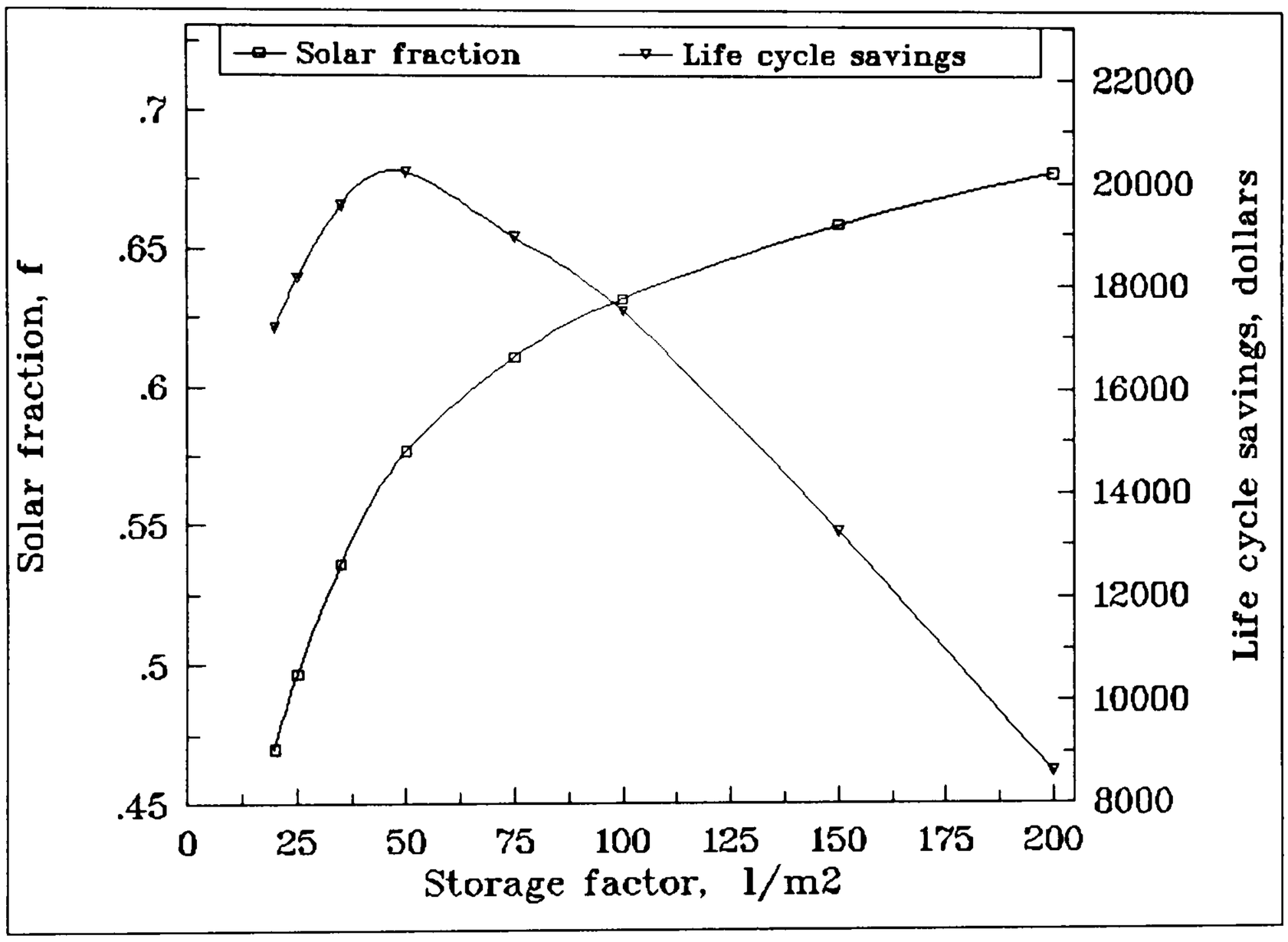

Fig. 5.9 Effect of storage capacity on annual solar fraction

Further simulations were run to investigate the effect of storage capacity on solar fraction at different collector to floor area factors, F_{cf}. The results were used to plot the graphs of figs. 5.10 and 5.11. Fig. 5.10 shows the variation of the annual solar fraction with the storage factor, F_s, at different collector to floor area factors, F_{cf}. As expected, the solar fraction increases with the size of the collector; however, this increase is significant when changing F_{cf} from 0.1 to 0.3 (see fig. 5.11). As F_{cf} increases beyond 0.3 it can be seen that the solar fraction does not increase at the same rate. This can be attributed to the fact that the heat losses increase as a result of the higher water temperatures in the system.

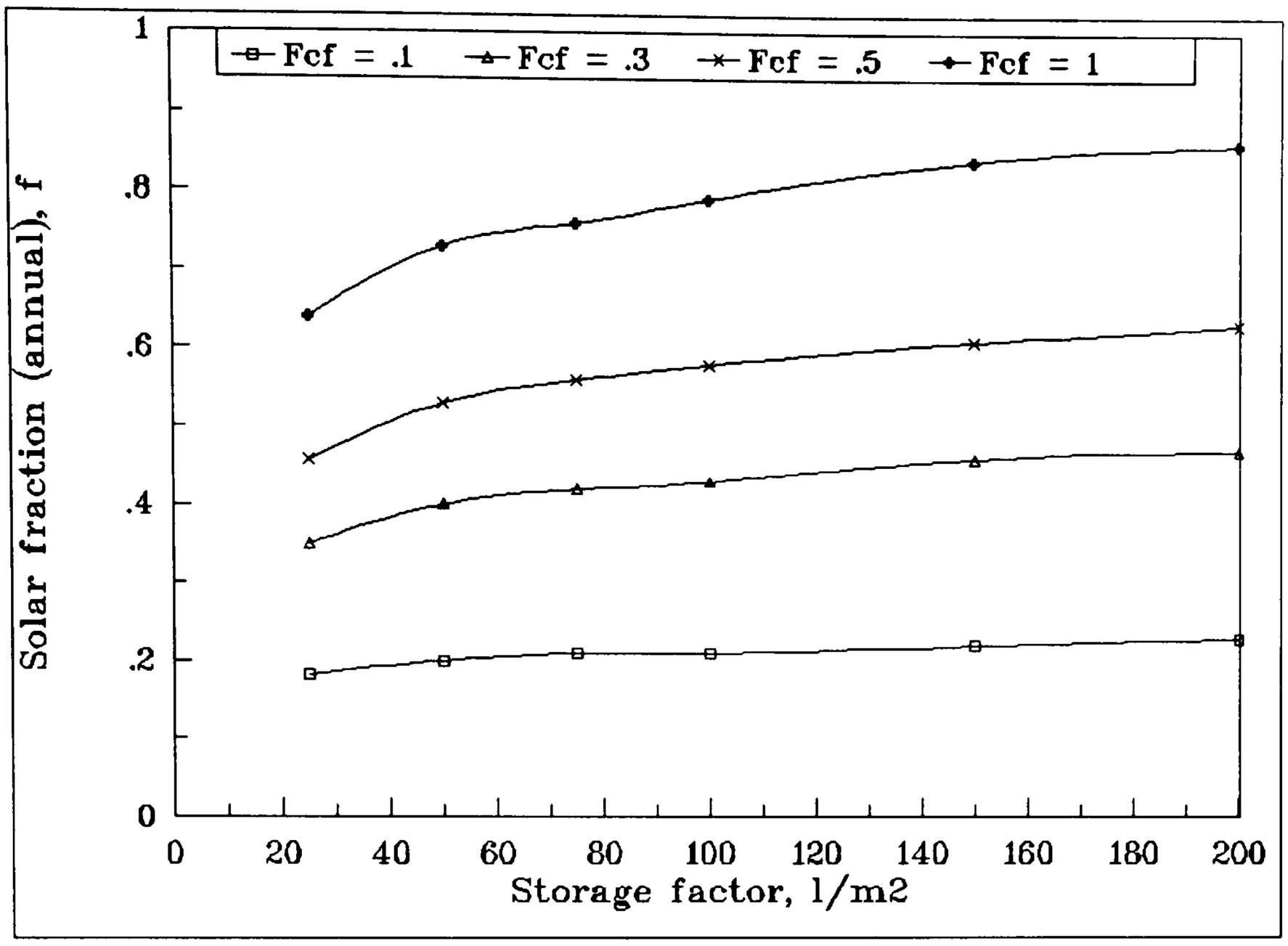

Fig. 5.10 Effect of storage capacity on the annual solar fraction, for different collector to floor area factors, F_{cf}

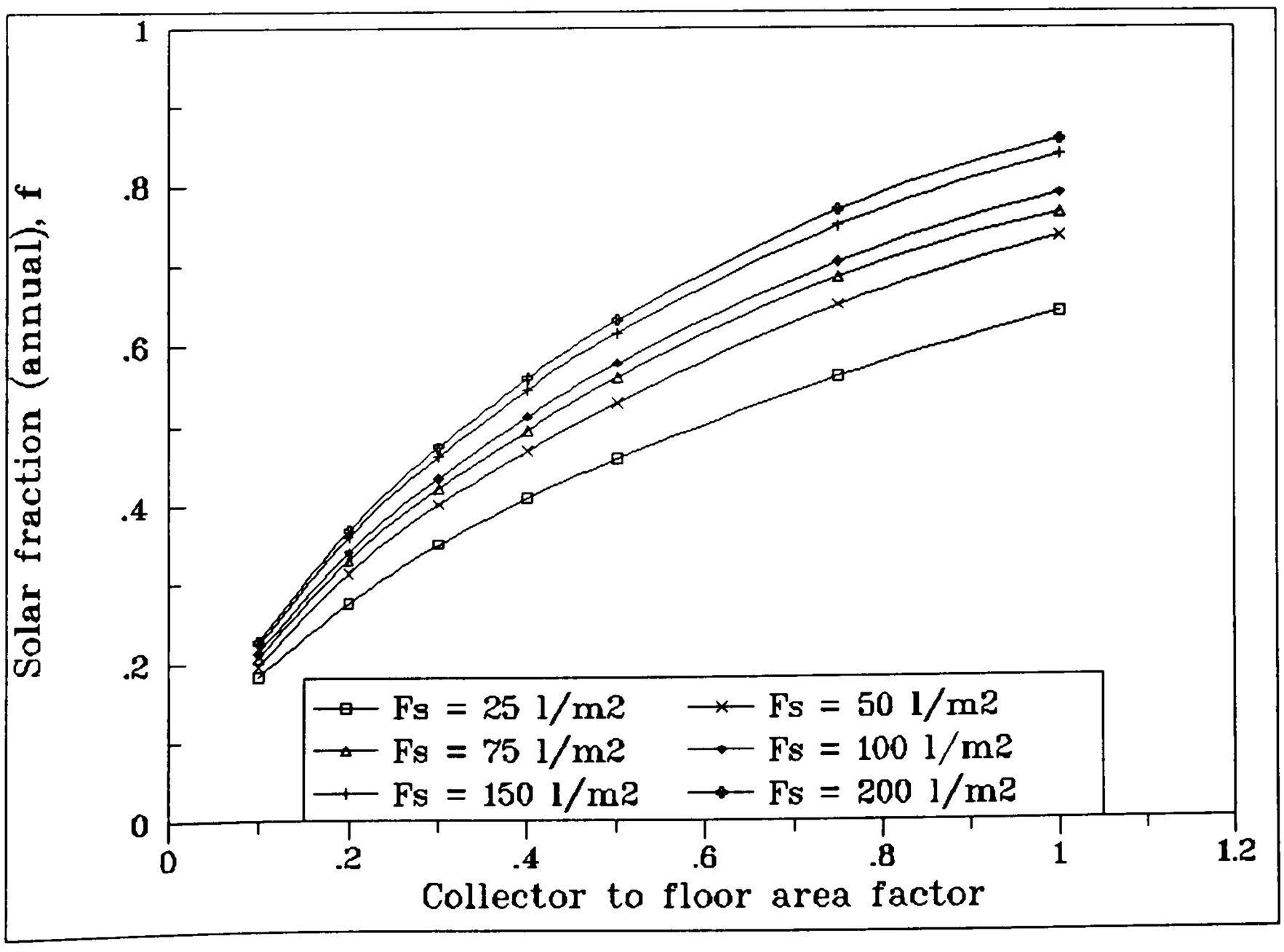

Fig. 5.11 Effect of collector to floor area factor, F_{cf}, on the annual solar fraction, for different storage factors, F_s

With regard to the effect of changing the storage factor, F_s, it can be seen from fig. 5.11 that the solar contribution increases with an increase in F_s. However, it is interesting to note the following:

(a) The change is not significant at low collector to floor area factors, F_{cf}. For example, when changing from 25 l/m^2 to 200 l/m^2, there is an increase in the solar fraction which is approximately 0.04 in the case of F_{cf} = 0.1 as compared to an increase of approximately 0.22 in the case of F_{cf} = 1.0 (see fig. 5.10).

(b) There is a significant increase in the annual solar fraction when changing the storage factor from 25 to 50 l/m^2 and then the rate of increase becomes smaller. This is in agreement with the graph of fig. 5.9, which relates the storage factor with the system economics and shows that the life cycle savings reach their maximum at a storage factor of about 50 l/m^2.

5.4.4 Heat exchangers

The efficiency of collectors in a solar heating system is influenced by all other components in the system. In order to minimise the heat loss from the collector, it should be supplied with liquid at the lowest available temperature. This is possible if thermal stratification occurs in the storage tank so as to maintain a warm, lower density liquid layer near the top of the tank, and a colder, denser liquid layer near the bottom of the tank. However, according to Ward *et al.* (1977), very little stratification is possible in the storage tank, since lower rates of water flow through the collector loop are too high for maintenance of stratification in the storage tank. In addition, the resulting benefits of stratification from installation of baffles or other devices to retard mixing in the tank are insufficient to justify the cost.

Water from the bottom of the storage tank should be circulated directly or indirectly to the collector. An optional heat exchanger, hereinafter called a collector–storage heat exchanger, could be employed in the collector and storage subsystem, in order to transfer heat from the collector fluid to the storage tank. Such an arrangement, however, would increase the capital cost of the system and would affect the system thermal performance; the latter is to be investigated in the present study.

In addition to dependence on heat input from the collector, storage temperatures are affected by the rate of heat delivery to the load, dependent, in turn, on the characteristics of the load heat exchanger. It is an advantage for the solar system if it can lower the liquid temperature in the storage tank as much as possible. The type of heat exchanger used and the arrangement for heat delivery can bear importantly on the minimum water temperature achieved in the storage tank. Selection and sizing of heat exchangers are therefore important in system design.

A number of simulations were run to investigate the effect of the collector–storage heat exchanger effectiveness, ε_c, on the system performance. The results were used to plot the graphs of figs. 5.12 to 5.14.

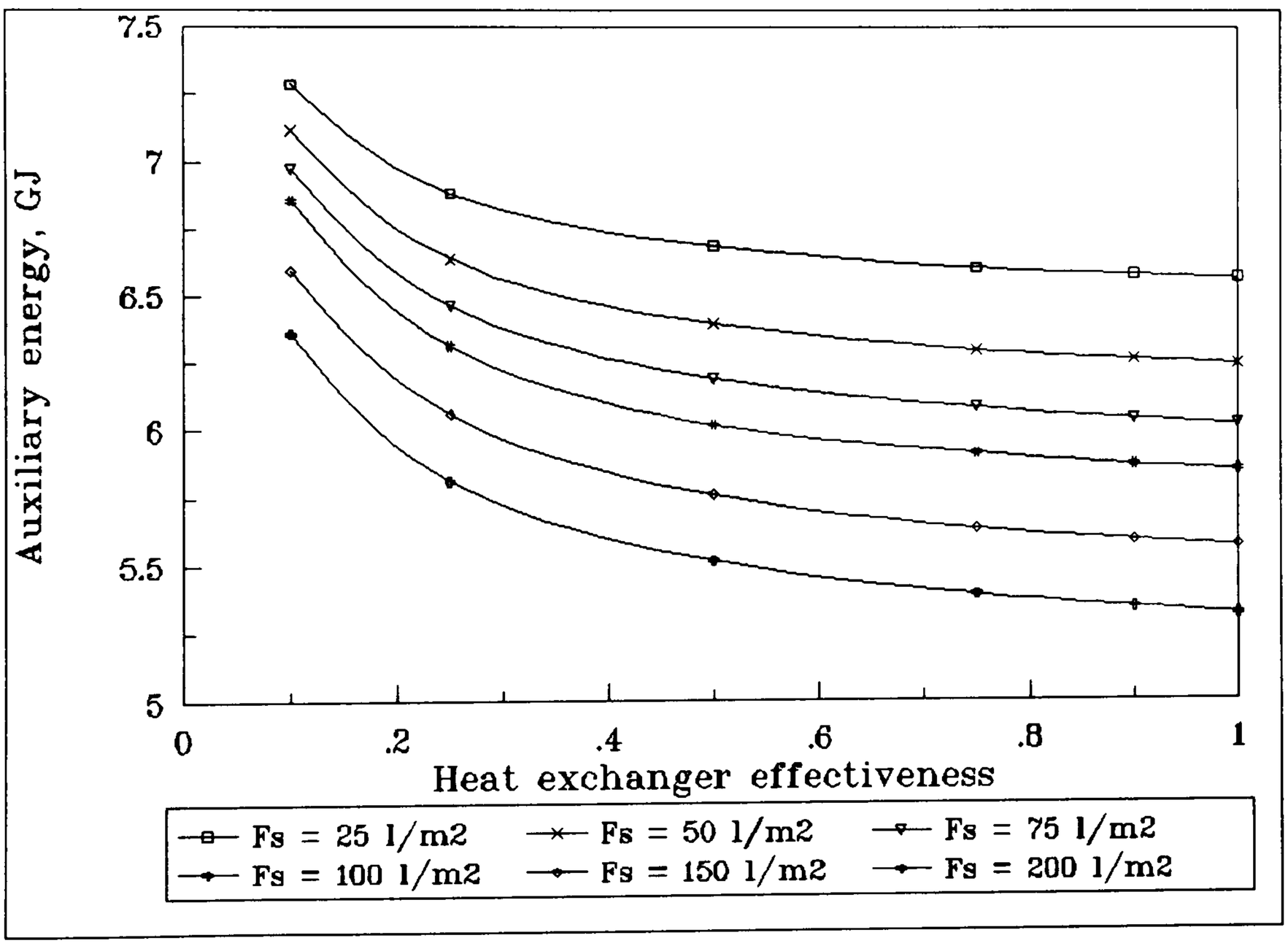

Fig. 5.12 Effect of collector–storage heat exchanger effectiveness, ε_c, on the auxiliary energy demand, at different storage factors, F_s

It can be seen from the graphs that the best results, i.e minimum auxiliary energy consumption, are obtained with maximum storage capacity and with effectiveness equal to 1. However, it is interesting to note that there is a significant decrease in the auxiliary energy, thus an important increase in the solar fraction, when increasing the effectiveness from 0.1 to 0.5 while for values beyond 0.5 the effect is not

significant (see fig. 5.12). This is also shown in fig. 5.13, which illustrates the variation of the collection average efficiency and the solar fraction with the heat exchanger effectiveness, at a storage capacity of 50 l/m^2.

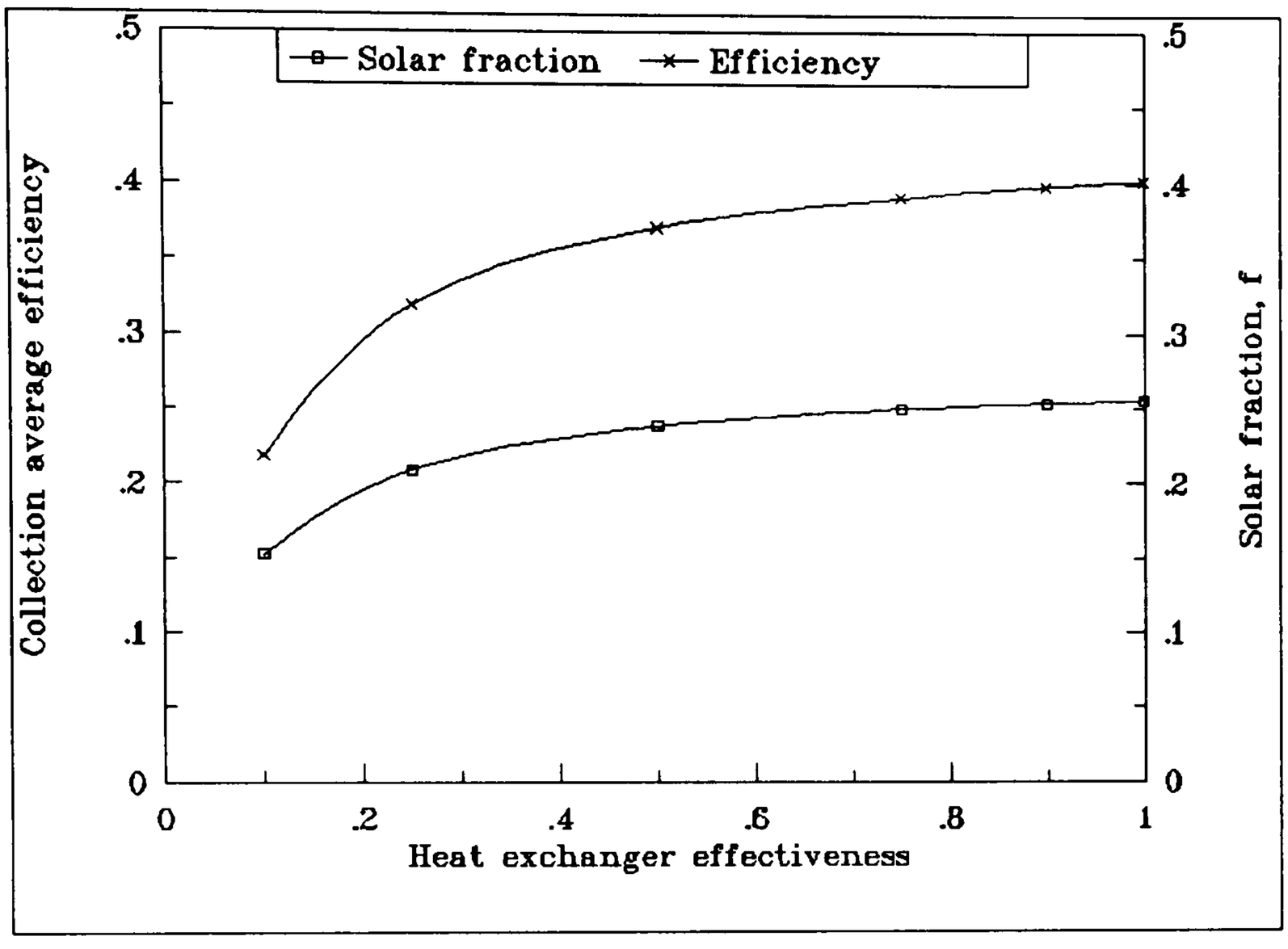

Fig. 5.13 Effect of collector–storage heat exchanger effectiveness, ε_c, on solar fraction and collector average efficiency

The effect of increasing ε_c from 0.1 to 0.5 is more distinct in the case of collection efficiency which changes from approximately 0.22 to 0.37 (i.e a percentage increase of 67%) while the solar fraction changes from 0.15 to approximately 0.24 (i.e a percentage increase of 67% again). The best results are obtained with $\varepsilon_c = 1$; this condition is the same as that without a heat exchanger.

The effect of employing a heat exchanger in the collector–storage subsystem is clearly shown in the graph of fig. 5.14 which compares the variation of the monthly and annual solar fraction with and without a heat exchanger when the auxiliary source is in parallel and in series with the solar system. It is interesting to note that the best results are obtained without a heat exchanger and with the auxiliary energy source in parallel with the solar system. When the auxiliary is connected in series with the solar, the system performance is reduced as a result of increased tempera–tures and hence higher heat losses from the collector and the storage system.

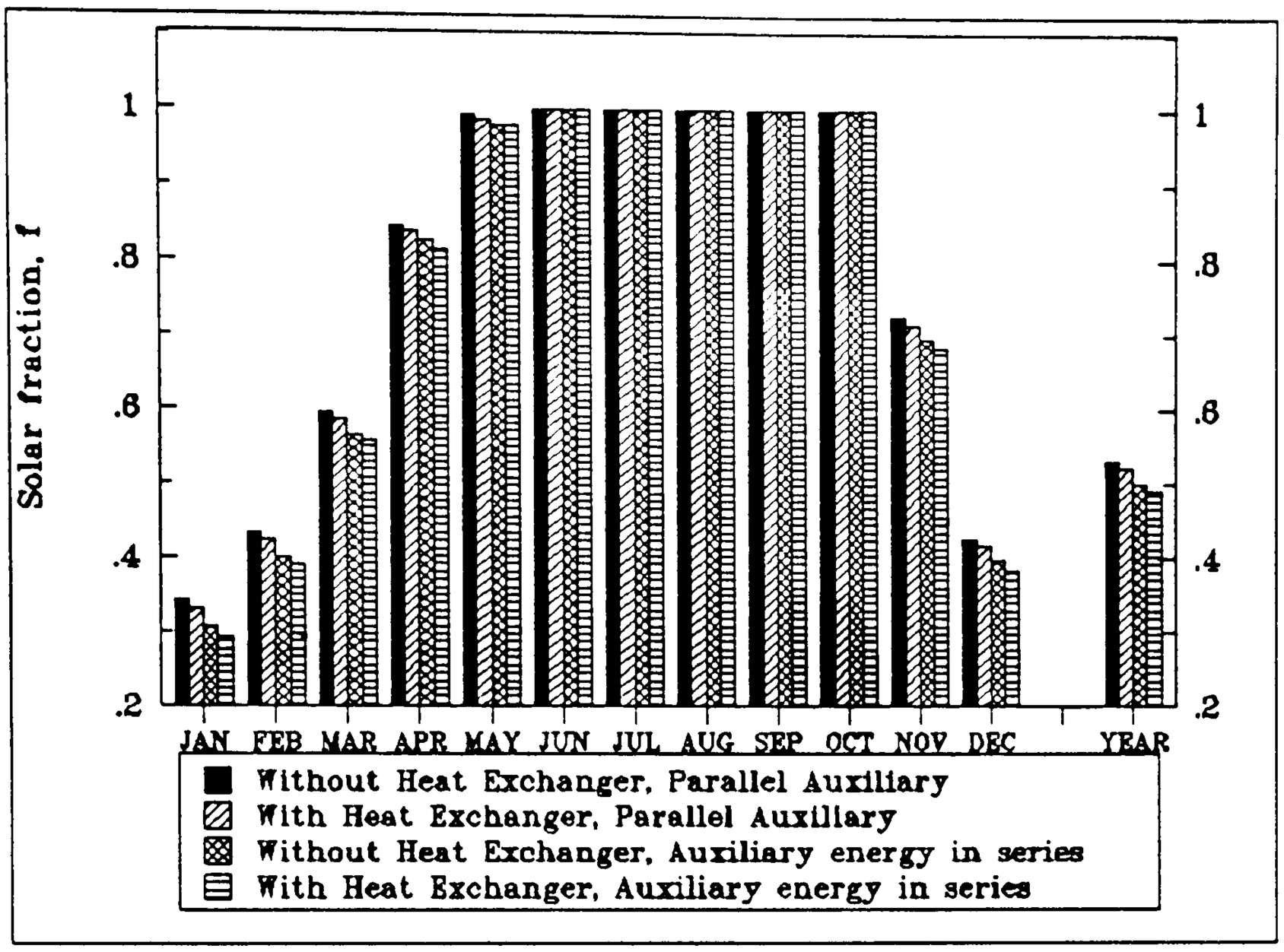

Fig. 5.14 Effect of collector–storage heat exchanger on the system monthly and annual solar fraction

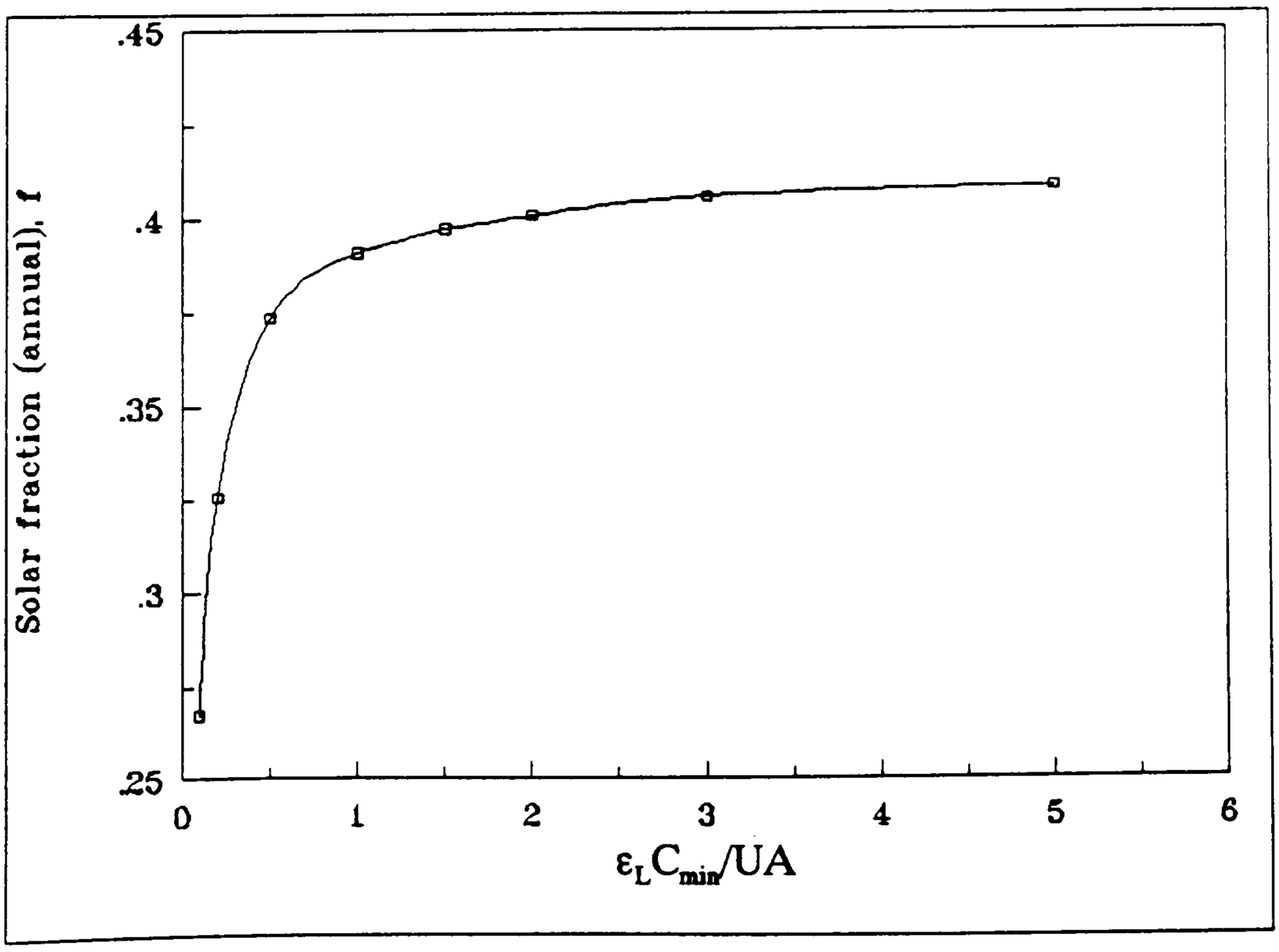

Fig. 5.15 Effect of load heat exchanger size

Fig. 5.15 shows the effect of the load heat exchanger size on the system performance. The size of the load heat exchanger is represented by the dimensionless parameter $\varepsilon_L C_{min}/UA$, where ε_L is the load heat exchanger effectiveness, C_{min} is the minimum capacitance rate of the heat exchanger and UA is the total building energy loss coefficient. This parameter has been found to provide a measure of the size of the heat exchanger needed to supply solar energy to a specified building (Klein *et al.* 1976). From the curve in fig. 5.15, it is seen that the change in system solar fraction due to too small a heat exchanger is significant for values of $\varepsilon_L C_{min}/UA$ less than 1. For values greater than 1 the change in system performance levels off. This is in agreement with Klein *et al.* (1976) who suggested that reasonable values of $\varepsilon_L C_{min}/UA$ for solar space heating systems are between 1 and 3. In the present study the simulation results have been obtained with $\varepsilon_L C_{min}/UA$ equal to 2.

5.4.5 Auxiliary heat

An auxiliary heat source is required as a backup to the heating system for use when the solar collector and storage subsystem is unable to meet heating demands. Although the collector and storage could be sized large enough to meet the full heating load throughout the heating season, the cost would be prohibitive, as indicated in the previous sections. An economical design involves a smaller solar system and an auxiliary unit capable of meeting the full heating demand (at design conditions) when solar collection is not possible and when stored heat is inadequate. This combination results in more effective use of the solar equipment throughout the heating season and a lower annual total cost.

There are several methods for supplying auxiliary heat in a liquid solar system for space heating. In virtually all practical solar heating designs, auxiliary heat is supplied to the fluid stream in which heat is distributed to the building. With hydronic distribution (individual fan coil units or radiators), a fuel–fired or electrically heated hot water boiler is used. If a central heat exchanger and ducted warm air are employed, auxiliary heat is most economically and practically supplied in a furnace or electric heater through which the solar heated air passes to the rooms.

In the present investigation two alternative solutions have been investigated, as described in section 5.3, namely auxiliary in parallel and auxiliary in series. A comparison of the two approaches can be made from the graph of fig. 5.14. It is evident that parallel auxiliary brings about higher solar fractions and is therefore more advantageous.

5.4.6 Effect of collector mass flux

Another factor that affects the performance of a solar space heating system is the collector mass flux, G, i.e the rate of water flow through the collector per unit area of collector, expressed in kg/h m^2. In order to investigate its effect on the system performance, a number of simulations were run for the first week of January and the results were used to plot the graph of fig. 5.16 which shows the variation of solar fraction with the collector mass flux.

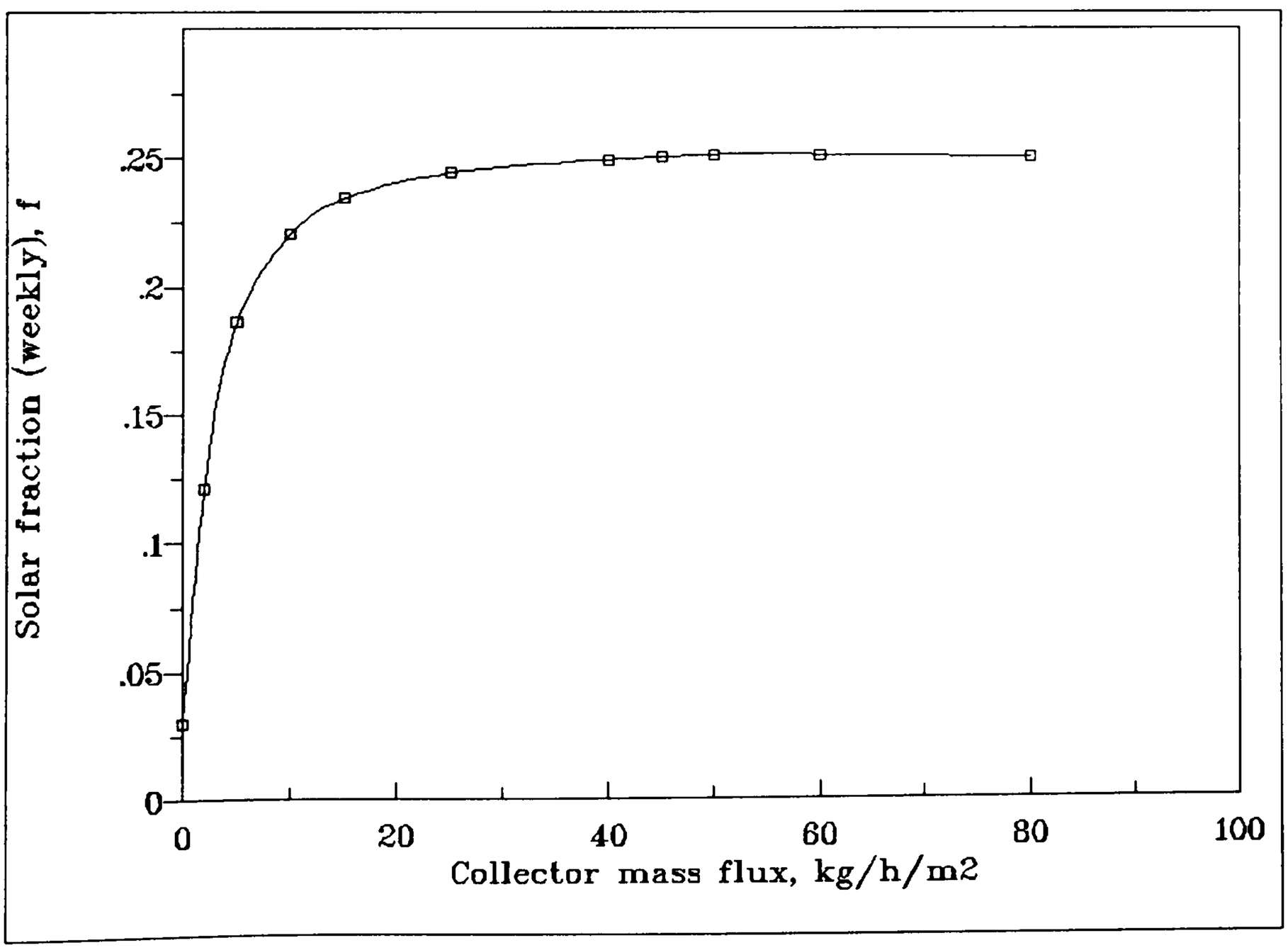

Fig. 5.16 Variation of solar fraction with collector mass flux

As the mass flux increases, the solar fraction increases too. This is explained by the fact that an increased flow rate through the collector is associated with a decrease in

the temperature rise in the collector which in effect causes lower heat losses and an increase in the useful energy gain. The solar fraction increases sharply as collector mass flux increases from 0 to 15 kg/h per m^2 and then increases at a much slower rate until it reaches a maximum corresponding to a collector mass flux of about 40 to 50 kg/h per m^2. Beyond this point, the solar fraction remains rather constant. This shows that there is no scope for maintaining a high flow rate of water through the collector. On the contrary, this will bring about an increased capital cost and higher pumping power which in fact will reduce the solar contribution to the system energy demand and will affect negatively its cost effectiveness. It appears, therefore, that the optimum collector mass flux is within the range of 40 – 50 kg/h per m^2 of collector.

5.5 Prediction of system performance

The simulation model developed can be used to predict the annual performance of a system. For this purpose the optimum design criteria, which have been investigated through simulations, were used to simulate the performance of the system. It is assumed that the system is required to meet the space heating demand for a residential house having a heat loss coefficient, UA, of 4000 kJ h^{-1} K^{-1}. The following design criteria have been used:

- Collector slope: 50° from horizontal
- Collector size: 70 m^2, based on 0.55 m^2/GJ annual heating load
- Storage tank: 3.5 m^3, based on 50 l/m^2 of collector
- Collector mass flow rate: 2800 kg/h, based on 40 kg/h per m^2 of collector
- Load heat exchanger: $\varepsilon_L C_{min}/UA = 2$
- Auxiliary energy: in parallel with the solar.
- Collector–storage heat exchanger: Not applicable

A summary of the results is shown in Table 5.4, which shows the monthly values of total solar radiation , useful solar energy collected, heating load, auxiliary heat used, solar fraction. Under these conditions, the predicted annual solar fraction is 0.58, which means that 58% of the annual heating load is met by solar while the rest is supplied by the auxiliary source.

Month	Q_{ins} (GJ)	Q_u (GJ)	Load (GJ)	Q_{aux} (GJ)	f	η
Jan	27.181	11.15	28.84	17.65	0.39	0.41
Feb	31.234	12.32	24.70	12.67	0.49	0.39
Mar	38.395	13.51	20.26	7.18	0.65	0.35
Apr	40.670	9.86	10.20	1.25	0.88	0.24
May	41.300	4.19	2.81	0	1	0.10
Jun	40.180	1.6	0.32	0	1	0.04
Jul	43.680	1.3	0.09	0	1	0.03
Aug	43.890	1.39	0.10	0	1	0.03
Sep	41.510	1.48	0.39	0	1	0.04
Oct	38.640	3.72	3.25	0	1	0.10
Nov	31.010	8.59	11.34	2.30	0.80	0.28
Dec	28.070	11.65	23.60	12.24	0.48	0.42
Year	445.76	80.76	125.90	53.29	0.58	0.18

Table 5.4 Predicted performance of a residential solar space heating system, at optimum design criteria

It is seen from the above results that the useful energy collected during the summer period is very small and in fact nearly zero, which is in agreement with theory. According to Duffie and Beckman (1980), the useful heat gain by the collector, Q_u, is :

$$Q_u = F_R A [S - U_L (T_i - T_a)] \quad (5.2)$$

where F_R is the collector heat removal factor, defined as the ratio of the useful energy collected to the useful energy which would be collected if the entire collector surface were at the temperature of the fluid entering the collector. Mathematically, F_R, is given by:

$$F_R = \frac{\dot{m}\ c\ (T_o - T_i)}{A_c\ [S - U_L\ (T_i - T_a)]} \tag{5.3}$$

where, S is the absorbed solar energy per unit area, T_i and T_o are the temperatures of the water at the collector inlet and outlet respectively, U_L is the collector heat loss coefficient, and $\dot{m}$ is the water flow rate through the collector.

In fact, during the summer period, a high amount of energy is accumulated in the storage tank since there is no demand for heating, except from heat losses from the tank. As a result of this, the storage tank is maintained at relatively high temperatures. This means that the collector inlet temperature is high and the temperature rise through the collector is nearly zero. In effect, the collector heat removal factor is nearly zero, which explains why the useful heat gain, Q_u, is zero.

Another interesting piece of information is that the solar contribution to the system heating demand is very high at the beginning and the ending of the heating season. The solar fraction for example during the month of November is about 0.80. In the heart of winter season, namely in January, the solar fraction is about 0.39, which means that 39% of the monthly heating load is met by solar. This is so because in January the weather is colder than that of November and therefore the heating load is higher so that the solar system can meet only a part of it.

The results of the simulation were used to plot the graphs of figs. 5.17 and 5.18. Fig. 5.17 shows the variation of predicted monthly energy supply by solar and auxiliary, at optimum design criteria, assuming electricity is used as auxiliary, while fig. 5.18 illustrates the variation of the monthly average efficiency of collector.

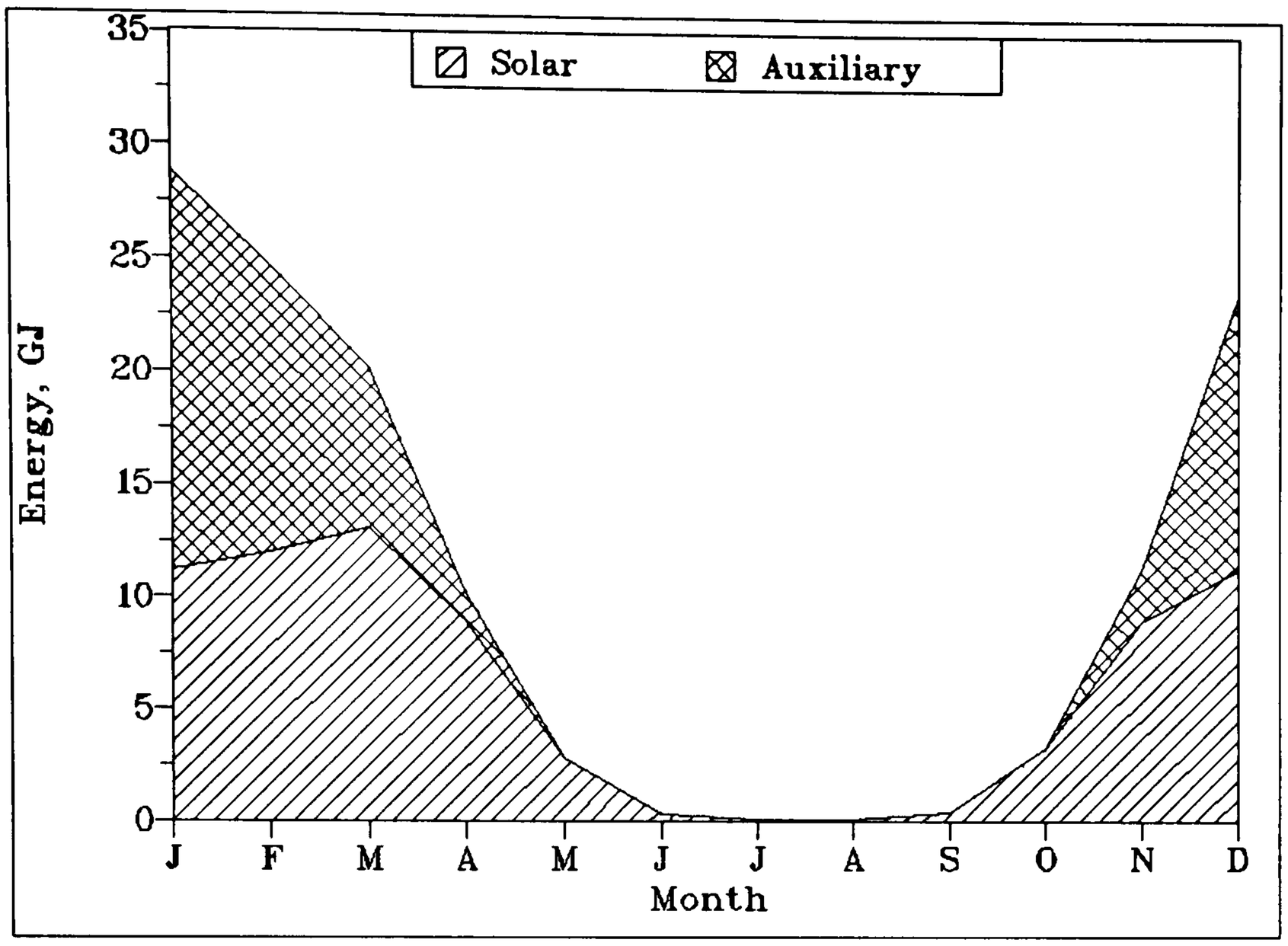

Fig. 5.17 Predicted monthly energy supply by solar and auxiliary, assuming optimum design criteria: $\beta = 50^{o}$ from horizontal, $A_c = 70\ m^2$ (0.55 m^2/GJ), $F_s = 50\ l/m^2$, $G = 40\ kg/h\ m^2$, auxiliary in parallel, $\varepsilon_L C_{min}/UA = 2$

It is interesting noting that the variation of the collector average efficiency shown in fig. 5.18 follows the pattern of variation of the space heating load (solar + auxiliary) in fig. 5.17. The collector average efficiency is maximum in the heart of the heating season (December and January) and decreases to nearly zero during the summer (no heating) season, as does the heating load. During the period of June to September, the collectors operate at high temperatures and therefore a high temperature difference between the collector and the surroundings which results to a high $\Delta T/I_T$, corresponding to low, almost zero, efficiencies.

The above investigations indicate that the system is under–utilised for a long period of time and this is certainly one of the reasons that make solar space heating non competitive to conventional systems. The problem is more distinct in the case of Cyprus where the heating season is relatively short. The situation, however, could be better if a hot water subsystem is integrated in the system, so that the available energy is utilised throughout the year. This possibility is investigated in Chapter 6.

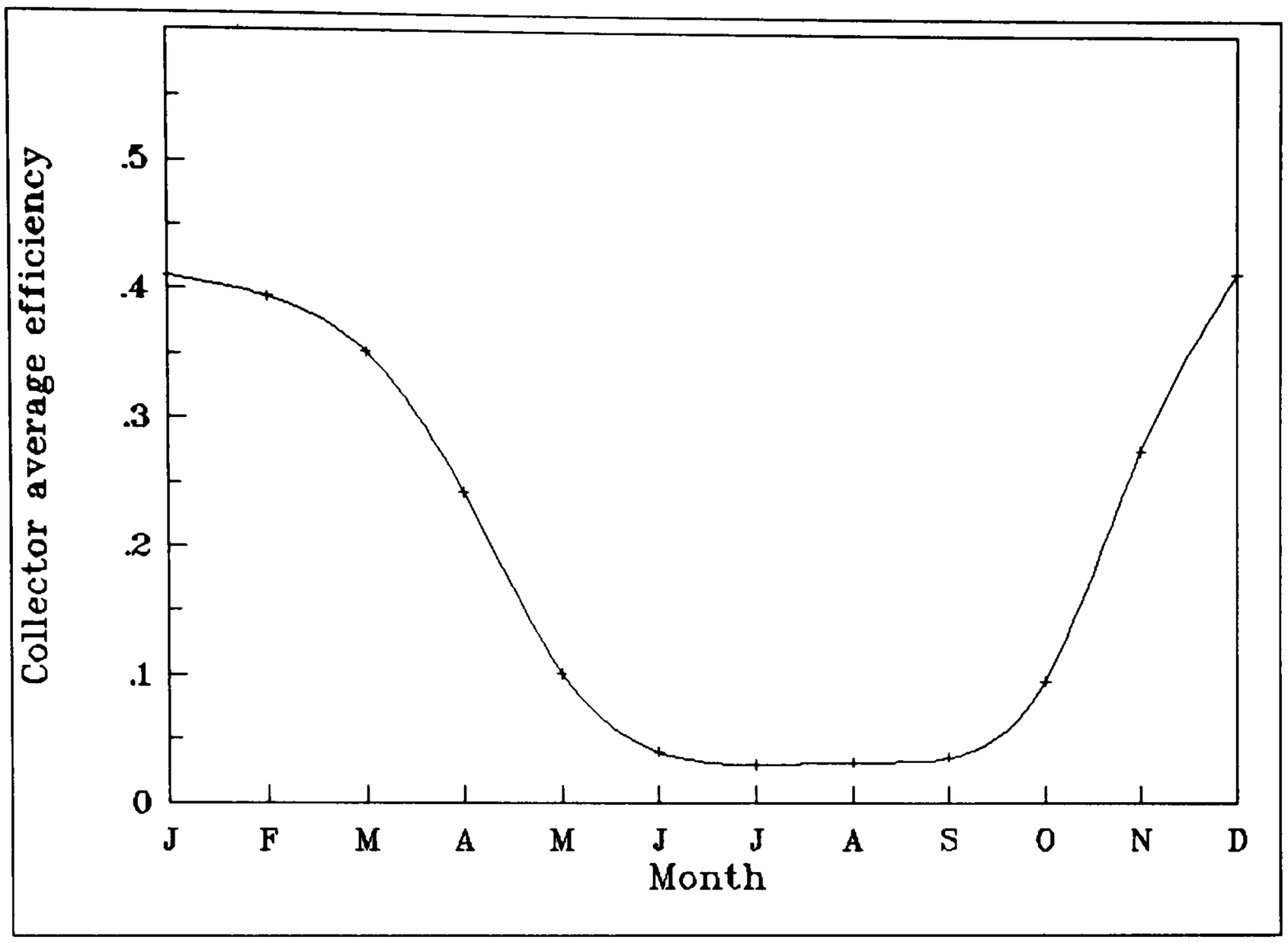

Fig. 5.18 Variation of collector monthly average efficiency

CHAPTER 6

MODELLING AND SIMULATION OF COMBINED SOLAR WATER AND SPACE HEATING SYSTEMS

6.1 Introduction

In the previous chapters, some design criteria were investigated, separately for hot water and space heating systems respectively. However, in most of solar heating applications in buildings, space heating and hot water systems can be combined together in an integrated system which will provide domestic hot water throughout the year, plus space heating during the heating season. This system is more convenient and economical as compared to single solar space heating, because, during the warm months of the year, the solar collectors which would otherwise be unused, can supply practically all of the required domestic water heating.

This chapter, aims to model such a system, using TRNSYS component models, and simulate its performance, in order to investigate and confirm the validity of the optimum design criteria, as done separately for solar water and space heating systems.

6.2 System configuration

Fig. 6.1 illustrates the schematic diagram of a combined solar space and water heating system capable of meeting the requirements of both, domestic hot water and space heating of a building. It comprises the collector and storage subsystem, the domestic hot water subsystem, separate auxiliary sources of energy for domestic hot water and space heating, heat exchangers, pumps and control devices.

The system is arranged to collect solar energy in a non-freezing liquid, such as water

with antifreeze additives, via an optional collector–storage heat exchanger, and supply heat from storage to the space heating and service hot water equipment. When solar energy cannot meet the demand of either domestic water or space heating, auxiliary heat is added from one or both of the conventional auxiliary units shown. Heat from the solar storage tank may be distributed to the living spaces either in hot water or in warm air, as described in Chapter 5. In the simulations which follow, a water to air load heat exchanger is assumed.

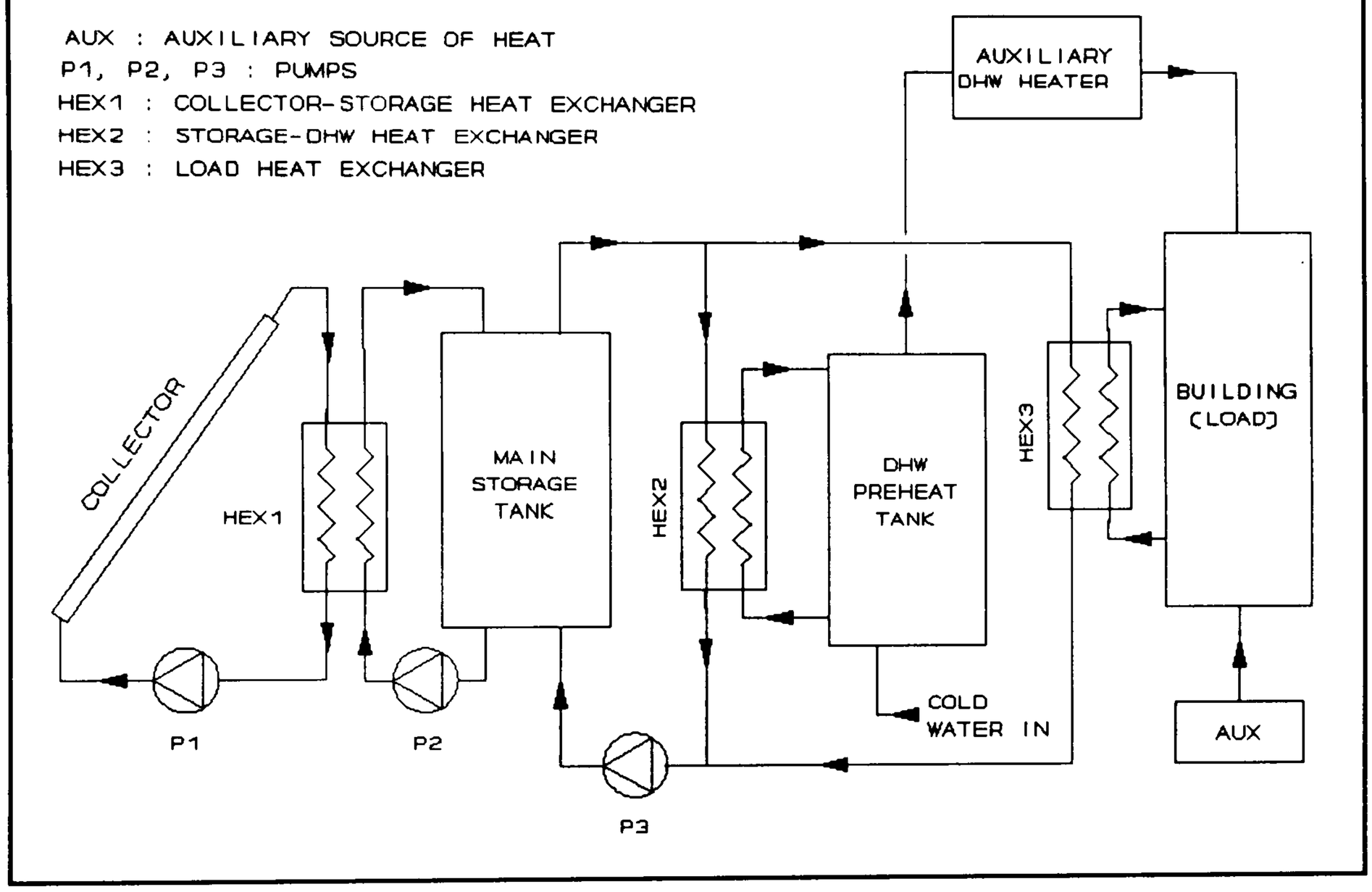

Fig. 6.1 Schematic diagram of a combined solar water and space heating system

6.3 The simulation model

Like the solar water and space heating systems described in the previous chapters, the combined solar water and space heating system is modular and the simulation model for the system is formulated by connecting the models of each of the system components. There is, however, a characteristic of the system under investigation which distinguishes it from the previous ones: the solar equipment in the combined solar water and space heating systems, for some period of the year, has to perform

a dual duty, i.e. supply heat to the building space and produce service hot water at the same time. This means that at a certain point of the system, the water flow streams returning from the space heating circuit and the service hot water subsystem must be mixed. This role is undertaken by a Tee–piece TYPE 11, so that the storage tank "sees" both, service hot water and space heating loads.

The simulation platform is synthesized from a number of TRNSYS components which include the collector–storage subsystem, the domestic water heating subsystem, the space heating load, the weather generator, etc. A complete list of the components is presented in Appendix E, together with the simulation model concerning the system under investigation.

With regard to service hot water load, although the hot water demand is subject to a high degree of variation from day to day and from consumer to consumer, it is impractical to use anything but a repetitive daily profile. For the present simulation, hot water consumption profile DOM4 (see Table 4.1 and fig. 4.1) will be used. The weather data used is the same as that used for the previous simulations and is shown in Table 4.2. The weather data file, CYDATA.DAT, is listed in Appendix A.

The system simulation model, including all the component parameters and inputs, is described in the simulation input file JM4.DAT and is shown in Appendix E.

As in the previous models, a large number of parameters are required as inputs to the system model and some of these are shown in Table 6.1. The simulation concerns residential applications of combined water and space heating. For this purpose a typical Cypriot house having a floor area of 200 m^2 and characterised by a heat loss coefficient, UA, of 4000 kJ h^{-1} $^oC^{-1}$ is used. It must be noted, however, that the simulation model can be used to simulate the performance of any other building and at any other conditions, provided the appropriate inputs and parameters are used.

In addition to the above component models, a number of equations are included in the system model, other than those contained in the component models, such as for example the equations defining the collector average efficiency for the year and the annual solar fraction, which are represented by EFBAR and FRACT respectively,

instead of the symbols η and f used in the text. These are defined as follows:

$$EFBAR = \frac{QU}{QINS} \tag{6.1}$$

where, QU is the yearly useful heat gain by the collector, and

QINS is the yearly solar energy incident on the collector.

$$FRACT = \frac{TLOAD - TAUX}{TLOAD} \tag{6.2}$$

where, TLOAD is the total heating load (water and space heating), and

TAUX is the total auxiliary heat supplied to the system.

The performance index will be the system solar fraction, f, in this case denoted by FRACT, which is defined as the fraction of the load provided by solar energy.

The following information is printed at monthly intervals during the simulation, except for the last two, i.e. the yearly collector efficiency EFBAR and the solar fraction FRACT, which are printed at the end of the year (see Appendix E):

QINS	: Incident solar energy on the collector, kJ
QU	: Useful solar heat gain by the collector, kJ
HLOAD	: Space heating load, kJ
HAUX	: Auxiliary heat for space heating, kJ
HWLOAD	: Domestic hot water load, kJ
HWAUX	: Auxiliary heat for domestic hot water, kJ
TLOAD	: Total heating load (space + hot water), kJ
TAUX	: Total auxiliary heat for space and water heat kJ
QINPH	: Heat supplied from solar to hot water tank, kJ
QPLOAD	: Heat supplied from hot water tank to load, kJ
EFBAR	: Collector yearly average efficiency
FRACT	: Yearly solar fraction

The system model has the ability to calculate and print additional information, such as temperatures, heat losses from tanks, etc, provided the appropriate parameters and inputs are properly set.

1. Collector–storage subsystem	
A_c	10 – 200 m^2
G_{test}	54 kg h^{-1} m^{-2}
G	50 kg h^{-1} m^{-2}
$F_R(\tau\alpha)_n$	0.78
F_RU_L	24.4 kJ h^{-1} K^{-1} m^{-2}
ε_c	0.1 – 1.0
β	0 – 90° from horizontal
ρ_g	0.2
V_s	0.5 – 10.0 m^3
U_s	1.2 kJ h^{-1} K^{-1} m^{-2}
2. Domestic water heating subsystem	
V_p	180 l
U_p	1.2 kJ h^{-1} K^{-1} m^{-2}
T_{req}	50 °C
ε	0.75
R_p	2
$\dot{m}_{sp}$	500 kg h^{-1}
M_D	As per profile DOM4 (see fig. 4.4)
3. Building space heating load	
UA	4000 kJ h^{-1} K^{-1}
T_R	20 °C
$\varepsilon_L C_{min}$	400 – 40000 kJ h^{-1} K^{-1}

Table 6.1 System simulation parameters

In addition to thermal performance, the system model is designed to perform economic analysis based on a number of assumptions concerning the economic parameters. Following the parameter listing, the output of the economic analysis contains the following information:

1. The collector area.
2. The initial cost of the system, i.e the sum of area dependent and fixed costs.
3. The amount of down payment.
4. The credits.
5. The resale value.
6. The mortgage payment.
7. The principal remaining on the loan at the end of each year.
8. The amount of the annual payment that went to interest in each year.
9. The amount of depreciation deduction taken by an income producing system in each year (if applicable).
10. In year zero of the analysis, this is the down payment. In subsequent years it is the annual mortgage payment. If the length of the analysis is less than the term of the mortgage, the value in this column for the last year of the analysis will be the last year's mortgage payment plus the remaining mortgage principal.
11. The amount of insurance and maintenance costs.
12. The property tax payments.
13. The savings in fuel.
14. The net annual cash flow which is the sum of items 13 and 14 minus items 10, 11 and 12.
16. The present worth, which is the value printed in output 14, discounted back to year zero at the market discount rate.
17. The rate of return.
18. Payback periods.
19. The total out of pocket cost of the system.
20. The present worth of all costs associated with the solar system.
21. The present worth of the fuel costs of the conventional system.
22. The constant cost per unit of delivered energy of the system.
23. The constant cost per unit of delivered energy for the conventional system
24. The present worth of cumulative net cash flow, i.e the difference between items 21 and 20.

6.4 Optimisation of design criteria

In Chapters 4 and 5, a number of optimum design criteria have been optimised, separately for service hot water and space heating systems respectively. A summary of the optimum values of the most important criteria, (electricity backup) is presented in Table 6.2 for comparison. It can be seen from Table 6.2 that certain design criteria, such as for example, the storage factor and the collector mass flux were found to be the same for both water and space heating systems. Consequently, the same values will apply to a combined solar water and space heating system.

Design criteria	**Optimum values**	
	Domestic hot water	**Space heating**
Collector tilt angle, β, degrees	35	50
Collector to load factor, F_{cl}, m^2/GJ	0.45	0.55
Collector to consumer factor, F_{cc}, m^2/consumer	1	N.A
Collector to floor area factor, F_{cf}, m^2/m^2	N.A	0.35
Storage factor, F_s, l/m^2	50	50
Collector mass flux, G, kg/h m^2	50	50
Space heating load heat exchanger, $\varepsilon_L C_{min}/UA$	N.A	1 – 3
N.A = Not Applicable		

Table 6.2 Summary of optimum design criteria for separate solar water and space heating systems, for residential applications

However, a number of other design criteria, like for example the collector tilt angle and the collector size, differ. It is, therefore, necessary to investigate the optimum values or ranges of values for which the system performance is maximum at

minimum costs. This task is performed by conducting an economic analysis of the system, with the use of the Economics Analysis subroutine of TRNSYS, as done with the previous simulations.

The life cycle savings and the payback period for the system, as defined in chapter 5, are used as the main economic criteria for evaluating and optimising the system design criteria. The economic parameters used in the simulation are the same as those used for the solar space heating system simulation (see Table 5.2).

6.4.1 Optimisation of collector tilt angle

From the literature review, it is clear that there is a wide range of optimum collector tilt angles as recommended by different investigators, for combined water and space heating systems. Lunde (1980), for example, suggests that the optimum tilt angle for a year round water and space heating system is $\phi \pm 15^{o}$, where ϕ is the location latitude; Carg (1982) suggests 0.9ϕ to ϕ, while Lof and Tybout (1973) recommend ϕ+(0 to 30°). For Cyprus, the above recommendations would mean 20 to 50°, 32 to 35°, and 35 to 65° respectively, i.e, a range from 20 to 65°, which is very wide to be considered as a recommendation for design purposes. There is, therefore, scope for investigating a narrower range of design tilt angles.

In the previous chapters, the optimum collector tilt angle has been investigated, separately for solar hot water and space heating respectively. Simulations have shown that for a solar hot water system, which is a year round application, the optimum collector slope is 35°, i.e the location latitude, while for a space heating system only, which is a winter application only, the optimum collector tilt angle is 50°, i.e. location latitude plus 15°. The above findings may lead to the conclusion that for a combined hot water and space heating system, which implies year round utilisation of solar collectors, the optimum collector tilt should be within the range of 35 to 50°, i.e ϕ to $\phi+15^{o}$.

In the present work, the optimum tilt angle is investigated, based on the yearly performance of the system. For this purpose, the system solar fraction and the yearly

heat gain by the collector are taken as the indices of comparison. A number of simulations were run for different tilt angles from 0 to 90°. Computations are carried out assuming that the collector is oriented to face due south and the ground reflectivity is taken equal to 0.2. The results of the simulations were used to plot the graphs of figs. 6.2 and 6.3.

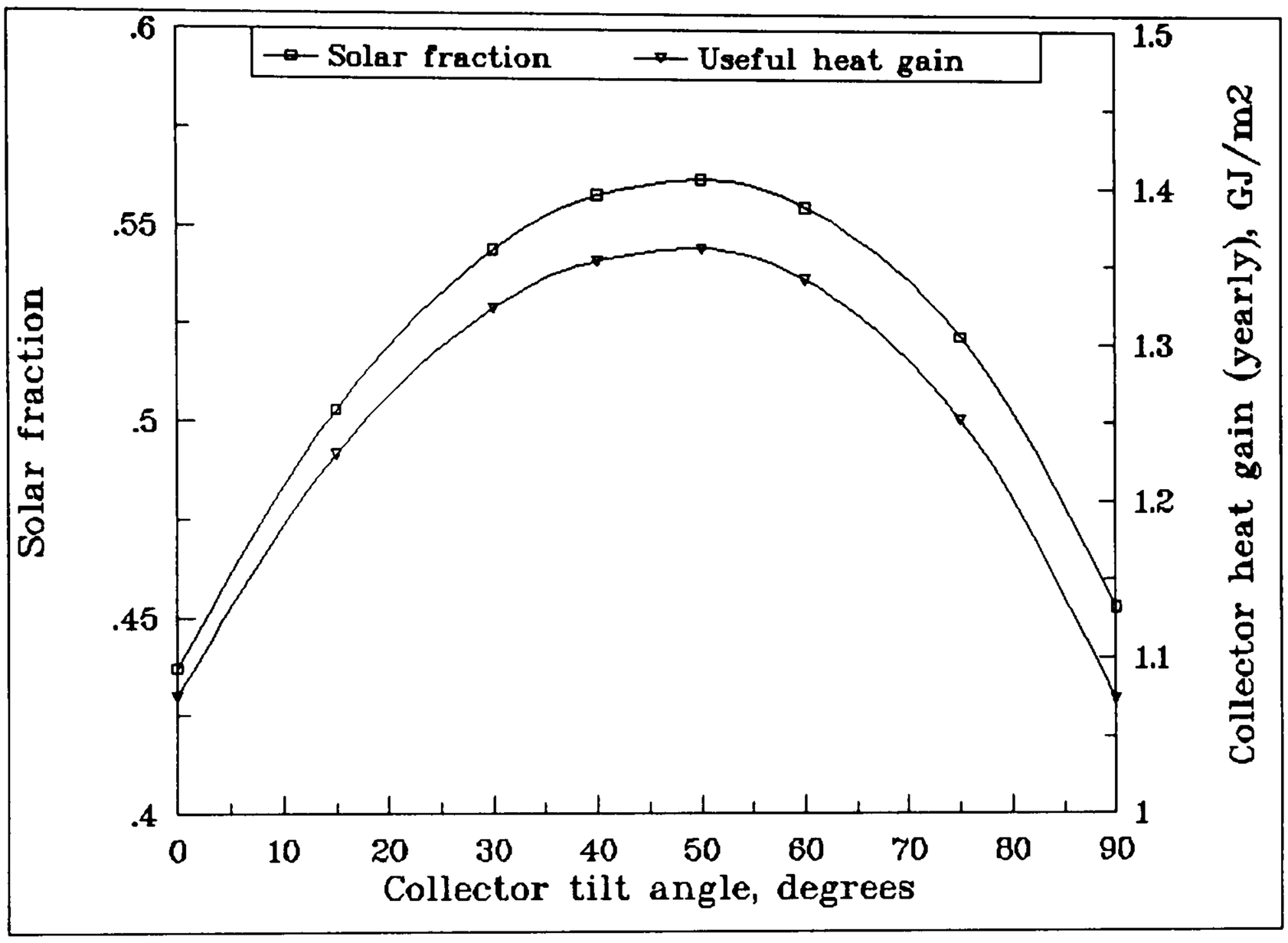

Fig. 6.2 Variation of annual solar fraction and collector heat gain with collector tilt angle

Fig. 6.2 shows the variation of the annual solar fraction and the collector useful heat gain with the collector tilt angle. Both plots have a maximum which corresponds to a tilt angle of about 50° from horizontal, which is the optimum tilt angle. Compared to the location latitude, ϕ, this tilt is ϕ+15°. However, there is a range of tilt angles within which yearly solar fraction and useful heat gain do not deviate considerably from maximum. This is clearly shown in fig. 6.3 which shows the variation of relative solar fraction with deviation of tilt angle from optimum. Relative solar fraction is defined as the ratio of the system annual solar fraction at any tilt angle to the solar fraction corresponding to the optimum tilt angle.

It is clearly shown that the solar fraction is reduced by approximately 1% when β_{opt} is changed by ±10°, and by less than 2% when β_{opt} is changed by ±15°. This may lead to the conclusion that the solar system may perform at nearly maximum performance if the tilt angle is within the range of ϕ and ϕ+30°, i.e, $\beta_{opt}=(\phi+15)\pm15°$. This is in agreement with what has been suggested by Tybout and Lof (1970), who recommend ϕ+(10 to 20)±10°.

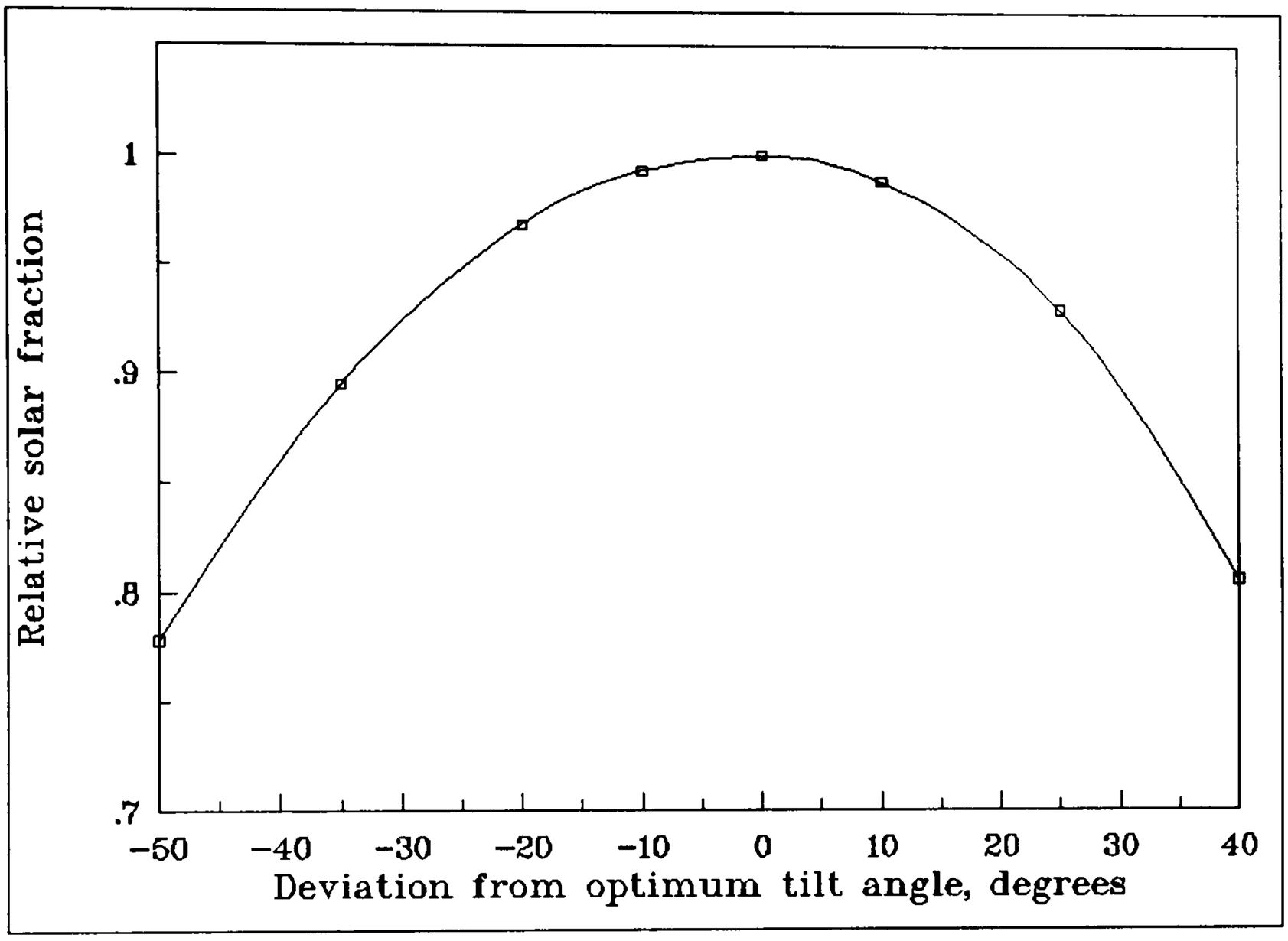

Fig. 6.3 Variation of relative solar fraction (f/f_{opt}) with deviation of collector tilt angle from optimum tilt

6.4.2 Optimisation of collector size

The optimum collector size is the collector surface area which will bring about maximum savings throughout the lifetime of the system, taking into consideration both the water and space heating loads. A number of simulations were run with the collector tilt angle fixed to 50° from horizontal, for different collector areas ranging from 10 m^2 to 200 m^2 in order to investigate the optimum collector size. This range corresponds to 0.05 – 1.55 m^2 of collector per GJ of yearly total heating load. The system was simulated at one hour time–step and a summary of simulation results is

shown in Table 6.3. The simulation results have been used to plot a number of graphs to correlate the yearly collector efficiency and solar fraction with the collector size and the collector load factor F_{cl}, as shown in Figs. 6.4 and 6.5.

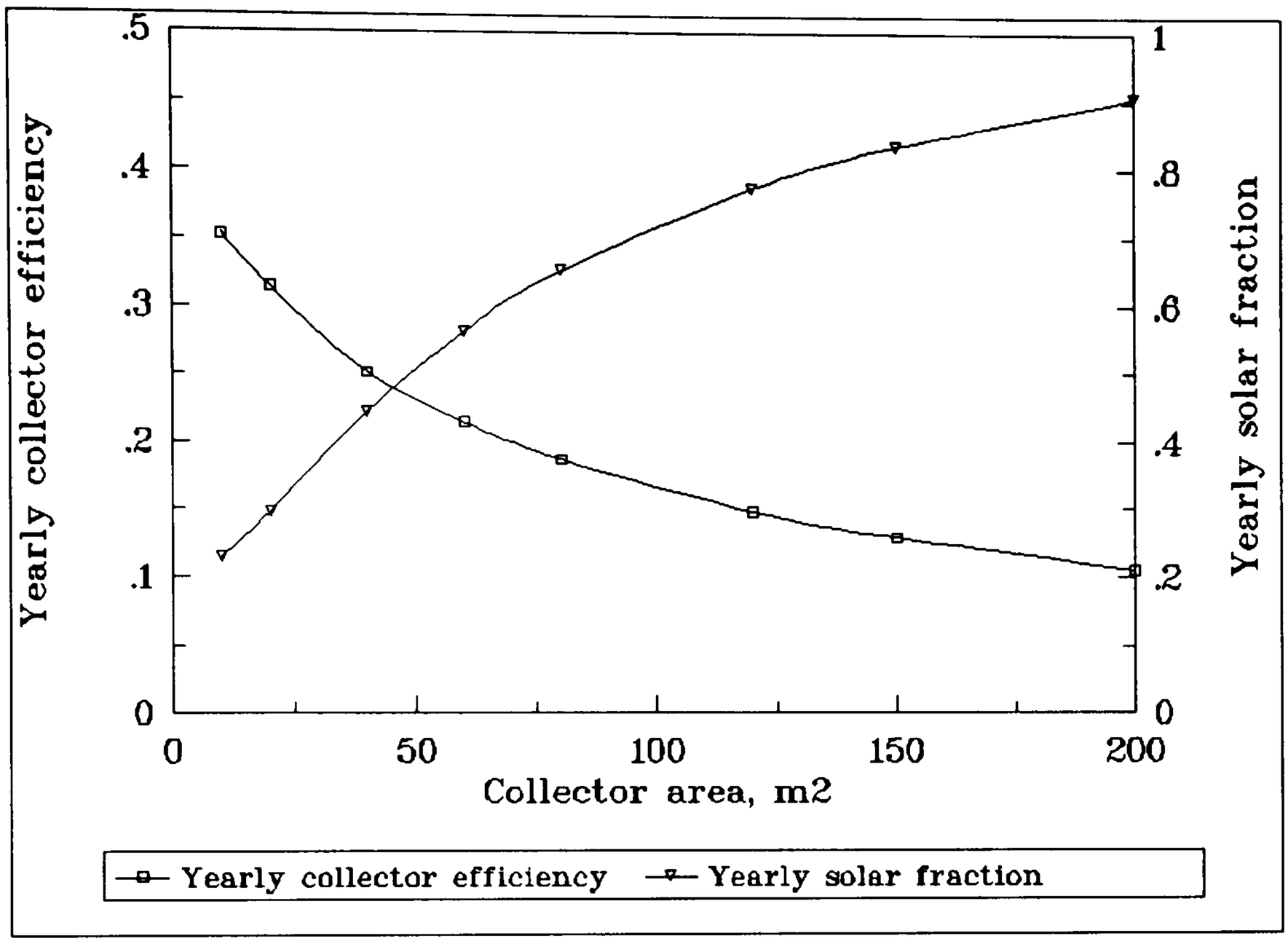

Fig. 6.4 Yearly collector efficiency and solar fraction as a function of collector size

The yearly collector efficiency and solar fraction are shown in fig. 6.4 as a function of collector size. It is clearly seen from these plots that as the collector area is increased, the efficiency decreases and the solar fraction increases. For a small collector of 10 m^2, for example, the yearly efficiency is about 35 per cent; for the 200 m^2 collector, the yearly efficiency decreases to nearly 10 per cent, which is a considerable reduction. The situation is, however, different with the solar fraction, which increases with the collector size. This means that, a large collector will have an increased contribution to the system heat demand but for a large fraction of the time it will operate at higher temperatures, thus lower efficiencies, and the energy delivery per unit area of collector will be reduced. This is also demonstrated in fig. 6.5, which relates the yearly collector efficiency and the solar fraction with the collector to load factor, F_{cl}.

A_c m^2	V_s m^3	HLOAD GJ	HAUX GJ	HWLOAD GJ	HWAUX GJ	QU GJ	QINS GJ	TAUX GJ	TLOAD GJ	QINPH GJ	QPLOAD GJ	FBAR (η)	FRACT (f)
10	0.5	127.7	101.3	7.781	2.2926	22.46	63.68	104.30	135.5	5.479	4.842	0.353	0.230
20	1	127.5	92.88	7.781	2.418	40.02	127.36	95.29	135.3	6.026	5.340	0.314	0.296
40	2	126.9	72.90	7.781	1.815	63.96	254.72	74.71	134.7	6.721	5.935	0.251	0.445
60	3	126.2	57.16	7.781	1.551	81.66	382.08	58.71	134.0	7.044	6.196	0.214	0.562
80	4	125.5	45.00	7.781	1.330	95.01	509.44	46.32	133.3	7.307	6.410	0.187	0.652
120	6	123.9	29.06	7.781	0.900	113.40	764.16	29.96	131.7	7.822	6.828	0.148	0.773
150	7.5	127.7	20.78	7.781	0.721	122.90	955.2	21.50	130.5	8.058	7.004	0.129	0.835
200	10	120.8	11.60	7.781	0.530	134.0	1273.6	12.13	128.6	8.336	7.201	0.105	0.906

Table 6.3 Summary of simulation results for different collector sizes

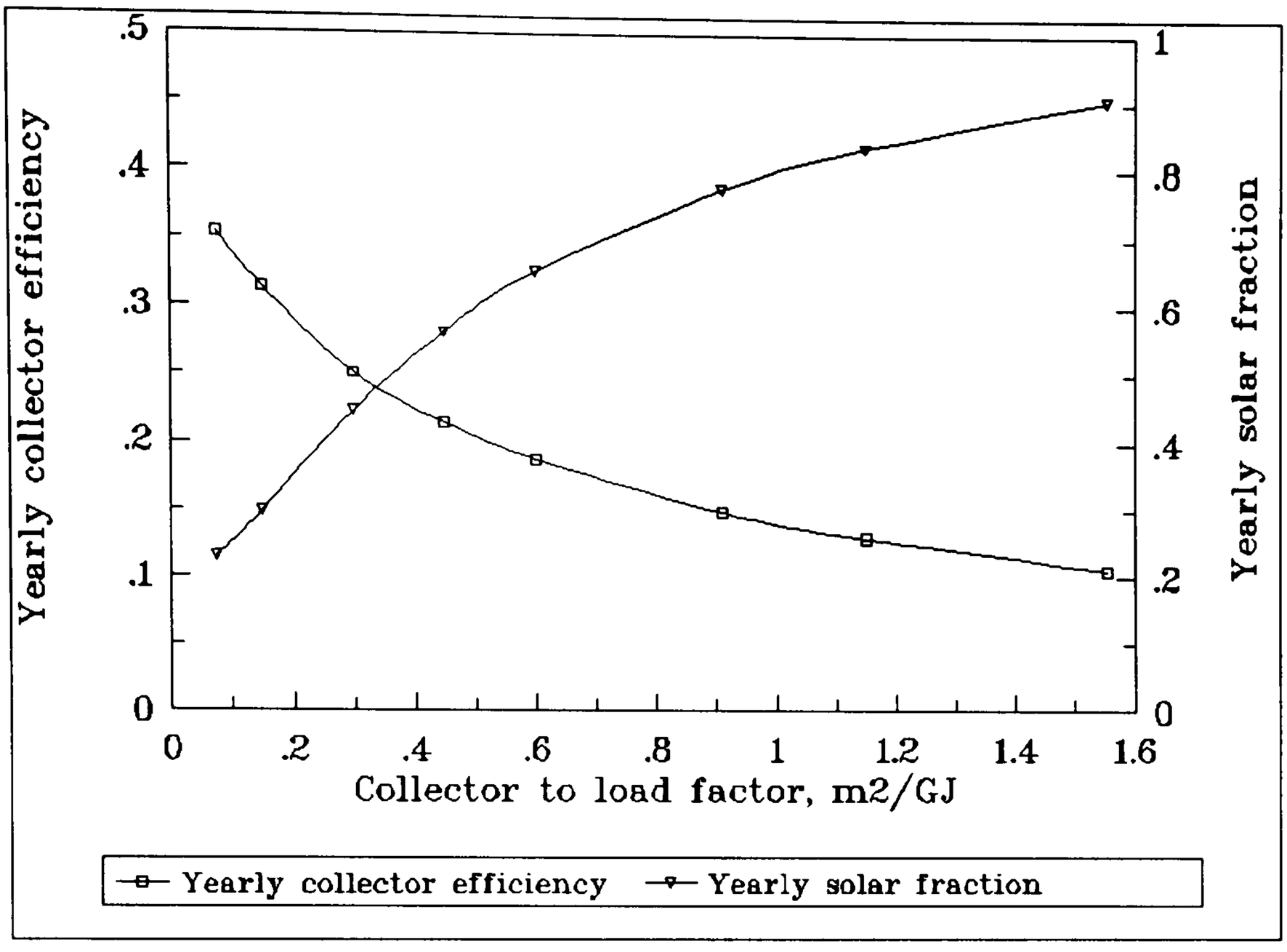

Fig. 6.5 Yearly collector efficiency and solar fraction as a function of collector to load factor, F_{cl}

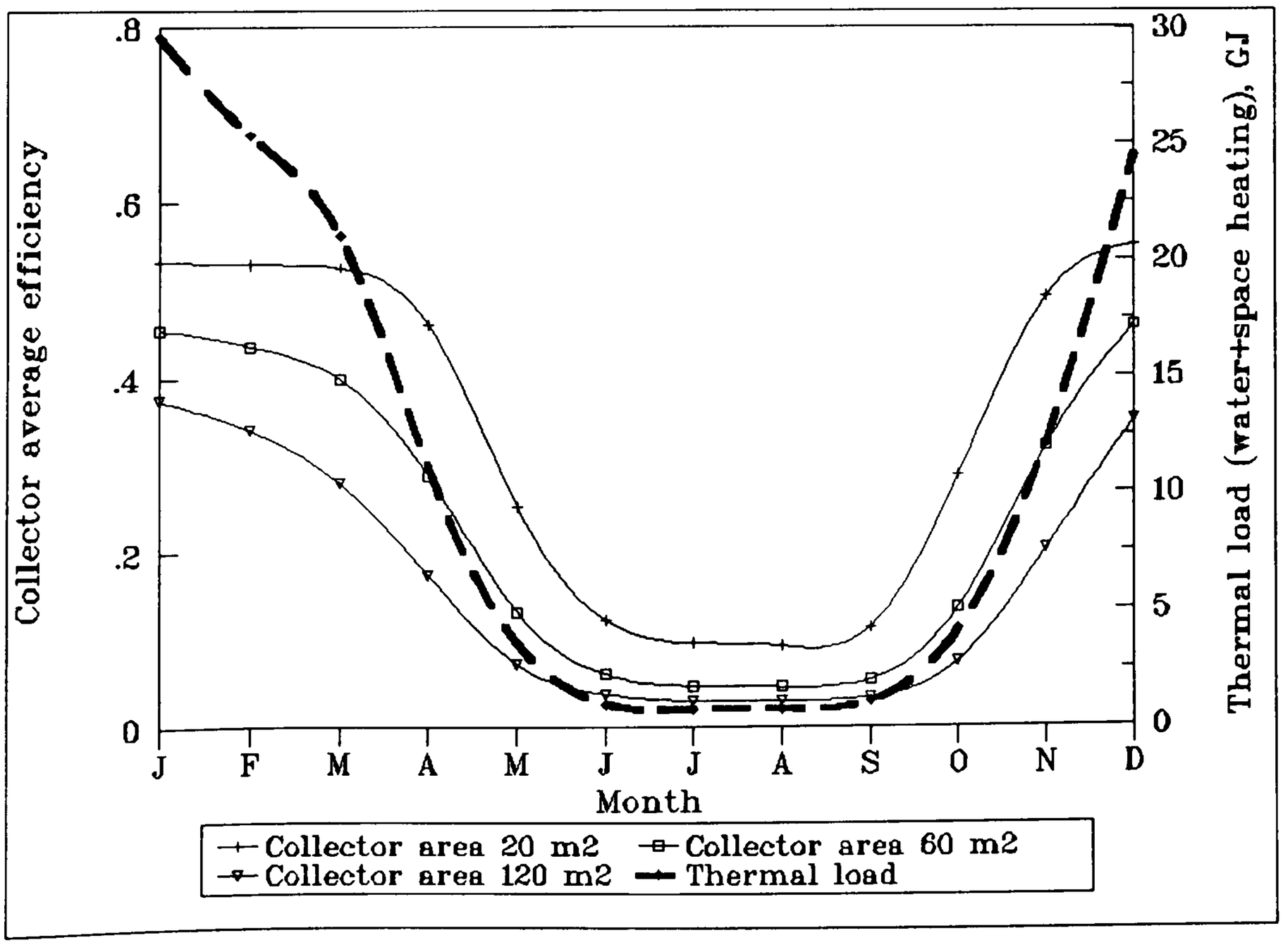

Fig. 6.6 Variation of total heating load and collector average efficiency for three different collector sizes (20, 60 and 120 m^2)

For a collector to load factor of 0.1 m^2/GJ for example, the collector average efficiency for the year is about 31.4 per cent while for a high F_{cl} of 1 m^2/GJ, the efficiency reduces drastically to only 10.5 per cent. However, since the collector yearly efficiency is, in fact, an average value of low and high efficiencies, this term does not necessarily represent the real facts. This is clearly shown in fig. 6.6 which represents the variation of monthly average efficiency of collector for three different sizes of collectors, namely 20, 60 and 120 m^2. Thus, for a collector size of 20 m^2 for example, which corresponds to a collector to load factor of 0.1 m^2/GJ, the monthly efficiency of collector is as high as 53 per cent in January, when the heating (space and service hot water) load is at its maximum, and gradually goes down to nearly 10 per cent in the summer season when the heating load is minimum (only service hot water is needed).

The monthly efficiency curve follows the pattern of the monthly space heating and service hot water load, as indicated in fig. 6.6. High efficiencies are associated with high heating loads and low efficiencies with low heat demand. The situation is, however, better when compared to the solar space heating system described in Chapter 5, where none of the collectors are utilised in summer. As a result of this, we have full coverage of the hot water heat demand in summer and therefore much better utilisation of the solar equipment. This in turn, will have a positive effect on the cost effectiveness of the system because it will pay back earlier than a simple solar space heating system similar to that presented in Chapter 5.

Another interesting piece of information from fig. 6.6, is the effect of increased collector size on the monthly collector efficiency. It is seen that the smaller systems always show higher efficiencies, and in winter this difference is more significant. Larger collectors run at higher temperatures than the smaller collectors and thus heat losses are higher. On the other hand, a large collector brings about a higher solar fraction and therefore reduced energy bills, but it is also associated with higher capital costs. For example, a system consisting of 40 m^2 of collector coupled to the appropriate size of storage tank, would require a capital cost of about 9,000 US dollars and would have an annual solar fraction of approximately 0.445 while a larger system of say 80 m^2 would cost about 18,000 US dollars and would have an increased solar fraction of 0.652 which means increased energy savings.

It is, therefore, necessary to investigate the cost effectiveness of the system and consequently determine the optimum economic size of the collector. For this purpose, an economic analysis is made, assuming a number of economic parameters. These are shown in the simulation input file JM4.DAT of Appendix E, under the label "UNIT 29 TYPE 29 ECONOMIC ANALYSIS", and some of them are listed in Table 5.2 of Chapter 5. One of the major parameters which is very decisive on the cost effectiveness of the system is the cost of conventional energy and the cost of solar equipment. For the purpose of this study, the energy produced from diesel oil fired boilers is priced at 7.4 dollars per GJ while electricity is priced at about 36 dollars per GJ. There is a significant difference in favour of diesel oil, for the reason that the latter is almost free of tax as compared to other energy forms like petrol and LPG on which a high tax is imposed.

The economic scenario used in the present simulation assumes a 20 year lifetime of solar equipment and an annual rate of increase in fuel price of 5%. A number of simulations were run, for different collector sizes and for diesel and electricity as backup energy sources. Some of the results are summarised in Table 6.4 for comparison purposes. The results of the simulation have been used to plot the graphs of figs. 6.7 and 6.8 which relate the life cycle savings with the collector size and the collector to load factor, respectively.

It is clearly shown from fig. 6.7 that when the system uses diesel oil as backup energy the life cycle savings are negative at large collector sizes and they become zero when the collector area is approximately 50 m^2. This is a critical condition indicating the point at which the optimum solar system design can compete with the conventional system. Beyond this point, the life cycle savings become positive and they increase as the collector area decreases. The form of the curve indicates that the life cycles savings tend to reach their maximum at very small or nearly zero collector area. An evaluation based on the payback period of the system, shows that at the critical condition where the life cycle savings are zero, the payback period is around 15 years but it drops down to 8 years when the collector area is only 10 m^2 or 0.6 m^2 per GJ of annual heating load. The above findings are good indications that, for the economic scenario assumed in the simulation, the solar system cannot compete with the diesel oil fired heating system.

A_c (m^2)	Diesel–oil backup			Electricity backup		
	f	LCS (dollars)	Payback (years)	f	LCS (dollars)	Payback (years)
10	0.230	6308	8	0.230	46088	3
20	0.296	4576	11	0.296	51754	3
40	0.445	1637	14	0.445	65689	4
60	0.562	–2329	16	0.562	74639	5
90	0.652	–7098	18	0.652	79677	6
120	0.773	–18506	> 20	0.773	80665	7
150	0.835	–27296	> 20	0.835	77309	8
200	0.906	–44597	> 20	0.906	66690	9

Table 6.4 Summary of simulation results, diesel oil and electricity backup

The situation is better and in favour of solar when the comparison is made with electricity as backup energy source. Figures 6.7 and 6.8 show that the life cycle savings are positive for all sizes of collectors. This is a good indication that the economic scenario is favourable to solar energy and that the solar heating system is the economic choice. As collector area increases, the life cycle savings increase until they reach a maximum which corresponds to the optimum collector size. As the collector size is further increased, the savings decrease as a result of excessive capital costs which force the solar savings to decrease.

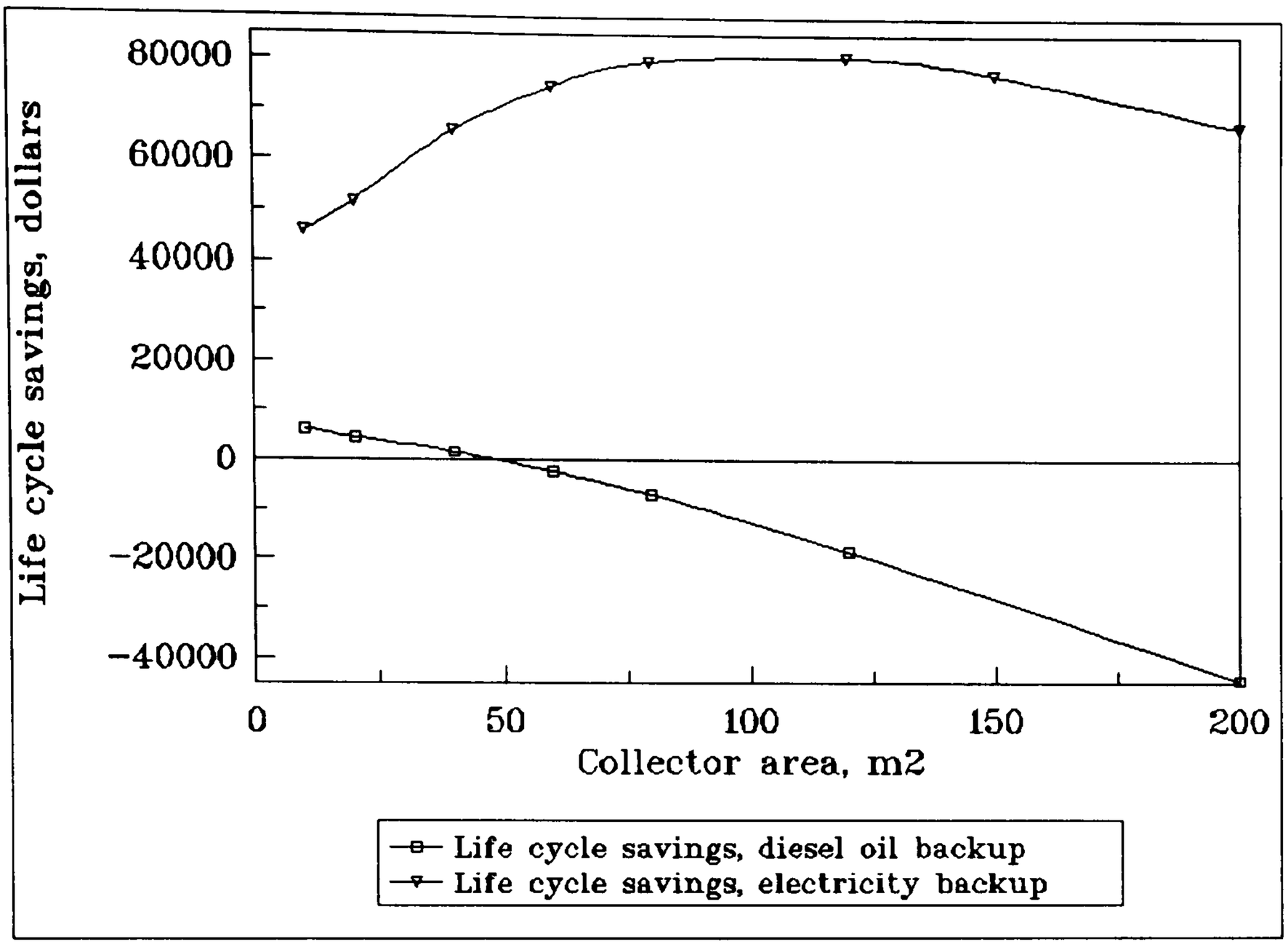

Fig. 6.7 Life cycle savings as a function of collector size, for diesel and electricity backup energy

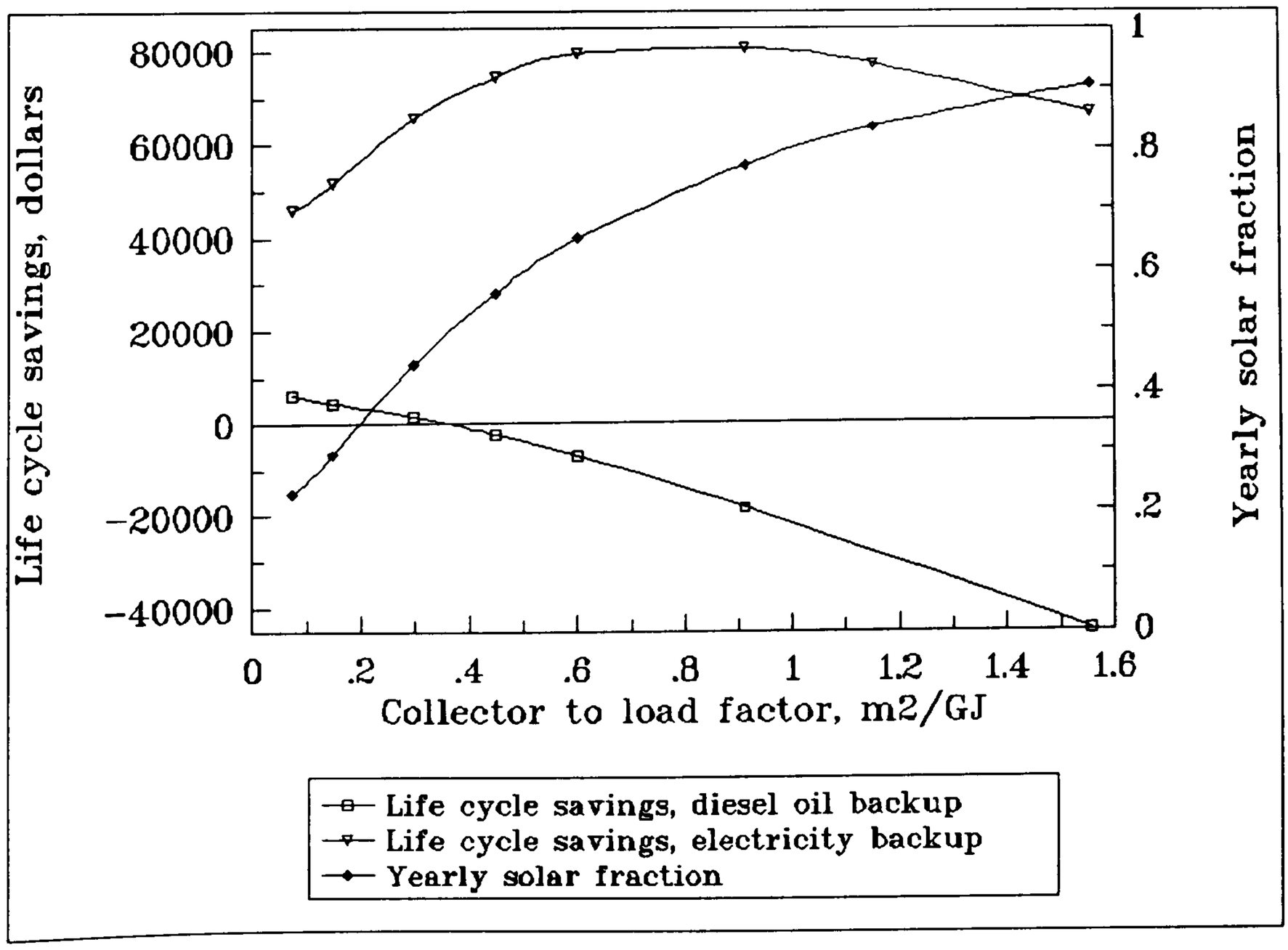

Fig. 6.8 Life cycle savings and yearly solar fraction as a function of the collector to load factor, F_{cl}, for diesel and electricity backup energy

The optimum collector size occurs at a collector to load factor of approximately 0.6 m^2 per GJ of annual total heating load. This is slightly greater than the corresponding values found for simple solar water and solar space heating system, i.e 0.45 and 0.55 m^2/GJ respectively. The above increase was expected and it is attributed to the fact that the combined water and space heating systems is by nature associated with higher heating loads which impose a greater utilisation of the solar equipment. The solar fraction corresponding to the optimum collector size is approximately 65% and the payback period is about 5 years.

A detailed account of the annual energy balance of the optimised system is shown by the pie chart of fig. 6.9.

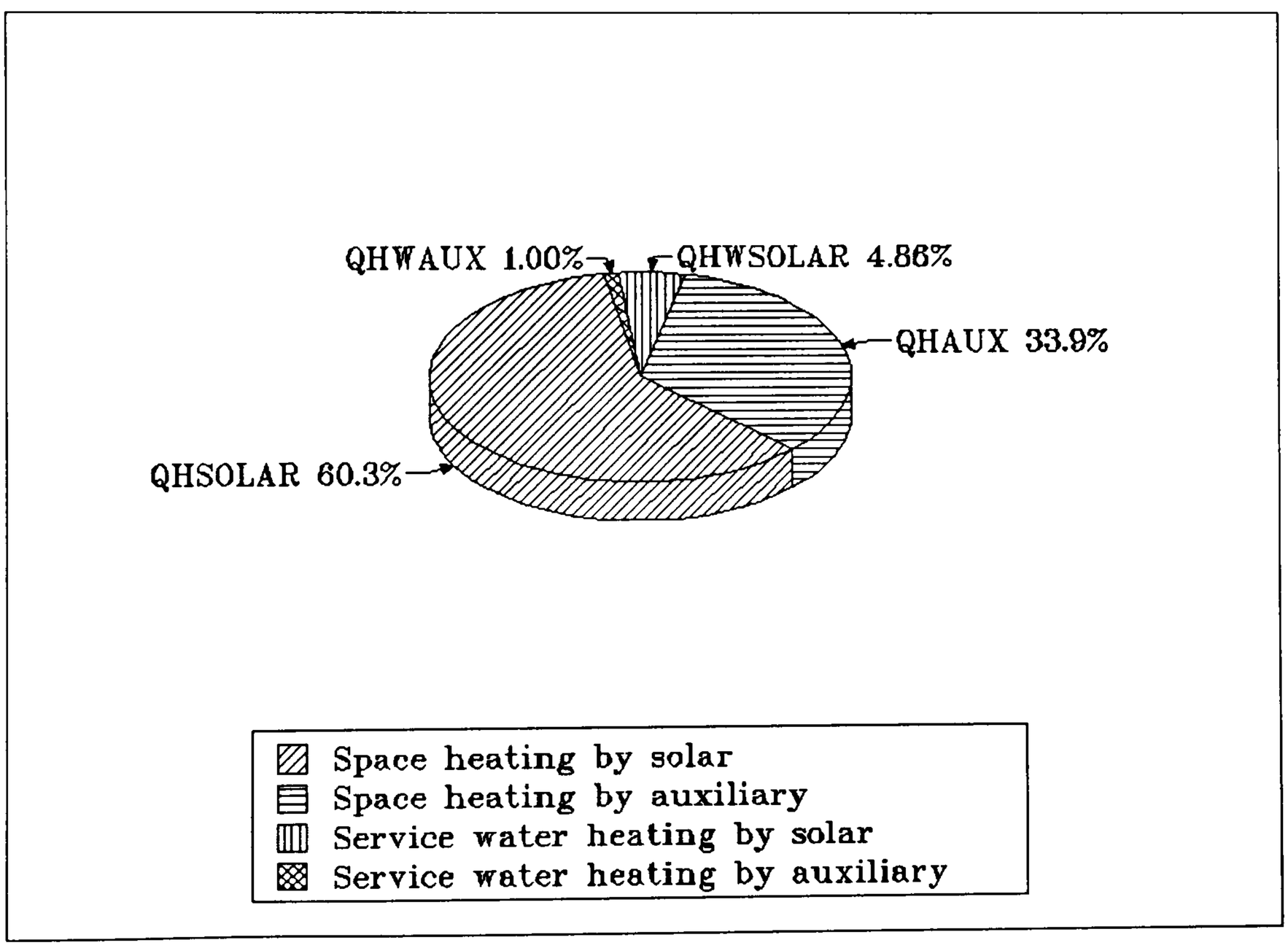

Fig. 6.9 A breakdown of the annual energy balance at optimum collector size

In conclusion, it can be said that the combined solar water and space heating system can compete with the conventional electric heating system and the optimum collector size under the economic scenario assumed is 0.6 m^2 per GJ of annual water and space heating load.

6.4.3 Effect of heat exchangers effectiveness

As it is shown in the schematic diagram of fig. 6.1, the system under consideration may include up to three heat exchangers. These are the collector–storage heat exchanger (HEX1), which is optional, the service hot water preheater tank heat exchanger (HEX2), which is again optional, and the load heat exchanger (HEX3), which is needed to transfer heat from the solar system to the building space. The first two exchangers are optional in the sense that they can be omitted under certain conditions of operation. The collector–storage heat exchanger is employed to separate the collector–storage circuit from the storage–load circuit. This is necessary if antifreeze additives are used to protect the collector from freezing during extremely low ambient air temperatures. In view of the fact that a heat exchanger may bring about a decrease in the system solar fraction, as found in Chapter 4, it would be advisable to omit it wherever possible. This is the case of simple space heating where the water circulating in the system is not consumable and once the chemical additives are added in the system they last for a long period of time. The second heat exchanger (HEX2), however, is necessary if the collector–storage heat exchanger is not employed, in order to separate the service hot water from the main system and thus maintain it free of the system chemical additives.

In order to investigate the effect of the effectiveness of the two heat exchangers (HEX2 and HEX3) on the system overall performance, a number of simulations were run for different values of effectiveness for the system operating at optimum design criteria (based on electricity as backup energy) i.e, collector tilt angle 50°, collector to load factor 0.6 m^2/GJ, collector mass flux 50 kg/h m^2, storage factor 50 l/m^2. Two different scenarios are examined:

(a) The collector storage heat exchanger is omitted and HEX2 is active; this is done by fixing the parameter concerning the heat exchanger effectiveness in UNIT 21 (collector–storage subsystem) of the simulation file equal to minus one, and varying parameter 10 of UNIT 23 (Domestic water heating subsystem) within a selected range of values, namely 0.5 to 1.

(b) The two heat exchangers are active. In this scenario, the corresponding parameters concerning the effectiveness, ε, are varied within the desired ranges of values, i.e 0.1 to 1.0.

The simulation with the first scenario, showed that the sensitivity of yearly solar fraction to the effectiveness of the heat exchanger of the hot water preheater is nearly non–existent. Even for low effectiveness such as 0.1, for example, the solar yearly fraction of the system is maintained at nearly the same levels as with a high effectiveness. This is attributed to the fact that the service hot water load is only a small fraction of the total load (around 6%).

With the effectiveness of the preheater heat exchanger fixed to 0.75, a second set of simulations have been conducted based on the second scenario. The sensitivity of yearly solar fraction and annual useful heat gain by collector to the effectiveness of the collector–storage heat exchanger, as predicted by the simulation results, is illustrated in fig. 6.10.

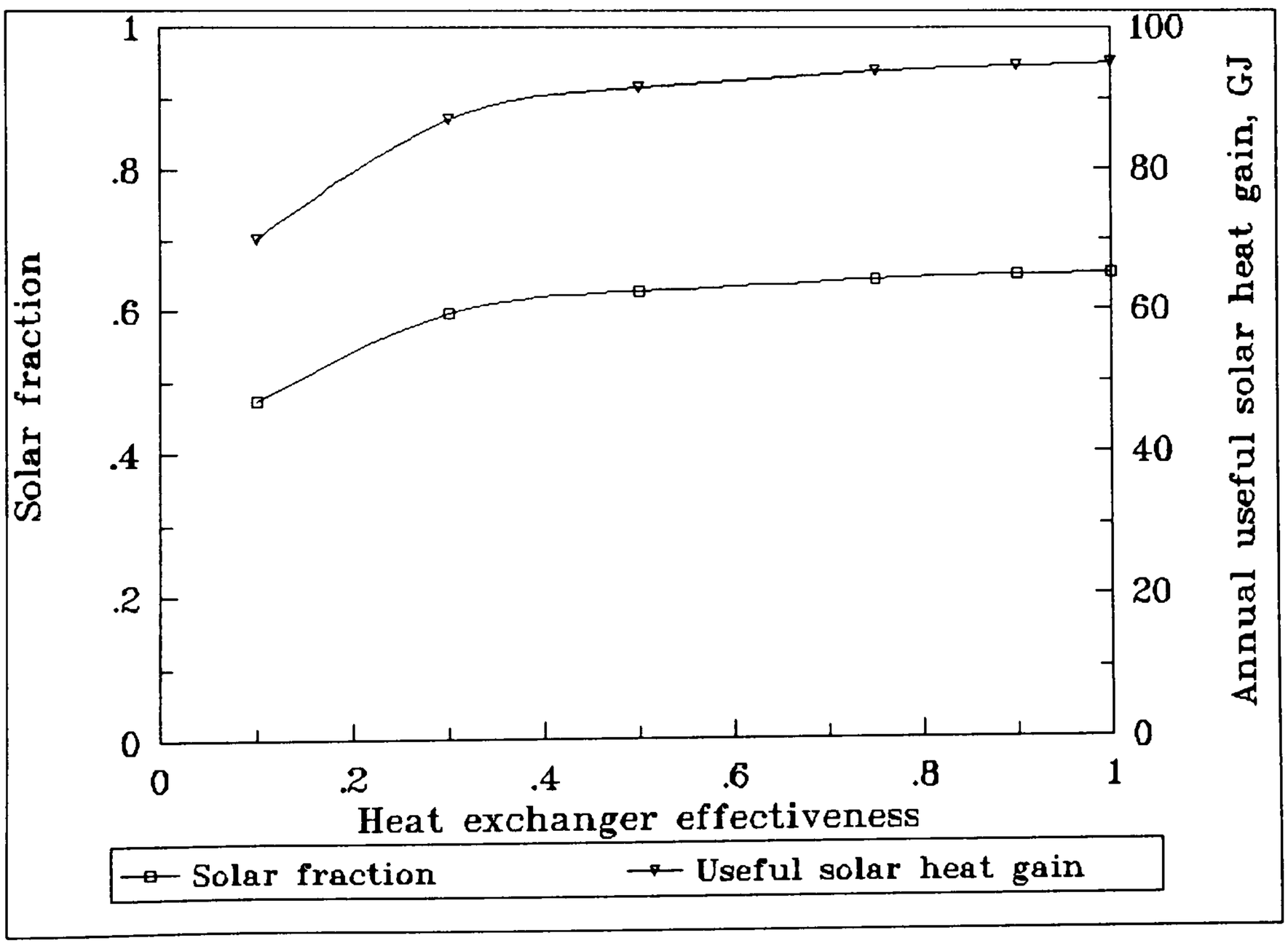

Fig. 6.10 The effect of effectiveness of collector–storage heat exchanger on the annual solar fraction and collector useful heat gain

At low effectiveness, the annual useful heat gain by the collector is relatively low as a result of poor heat transfer from solar collector to storage tank. Effectively, the solar fraction is also low. As the effectiveness increases the useful solar heat gain and the solar fraction are increased, until they reach a value beyond which the rate

of increase is very small. It is, therefore, clear that the system performance is sensitive to the collector–storage heat exchanger effectiveness particularly within the range of 0.1 to 0.3, and a high effectiveness is associated with high solar fraction. The best results are certainly achieved when the effectiveness approaches unity, which is equivalent to a situation where the heat exchanger is omitted.

In conclusion, we can say that of the two heat exchangers it is more beneficial and therefore advisable to include a heat exchanger in the hot water preheat tank in order to separate the service hot water circuit from the main system, and avoid using the collector–storage heat exchanger in order to obtain the maximum possible performance of the system.

As regarding the load heat exchanger, HEX3, its effect on solar fraction has been investigated in Chapter 5. In that case, the system performance and particularly solar fraction has been related to the dimensionless parameter $\varepsilon_L C_{min}/UA$, which concerns the space heating load. It has been shown that the system performance is optimum for values of $\varepsilon_L C_{min}/UA$ within the range of 1 to 3, which is certainly applicable to the combined solar space and water heating system under consideration.

6.5 Optimisation of a hotel application

In the preceding section, the optimisation concerned residential applications including flats having similar or nearly similar characteristics, concerning service water and space heating loads. A hotel application, however, is characterised by the following specific features:

(a) A hotel is a profit making organisation; this implies that a short payback is of utmost importance.

(b) The floor area corresponding to each occupant in a hotel is much smaller than that of a residential application. For a typical average sized hotel in Cyprus, for example, the floor area per occupant is about 25 m^2 compared to about 50 m^2 per occupant for residential applications.

(c) As a result of (b) the ratio of space heating load to service water heating load is much smaller than a residential application.

A set of simulations have been conducted for different collector sizes in order to evaluate the cost effectiveness of a combined solar water and space heating in hotels and investigate the optimum collector size. The simulation concerns a hotel in Nicosia, having 50 guest rooms and other commonly used areas. The space heat loss coefficient for the building is 24000 kJ h^{-1} $^{-o}C^{-1}$ and the service hot water demand is based on the daily consumption profile HOT1 (see Table 4.1, fig. 4.5). The economic scenario assumes that hotel is a profit making organisation. It also assumes that diesel oil is used as backup energy and its inflation rate is 5% per year. The rest of the parameters are the same as those shown in Table 5.2.

The simulation analysis model was designed to give outputs of thermal performance and economic analysis. The simulation results were plotted in figs. 6.11 – 6.13 to correlate the collector size with the system life cycle savings, payback period, solar fraction and collector average efficiency.

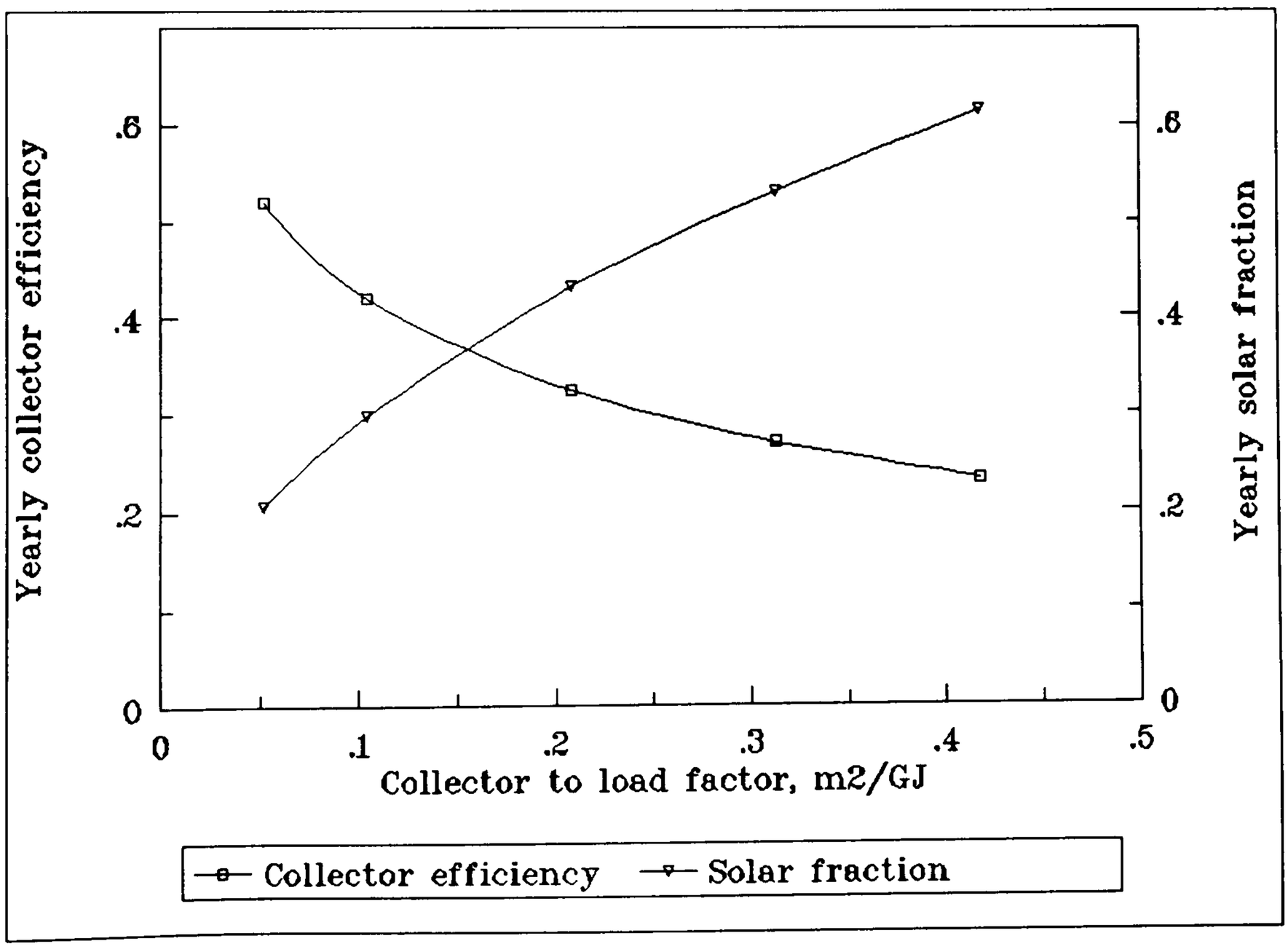

Fig. 6.11 Yearly collector efficiency and solar fraction as a function of collector to load factor, hotel application

Fig. 6.11 shows the variation of yearly collector efficiency and solar fraction as a function of collector to load factor, F_{cl}. The graph pattern is in agreement with that

obtained for a residential application, i.e low efficiencies and high solar fractions at large collector sizes, and high efficiencies and low solar fraction at small collectors.

Fig. 6.12 indicates that the life cycle savings are low at large collector sizes, they increase as the collector area decreases and reach a maximum which corresponds to the optimum collector size. The curve tends to decline as the collector area decreases furthermore. The payback period, however, follows a different pattern. Small collector sizes are associated with short payback periods which become longer as the collector area increases. The optimum collector area is 75 m^2 and the payback period for this size of collector is slightly greater than 8 years.

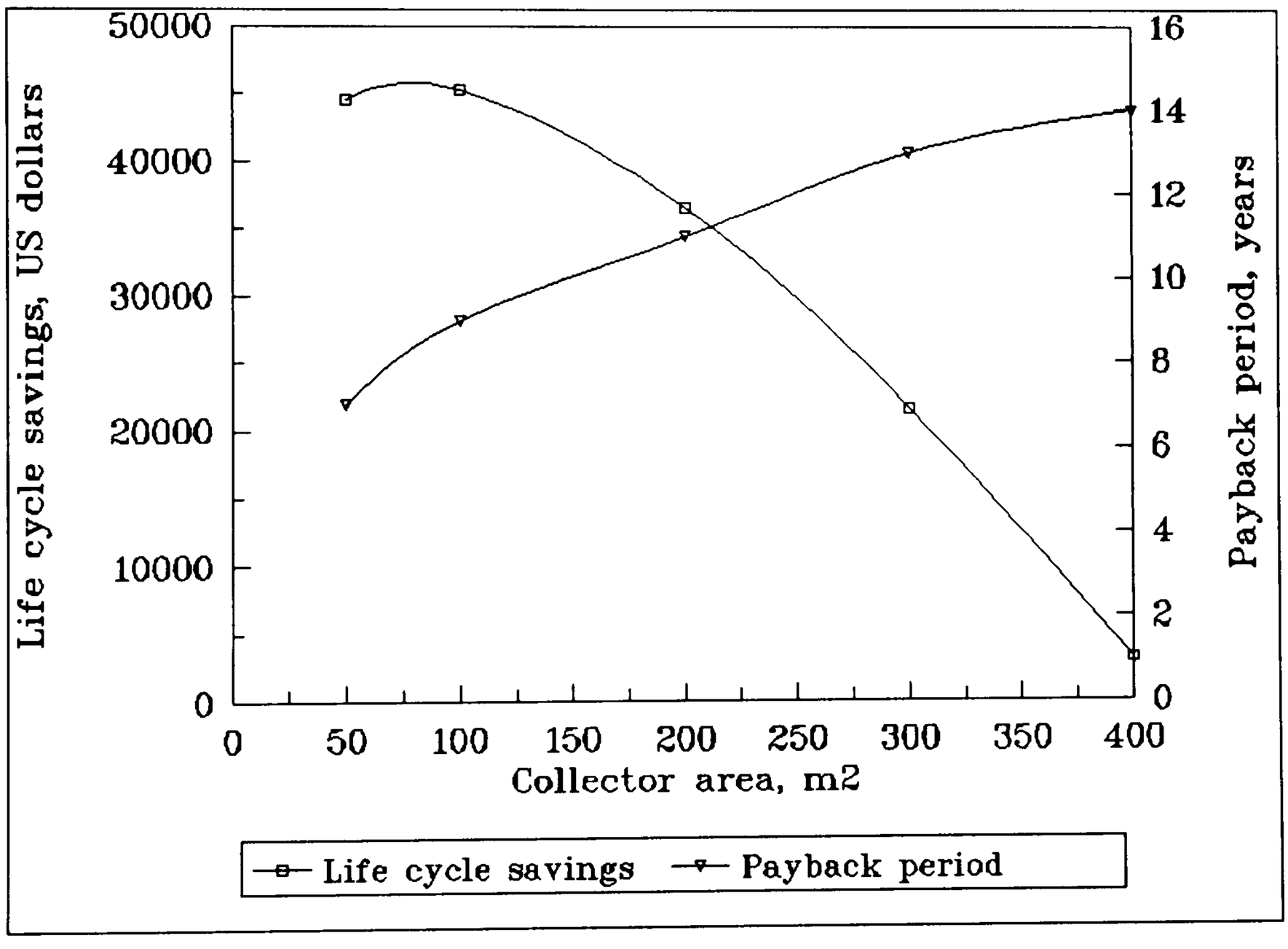

Fig. 6.12 Variation of life cycle savings and payback period with collector area, hotel application

The effect of collector to load factor F_{cl} on the system life cycles and solar fraction is shown in fig. 6.13 and follows the pattern of collector area plot. The optimum F_{cl} is 0.08 m^2 per annual GJ and the solar fraction corresponding to the factor is 0.25, i.e 25% of the total heating load is met by solar while the rest is supplied from the auxiliary energy source. A breakdown of the annual energy balance of the system is shown in fig. 6.14.

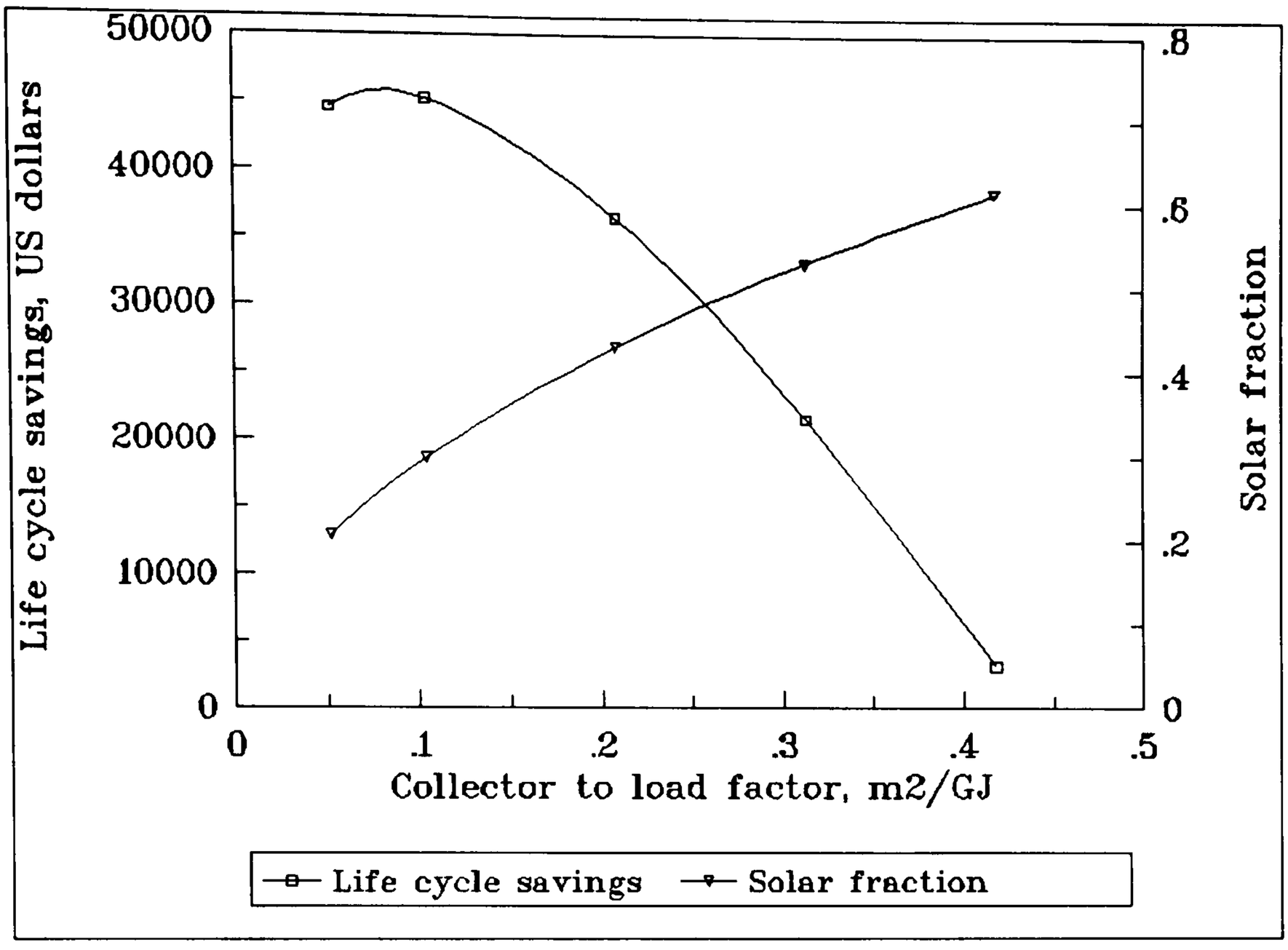

Fig. 6.13 Variation of life cycle savings and solar fraction with collector to load factor F_{cl}, diesel oil backup, hotel application

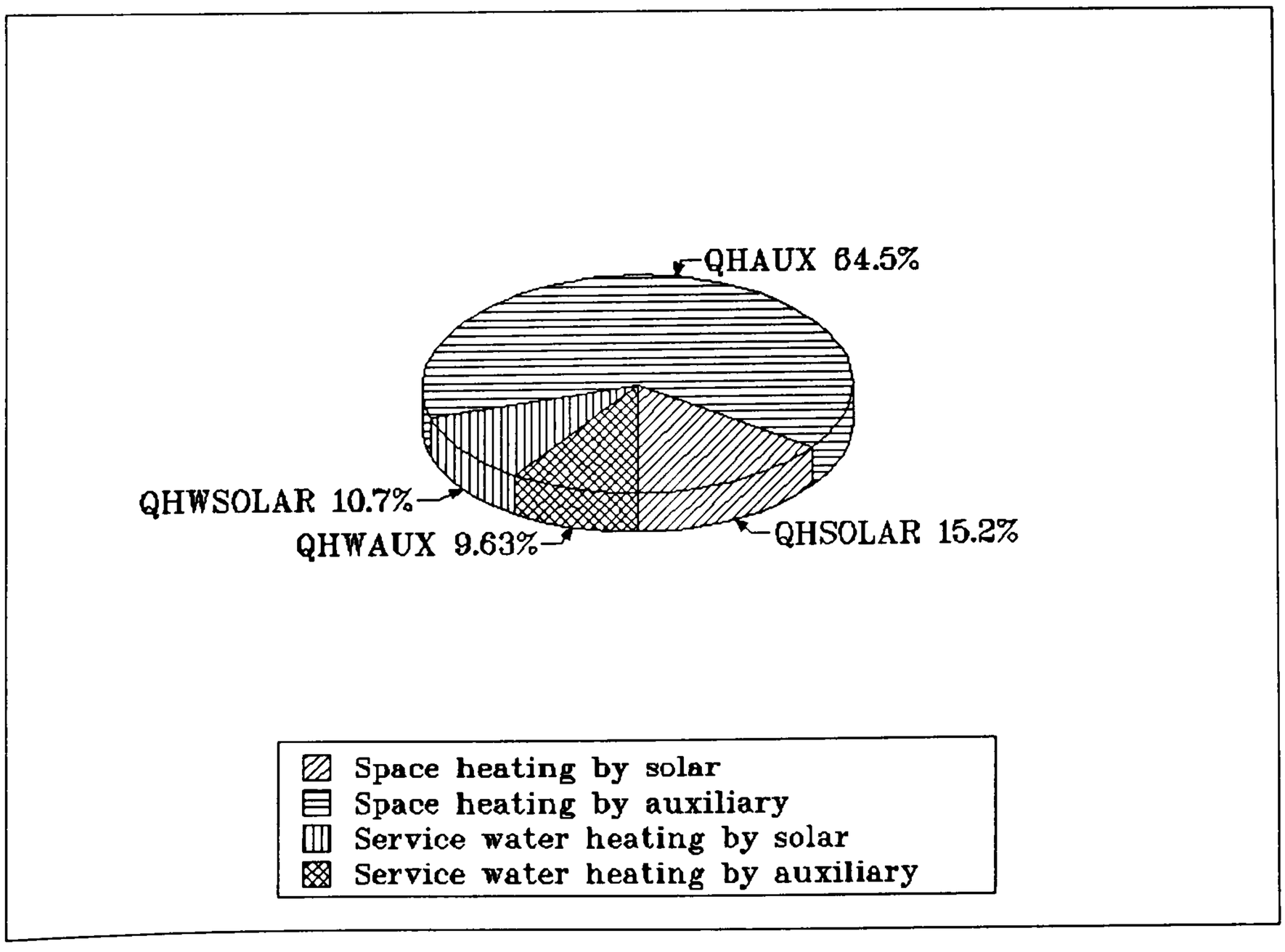

Fig. 6.14 A breakdown of the hotel annual energy balance at optimum collector size, hotel application

The life cycle savings in the present simulation are positive for a large range of collector size but the optimum collector size is very small and only a small proportion of heating load is covered. In addition, the above optimum is associated with a payback period higher than 8 years which is relatively high for a profit making organisation such as a hotel. We can, therefore, conclude that on the basis of the economic scenario used in the simulation, solar water and space heating systems in hotels are not competitive with fuel oil fired conventional systems.

Based on the results obtained for the economic scenarios used in the simulation, it may be anticipated that the results concerning the cost effectiveness of the solar system when compared to electricity, will certainly be much better and in favour of solar because of the higher cost of electric energy in Cyprus. However, the possibility of using electricity for water and space heating in hotels is rather remote for Cyprus.

6.6 The effect of a hypothetical economic scenario

As mentioned before, the optimisation of the system was performed, based on certain economic scenarios which assume a number of economic parameters. However, since the economic analysis is done for a certain period of time, namely 20 years, it was necessary to make some projections into the future, based on the trend observed during the last few years. It has been assumed, for example, that the inflation rate for both backup and conventional fuels is 5% per year and that the nominal market discount rate is 9% per year. The question which arises is how sensitive is the cost effectiveness of the solar system under consideration to the fuel inflation rate i_F. To investigate this, a set of simulations were run for four different economic scenarios, in which the key parameter is the fuel inflation rate per year. Thus, in addition to the scenario already examined, where i_F was taken as 5% per year, projections are made for fuel inflation rates of 1%, 10%, 15%, and 20%. The simulations concern residential applications using diesel oil as backup energy. The effect of the fuel inflation rate on the collector optimum size is illustrated in fig. 6.15.

It is clearly shown that an increase in the fuel inflation rate is associated with an

increase in the optimum collector size and such an increase is in favour of the solar system. Thus, the optimum collector sizes for a system using diesel oil as backup are approximately 0.25, 0.35 and 0.85 m^2 per annual GJ of heating load respectively for 10, 15 and 20% fuel inflation rates per year.

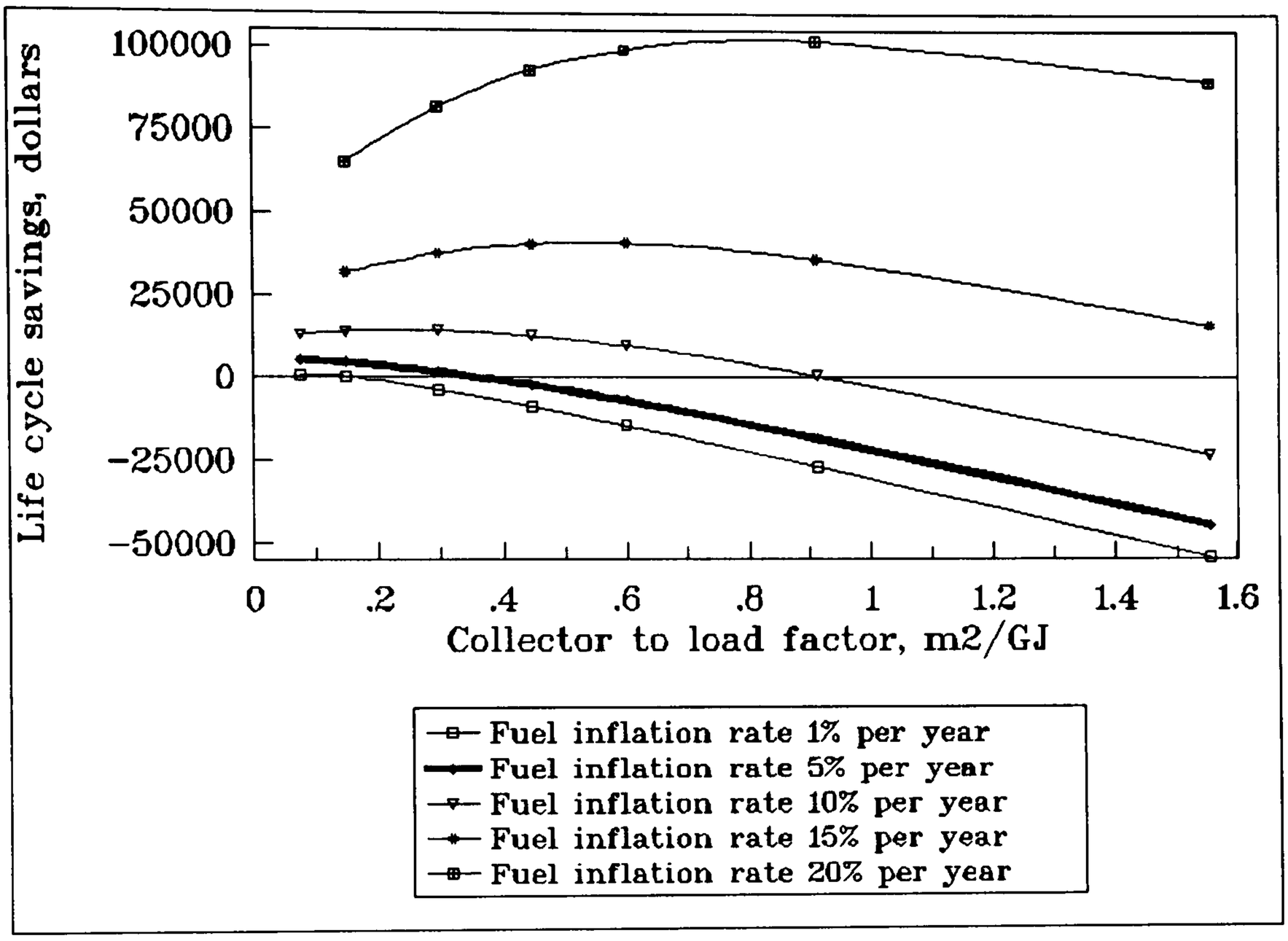

Fig. 6.15 Effect of fuel inflation rate per year on the collector optimum size

Another interesting piece of information from fig. 6.15 concerns the critical condition i.e. the point where the life cycle savings are zero. For i_F=1% per year, this point corresponds to a collector size of approximately 0.15 m^2/GJ while for a higher inflation rate like for example 10%, the life cycle savings are zero for a collector size equal to 0.9 m^2/GJ.

In conclusion we can say that the optimum size of the collector and consequently the cost effectiveness of the system is very sensitive to the fuel inflation rate per year.

CHAPTER 7

MODELLING AND SIMULATION OF SOLAR ASSISTED HEAT PUMP SYSTEMS

7.1 Introduction

A heat pump is by definition, a refrigeration system which has the ability to "pump" heat from a low temperature sink and elevate it to a higher temperature. The majority of existing heat pump systems utilise atmospheric (ambient) air as their heat source. Thus in a space heating application, the heat pump takes heat from low temperature outdoor air and transfers it to the room to be heated, at a higher temperature. Its performance is characterised by its coefficient of performance (COP) which is defined as the ratio of heat output over the work supplied to the compressor and is usually greater than unit.

One of the major characteristics of a heat pump is that its performance , or more particularly its COP, varies with the source temperature. In fact, the heat pump COP decreases as the heat source temperature drops. Thus, the COP of a typical air source heat pump reduces from 2.7 at an ambient air temperature of 15°C to about 2.1 when operating at 0°C (Reay and Macmichael, 1979). Bearing in mind that the heating load of a building increases with a decrease in the ambient air temperature, the above characteristic is a disadvantage for a heat pump system. On the other hand, as explained in Chapter 5, the energy collected by a solar space heating system in winter is, very often, low in temperature to be useful for direct heating but it is high enough to be used by a water source heat pump. Such a combination will not only mean a better utilisation of the solar energy collected but will indirectly cause an improvement in the collector efficiency as a result of lower operating temperatures in the collector–storage subsystem. For the above reasons, the combination of a heat pump and a solar system may prove an efficient and probably a cost–effective

method of space heating. The present study is a performance analysis and cost optimisation of a solar–assisted heat pump system for residential space heating.

7.2 System description

As mentioned above, the solar assisted heat pump (SAHP) system under investigation is a combination of a base solar system and a heat pump system as illustrated in fig. 7.1. The base solar system consists of a solar collector, a storage tank, a domestic hot water preheating system, a liquid–to–air heat exchanger coil in the building supply duct, auxiliary space and water heaters and all necessary controls.

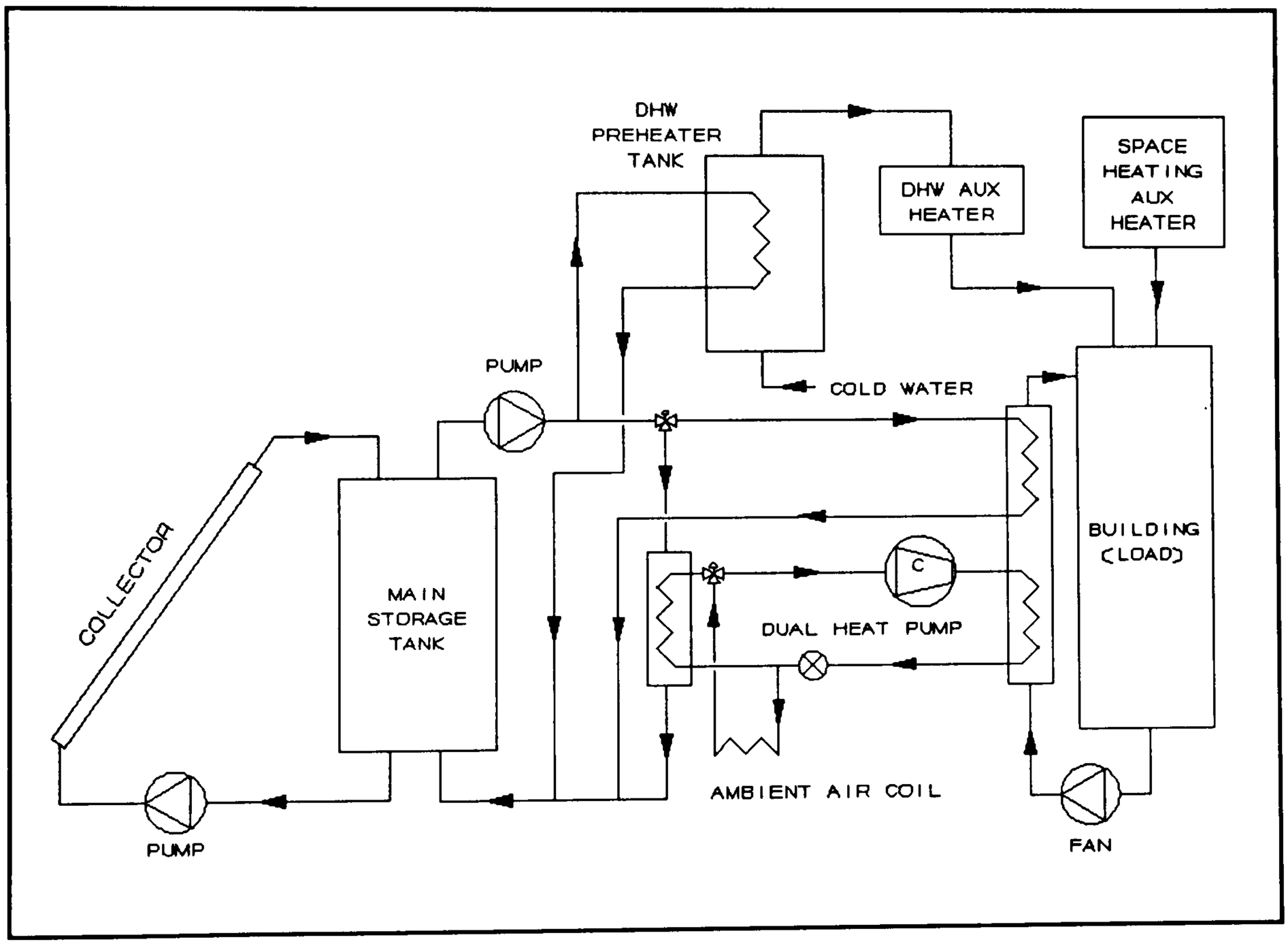

Fig. 7.1 Schematic diagram of a dual type solar assisted heat pump system

The heat pump subsystem, which is exclusive for space heating, comprises a dual source heat pump which has two evaporators, one placed in a liquid stream taking hot water from the storage tank, and a second one which is placed outdoors to absorb heat from atmospheric air. This allows the heat pump to use either the hot water of the storage tank or the ambient air as the heat source, depending on which one results in a higher coefficient of performance (COP), i.e the highest source temperature.

The service hot water subsystem consists of a preheat tank which incorporates a heat exchanger connected to the main storage tank, an auxiliary heater, and all necessary controls. The auxiliary heater makes up energy, when necessary, to elevate the temperature of service hot water leaving the preheat tank to 50°C. The hot water load is assumed to follow the daily pattern described by consumption profile DOM4 (see Table 4.1). The cold water is assumed to enter the preheat tank at 18°C.

Solar energy is absorbed by the solar collectors and stored into the main storage tank. Provided that there is sufficient energy in the storage tank, the pump will circulate the storage water to the load (service hot water and space heating). There is, however, a difference from the system presented in Chapter 6 (combined solar space and water heating) and it concerns the space heating load. In the system described in chapter 6 the hot water from the storage tank is supplied to the building through the load heat exchanger; in this system, the hot water from the main storage tank may be supplied directly to the space through the load heat exchanger and thus heat the building, or to the evaporator of the heat pump so that heat is extracted from the hot water heat source and supplied to the building through the heat pump. The different modes of operation of the system are described in the section which follows.

7.3 The simulation model

The complexity of the thermal analysis of solar–heat pump systems makes the use of computer simulations the only method capable of adequately determining the system dynamics. The solar system modelled is a conventional liquid based system. The collector model is a simplified adaptation of the Hottel and Whillier (1958) model with a constant heat removal factor, (F_R), transmittance – absorptance product, ($\tau\alpha$), and heat loss coefficient (U_L). The values of the above parameters used in the simulations are listed in Table 7.2

The simulation model includes a number of TRNSYS component models, which include the collector–storage subsystem model, the service hot water subsystem model, the dual source heat pump model, the weather generator, economic analysis subroutine, etc., as described in Appendix F. The weather data used is the same as

that used for the previous simulations and is shown in Table 4.2, Chapter 4. The weather data is shown in the file **CYDATA.DAT** (see Appendix A). The system model is listed in file **JM5.DAT** in Appendix F.

The dual source heat pump model (**TYPE 20**) models the performance of a heat pump having two evaporators; a liquid source evaporator to utilize heat from a solar system or other processes, and an ambient air source to be used when the outdoor temperature, T_a, exceeds the water source temperature, T_{so}, or if the liquid source temperature, T_{so}, approaches its freezing point. The model also allows a direct heating mode in which the hot water source bypasses the heat pump and delivers energy across a heat exchanger whenever its temperature exceeds a user specified minimum, $T_{sh,min}$.

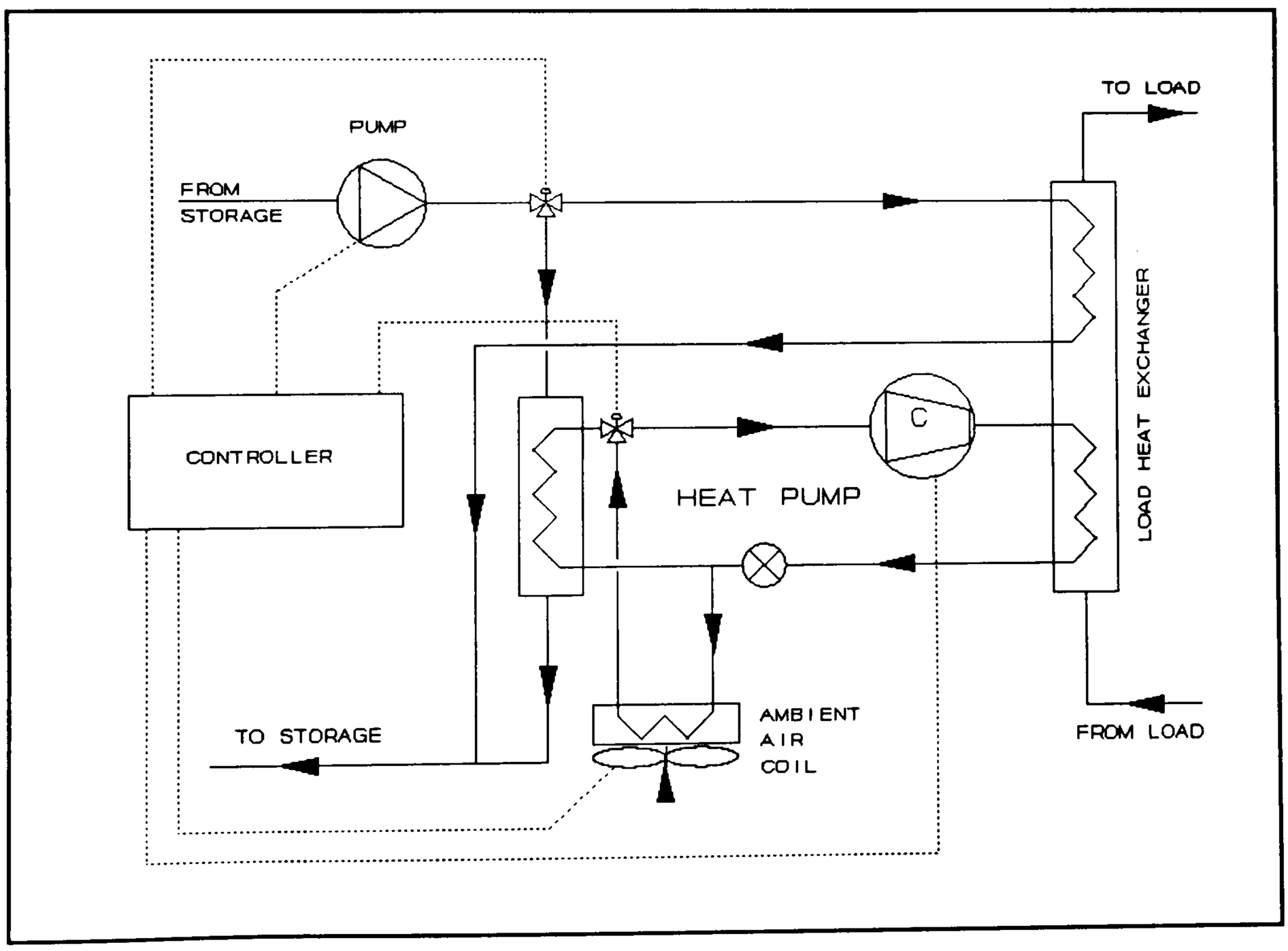

Fig. 7.2 Schematic of dual source heat pump configuration

A schematic of the dual source heat pump considered by this component is shown in fig. 7.2. The entire system is controlled by a single control input, γ_{htr}. If the value of this control function is 0, then no heating is required and the heat pump delivers no energy. If, on the other hand, γ_{htr} is 1, then an internal controller determines the

heating mode. Direct liquid source heating occurs if the storage water temperature T_{so} is greater than T_{sh}. Otherwise, heat pump heating occurs using either the water or ambient source, whichever has the higher temperature. If, however, either source temperature falls below user specified minima, then the heat pump is not allowed to operate. The performance of the heat pump is determined with user–supplied steady–state performance data as a function of the inlet fluid temperature to the evaporator only. No dependence upon the condenser conditions is considered.

The heat pump performance data is read and interpolated using subroutine DATA which is provided in a file accessed through a Fortran logical unit. A set of data for each evaporator source is required. The data consists of between 2 and 10 evaporator inlet temperatures. For each temperature, corresponding values of heat pump capacity, energy absorbed by the evaporator, and electrical energy required must be provided. Performance data is read in free format. The first values in the data file must be the evaporator temperatures in increasing order. Next are the values of capacity, energy absorbed, and electrical input at the lowest evaporator temperature, followed by values at the next higher evaporator temperature, etc.

For the present simulation, a 3–ton heat pump has been chosen from the CARRIER range of heat pumps, namely heat pump model 38Y030.00/40AQ030. Its performance data have been adapted to the above model and written in the files **LHPDATA.DAT** and **AHPDATA.DAT** (see Appendix G), for liquid–to–air and air–to–air heat pump modes respectively. These files are accessed through the Fortran logical units 11 and 12 respectively (see Appendix F, Simulation file **JM5.DAT**).

The simulation model offers the flexibility to determine many energy quantities such as the incident solar energy on the collector, useful solar heat gain by the collector, space and water heating loads, auxiliary heat required, electrical energy required by the heat pump (Q_{ei}), energy delivered to the building by direct water source heating (Q_{dh}), energy absorbed by the heat pump evaporator (Q_{abs}), energy delivered by heat pump (Q_{hp}), the coefficient of performance of the heat pump (COP), etc. For the present simulation, however, only the quantities which are necessary for the optimisation of the system and comparison with the systems presented in the preceding sections will be obtained.

There are four possible operating modes of the system, as shown in Table 7.1, and the operating strategies are described below:

Mode A. If the storage water temperature (T_{so}) is smaller than T_{dh} and $T_{sh,min}$, and the ambient air temperature (T_a) is below $T_{a,min}$, then the heat pump is out of operation. In such a case, the auxiliary heaters are activated in order to meet the space and DHW heating loads.

MODE	CONDITION	OPERATION
A	$T_{so} < T_{dh}$ $T_{so} < T_{sh,min}$ $T_a < T_{a,min}$	Heat pump OFF, auxiliary heaters ON
B	$T_{so} > T_{dh}$	Heat pump OFF, direct (solar) heating, collector–storage–load
C	$T_{so} < T_{dh}$ $T_{so} \geq T_{sh,min}$ $T_{so} \geq T_a$ $T_a < T_{a,min}$	Heat pump ON, water–to–air, collector–storage–heat pump
D	$T_{so} < T_{dh}$ $T_a \geq T_{a,min}$ $T_a > T_{so}$ $T_{so} < T_{sh,min}$	Heat pump ON, air–to–air

T_a = Ambient air temperature, °C

$T_{a,min}$ = Minimum ambient temperature necessary for ambient air source heat pump operation, °C

T_{dh} = Minimum water temperature necessary for direct heating (collector–storage–load), °C

T_{so} = Temperature of water leaving the storage tank, °C

$T_{sh,min}$ = Minimum water temperature necessary for heat pump operation using storage water source, °C

Table 7.1 Operating modes for a SAHP system employing a dual source heat pump

Mode B. If the storage water temperature (T_{so}) is equal or greater than the design flow temperature for heating (T_{dh}), then heat from the storage tank is transferred directly to the building through the load heat exchanger. The heat pump is again out of operation.

Mode C. If the storage water temperature (T_{so}) is lower than the design flow temperature (T_{dh}) but greater than the preset design minimum temperature ($T_{sh,min}$) and at the same time this temperature is greater or equal to the ambient air temperature (T_a), then the heat pump is activated to operate on the water–to–air mode, i.e it pumps heat from the warm water coming from the storage tank and transfers the elevated heat to the building.

Mode D. If the storage water temperature (T_{so}) is smaller than the design flow temperature (T_{dh}), and the ambient air temperature is equal or greater than the minimum design temperature for air source operation ($T_{a,min}$), and at the same time the ambient air temperature is greater than the storage temperature (T_{so}), then the heat pump operates on the air–to–air mode.

Since the storage temperature in this system can hover near 0°C, the relative error test often forces wasteful computations to converge temperatures to within a few tenths of a degree. For this reason, it has been selected to use the absolute error tolerances, specified by the card TOLERANCES, – 0.05 –0.05.

Simulations for long term performance, are carried out on an hour–by–hour basis using the meteorological data used in the previous Chapters and the space heating and domestic hot water load. In each simulation, a range of collector areas and storage factors are used, and plots of one performance index versus another are produced for evaluation of system performance for ranges of area and other parameters. The simulation parameters are listed in Table 7.2.

The economic parameters are the same as those used in the preceding simulations, the only difference being in the fixed costs, which in this case also include the cost of the heat pump. It is also important to note that the simulations assume that electricity is used as backup fuel, simply because the heat pump is electrically driven.

1. Collector–storage subsystem	
A_c	10 – 200 m^2
G_{test}	54 kg h^{-1} m^{-2}
G	50 kg h^{-1} m^{-2}
$F_R(\tau\alpha)_n$	0.78
F_RU_L	24.4 kJ h^{-1} K^{-1} m^{-2}
β	50° from horizontal
V_s	0.5 – 10.0 m^3
U_s	1.2 kJ h^{-1} K^{-1} m^{-2}
2. Domestic water heating subsystem	
V_p	180 l
U_p	1.2 kJ h^{-1} K^{-1} m^{-2}
T_{req}	50 °C
ε	0.75
M_D	As per profile DOM4 (see fig. 4.4)
3. Building space heating load	
UA	4000 kJ h^{-1} K^{-1}
T_R	20 °C
$\varepsilon_L C_{min}$	8000 kJ h^{-1} K^{-1}
4. Dual source heat pump	
T_{dh}	35 °C
$T_{sh,min}$	15 °C
$T_{a,min}$	5 °C

Table 7.2 Simulation parameters for the SAHP system

It must be noted, however, that the simulation model offers the flexibility to the user to assume a scenario which will use electricity for the heat pump and any other fuel for the auxiliary sources of heat. The need for such a scenario will depend on the economic performance of the system with electricity as energy source.

The system model with all parameters and inputs concerning a certain scenario is presented in the simulation file **JM5.DAT** (see Appendix F).

7.4 System performance

The energy required to meet the space and water heating load (Q_{load}) comes from the following possible sources:

(a) Solar energy, either directly from storage to load or indirectly from the storage water through the heat pump operating at the water–to–air mode (Q_{sol})

(b) Energy absorbed from the ambient air by the heat pump (Q_{air})

(c) Electric energy required by the heat pump (Q_{ei})

(d) Auxiliary energy (Q_{aux}).

For a longterm simulation, the change in the amount of energy in the storage tank is negligible and the annual system energy balance is:

$$Q_{sol} + Q_{air} + Q_{ei} + Q_{aux} = Q_{load} \tag{7.1}$$

A useful index of system performance of these systems is the Solar–Air Fraction, **SAF**, which is the ratio of "non–purchased" energy (free energy from solar and ambient air) to the total heating load. This ratio is analogue to the solar fraction, f, used for conventional solar heating systems. The solar–air fraction is defined as:

$$SAF = \frac{Q_{sol} + Q_{air}}{Q_{load}} \tag{7.2}$$

The heat pump is driven by electricity while the auxiliary energy may be supplied by diesel oil, gas or electricity. Thus, SAF can also be expressed in terms of the energy required by the heat pump, Q_{ei}, and the auxiliary energy needed by the system, Q_{aux},

and is given by the formula:

$$SAF = \frac{Q_{aux} + Q_{ei}}{Q_{load}} \tag{7.3}$$

The components of a solar assisted heat pump system (SAHP) could be sized to meet the entire space heating and domestic hot water load of a building. However, design should be based on sizing the various components for the most cost effective system operation.

In the preceding Chapters, a number of design criteria were optimised, separately for solar space heating systems and solar water heating systems and for combined water and space heating systems. For the present system, the simulations are run using the optimum design criteria and configurations investigated in the preceding simulations and the emphasis will be given to the performance of the system in comparison with the conventional solar heating systems.

It must be appreciated, however, that owing to the fact that dual source heat pumps are not commercially available for use in solar–heat pump systems, the economic analysis is made on the assumption that the costs of such a system is equal or slightly greater than that of a conventional heat pump.

7.5 Discussion of simulation results

A set of simulations runs for different collector areas were conducted in order to evaluate the performance of the system as a function of the collector size. It is noted that the space heating loads differ slightly with collector area since the storage tank losses are counted as heat inputs to the heated space. The results of the system simulations are shown in Table 7.3 and they concern the following items (yearly):

(a) Space heating load, HLOAD

(b) Space heating auxiliary, HAUX

(c) Service hot water load met by solar, HWSOLAR

(d) Service hot water load met by auxiliary energy, HWAUX

A_c m^2	F_{cl} m^2/GJ	HLOAD GJ	HAUX GJ	HWSOL GJ	HWAUX GJ	QU GJ	QINS GJ	QDH GJ	QHP GJ	QABS GJ	QEI GJ	η	SAFH	SAF
10	0.077	122.3	16.14	5.50	2.30	21.11	63.68	0.58	105.4	70.28	34.97	0.332	0.582	0.607
20	0.153	123.0	14.76	5.65	2.14	37.44	127.36	4.70	103.5	69.79	33.66	0.294	0.607	0.630
40	0.299	125.8	12.78	6.09	1.70	62.44	254.72	15.24	97.76	67.24	30.83	0.245	0.654	0.740
60	0.440	128.7	10.26	6.37	1.43	80.99	382.08	26.09	92.36	64.43	28.45	0.212	0.699	0.717
80	0.577	130.9	7.32	6.56	1.24	94.76	509.44	37.48	86.12	60.59	26.17	0.186	0.744	0.759
120	0.847	133.9	2.10	6.87	0.93	115.50	764.16	59.33	72.51	51.52	21.67	0.151	0.823	0.832
200	1.367	138.5	0.60	7.29	0.51	140.30	1273.60	90.84	47.12	33.96	13.74	0.110	0.896	0.902

Table 7.3 Summary of simulation results for different collector sizes

(e) Useful solar heat gain, QU

(f) Incident solar radiation on the collector, QINS

(g) Heat supplied to the building by the heat pump, QDH

(h) Heat supplied to the building by the heat pump, QHP

(i) Heat absorbed by the evaporator of the heat pump either from air or from water, QABS

(j) Energy input to compressor, QEI

(k) Collector average efficiency, η

(l) Solar–air fraction, SAF

(m) Space heating solar air fraction, SAFH

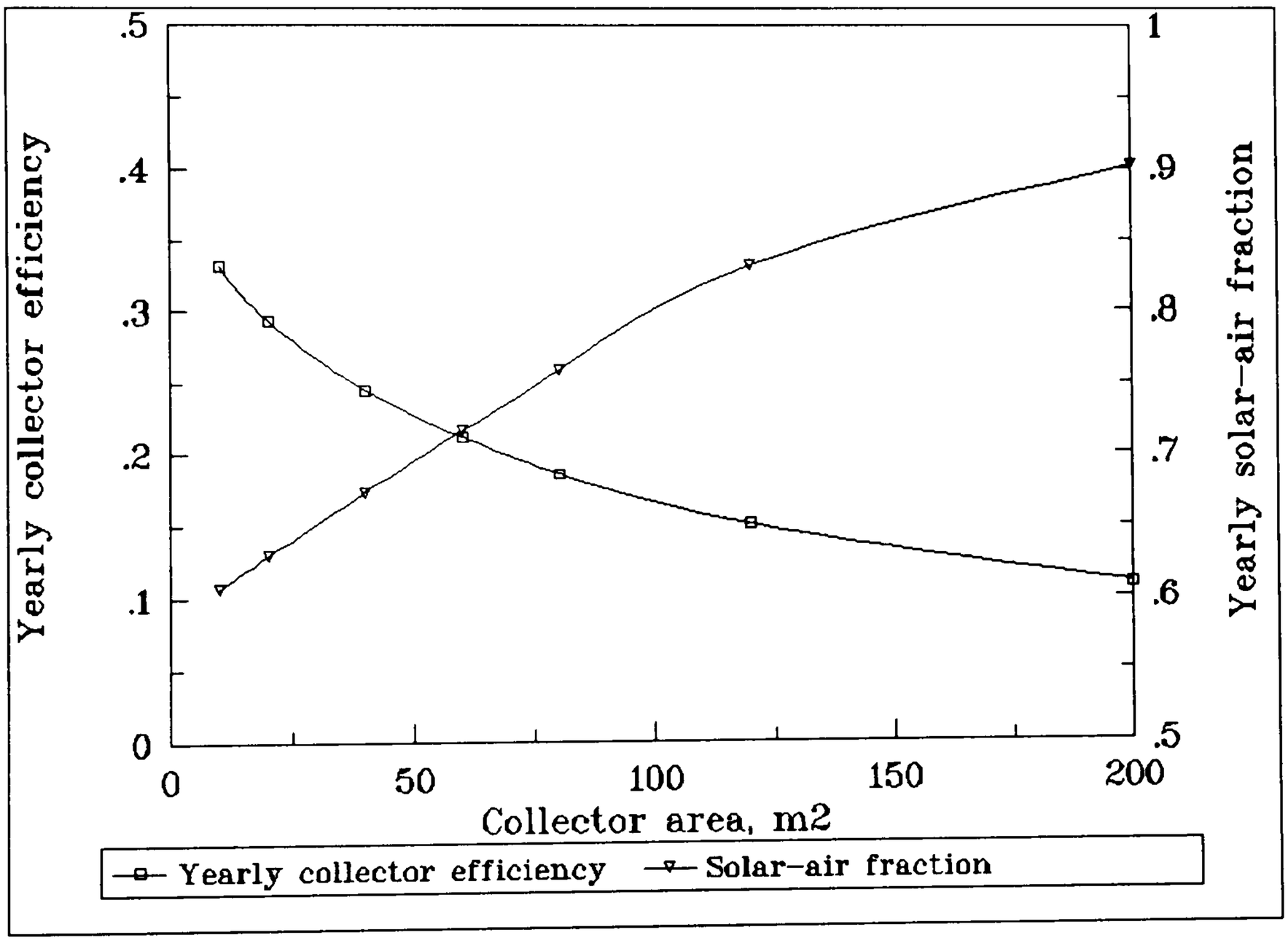

Fig. 7.3 Yearly collector efficiency and solar–air fraction as a function of collector size

The above results have been used to plot a number of graphs. Thus, in fig. 7.3 the yearly collector efficiency and solar–air fraction were plotted as a function of collector area. It is clearly seen that the curve patterns are the same as those of the systems evaluated in the preceding Chapters. The collector average efficiency is high at low collector sizes and decreases as the collector area increases. However, the solar–air fraction is low at small collector areas and increases as the collector area

increases. The rate of increase in SAF is decreasing as the collector area increases. This is a result of the reduced collector efficiency associated with increased collector size.

The collector average efficiency and solar–air fraction were also plotted as a function of the collector to load factor, F_{cl}, as shown in fig, 7.4, and obviously these plots follow the patterns of the curves of fig. 7.3, i.e the collector efficiency decreases as F_{cl} increases and the solar–air fraction increases as F_{cl} increases.

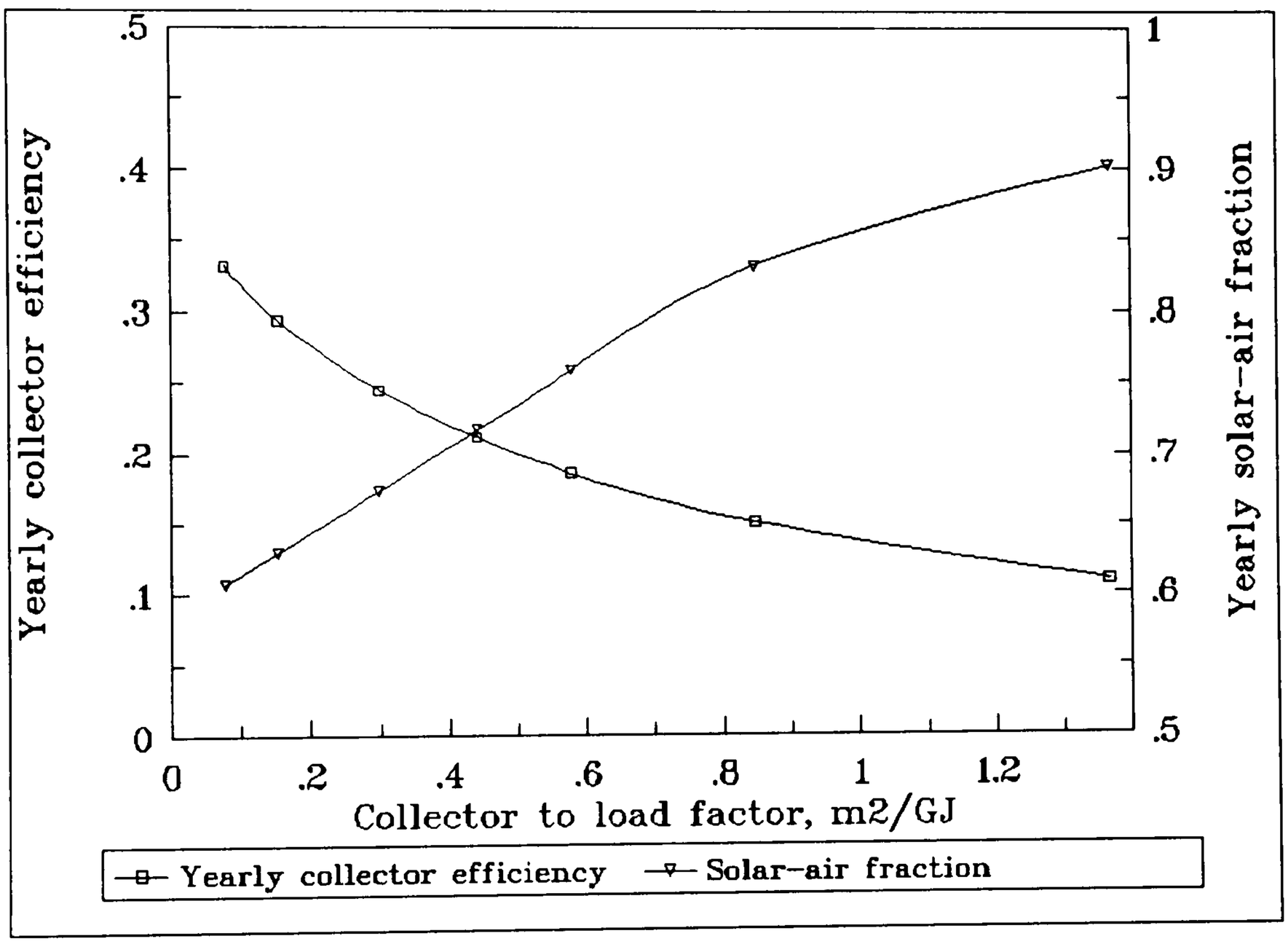

Fig. 7.4 Yearly collector efficiency and solar–air fraction as a function of collector to load factor

It is interesting to observe the variation of the collector efficiency on a monthly basis. For this purpose the monthly average efficiency of collector has been plotted for three different collector sizes, 20, 60 and 120 m^2, as shown in fig. 7.5. Superimposed to this graph is the variation of total load (service hot water and space heating). It is clearly demonstrated that the collector efficiency is lower at larger collector sizes. The collector efficiency is higher during the winter months when the load is maximum, and gets to a minimum during the summer months when the load is minimum (service hot water only). Another interesting piece of information is that

the variation of the efficiency follows the pattern of the thermal load, i.e high in winter and low in summer.

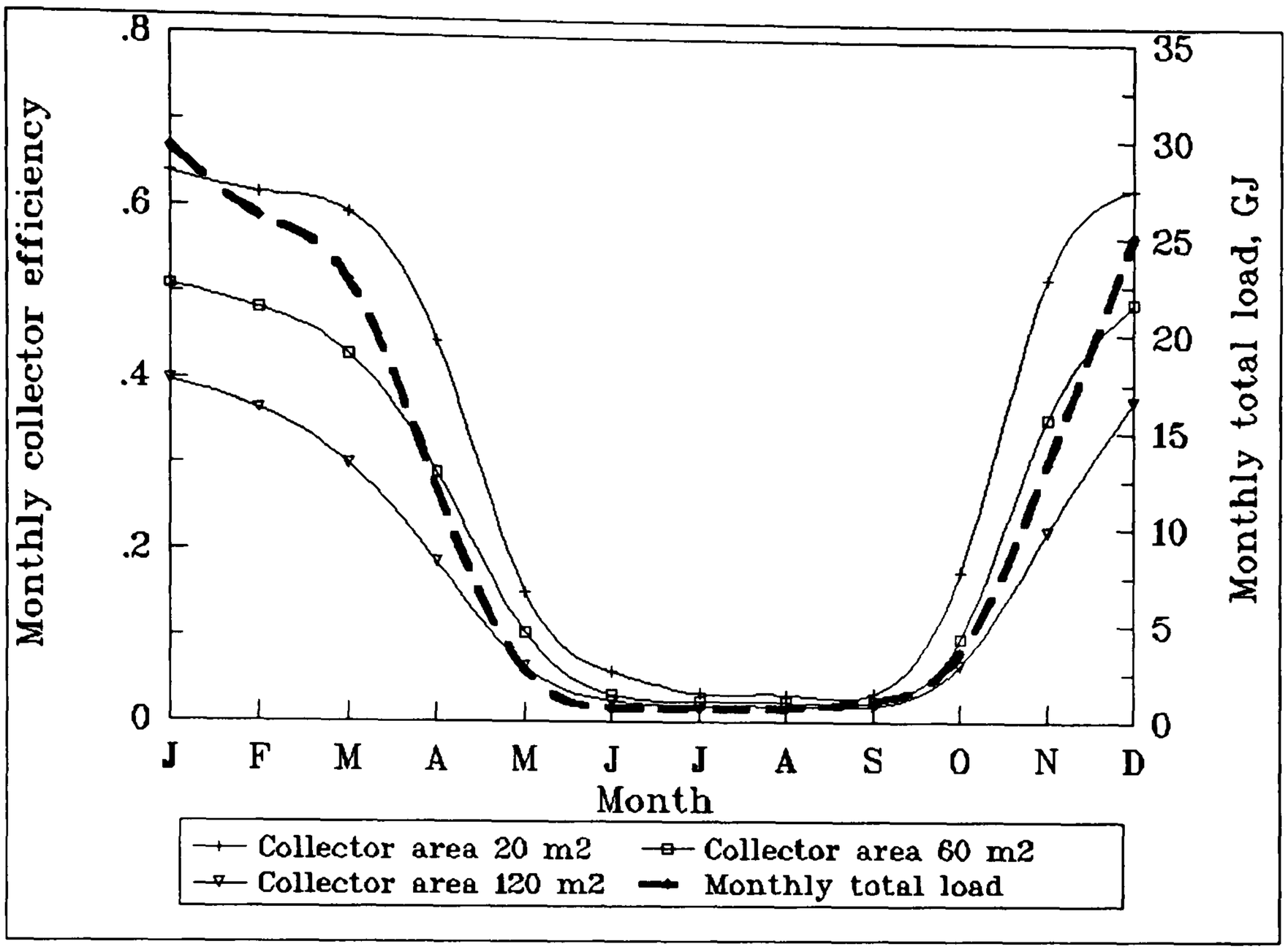

Fig. 7.5 Monthly collector efficiency at different collector sizes

It has been demonstrated by fig. 7.3 that the solar–air fraction, i.e. the ratio of non–purchased (free) energy to the total load increases with the collector area. It is useful if a comparison is made with the solar fraction of a system that does not include a heat pump. For this purpose another set of simulations were run with modified parameters. Thus, parameters 4, 5 and 6 of UNIT 20 in the simulation file JM5.DAT (see Appendix F), were modified to read 25 °C, 100 °C and 100 °C respectively so that the heat pump is put in operation only if the water temperature in the storage tank is higher than 100 °C, which is in fact impossible. This means that the system will operate as a conventional solar water and space heating system without the intervention of the heat pump.

The results of these simulations have been used together with the results of the previous set of simulations to plot the graphs of fig. 7.6 which shows the fraction of the load met by a SAHP system and the fraction of the load met by a conventional solar heating system without the heat pump, as a function of the collector to load

factor. Both fractions increase with the collector size. It is, however, interesting to note that at low F_{cl}, the solar–air fraction is much higher than the solar fraction of a conventional solar heating system and the difference represents the fraction of the load met by the heat extracted from the ambient air by the heat pump. This demonstrates clearly the importance of including the heat pump in the system. This difference, however, decreases as the collector size increases. This is explained by the fact that at large collector sizes, the building thermal load is, to a great extent, met by direct solar heating as a result of high amounts of energy collected by the solar system which, in turn, minimises the heat pump intervention.

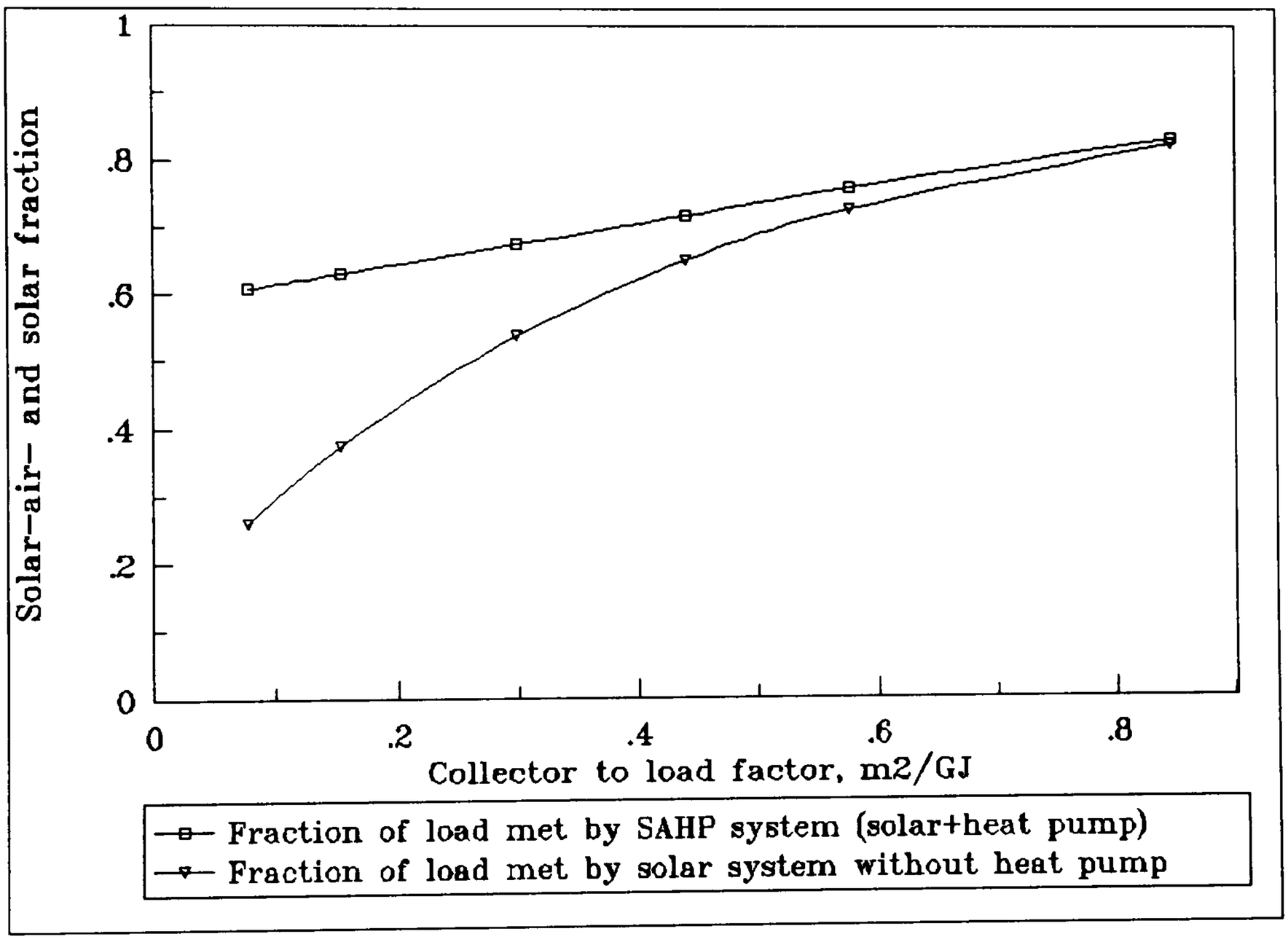

Fig. 7.6 Comparison of the fraction of load met by a SAHP system with the fraction met by a conventional solar heating system

The above is also demonstrated by the plots of fig. 7.7 which illustrates the variation of the heat delivered to the building by the heat pump and by direct solar heating. It is very clearly shown that the heat delivered to the building by the heat pump as well as the heat absorbed by the evaporator and the energy input to compressor decrease as the collector size increases, while the energy delivered by direct solar heating increases with the collector size. As a result of the above, the contribution of the heat pump is reduced as the collector size is increased.

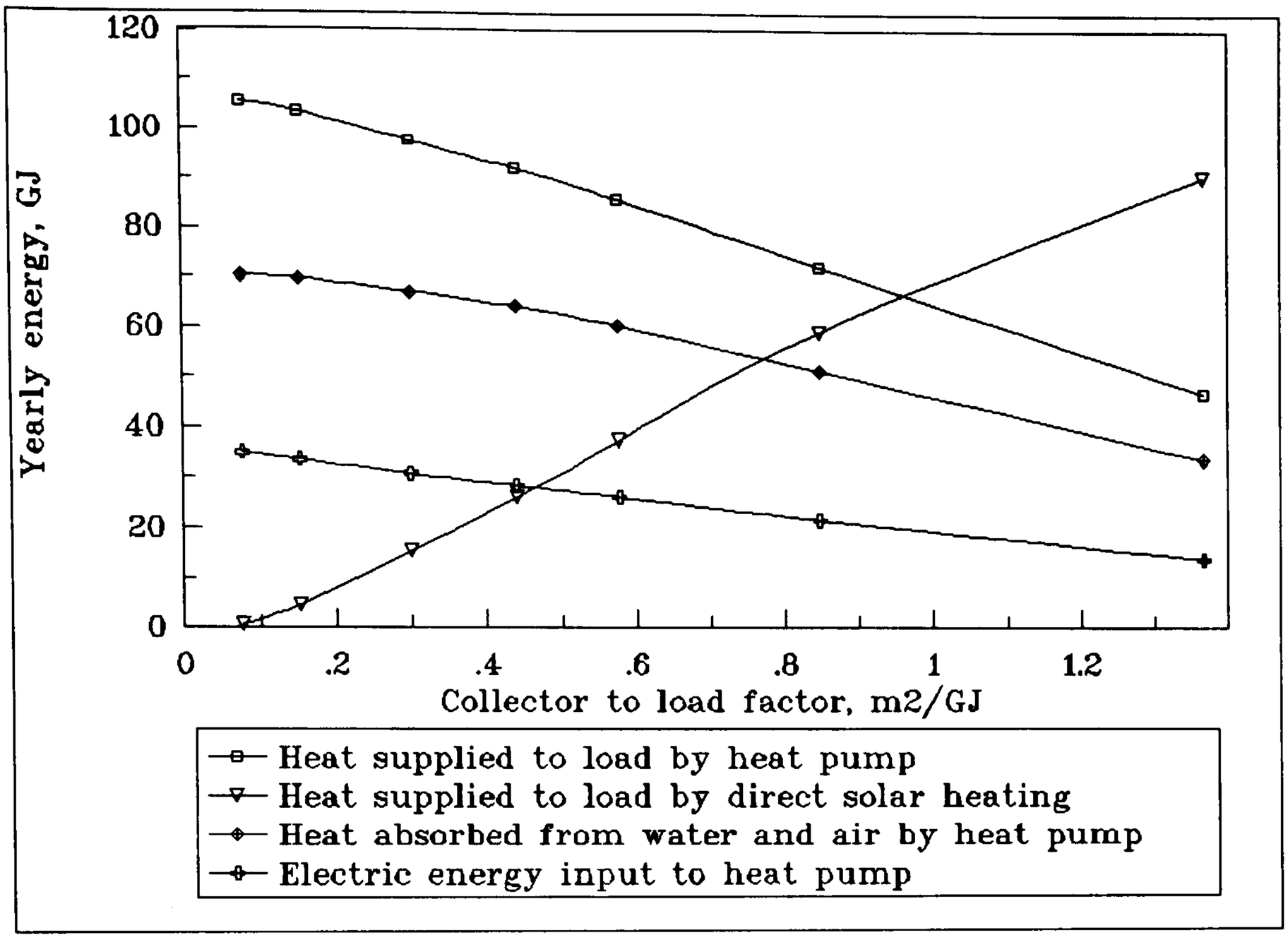

Fig. 7.7 Yearly energy quantities as a function of the collector to load factor, F_{cl}

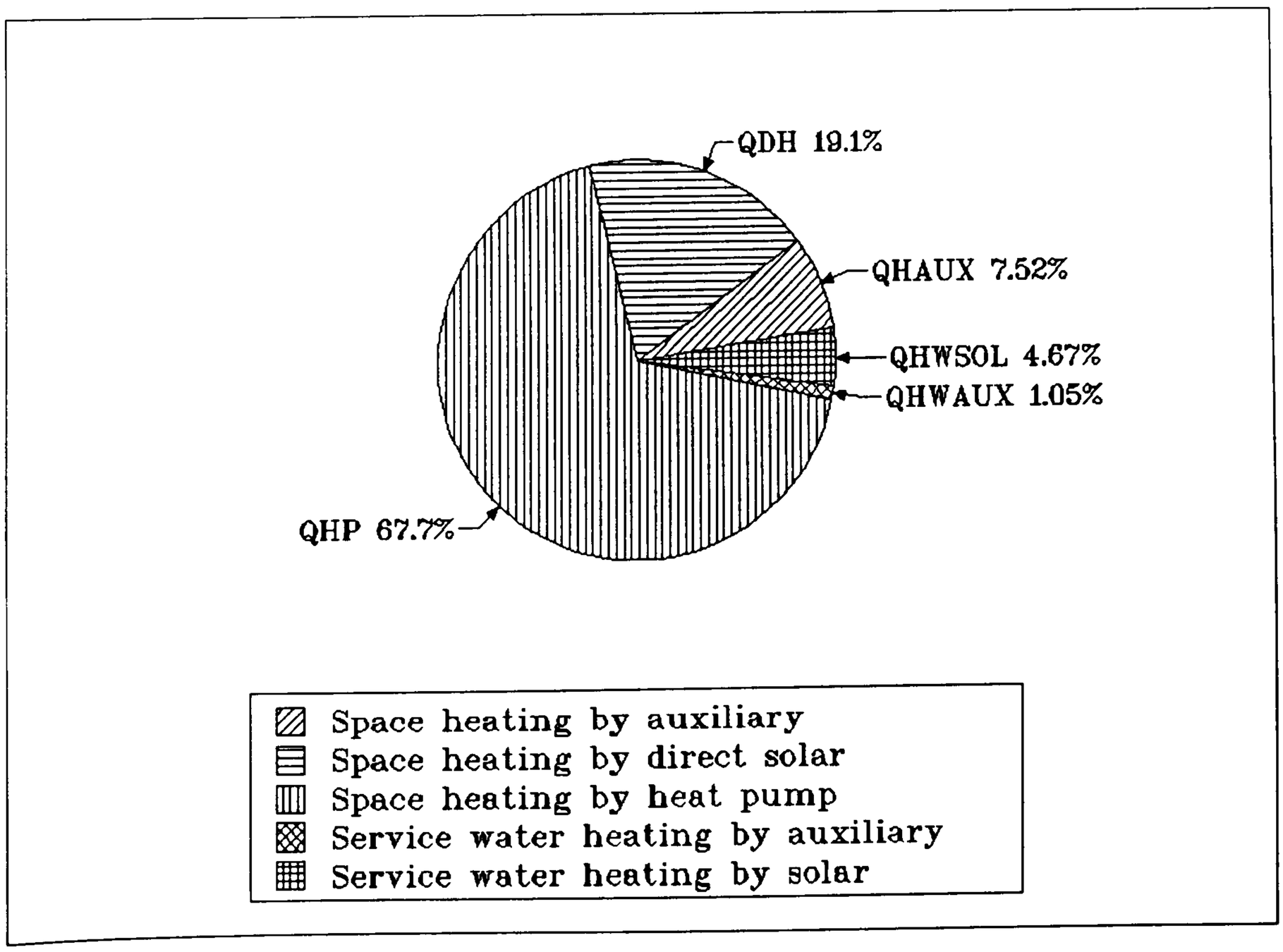

Fig. 7.8 An account of the system annual energy balance with F_{cl} = 0.44 m^2/GJ

The contribution of each source of energy involved in a SAHP system with a collector area of 60 m^2 (0.44 m^2 per annual GJ) is illustrated in fig. 7.8. It is clearly shown that of the system total load, 19.1% is met by direct solar heating, 67.7% is met by the solar assisted heat pump, 7.52% is met by the space heating auxiliary heat source, 4.87% by solar water heating and 1.05% by the DHW auxiliary heat source.

7.6 Effect of storage factor

One peculiar characteristic of the solar assisted heat pump system (SAHP) is that the dual source heat pump has the flexibility to absorb heat from the storage tank water even if its temperature is as low as 5°C. It is therefore expected that larger storage sizes may benefit the SAHP systems more than the conventional solar heating systems. To investigate the effect of the storage size on the system solar–air fraction and compare it with a conventional solar heating system, a set of simulations were run for two collector to load factors (F_{cl} = 0.077, 0.440 m^2 per annual GJ), at different storage factors (F_s = 50, 75, 100 and 150 litres of water per m^2 of collector). The results of the simulations have been used to plot the graphs of fig. 7.9 which show the fraction of load met by conventional solar and combined solar–heat pump system as a function of storage factor F_s.

As it can be seen from fig. 7.9, all the plots remain almost horizontal, which shows that the effect of F_s on the system performance is negligible in both, the SAHP and the conventional solar system; in fact, an increased storage size brings about a slight increase in the system performance. This is more distinct in the case of low collector to load factors, i.e small collector sizes. This is because at low collector sizes, the storage temperature is at low levels for most of the time and the collectors operate near their maximum efficiency, so that an increased storage does not bring a significant improvement in the system performance. As a result of low water temperatures in the storage tank, the heat pump runs out of water–source heat for most of the time and operates on its air–to–air mode.

At larger collector sizes, increased storage factors show a slightly larger improvement in the SAHP system performance which, however, is not significant. In conclusion,

we could say that the effect that an increased storage size has on the system performance is very little and not significant to justify the extra investment costs.

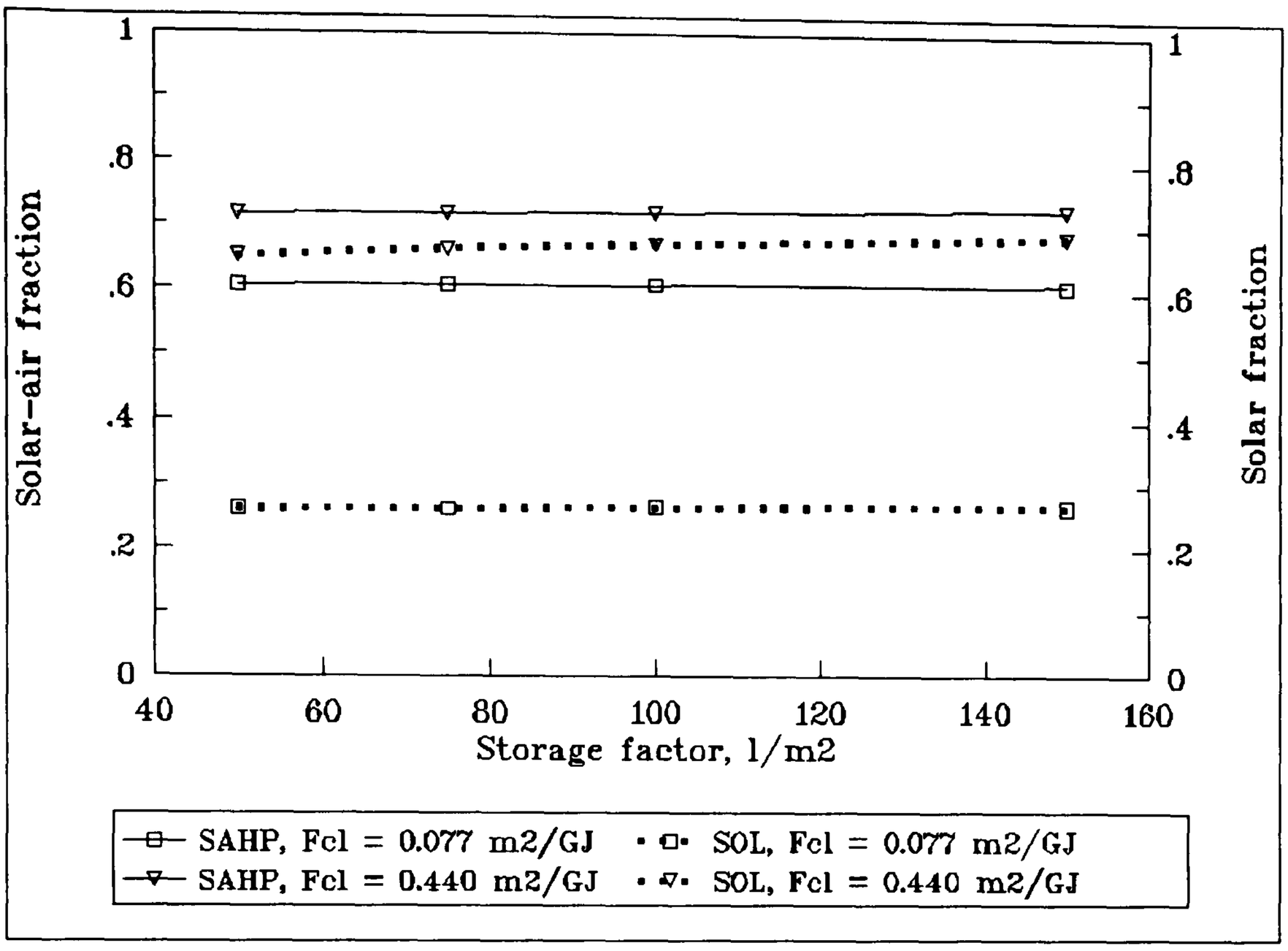

Fig. 7.9 Effect of storage size on the performance of a SAHP system at different collector to load factors (F_{cl} = 0.077, 0.440 m^2 per annual GJ)

7.7 An economic evaluation

As mentioned before, the economic analysis in the present simulations is based on an economic scenario which assumes that electricity is used as backup fuel, simply because the heat pump is electrically driven.

Using the same economic parameters as in the previous systems, with the exception of the fixed costs which in this case they are increased to account for the cost of the heat pump, a set of simulations were run to investigate the system life cycle savings and the payback periods for different collector sizes. These were plotted in fig. 7.10 which shows the effect that the collector to load factor has on the life cycle savings. Superimposed to this graph is also the variation of the solar air fraction.

It is clearly seen in fig. 7.10 that the life cycle savings for the period of the economic analysis are negative for all sizes of collector. As compared to the solar–air fraction which increases with the collector size, the life cycle savings decrease as the collector size is increased but their highest value is always negative. In addition to the above, the simulations showed that the payback period exceeds the period of economic analysis which is 20 years. These are indications that the solar assisted heat pump system is not a cost effective alternative. This is attributed to the high cost of the heat pump and to the use of electric energy as motive power for the heat pump. The situation might be better and perhaps in favour of SAHP system if summer cooling is required. Such an investigation, however, is beyond the scope of this study.

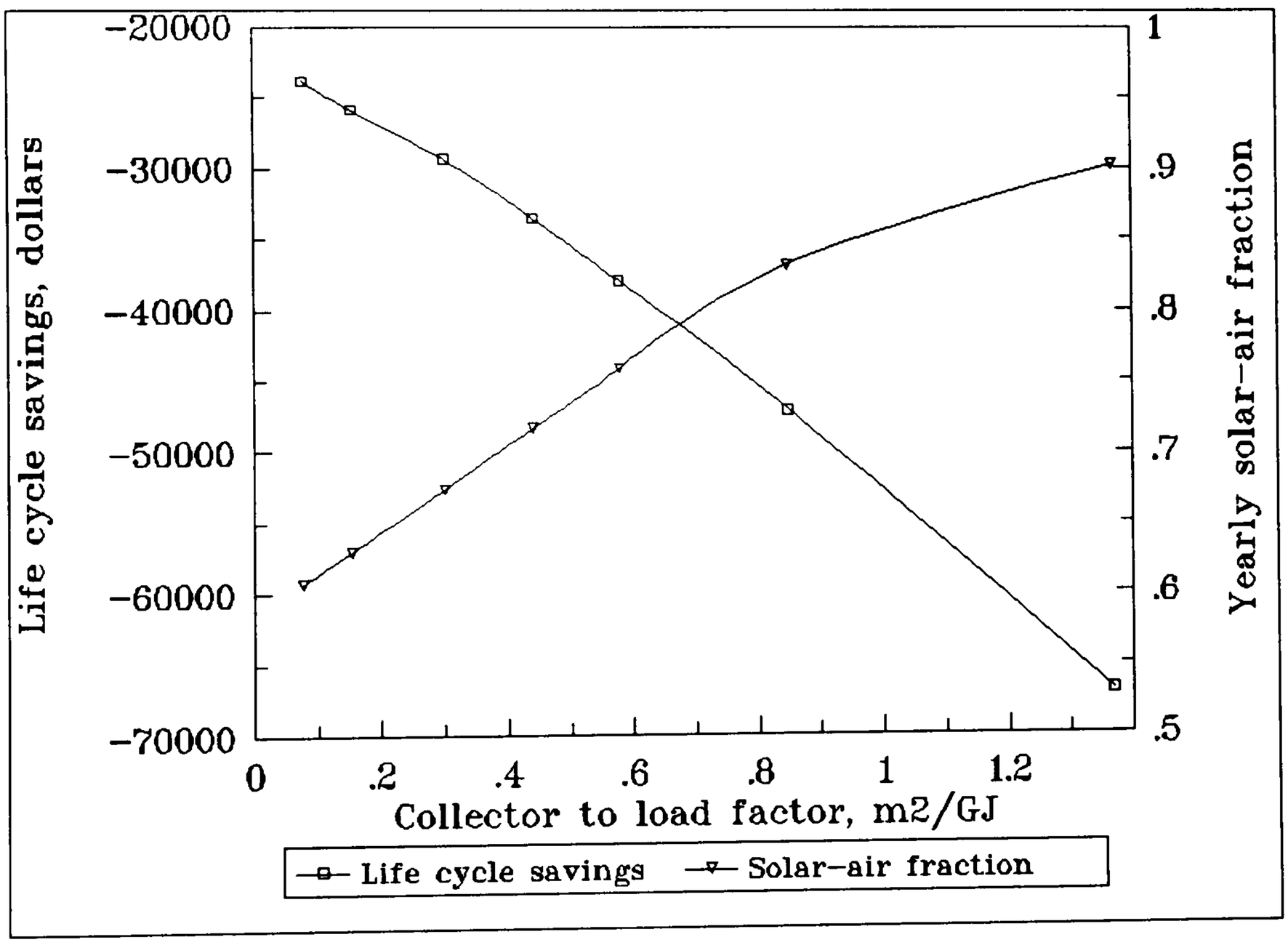

Fig. 7.10 Effect of collector to load factor on the life cycle savings

CHAPTER 8

CONCLUSIONS AND RECOMMENDATIONS FOR FUTURE WORK

8.1 Conclusions

The purpose of this work was to develop suitable simulation models for solar heating systems, use them to simulate the thermal performance of such systems and investigate some of the optimum design criteria applicable to the Cyprus climatic and socioeconomic conditions. To this effect, five solar energy systems have been modeled and simulated using the transient simulation capabilities of TRNSYS. These include thermosyphon solar water heating systems, forced circulation solar water heating systems, solar space heating systems, combined solar water and space heating systems and solar assisted heat pump systems for space and water heating. The resultant thermal performance data revealed some original information about the performance and cost effectiveness of these systems.

The simulation models that have been developed and incorporated within TRNSYS are powerful and versatile, firstly because they contain a large number of key parameters and inputs affecting the performance of the solar heating systems they represent, and secondly because they offer the possibility to the designer to modify the value of any parameter in the system under investigation so that the thermal performance and cost effectiveness of the system can be evaluated under the modified conditions. It is through this experimental approach that the heating systems have been investigated.

This study thoroughly analyses the various heating systems for solar water and/or space heating and evaluate the cost effectiveness and the performance of such systems. The current understanding is such that both the consumer and the designer

of solar water and space heating systems have little idea of how much the solar energy is likely to contribute to the heating load.

The major design criterion that has been evaluated in this study is the collector size which is expressed in terms of the collector to load factor, F_{cl}, which is defined as the ratio of collector area to the annual heating load, in m^2 per annual GJ of heating load. The main performance index is the system annual solar fraction, f, defined as the fraction of the annual heating load met by solar. A general conclusion revealed from the simulations concerns the collector efficiency as a function of the collector size. Thus, the smaller systems, characterised by a small collector to load factor, show higher efficiencies. The difference is more significant during the spring and autumn season. For a given collector size, however, the efficiency curve follows the pattern of the heat load.

The question of employing or not a heat exchanger in the collector–storage subsystem and its effect on the system performance have also been investigated. Simulations indicated an increase in the solar fraction when the system does not incorporate a heat exchanger in the collector–storage subsystem.

The need for an auxiliary heater in a solar heating system is greatly appreciated firstly because solar energy is intermittent and secondly because a self–sufficient and autonomous system is not cost effective. It was shown that the best position for the auxiliary heater in thermosyphon and active solar water heating systems is outside the storage tank, in line to the taps. It has been demonstrated that this arrangement brings about an increase in the yearly average collector efficiency of about 25% as compared to the other alternative arrangement where the auxiliary is built–in the storage tank. The corresponding increase in the system annual solar fraction is about 30%. This finding is very interesting for the Cyprus solar industry because in the traditional thermosyphon solar water heater the auxiliary heater is built–in the storage tank. This means that there is space for improvements in the system configuration which will increase its performance and result in more energy savings. In solar space heating systems the auxiliary heater should be located either in line with the load or in parallel with the solar system, but in no case in the storage tank since this will result in a considerable degradation in the efficiency of the system for the reasons

mentioned above.

The economic feasibility of solar water and space heating for Cyprus was studied by comparing the life cycle savings of these systems to those of the conventional systems assuming a number of economic scenarios in which the costs of conventional and backup energies were taken into account. Economic simulations revealed the following conclusions:

(a) Solar water heating is a cost effective application if compared to electric water heating. Thus, a typical Cypriot thermosyphon solar water heater which uses an electric backup heater, is a cost effective method of providing service hot water to a family of four and its payback period is as low as 3 years, depending on the daily hot water consumption profile. However, when the comparison is made with diesel oil fired systems, the payback period is much greater and of the order of 8 years. This concerns mostly large scale applications such as hotels and hotel apartments, hospitals etc, where the conventional method of service hot water production is by oil fired boiler systems. In such applications, payback periods of the order of 7 years and higher are not considered favourable.

(b) Solar space heating can not compete with conventional fuel oil fired heating systems. The life cycle savings for the solar system are negative for a large range of collector sizes and the payback period is very high. However, when the comparison is made with electric heating systems, solar space heating is a cost effective alternative for residential applications. At optimum system design criteria the payback period is of the order of 5 to 6 years. For large scale applications, however, like hotels, solar space heating is not feasible owing to the fact that the competitive fuel in this type of buildings is diesel oil. The life cycle savings under these conditions are very low and they are associated with high payback periods.

(c) In case where both service hot water and space heating are required the cost effectiveness of the system is improved as a result of greater utilisation of solar equipment throughout the year, but not as much as to make the solar system compete with conventional diesel oil fired systems.

(d) In systems where a dual source heat pump is used in combination with a solar system there is a significant improvement in the thermal performance of the system at small collector sizes if a dual source heat pump is employed. However, life cycle savings are not high enough to justify the high capital costs for the heat pump. The situation might be better and perhaps in favour of solar assisted heat pump systems if summer cooling is required.

Another important aspect which concerns solar domestic hot water systems is the effect that the daily hot water consumption pattern has on the performance and cost effectiveness of the system. It has been demonstrated that solar water heating systems are insensitive to the hourly distribution of hot water usage. This is very clearly shown in the case of thermosyphon solar water heating systems where performance simulations were run for different daily hot water consumption profiles. A comparison of the results obtained with three different consumption patterns, based on the same thermal load, showed that the annual solar fraction of a thermosyphon solar water heater may vary from 0.63 to 0.65. An economic comparison showed that the payback periods of the same system are the same, irrespective of consumption pattern, when compared to electric water heating systems and they vary from 7 to 8 years when compared to diesel oil fired systems.

The effect of thermal stratification in the storage tank of a solar water heating system has also been investigated. Simulation results showed an increase in the collector average efficiency and a lower and not significant increase in the annual solar fraction in favour of the stratified storage tank. However, it is difficult to maintain thermal stratification because of the mixing motion caused by pumping the water to the collector and the load heat exchanger, in addition to the mixing effect of natural convection occurring within the storage tank. Accordingly, in the design of solar heating systems, it is not wise to count on much performance advantage from stratification of a water storage tank.

The system simulations enabled the optimisation of some design criteria which are useful to designers of solar heating systems. These criteria concern mainly the collector and the storage tank. For the collector, it was considered that a factor related to the load, namely F_{cl}, would be a good design criterion since a solar system

should be designed to meet a certain thermal load. Another criterion which concerns only the solar water heating system is the collector to consumer factor, F_{cc}, which specifies the collector area required for each consumer of service hot water in the building. For space heating systems, in addition to F_{cl}, the collector area is also related to the building floor area by the collector to floor area factor, F_{cf}.

It has been found that the optimum values of some design criteria are dependent on the economic scenarios and particularly the incremental costs incurred by solar equipment, the cost of conventional energy and the cost of backup energy. A summary of the optimum design criteria is presented in Table 8.1.

It can be seen from Table 8.1 that the optimum tilt angle for the solar collector is 35° from horizontal for solar water heating systems and 50° for space heating and combined water and space heating systems. It has been, however, shown that the system annual solar fraction is reduced by approximately 1% when β_{opt} is changed by ±10°, and by less than 2% when β_{opt} is changed by ±15°.

The optimum collector to load factor for residential service hot water systems is 0.45 m^2 per annual GJ of thermal load when electricity is considered as backup energy source; this factor results to an annual solar fraction of about 0.80 to 0.85. In hotel applications, however, where the backup energy source is traditionally diesel oil, the optimum collector to load factor varies from 0.3 to 0.4 m^2 per annual GJ, depending on the load profile, and the corresponding solar fraction is 0.65 to 0.80. In systems where service hot water and space heating are required the collector to load factor increases to 0.6 m^2 per GJ of thermal load as a result of increased load but the corresponding solar fraction is only 0.65 as a result of reduced utilisation of the solar equipment during the off–heating season. The situation is, however, better than the case where only space heating is provided.

The annual solar fraction of solar water and space heating systems is maximised at a collector mass flux within the range of 40 – 50 kg/h per m^2 of collector. A higher mass flux may result to a slight increase in the solar fraction which, however, does not justify the maintenance of high flow rates of water through the collector since this will bring about an increased capital cost and higher pumping power which in fact

DESIGN CRITERIA	SYSTEM		
	SOLAR WATER HEATING	SOLAR SPACE HEATING	COMBINED SOLAR WATER AND SPACE HEATING
Collector orientation	Due south		
Collector tilt angle, β, *degrees*	35	50	50
Collector to load factor, F_{cl}, *m^2 per annual GJ*	0.45 RD 0.3 – 0.4 HD	0.55 RE	0.60 RE
Collector to consumer factor, F_{cc}, *m^2 per consumer*	1.0 RD 0.8 – 1.2 HD	N.A	N.A
Collector to floor area factor, F_{cf}, *m^2 per m^2 of floor area*	N.A	0.35 RE	N.A
Storage factor, F_s, *litres per m^2*	50	45 – 50	50
Collector mass flux, G, *kg/h per m^2*	40 – 50	40 – 50	40 – 50
$\varepsilon_L C_{min}/UA$	N.A	1 – 3	1 – 3
Auxiliary heater	Outside the storage tank, in line to the load		
Collector–storage heat exchanger	NO	NO	NO
Solar fraction	0.80–0.85 RD 0.65–0.80 HD	0.6 RE	0.65 RE
R = Residential, H = Hotel, E = Electricity backup, D = Diesel oil backup N.A = Not Applicable			

Table 8.1 Summary of optimum design criteria for solar heating systems

will reduce the solar contribution to the system energy demand and will affect negatively its cost effectiveness. Lower flow rates, however, can reduce energy collection significantly.

The size of load heat exchanger affects the performance of a solar heating system because the rate of heat transfer across the load heat exchanger directly influences the temperature of the storage tank, which in turn, influences the collector inlet temperature. The dimensionless parameter $\varepsilon_L C_{min}/UA$ provides a measure of the size of the load heat exchanger needed to supply heat to a specified building. Simulation results revealed that the dependence of system performance on the size of the load heat exchanger is asymptotic and only relatively small improvements of the system performance can be realised if the value of $\varepsilon_L C_{min}/UA$ is increased beyond 2 or 3 and best results are obtained within the range of 1 to 3.

The optimum collector size and consequently the cost effectiveness of a solar heating system is sensitive to the fuel inflation rate per year. It has been found that, for a combined solar water and space heating system using diesel oil as backup fuel, the optimum collector sizes are approximately 0.25, 0.35 and 0.85 m^2 per GJ of annual thermal load respectively for 10%, 15% and 20% fuel inflation rates. The values listed in Table 8.1 assume a fuel inflation rate of 5%.

8.2 Recommendations for future work

The simulation models developed in the present work can be used to produce a user friendly computer package, suitable for designers of solar water and space heating systems. Such a package should be in the form of interacting questions and answers between the computer and the user–designer. The questions should be short and comprehensive and should cover all the aspects of the system design, such as type of application, type of system, weather data, load characteristics, collector performance characteristics, operating conditions, cost of solar equipment, cost of backup energy, etc. Based on the answers/inputs of the user–designer, the computer should determine the thermal performance of the system and investigate its cost effectiveness for different economic scenarios.

Further research is also required into the solar assisted heat pump system. It has been pointed out that year–round usage of a solar heating system, like for example a combined solar water and space heating system, gives greater cost effectiveness as compared to two separate systems providing hot water and space heating, because of greater savings on conventional fuels in return for a relatively small additional capital investment. On the other hand, the solar assisted heat pump system has been proved a non cost effective method of solar heating as a result of the high capital costs of the heat pumps as compared to traditional methods of heating. The above lead to the conclusion that for Cyprus, where the annual cooling load is higher than the heating load by about 1.5 times, a combined solar space heating and cooling system is likely to be much more cost effective than single space heating, by the use of a solar assisted heat pump system. The heat pump will provide cooling during the summer period while in winter it will operate in combination with the solar system to provide space heating. Service hot water will be provided by the solar system throughout the year.

There is a need, however, for investigating the cost effectiveness of such a system. This can be achieved by modelling, simulation and optimisation of the system. There are a number of basic system parameters, other than the collector to load factor, which should also be investigated. These include the heat pump to collector size and the storage to heat pump size. Another important aspect of the system which needs further investigation is the control strategy concerning the storage temperatures at which the system should switch from direct solar heating to the heat pump water–source mode of operation and the outdoor air–source mode of operation.

APPENDICES

Appendix A. Simulation weather data file CYDATA.DAT

```
1NICOSIA        CY      35.00       .00       .00
8568 11943 15841 20625 23261 25307 25761 22830 18841 13886  9898  8273
  59    61    67    75    95   114   132   129   123   102    78    68
10.3  10.9  13.2  17.1  21.9  26.3  29.0  28.8  25.8  21.5  16.4  12.0
```

Appendix B1. Simulation input file JM1.DAT

A THERMOSYPHON SOLAR WATER HEATING SYSTEM
(Performance and Economic analysis)

```
ASSIGN EC101E3N.OUT 6
ASSIGN CYDATA.DAT 10
SIMULATION 0 8760 1
TOLERANCES -0.1 -0.1
WIDTH 72
UNIT 54 TYPE 54 WEATHER DATA GENERATOR
PARAMETERS 20
1 1 10 1 2 1 1
3.09 4.12 3.61 4.12 4.64 5.15 5.15 4.64 4.12 3.61 3.09 3.09
100
UNIT 16 TYPE 16 SOLAR RADIATION PROCESSOR
PARAMETERS 7
3 1 1 1 35 4871 0
INPUTS 6
54,7 54,19 54,20 0,0 0,0 0,0
0 0 0 .2 42 0
UNIT 45 TYPE 45 THERMOSYPHON SOLAR WATER HEATER
PARAMETERS 40
1 3 .78 24.4 54 .7 42 -1 20 .012 .026 1.9 3 1 1.15 .02 2.0 2 1.6
.02 .52 2 .5 1 .18 .5 .25 4.19 1000 0 2 5.5 1 25 10800 .3 .37 45
1 2
INPUTS 9
16,6 16,4 16,5 16,9 0,0 54,4 0,0 14,1 54,4
0 0 0 0 .2 0 18 0 0
*FUEL (Electricity) COST MULTIPLIER
EQUATIONS 4
MULT=0.000036
FUELC1=[45,10]*MULT
FUELC2=[45,8]*MULT+[45,10]*MULT
TLOAD=[45,8]+[45,10]
UNIT 14 TYPE 14 LOAD
PARAMETERS 60
0 0 6 0 6 5 7 5 7 15 8 15 8 5 9 5 9 0 12 0
12 5 14 5 14 10 15 10 15 15 16 15 16 5 18 0 18 10 19 10
19 15 20 15 20 20 21 20 21 10 22 10 22 5 23 5 23 0 24 0
UNIT 24 TYPE 24 INTEGRATOR
INPUTS 5
16,6 45,2 45,7 45,8 45,10
0 0 0 0 0
UNIT 1 TYPE 24 FUEL COST INTEGRATOR
PARAMETERS 1
9000
INPUTS 3
```

```
FUELC1 FUELC2 TLOAD
0 0 0
UNIT 29 TYPE 29 ECONOMIC ANALYSIS
PARAMETERS 31
2 3 100 200 2 0 20 30 9 3 8 1 5 9 0 0 1 0 2 1
150 20 5 5 1 1 2 0 0 0 0
INPUTS 3
1,1 1,2 1,3
0 0 0
UNIT 25 TYPE 25 PRINTER
PARAMETERS 1
-1
INPUTS 6
24,1 24,2 24,3 24,4 24,5 45,9
TSOLS TQU TQENV TQSUP TQAUX DELTAU
END
```

Brief description of TRNSYS components included in the simulation model

TYPE 45: Thermosyphon collector–storage subsystem; it consists of a flat plate solar collector, a stratified storage tank (either vertical or horizontal cylinder), a check valve to prevent reverse flow, and water as the working fluid.

TYPE 54: Weather generator, to produce hourly weather data from monthly averages.

TYPE 16: Solar radiation processor, to convert the solar data into a form usable by the collector–storage subsystem.

TYPE 24: Quantity integrator, to integrate energy quantities.

TYPE 14: Domestic hot water load, which describes the daily hot water consumption pattern.

TYPE 25: Printer, to output the monthly or yearly results of the simulation.

TYPE 29: Economic analysis, to evaluate the economics of the system.

Appendix B2. Economic analysis of a thermosyphon solar water heating system (simulation results extracted from the simulation output file)

****ECONOMIC PARAMETERS****

INPUT 1. FIRST YEAR FUEL COST OF SOLAR BACKUP FUEL .	45.92	$
INPUT 2. FIRST YEAR FUEL COST OF CONV. SYSTEM	272.33	$
INPUT 3. ANNUAL SYSTEM ENERGY REQUIREMENT.....	7.56	GJ/YR
P3. AREA DEPENDENT COSTS.....	100.00	$/M2
P4. FIXED COSTS.....	200.00	$
P6. SOLAR SYSTEM THERMAL PERFORMANCE DEGRADATION....	.00	%/YR
P7. PERIOD OF THE ECONOMIC ANALYSIS.....	20.00	YEARS
P8. DOWN PAYMENT(% OF ORIGINAL INVESTMENT).....	30.00	%
P9. ANNUAL INTEREST RATE ON MORTGAGE.....	9.00	%
P10. TERM OF MORTGAGE.....	3.00	YEARS
P11. ANNUAL NOMINAL(MARKET) DISCOUNT RATE.....	8.00	%
P12. EXTRA INSUR.,MAINT. IN YEAR 1(% OF ORIG.INV.)..	1.00	%
P13. ANNUAL % INCREASE IN ABOVE EXPENSES.....	5.00	%
P14. EFFECTIVE FEDERAL-STATE INCOME TAX RATE.....	9.00	%
P15. TRUE PROP. TAX RATE PER $ OF ORIGINAL INVEST...	.00	%
P16. ANNUAL % INCREASE IN PROPERTY TAX RATE.....	.00	%/YEAR
P17. CALC.RT. OF RETURN ON SOLAR INVTMT?YES=1,NO=2..	1.00	
P18. RESALE VALUE (% OF ORIGINAL INVESTMENT).....	.00	%
P19. INCOME PRODUCING BUILDING? YES=1,NO=2.....	2.00	
P20. DPRC.: STR.LN=1,DC.BAL.=2,SM-YR-DGT=3,NONE=4...	1.00	
P21. IF 2, WHAT % OF STR.LN DPRC.RT.IS DESIRED?.....	150.00	%
P22. USEFUL LIFE FOR DEPREC. PURPOSES.....	20.00	YEARS
P23. THE ANNUAL RATE OF BF RISE.....	5.00	%/YEAR
P24. THE ANNUAL RATE OF CF RISE.....	5.00	%/YEAR
P25. ECONOMIC PRINT OUT BY YEAR=1, CUMULATIVE=2.....	1.00	
P27. CONSIDER FEDERAL TAX CREDIT?YES=1,NO=2.....	2.00	
P28. STATE CREDIT IN TIER ONE.....	.00	%
P29. STATE CREDIT IN TIER TWO.....	.00	%
P30. STATE CREDIT TIER ONE BREAK.....	.00	$
P31. STATE CREDIT TIER TWO BREAK.....	.00	$

COLLECTOR AREA= 3. M2
INITIAL COST OF SYSTEM = $ 500.
DOWN PAYMENT = $ 150.
STATE + FEDERAL CREDITS = $ 0.
RESALE OR SALVAGE VALUE = $ 0.
THE ANNUAL MORTGAGE PAYMENT FOR 3 YEARS = $ 138.

	****INFORMATION****			*******COSTS*******			***SAVINGS***		**NET CASH FLOW***		
YR	END OF YR PRINC	IN-TEREST PAID	COMM DEPREC DEDUCT	LOAN PAYMT	MAINT & INS	PROP TAX	FUEL BILL SAVED	CREDIT CHG TX RESALE	AN-NUAL	CUMU-LATIVE	PRE-SENT WORTH
0	350	0	0	150	0	0	0	0	-150	-150	-149
1	243	32	0	138	5	0	226	3	86	-64	80
2	127	22	0	138	5	0	238	2	97	33	82
3	0	11	0	138	6	0	250	1	107	140	85
4	0	0	0	0	6	0	262	0	256	396	188
5	0	0	0	0	6	0	275	0	269	665	183
6	0	0	0	0	6	0	289	0	283	948	178
7	0	0	0	0	7	0	303	0	296	1244	173
8	0	0	0	0	7	0	319	0	312	1556	168
9	0	0	0	0	7	0	335	0	328	1884	164
10	0	0	0	0	8	0	351	0	343	2227	159
11	0	0	0	0	8	0	369	0	361	2588	155
12	0	0	0	0	9	0	387	0	378	2966	150
13	0	0	0	0	9	0	407	0	398	3364	146
14	0	0	0	0	9	0	427	0	418	3782	142
15	0	0	0	0	10	0	448	0	438	4220	138
16	0	0	0	0	10	0	471	0	461	4681	134
17	0	0	0	0	11	0	494	0	483	5164	131
18	0	0	0	0	11	0	519	0	508	5672	127
19	0	0	0	0	12	0	545	0	533	6205	123
20	0	0	0	0	13	0	572	0	559	6764	120
TOTALS		65	0	564	165	0	7487	6	6764		2677

THE RATE OF RETURN ON THE SOLAR INVESTMENT(%)= 81.7

YRS UNTIL UNDISC. FUEL SAVINGS = INVESTMENT	3.
YRS UNTIL UNDISC. NET CASH FLOW = MORTGAGE PRINCIPAL	3.
UNDISCOUNTED CUMULATIVE NET CASH FLOW = $	6764.
PRESENT WORTH OF TOTAL COSTS WITH SOLAR = $	1233.
PRESENT WORTH OF ENERGY COSTS W/O SOLAR = $	3910.
ANNUALIZED TOTAL COST WITH SOLAR = $/GJ	17.
ANNUALIZED ENERGY COST W/O SOLAR = $/GJ	53.
PRESENT WORTH OF CUMULATIVE NET CASH FLOW = $	2677.

Appendix C. Simulation input file JM2.DAT

A FORCED CIRCULATION SOLAR WATER HEATING SYSTEM
(Performance and Economic analysis)

ASSIGN JM2CEM.OUT 6
ASSIGN CYDATA.DAT 10
SIMULATION 0 8760 1
TOLERANCES -0.1 -0.1
WIDTH 72
UNIT 54 TYPE 54 WEATHER DATA GENERATOR
PARAMETERS 20
1 1 10 1 2 1 1 3.09 4.12 3.61 4.12 4.64 5.15 5.15 4.64 4.12 3.61 3.09
3.09 100
UNIT 16 TYPE 16 SOLAR RADIATION PROCESSOR
PARAMETERS 7
3 1 1 1 35 4871 0
INPUTS 6
54,7 54,19 54,20 0,0 0,0 0,0
0 0 0 .2 50 0
UNIT 1 TYPE 1 SOLAR COLLECTOR
PARAMETERS 12
1 1 30 4.19 2 54 .78 24.4 -1 4.19 1 .1
INPUTS 10
3,1 3,2 3,2 54,4 16,6 16,4 16,5 0,0 16,9 16,10
0 0 0 0 0 0 0 .2 0 50
UNIT 2 TYPE 2 PUMP CONTROLLER
PARAMETERS 3
3 10 1
INPUTS 3
1,1 4,1 2,1
20 50 0
UNIT 3 TYPE 3 PUMP
PARAMETERS 1
1500
INPUTS 3
4,1 4,2 2,1
50 0 0
UNIT 6 TYPE 6 AUXILIARY HEATER
PARAMETERS 3
108000000 50 4.19
INPUTS 3
4,3 4,4 0,0
50 0 1
UNIT 14 TYPE 14 LOAD
PARAMETERS 72
0 0 5 0 5 20 6 20 6 100 7 100 7 140 8 140 8 80 9 80
9 50 10 50 10 20 13 20 13 40 14 40 14 60 15 60 15 80 18 80

16 110 17 110 17 120 18 120 18 150 19 150 19 180 20 180 21 180 21 100
22 100 22 50 23 50 23 20 24 20 24 0
* Assumes 1200 litres consumption daily, based on consumption profile DOM4
UNIT 4 TYPE 4 STORAGE TANK
PARAMETERS 6
1 1.5 4.19 1000 1.2 2
INPUTS 5
1,1 1,2 0,0 14,1 0,0
18 0 18 0 20
DERIVATIVES 1
50
*** FUEL COST MULTIPLIER**
EQUATIONS 4
MULT=0.000018
FUELC1=[6,3]*MULT
FUELC2=[6,3]*MULT+[4,6]*MULT
LOAD=[6,3]+[4,6]
UNIT 24 TYPE 24 INTEGRATOR
INPUTS 5
16,6 1,3 4,5 4,6 6,3
0 0 0 0 0
UNIT 20 TYPE 24 FUEL COST INTEGRATOR
PARAMETERS 1
9000
INPUTS 3
FUELC1 FUELC2 LOAD
0 0 0
UNIT 29 TYPE 29 ECONOMIC ANALYSIS
PARAMETERS 31
2 30 70 500 2 0 20 10 9 15 9 1 5 9 0 0 1 0 2 1 150 20 10 10 1
1 2 0 0 0 0
INPUTS 3
20,1 20,2 20,3
0 0 0
UNIT 25 TYPE 25 PRINTER
PARAMETERS 1
–1
INPUTS 6
24,1 24,2 24,3 24,4 4,7 24,5
TSOL TQU TQENV TQLOAD DELTAU QAUX
END

Brief description of TRNSYS components included in the simulation model

TYPE 1: Solar collector; this component models the thermal performance of a flat plate solar collector using either performance data or theory. The total collector array may consist of collectors connected in series and in parallel. The thermal

performance of the collector array is determined by the number of modules in series and the characteristics of each module.

TYPE 2: On/off Differential Controller; this component controls th operation of the pump which circulates the working fluid through the collector–storage subsystem.

TYPE 3: Pump; this model computes a mass flow rate using a variable control function which must be between 0 and 1, and a fixed (user specified) maximum flow capacity.

TYPE 4: Stratified fluid storage tank; the thermal performance of a fluid–filled sensible energy storage tank, subject to thermal stratification, can be modelled by assuming that the tank consists of N ($N \leq 15$) fully mixed equal volume segments, where N is the number of segments. If N is equal to 1, the storage tank is modelled as a fully mixed tank and no stratification effects are possible.

TYPE 6: Auxiliary heater; it is modeled to elevate the temperature of a flowstream using either an internal or external control or a combination of both. The auxiliary heater employs a temperature dead band.

TYPE 54: Weather generator, to produce hourly weather data from monthly averages.

TYPE 16: Solar radiation processor, to convert the solar data into a form usable by the collector–storage subsystem.

TYPE 24: Quantity integrator, to integrate energy quantities

TYPE 14: Domestic hot water load, which describes the daily hot water consumption pattern.

TYPE 25: Printer, to output the monthly or yearly results of the simulation.

TYPE 29: Economic analysis, to evaluate the economics of the system.

Appendix D. Simulation input file JM3.DAT

A SOLAR SPACE HEATING SYSTEM
(Performance and Economic analysis)

```
ASSIGN J3YOPT.OUT 6
ASSIGN CYDATA.DAT 10
SIMULATION 0 8760 1
TOLERANCE -0.1 -0.1
WIDTH 72
UNIT 54 TYPE 54 WEATHER DATA GENERATOR
PARAMETERS 20
1 1 10 1 2 1 1 3.09 4.12 3.61 4.12 4.64 5.15 5.15 4.64 4.12 3.61 3.09  3.09 100
* Parameters 8-19 represent monthly average wind speeds
UNIT 16 TYPE 16 SOLAR RADIATION PROCESSOR
PARAMETERS 7
3 1 1 1 35 4871 0
INPUTS 6
54,7 54,19 54,20 0,0 0,0 0,0
0 0 0 .2 50 0
UNIT 1 TYPE 1 SOLAR COLLECTOR
PARAMETERS 12
1 1 70 4.19 2 50 .78 24.4 -1 4.19 1 .1
INPUTS 10
3,1 3,2 3,2 54,4 16,6 16,4 16,5 0,0 16,9 16,10
40 0 0 0 0 0 0 .2 0 50
UNIT 2 TYPE 2 PUMP CONTROLLER
PARAMETERS 3
3 10 1
INPUTS 3
1,1 4,1 2,1
40 40 0
UNIT 3 TYPE 3 PUMP
PARAMETERS 1
2800
INPUTS 3
4,1 4,2 2,1
40 0 0
UNIT 4 TYPE 4 STORAGE TANK
PARAMETERS 6
1 3.5 4.19 1000 1.2 -2
INPUTS 5
1,1 1,2 12,1 12,2 0,0
40 0 0 0 18
DERIVATIVES 1
40
UNIT 12 TYPE 12 DEGREE-DAY HOUSE
PARAMETERS 6
```

1 4000 20 1800 4.19 8000
INPUTS 4
4,3 4,4 54,4 4,5
40 0 0 0
*** Fuel cost multiplier**
EQUATIONS 4
MULT=0.0000074
FUELC1=[12,6]*MULT
FUELC2=[12,3]*MULT
FRACT=1-[24,5]/[24,4]
UNIT 24 TYPE 24 INTEGRATOR
INPUTS 5
16,6 1,3 4,5 12,3 12,6
0 0 0 0 0
UNIT 20 TYPE 24 FUEL COST INTEGRATOR
PARAMETERS 1
9000
INPUTS 3
FUELC1 FUELC2 12,3
0 0 0
UNIT 29 TYPE 29 ECONOMIC ANALYSIS
PARAMETERS 31
2 70 220 200 2 1 20 50 9 15 9 1 3 9 0 0 1 0 2 1 100 20 5 5 1 1 2 0 0 0 0
INPUTS 3
20,1 20,2 20,3
0 0 0
UNIT 25 TYPE 25 PRINTER
PARAMETERS 1
-1
INPUTS 7
24,1 24,2 24,4 24,5 FRACT 24,3 4,7
QINSOL QU LOAD QAUX FRACT QENV DELTAU
END

Brief description of TRNSYS components included in the simulation model

TYPE 1: Solar collector; this component models the thermal performance of a flat plate solar collector using either performance data or theory. The total collector array may consist of collectors connected in series and in parallel. The thermal performance of the collector array is determined by the number of modules in series and the characteristics of each module.

TYPE 2: On/off Differential Controller; this component controls th eoperation of the pump which circulates the working fluid through the collector-storage subsystem.

TYPE 3: Pump; this model computes a mass flow rate using a variable control function which must be between 0 and 1, and a fixed (user specified) maximum flow capacity.

TYPE 4: Stratified fluid storage tank; the thermal performance of a fluid–filled sensible energy storage tank, subject to the rmal stratification, can be modelled by assuming that the tank consists of N ($N \leq 15$) fully mixed equal volume segments, where N is the number of segments. If N is equal to 1, the storage tank is modelled as a fully mixed tank and no stratification effects are possible.

TYPE 12: Energy/(Degree Day) space heating load, as described in Chapter 5.

TYPE 54: Weather generator, to produce hourly weather data from monthly averages.

TYPE 16: Solar radiation processor, to convert the solar data into a form usable by the collector–storage subsystem.

TYPE 24: Quantity integrator, to integrate energy quantities

TYPE 25: Printer, to output the monthly or yearly results of the simulation.

TYPE 29: Economic analysis, to evaluate the economics of the system.

Appendix E. Simulation input file JM4.DAT

A COMBINED SOLAR WATER AND SPACE HEATING SYSTEM
(Performance and Economic analysis)

```
ASSIGN JM4.OUT 6
ASSIGN CYDATA.DAT 10
SIMULATION 0 8760 1
TOLERANCES -0.1 -0.1
WIDTH 72
UNIT 54 TYPE 54 WEATHER DATA GENERATOR
PARAMETERS 20
1 1 10 1 2 1 1 3.09 4.12 3.61 4.12 4.64 5.15 5.15 4.64 4.12 3.61 3.09
3.09 100
* Parameters 8-19 represent monthly average wind speeds
UNIT 16 TYPE 16 SOLAR RADIATION PROCESSOR
PARAMETERS 7
3 1 1 1 35 4871 0
INPUTS 6
54,7 54,19 54,20 0,0 0,0 0,0
0 0 0 .2 50 0
UNIT 21 TYPE 21 LIQUID COLLECTOR-STORAGE SUBSYSTEM
PARAMETERS 17
60 1 3000 4.19 3000 4.19 50 .78 24.4 .1 100 -1 3 1000 1.2 2 40
INPUTS 10
11,1 11,2 54,4 0,0 16,6 16,4 16,5 0,0 16,9 16,10
20 0 0 18 0 0 0 .2 0 50
UNIT 14 TYPE 14 DOMESTIC HOT WATER CONSUMPTION PROFILE
PARAMETERS 70
0 0 5 0 5 5 6 5 6 10 7 10 7 14 8 14 8 10 9 10 9 5 10 5 10 2
13 2 13 4 14 4 14 6 15 6 15 8 16 8 16 11 17 11 17 12 18 12 18 15
19 15 19 18 21 18 21 10 22 10 22 5 23 5 23 2 24 2 24 0
* Assumes 40 l per person, as per consumption profile DOM4
UNIT 23 TYPE 23 DOMESTIC WATER HEATING SUBSYSTEM
PARAMETERS 14
-160 0.18 1000 4.19 1.2 2 50 4.19 500 0.75 5 1 40 90
INPUTS 5
21,1 0,0 0,0 0,0 14,1
40 500 18 18 0
UNIT 11 TYPE 11 TEE-PIECE
PARAMETERS 1
1
INPUTS 4
23,1 23,2 12,1 12,2
40 0 0 0
UNIT 12 TYPE 12 DEGREE-DAY HOUSE
PARAMETERS 6
1 4000 20 1800 4.19 8000
```

```
INPUTS 4
21,1 21,2 54,4 21,4
40 0 0 0
*FUEL COST MULTIPLIER
EQUATIONS 9
AC=60
MULT=0.0000037
HWLOAD=[14,1]*4.19*(50-18)
FUELC1=[12,6]*MULT+[23,7]*MULT
FUELC2=[12,3]*MULT+(HWLOAD)*MULT
TLOAD=[12,3]+(HWLOAD)
TAUX=[12,6]+[23,7]
FRACT=1-[24,7]/[20,3]
EFBAR=[24,5]/([24,6]*AC+0.000000000000001)
UNIT 24 TYPE 24 INTEGRATOR
INPUTS 9
12,3 12,6 HWLOAD 23,7 21,3 16,6 TAUX 23,5 23,6
0 0 0 0 0 0 0 0 0
* HLOAD HAUX HWLOAD HWAUX QU QINS TAUX QINPH QPLOAD
UNIT 20 TYPE 24 FUEL COST INTEGRATOR
PARAMETERS 1
9000
INPUTS 3
FUELC1 FUELC2 TLOAD
0 0 0
UNIT 29 TYPE 29 ECONOMIC ANALYSIS
PARAMETERS 31
2 60 220 200 2 1 20 50 9 15 9 1 3 9 0 0 1 0 2 1
100 20 5 5 1 1 2 0 0 0 0
INPUTS 3
20,1 20,2 20,3
0 0 0
UNIT 25 TYPE 25 PRINTER 1
PARAMETERS 1
-1
INPUTS 10
24,1 24,2 24,3 24,4 24,5 24,6 24,7 20,3 24,8 24,9
HLOAD HAUX HWLOAD HWAUX QU QINS TAUX TLOAD QINPH
QPLOAD  UNIT 26 TYPE 25 PRINTER 2
INPUTS 2
EFBAR FRACT
EFBAR FRACT
END
```

Brief description of TRNSYS components included in the simulation model

TYPE 21: Collector-storage subsystem; this unit consists of a flat plate solar collector, an optional heat exchanger, a water storage tank, pumps and a controller.

TYPE 23: Domestic water heating subsystem; it consists of a preheat tank that supplies solar pre-heated water to an auxiliary heater which heats the water to the required supply temperatures. There is also an optional heat exchanger, built into the model which can be "removed" by specifying its effectiveness, ε, as -1.

TYPE 12: Energy/(Degree Day) space heating load, as described in Chapter 5.

TYPE 54: Weather generator, to produce hourly weather data from monthly averages.

TYPE 16: Solar radiation processor, to convert the solar data into a form usable by the collector-storage subsystem.

TYPE 24: Quantity integrator, to integrate energy quantities

TYPE 14: Domestic hot water load, which describes the daily hot water consumption pattern.

TYPE 25: Printer, to output the monthly or yearly results of the simulation.

TYPE 29: Economic analysis, to evaluate the economics of the system.

Appendix F. Simulation input file JM5.DAT

A SOLAR ASSISTED HEAT PUMP SYSTEM
(Performance and Economic Analysis)

```
ASSIGN JM5AC60.OUT 6
ASSIGN CYDATA.DAT 10
ASSIGN LHPDATA.DAT 11
ASSIGN AHPDATA.DAT 12
SIMULATION 0 8760 1
TOLERANCES -0.05 -0.05
WIDTH 72
EQUATIONS 11
* Electricity MULT=0.000036  $/kJ
* Diesel oil  MULT=0.0000074 $/kJ
AREA=60
MULT=0.000036
EFF=[24,2]/(AREA*[24,1]+0.0000000000001)
HAUX=[8,2]*60000
HWLOAD=[14,1]*4.19*(50-18)
SAFH=([34,1]-[24,7]-[34,2])/([34,1]+0.0000000001)
TLOAD=[12,3]+(HWLOAD)
SAFO=([34,3]-[24,7]-[34,2]-[23,7])/([34,3]+0.00000000001)
HEATAD=[20,3]+[20,4]+HAUX
FUELC1=[12,6]*MULT+[23,7]*MULT+[20,6]*MULT
FUELC2=[12,3]*MULT+(HWLOAD)*MULT
ACCELERATE 1
20 1
UNIT 54 TYPE 54 WEATHER DATA GENERATOR
PARAMETERS 20
1 1 10 1 2 1 1 3.09 4.12 3.61 4.12 4.64 5.15 5.15 4.64 4.12 3.61
3.09
3.09 100
UNIT 16 TYPE 16 SOLAR RADIATION PROCESSOR
PARAMETERS 7
3 1 1 1 35 4871 0
INPUTS 6
54,7 54,19 54,20 0,0 0,0 0,0
0 0 0 .2 50 0
UNIT 21 TYPE 21 LIQUID COLLECTOR-STORAGE SUBSYSTEM
PARAMETERS 17
60 1 3000 4.19 3000 4.19 50 .78 24.4 .1 100 -1 3 1000 1.2 2 40
INPUTS 10
20,1 20,2 54,4 0,0 16,6 16,4 16,5 0,0 16,9 16,10
20 0 0 20 0 0 0 .2 0 50


UNIT 14 TYPE 14 DOMESTIC HOT WATER CONSUMPTION PROFILE
PARAMETERS 70
```

0 0 5 0 5 5 6 5 6 10 7 10 7 14 8 14 8 10 9 10 9 5 10 5 10 2
13 2 13 4 14 4 14 6 15 6 15 8 16 8 16 11 17 11 17 12 18 12 18 15
19 15 19 18 21 18 21 10 22 10 22 5 23 5 23 2 24 2 24 0
UNIT 23 TYPE 23 DOMESTIC WATER HEATING SUBSYSTEM
PARAMETERS 14
-180 .18 1000 4.19 1.2 2 50 4.19 300 -1 5 1 40 90
INPUTS 5
21,1 0,0 0,0 0,0 14,1
40 200 18 18 0
UNIT 11 TYPE 11 TEE-PIECE
PARAMETERS 1
1
INPUTS 4
23,1 23,2 20,1 20,2
40 0 0 0
UNIT 12 TYPE 12 DEGREE-DAY HOUSE
PARAMETERS 6
4 4000 100000 20 4.19 8000
INPUTS 6
0,0 0,0 54,4 21,4 HEATAD 0,0
0 0 0 0 0 0
UNIT 8 TYPE 8 THERMOSTAT
PARAMETERS 7
3 1 0 100 20 18 1
INPUTS 2
12,4 0,0
20 100
UNIT 20 TYPE 20 DUAL SOURCE HEAT PUMP
PARAMETERS 10
4.19 1800 8000 35 15 5 11 12 10 10
INPUTS 5
21,1 21,2 54,4 12,4 8,1
20 0 0 18 0
UNIT 24 TYPE 24 INTEGRATOR 1
INPUTS 7
*Qins, Qu, Qenvst, Qhp, Qdh, Qabs, Qei
16,6 21,3 21,4 20,3 20,4 20,5 20,6
0 0 0 0 0 0 0
UNIT 34 TYPE 24 INTEGRATOR 2
INPUTS 5
12,3 HAUX TLOAD 23,7 23,6
0 0 0 0 0
UNIT 10 TYPE 24 FUEL COST INTEGRATOR
PARAMETERS 1
9000
INPUTS 3
FUELC1 FUELC2 TLOAD
0 0 0
UNIT 29 TYPE 29 ECONOMIC ANALYSIS
PARAMETERS 31

2 60 220 3000 2 1 20 50 9 15 9 1 3 9 0 0 1 0 2 1
100 20 5 5 1 1 2 0 0 0 0
INPUTS 3
10,1 10,2 10,3
0 0 0
UNIT 25 TYPE 25 PRINTER 1 FOR INTEGRATOR 1
INPUTS 7
24,1 24,2 24,3 24,4 24,5 24,6 24,7
QINS QU QENVST QHP QDH QABS QEI
UNIT 35 TYPE 25 PRINTER 2 FOR INTEGRATOR 2
INPUTS 10
34,1 34,2 21,6 20,7 EFF SAFH 34,3 SAFO 34,4 34,5
HLOAD HAUX DELTUS COPBAR EFF SAFH TLOAD SAFO HWAUX HWLOAD
END

Brief description of TRNSYS components included in the simulation model

TYPE 21: Collector–storage subsystem; this unit consists of a flat plate solar collector, an optional heat exchanger, a water storage tank, pumps and a controller. Based on the findings of the preceding simulations (Chapter 6), no heat exchanger will be employed in the collector–storage subsystem, so that the performance of the solar system is maximised and the capital cost is reduced.

TYPE 23: Domestic water heating subsystem; it consists of a preheat tank that supplies solar pre–heated water to an auxiliary heater which heats the water to the required supply temperatures. There is also an optional heat exchanger, built into the model which can be "removed" by specifying its effectiveness, ε, as −1.

TYPE 12: Energy/(Degree Day) space heating load, as described in Chapter 5.

TYPE 20: Dual source heat pump, a description of which is presented in detail in Chapter 7.

TYPE 11: Tee–piece, so that hot water from storage tank is supplied to both space heating and service hot water circuits.

TYPE 8: Thermostat, which is sensing room temperature through TYPE 12 (building load).

TYPE 54: Weather generator, to produce hourly weather data from monthly averages.

TYPE 16: Solar radiation processor, to convert the solar data into a form usable by the collector–storage subsystem.

TYPE 24: Quantity integrator, to integrate energy quantities

TYPE 14: Domestic hot water load, which describes the daily hot water consumption

pattern.

TYPE 25: Printer, to output the monthly or yearly results of the simulation.

TYPE 29: Economic analysis, to evaluate the economics of the system.

Appendix G. Performance data for heat pumps, adapted from CARRIER 38Y030.00/40AQ030, Condenser inlet temperature 20°C

PERFORMANCE DATA FROM LOGICAL UNIT 11 (LHPDATA.DAT)

X1	Y1	Y2	Y3
5.000E+00	3.240E+04	2.034E+04	1.206E+04
7.500E+00	3.560E+04	2.280E+04	1.250E+04
1.000E+01	3.852E+04	2.534E+04	1.318E+04
1.250E+01	4.220E+04	2.760E+04	1.380E+04
1.500E+01	4.572E+04	3.114E+04	1.458E+04
1.750E+01	4.900E+04	3.400E+04	1.510E+04
2.000E+01	5.292E+04	3.686E+04	1.606E+04
2.250E+01	5.700E+04	4.000E+04	1.700E+04
2.500E+01	6.000E+04	4.300E+04	1.750E+04
2.750E+01	6.300E+04	4.600E+04	1.800E+04

PERFORMANCE DATA FROM LOGICAL UNIT 12 (AHPDATA.DAT)

X1	Y1	Y2	Y3
−1.500E+01	1.469E+04	5.868E+03	8.820E+03
−1.000E+01	1.778E+04	8.208E+03	9.576E+03
−5.000E+00	2.095E+04	1.058E+04	1.037E+04
−2.000E+00	2.700E+04	1.300E+04	1.100E+04
2.000E+00	2.820E+04	1.750E+04	1.170E+04
5.000E+00	3.240E+04	2.034E+04	1.206E+04
7.500E+00	3.560E+04	2.280E+04	1.250E+04
1.000E+01	3.852E+04	2.534E+04	1.318E+04
1.500E+01	4.572E+04	3.114E+04	1.452E+04
2.000E+01	5.292E+04	3.686E+04	1.606E+04

X1 Evaporator source temperature, °C
Y1 Heat output, kJ/h
Y2 Heat absorbed by heat pump, kJ/h
Y3 Energy input to compressor, kJ/h

Appendix H. Publications

1. Michaelides I. M. and Votsis P. P. Energy analysis and development of solar energy in Cyprus. *Computing and Control Engineering Journal*, Vol 2, No 5, 211–215, (1991).

2. Michaelides I. M., Wilson D. R. and Votsis P. P. Exploitation of solar energy in Cyprus. *Renewable Energy,* Vol 1, No 5/6, 627–637, (1991).

3. Michaelides I. M., Lee W. C., Wilson D. R. and Votsis P. P. Computer simulation of the performance of a thermosyphon solar water heater. *Applied Energy,* **41**, 149–163, (1992).

4. Michaelides I. M., Lee W. C., Wilson D. R. and Votsis P. P. An investigation into the performance and cost effectiveness of thermosyphon solar water heaters. *Renewable Energy,* Vol. 2, No. 3, 219–225, (1992).

5. Michaelides I. M. Solar energy in Cyprus: Facts and Prospects. Proceedings *Second World Renewable Energy Congress*, 13–18 September 1992, Reading, U.K., Vol. 5, 2562–2567 (1992).

6. Michaelides I. M., Lee W. C., Wilson D. R. and Votsis P. P. An investigation of some performance criteria in the design of solar space heating systems. *Cairo Third International Conference on Renewable Energy Sources*, 30 December 1992 – 2 January 1993, Cairo, Egypt.

7. Michaelides I. M., Lee W. C., Wilson D. R. Computer simulation and optimisation of solar water heating systems. Accepted (13 February, 1993) for presentation at the *ISES Solar World Congress 1993,* 23–27 August 1993, Budapest, Hungary.

GLOSSARY

Absorber – the part of a solar collector that receives the incident solar radiation and transforms it into thermal energy.

Absorptance – the ratio of the radiation absorbed by a surface and the total energy falling on that surface measured as a percentage.

Active solar heating system – an assemblage of collectors, storage devices, and distribution equipment which converts solar energy into heat and distributes the heat in a controlled manner.

Angle of incidence – Angle between a ray striking a surface and line perpendicular to that surface at the point of impact. Normal, or perpendicular, rays have zero angle of incidence.

Annualized life cycle cost (ALCC) – the average yearly outflow of money (cash flow).

Auxiliary system – equipment using conventional energy sources to supplement the output provided by the solar energy system.

Backup system – see auxiliary system.

Beam radiation, direct radiation – the portion of the incident solar radiation that comes directly from the sun without scattering by the atmosphere or clouds; it casts shadows and can be focused.

Building overall heat loss coefficient – overall rate of heat loss from a building expressed in Watts per degree temperature difference between inside and outside; also known as the building "UA" value.

Capacitance rate – mass flow rate multiplied by the specific heat of the fluid flowing through a component such as a heat exchanger.

Collector aperture – the frontal opening of the collector which captures the sun's rays.

Collector efficiency – ratio of the energy collected by a solar collector during a time period to the radiant energy incident on the collector in the same time period.

Collector heat removal factor (F_R) – ratio of the actual useful energy output of a flat plate solar collector to the useful output if the entire absorber plate were as cool as the entering fluid.

Collector overall heat loss coefficient (U_L) – parameter characterizing the energy losses of the collector to the surroundings through the top, sides, and bottom of the collector.

Collector to consumer factor – the ratio of collector surface area to the number of service hot water consumers in a building.

Collector to floor area factor – the ratio of collector surface area to the floor area of a heated building.

Collector to load factor – the ratio of collector surface area to the annual thermal load of a building.

Dead band temperature differential – temperature difference of the differential controller. A heating system may be turned on by a thermostat at a room temperature of 19°C, but not turned off until the room reaches 21°C. In this case the controller has a dead band temperature difference of 2°C.

Degree–day (heating) – one day with the mean of the daily minimum and maximum ambient air temperatures one degree colder than 18 °C or other specified base temperature.

Design heating load – maximum predicted space heating load under design (near worst) conditions.

Diffuse radiation – sunlight scattered by atmospheric particles and gases; it arrives to the earth's surface from all directions and can not be focused.

Direct beam radiation – see beam radiation.

Discounted cash flow – present worth of a future payment.

Emittance – ratio of the radiant thermal energy emitted from an actual surface at a given temperature to the energy that would be emitted by a black body (a perfect absorber and emitter) at the same temperature.

Energy intensity – the amount of energy needed to produce a unit of Gross Domestic Product (GDP).

Flat plate collector – device used to collect solar energy in which the surface absorbing the incident solar radiation is essentially flat. No concentration of sunlight is employed; the absorber is about the same size as the aperture.

Heat exchanger – device used to transfer heat from one material to another, usually between two separate fluids.

Incident angle modifier – factor that accounts for reduction in collector optical efficiency during off–axis operation, a reduction caused by lower glazing transmission, lower effective absorptance and shading effects.

Insolation – radiation received from the sun, including ultraviolet, visible, and infrared. Total insolation includes both direct and diffuse radiation.

Life–cycle cost (LCC) – the sum of all the costs associated with an energy delivery

system over its lifetime or over a selected period of analysis, in today's dollars; it takes into account the time value of money.

Life–cycle economic analysis – method of comparing future costs in terms of today's money.

Life–cycle savings (LCS) or net present worth – the difference between the life cycle costs of a conventional fuel–only system and the life cycle cost of the solar plus auxiliary energy system.

Liquid–based solar heating system – heating system in which liquid (either water, anti–freeze, or a nonaqueous solution) is heated in solar collectors.

Longwave solar radiation – infrared radiant heat beyond about 3 microns in wavelength; emitted to some extent by all objects, even those at room temperature.

Market discount rate – the rate of return on the best alternative investment.

Passive solar heating – heating a building through use of the sun plus appropriate architectural details and construction techniques, and with the aid of very little(or no) mechanical equipment or energy.

Payback period (time) – the time needed for the cumulative fuel savings to equal the total initial investment, that is, how long it takes to get an investment back by savings in fuel.

Present worth – amount of money that must be invested today in order to have a specified worth at a future time.

Rate of return, Return on investment (ROI) – the market discount rate that will result in zero life–cycle savings, that is, the discount rate that makes the present worth of solar and non–solar alternatives equal.

Selective surface – surface having a high absorptance for solar radiation and a low emittance for thermal (longwave) radiation.

Solar collector – device designed to absorb incident solar radiation and transfer the energy to a fluid flowing in thermal contact with the absorbing surface.

Solar constant – intensity of solar radiation on a surface normal to and exposed to the sun, and located outside the earth's atmosphere at a distance from the sun equal to the earth's mean distance from the sun; the currently accepted value of solar constant is 1353 W m^{-2}, or 4871 kJ m^{-2} h^{-1}.

Solar degradation – deterioration of materials and components by exposure to sunlight.

Solar fraction – fraction of the thermal load supplied by solar energy.

Solar heating system – assembly of subsystems and components necessary to

convert solar energy into thermal energy for heating purposes, in combination with auxiliary energy when required.

Solar savings – the difference between the cost of a conventional system and a solar system.

Solar time – hour of the day as reckoned by the apparent position of the sun. Solar noon is mid–day, the moment when the sun reaches its maximum altitude for that day. It differs by up to an hour from local standard time.

Storage capacity – amount of energy that can be stored by a solar heating system for use at a later time.

Storage factor – the ratio of storage tank volume to the surface area of collector.

Stratification – in solar heating context, the formation of layers in a substance where the top layer is warmer than the bottom.

Subsystem – a major, separable, functional assembly of a system, such as a complete collector, thermal storage device etc.

Thermosyphon – circulation of fluid by convection, which occurs in a closed system as warm (less–dense) fluid rises and cooler (more–dense) fluid falls.

Transmittance – ratio of the radiation passing through a material to the radiation incident on the upper surface of the material.

Water–source heat pump – heat pump that transfers heat from a water source to an indoor air circulation system.

LIST OF REFERENCES

Ammar, A.A. 1989. Efficient collection and storage of solar energy. *Solar and Wind Technology*, Vol. 6, No. 6, pp. 643–652.

Anderson, J.V. 1979. Procedures for predicting the performance of air–to–air heat pumps in stand alone and parallel solar–heat pump systems. MSc thesis, University of Wisconsin–Madison.

Anderson, J.V., Mitchell, J.W. and Beckman, W.A. 1980. A design method for parallel solar heat pump systems. *Solar Energy* **25**, 155–163.

Aristodemou, N.E. *et al*, 1988. *Energy Planning and Conservation Project EC4 Hotels, Hotel Apartments and Offices*, June 1988.

ASHRAE, 1981. *Handbook of Fundamentals.* New York: American Society of Heating Refrigeration and Air conditioning Engineers.

Barley, C.D. 1979. Load optimization in solar space heating systems. *Solar Energy* **23**, 149–156.

Beckman, W.A., Klein, S.A. and Duffie, J.A. 1976. A design procedure for solar heating systems. *Solar Energy* **18**, 113–127.

Brandemuehl, M.J. and Beckman, W.A. 1979. Economic evaluation and optimization of solar heating systems. *Solar Energy* **23**, 1–10.

Braun, J.E., Klein, S.A. and Pearson, K.A. 1983. An improved design method for solar water heating systems. *Solar Energy* **31**, 597–604.

British Standards Institution, 1981. British Standard Code of Practice for Solar heating systems for domestic hot water. BS 5918:1981.

Buckles, W.E. and Klein, S.A. 1980. Analysis of solar domestic hot water heaters. *Solar Energy* **25**, 417–424.

Butz, L.W., Beckman, W.A. and Duffie, J.A. 1974. Simulation of a solar heating and cooling system. *Solar Energy* **16**, 129–136.

Carg, H.P. 1982. *Treatise on Solar Energy; Volume 1: Fundamentals of Solar Energy,* p. 378, Wiley, New York.

Carrington, C. G., Warrington, D.M. and Yak, Y.C., 1985. Structure of domestic hot water consumption. *Energy Research* **9**, 65–75.

Carvalho, N.J., Deimezis, N., Lecloux, M. and Karaderoglou, P. 1991. *Energy in Europe, Annual Energy Review,* Commission of the European Communities Directorate General for Energy, December 1991.

Commission of European Communities, 1991. *Energy in Europe* **18**, Directorate

General for Energy, December 1991.

CYS, 1980. CYS 119:1980 Method of Testing the Performance of Flat-plate Solar Collectors. Cyprus Organisation for Standards and Control of Quality, 1980.

CYS, 1984. CYS 100:1984 Specification for Solar Water Heaters. Cyprus Organisation for Standards and Control of Quality, 1984.

Department of Statistics and Research, 1982. *Census of Housing 1982*. Ministry of Finance, Republic of Cyprus.

Department of Statistics and Research, 1987. *Construction and Housing Statistics for 1987*. Ministry of Finance, Republic of Cyprus.

Department of Statistics and Research, 1990. *Construction and Housing Statistics for 1990*. Ministry of Finance, Republic of Cyprus.

Department of Statistics and Research, 1989. *Economic Report 1989.* Ministry of Finance, Republic of Cyprus.

Department of Statistics and Research, 1990. *Demographic Report 1990.* Ministry of Finance, Republic of Cyprus.

Department of Statistics and Research, 1990. *Industrial Statistics 1990.* Ministry of Finance, Republic of Cyprus.

Duffie, J.A. and Beckman, W.A, 1980. *Solar Engineering of Thermal Processes.* John Wiley, New York.

Duffie, J.A. 1980. Modelling and simulation of active systems. *Proceedings of the International Symposium on Solar Energy Utilisation, London, Ontario, Canada, 10–24 August 1980,* Pergamon Press.

Duff, W. and Winn, B. 1981. Modelling of solar thermal systems. *Solar Energy Handbook,* 17, 1–30.

Elsayed, M.M., 1989. Optimum orientation of absorber plates. *Solar Energy* **42**, 89–102.

Fahmy, M.F.M. and Sadek, M.A. 1990. Transient analysis of closed loop solar water heating system (effect of heat exchangers). *Energy Conversion and Management* **30**, 343–355.

Fanney, A.H., and Klein, S.A. 1987. Comparison of experimental and calculated performance of integral collector–storage solar water heaters. *Solar Energy,* **38**, 303–309.

Fanney, A.H. and Liu, S.T. 1980. Experimental system performance and comparison with computer predictions for six solar water systems. *ASHRAE Trans.* **86**, 823–834.

Felske, J.D. 1978. The effect of off–south orientation on the performance of flat plate solar collectors. *Solar Energy* **20**, 29–36.

Freeman, T.L., Mitchell, J.W. and Audit, T.E. 1979. Performance of combined solar heat pump systems. *Solar Energy* **22**, 125–135.

Gandhindasam, G. 1987. Effectiveness of solar water–heating systems. *Applied Energy* **28**, 153–160.

Gillet, W.B. and Rosenfeld, J.L.J. 1981. The thermal performance of solar water heaters in the United Kingdom. *Sun at Work in Britain,* **12/13**, 12–19.

Goyal, A.K., Kumar, A. and Sodha, M.S. 1987. Optimization of hybrid solar forced–convection water heating system. *Energy Conversion and Management* **27**, 367–377.

Gupta, C.L. and Carg, H.P. 1968. System Design in Solar Water Heaters with Natural Circulation. *Solar Energy* **12**, 163–182.

Gutierrez, G., Hincapie, F., Duffie, A. and Beckman, W.A. 1976. Simulation of forced circulation water heaters; effects of auxiliary energy supply, load type and storage capacity. *Solar Energy* **15**, 287–296.

Hadjioannou, L. 1987. Three Years of Operation of the Radiation Centre in Nicosia – Cyprus, *Meteorological Note Series No. 2*, Meteorological Service, March 1987.

Hatheway, F.M. and Converse, A.O. 1981. Economic comparison of solar–assisted heat pumps. *Solar Energy* **27**, 561–569.

Hottel, H.C. 1989. Fifty years of solar energy research supported by the Cabot Fund. *Solar Energy* **43**, 107–128.

Hottel, H.C. and Whillier, A. 1958. Evaluation of flat plate solar collector performance. *Transactions of the Conference on the use of solar energy*, **2**, Part I, 74, University of Arizona Press, Tucson, Arizona, 1958.

Hunn, B.D., Willcut, G.J.E. and McSweeny, T.B. 1977. Simulation and cost optimization of solar heating of buildings in adverse solar regions. *Solar Energy* **19**, 33–44.

Kern, J. and Harris, I. 1975. On the optimum tilt of a solar collector. *Solar Energy* **17**, 97–103.

Klein, S.A. *et al.* 1990. *TRNSYS, a Transient Simulation Program*. Solar Energy Laboratory, University of Wisconsin.

Klein, S.A., Beckman, W.A., and Duffie, J.A., 1976. A design procedure for solar heating systems. *Solar Energy* **18**, 113–127.

Kordatos, Y. and Varnalis, C. (editors), 1957. *Xenophon Memorabilia, III.viii. 8.*

Kovarik, M. and Lesse, P.F. 1976. Optimal control of flow in low temperature solar heat collectors. *Solar Energy* **18**, 431–435.

Kreider, J.F. and Kreith, F. 1977. *Solar Heating and Cooling*. McGraw Hill, Washington, 1977.

Kreider, J.F. and Kreith, F. 1981. *Solar Energy Handbook*. McGraw Hill, Washington, 1981.

Liu, B.Y. and Jordan, R.C. 1963. The long–term average performance of flat–plate solar collectors. *Solar Energy* **7**, 53–59.

Lof, G.O.G. and Tybout, R.A. 1973. Cost of house heating with solar energy. *Solar Energy* **14**, 253–278.

Lunde, P.J., 1979. Prediction of the performance of solar heating systems over a range of storage capacities. *Solar Energy* **23**, 115–121.

Lunde, P.J., 1980. *Solar Thermal Engineering.* Wiley, New York.

McArthur, J.W., Palm, W.T. and Lessman, R.C. 1978. Performance analysis and cost optimisation of a solar–assisted heat pump system. *Solar Energy* **21**, 1–9.

Meteorological Service, 1975. *Local climates in Cyprus. Meteorological Paper No. 6*. Ministry of Agriculture and Natural Resources, Republic of Cyprus.

Meteorological Service, 1985. *Solar Radiation and Sunshine Duration in Cyprus. Meteorological Paper No. 10.* Ministry of Agriculture and Natural Resources, Republic of Cyprus.

Michaelides I.M. 1985. *Performance of the HTI Experimental Solar Heating System*, Report, Higher Technical Institute, Nicosia (May 1985).

Michaelides, I.M., Wilson, D.R. and Votsis, P.P. 1991. Exploitation of solar energy in Cyprus. *Renewable Energy Vol. 1, No. 5/6,* 629–637.

Michaelides, I.M. 1992. Solar energy in Cyprus: Facts and prospects. *Proceedings Second World Renewable Energy Congress*, Reading, U.K., Vol. 5, 2562–2567 (13–18 September 1992).

Michaelides, I.M., Lee, W.C., Wilson, D.R. and Votsis, P.P. 1992. Computer Simulation of the Performance of a Thermosyphon Solar Water Heater. *Applied Energy* **41**, 149–163.

Michaelides, I.M., Lee, W.C., Wilson, D.R. and Votsis, P.P. 1992. An investigation into the performance and cost optimisation of Thermosyphon Solar Water Heaters. *Renewable Energy Vol. 2, No. 3,* 219–225.

Minnerly, B.V., Klein, S.A. and Beckman, W.A., 1991. A rating procedure for solar domestic hot water systems based on ASHRAE–95 test results. *Solar Energy* **47**,

405–411.

Morrison, G.L. and Braun, J.E. 1985. System modelling and operation characteristics of thermosyphon solar water heaters. *Solar Energy* **34**, 389–405.

Morrison, G.L. and Tran, H.N. 1984. Simulation of the long term performance of thermosyphon solar water heaters. *Solar Energy* **33**, 515–526.

Morrison, G.L., Gilliaert, D. and Tebaldi, P. 1992. Outdoor testing of solar water heaters – effects of load pattern and auxiliary boosting. *Solar Energy* **49**, 299–308.

Mutch, J.J. 1974. RAND Report R1498: Residential water heating, fuel consumption, economics and public policy.

Norton, B. and Probert, S.D. 1983. Recent advances in natural–circulation, solar–energy water heater designs. *Applied Energy* **15**, 15–42.

Norton, B. and Probert, S.D. 1984. Measured performances of natural–circulation solar energy water heaters. *Applied Energy* **16**, 1–26.

Ong, K.S. 1976. An improved computer program for the thermal performance of a solar water heater. *Solar Energy* **18**, 183–191.

Pafelias, Th., Beleshiotis, V., and Nikolinakou, E. Performance of Greek solar water heating systems. *Proceedings 3rd seminar on solar energy, Athens, May 1990,* 178–79.

Parker, G.J. 1981. The performance of a solar water heating system in a dwelling in Christchurch, New Zealand. *Solar Energy* **26**, 189–197.

Phillips, W.F. 1981. Integrated performance of liquid–based solar heating systems. *Solar Energy* **26**, 287–295.

Planning Bureau, 1990. *Economic Review 1990*, Nicosia, Cyprus.

Pott, P. and Cooper, P.I. 1976. An Experimental Facility to Test Flat–plate Solar Collectors Outdoors, *Technical Report No TR 9*, Commonwealth Scientific and Industrial Research Organisation.

Reay, D.A. and Macmichael, D.B.A. 1979. *Heat Pumps Design and Applications.* Oxford: Pergamon Press, 1979.

Rusch, E. 1978. *Solar Heating*. Landis & Gyr, 3rd edition, 1978.

Sema–Metra & Kittis Associates Ltd, 1985. *Renewable Energy and Energy Conservation Project, Energy Planning, Final Report*, January 1985.

Shitzer, A., Kalmanoviz, D., Zvirin, Y. and Grossman, G. 1979. Experiments with a flat plate solar water heating system in thermosyphonic flow. *Solar Energy* **22**, 27–35.

Swanson, S.R. and Boehm, R.F. 1977. Calculation of long term solar collector heating system performance. *Solar Energy* **19**, 129–138.

Szokolay, S.V. 1975. *Solar energy and building*. The Architectural Press Ltd, Great Britain.

Thornton, J. 1993. Solar domestic hot water TRNSYS work. *TRNSYS News,* Vol. 5 No. 1, p. 9.

Tiwari, G.N., Shukla, S.N. and Sodha, M.S. (1985). Performance of large solar water heating system: Thermosyphon mode. *Energy Conversion and Management*, Vol. 25, No. 1, 29–38.

Tybout, R.A. and Lof, G.O.G. 1970. Solar energy heating. *Natural Resources Journal,* **10**, 268. Appeared in Duffie and Beckman (1980), p. 473.

Ward, D.S., Smith, C.C. and Ward, J.C. 1977. Operational modes of solar heating and cooling systems. *Solar Energy* **19**, 55–61.